The author(s) shown below used Federal funds provided by the U.S. Department of Justice and prepared the following final report:

ELEMENTAL ANALYSIS OF GLASS AND PAINT MATERIALS BY LASER ABLATION INDUCTIVELY COUPLED PLASMA MASS SPECTROMETRY (LA-ICP-MS) FOR FORENSIC APPLICATION

Award No. **2003-IJ-CX-K004**

NIJ TECHNICAL REPORT 2006

Tatiana Trejos, Waleska Castro and Jose R. Almirall,
Research Programs Coordinator, Doctoral Student and Associate Professor
Department of Chemistry and Biochemistry and
International Forensic Research Institute
Florida International University

Miami, Florida

August 2006

ABSTRACT

Abstract:

The elemental analysis of materials has become an important yet underutilized type of evidence at many crime scenes, including scenes of hit-and-run accidents. Although the utility of trace elemental analyses and comparisons for glass or paint fragments has been shown to offer a high degree of discrimination between different sources of these materials, the lack of method development, validation of methods and publication of the results in the open literature have limited the adoption of this technology by the typical forensic laboratory. The proposed research has expanded on prior work in our group (TSWG contract with end date of December 2002) to develop a solution analysis-based standard method for the elemental analysis of glass from a large number of sources and develop a database of data from the analysis of a large number of glasses. One significant disadvantage to solution analysis is the time consuming nature of the sample preparation, using acid digestion of the glasses for metal analysis. The methodology described within this report utilizes a laser ablation-sampling source prior to the ICP-MS analyte detection. A direct comparison of the results for solution and laser ablation analyses also provides additional data to pursue a more comprehensive study of the LA method development for glass comparisons. The results of the studies described within this report and the results of several groups (ie. NITECRIME network) yields excellent precision and low bias for the analysis of glass samples encountered in forensic casework. Glass sample size and sample heterogeneity/homogeneity considerations are also addressed. The results from the analysis of paint samples for forensic purposes are also described.

TABLE OF CONTENTS

SECTION I. INTRODUCTION AND OBJECTIVES

1.1. THE ROLE OF TRACE EVIDENCE IN FORENSIC SCIENCE

Forensic science practitioners apply the fundamental principles first described by Locard (exchange principle) to search for evidence at crime scenes that could provide information about who, what and how a crime was committed. This principle is recognized as one of the most valuable contributions given to law enforcement by one pioneer scientist, Edmond Locard, who believed that "every contact leaves a trace". When a criminal comes into contact with a person or an object, a cross transfer of evidence can occur. With only a microscope and a rudimentary spectrometer, this visionary man incorporated his philosophy within a "police" laboratory and convinced the world that trace evidence could help to solve crimes (Saferstein, 1998).

Evidence can manifest itself in different forms and can be classified as physical, demonstrative and testimonial. Evidence in the form of actual objects is called "real" or "physical evidence"; it can be found in the form of a demonstration or audio-visual aid to assist the trier of fact (demonstrative evidence); or it can be in the form of words recounting things that have been done and inferences that have been drawn. (Testimonial or parole) (Sapir, 2002).

Forensic scientists usually work with "physical" evidence to decipher visible and often invisible clues that can result in the solution of a case. When the amount of physical evidence left and/or transferred at crime scenes is very small it is called "trace evidence". The examination of that evidence is usually undertaken for identification or comparison. For identification, the determination of the physical or chemical identity of a substance is the target purpose, such as the identification of an illicit drug or an explosive. On the

7

other hand, for comparison purposes, a suspect specimen has to be compared with a control specimen in order to determine whether or not they have a common origin (Saferstein, 1998).

Fragments of glass and paint can be compared to determine whether or not they originated from the same source. For example, when a vehicle strikes a pedestrian, the body may be lifted into the air and onto the hood and windshield of the vehicle. Fragments of glass and paint chips are often embedded in the victim's clothing. If it is shown that there is an association or "match" between fragments of glass and paint chips found at the crime scene and evidence recovered from the suspect, such as the suspect car, a question then arises as to the significance of such association.

Evidence that can be associated with a common source with a high degree of probability is often described as evidence exhibiting "individual characteristics". Examples of this are the matching of ridge characteristics of two fingerprints or the fitting together of two glass fragments in a manner of jigsaw puzzle. By contrast, evidence exhibiting "class characteristics" can be associated with a class but not with a single source. Class characteristics, nonetheless, may constitute an important part of the evidence that can help to solve a crime (Fisher, 1993).

Trace evidence such as glass and paint usually exhibit class characteristics and therefore the value of evidence will depend on the discrimination power of the techniques used for its comparison and the significance of the findings. The value of evidence can also be enhanced by cross transfer of evidence between victim and suspect, multiple transfer of evidence and rarity of the characteristics of the evidence. For instance, the value of the match of one-layer paint chip from the suspect car is not nearly as great as

the match of a multi-layer paint chip. In addition, if there is also a match of glass fragments from the same suspect car, the evidence of glass and paint together will have a greater significance of having originated from the same source.

In the field of trace evidence the target objective is to develop techniques with great sensitivity, great discrimination power and minimum sample manipulation. In order to evaluate the value of new techniques, it is useful to consider an overall description of the techniques as well as the nature of the samples. The following sections discuss the nature of the chemical composition and manufacture of glass and paint in addition to the significance of elemental composition in forensic examinations.

1.2. FORENSIC SIGNIFICANCE OF EXAMINATION OF GLASS FRAGMENTS

1.2.1. History of the glass industry

Glass is defined as an inorganic production of fusion that has been cooled to a rigid condition without crystallization (ASTM, 2000). This material is composed of a mixture of inorganic materials that are responsible of its different physical properties. Some inorganic components are responsible for the glass structure; others are added intentionally to decrease the cost of manufacture or to provide desired properties such as heat resistance. In old days, however, the glassmaking was rudimentary and the production methods were discovered by trial and error (Koons, 2002).

Glass can be naturally produced by volcanic activity. It was first formulated in 1500 B.C. by the Egyptians to be used mainly in the manufacture of vessels and jewelry. Later, press molded glass was formulated in Alexandria (400 B.C.) and the Syrians

introduced (200 B.C.) the first examples of flat glass for use in windows. The quality of manufacturing of glass was improved by the Romans who were known for their contributions in oven technology. The formulas to produce clear glass were lost with the fall of the Roman Empire and were not redeveloped until the 13th century. The Germans in the 19th century manufactured optical glass and heat-resistant glass for use in thermometers and cooking wear (Koons, 2002).

Since then, the manufacture of glass has been in constant changes in order to look for better quality, automated processes and cheaper products.

Nowadays, glass is one of the products most utilized in society for many reasons. Glass production ranges from simple glass containers to advanced micro-components.

1.2.2. Formulations and raw materials

Glass can be classified in different groups according to their intended use as: flat glass (for architecture and automobiles), containers (bottles and jars), glass fibers (for insulation) and specialty glass. They can also be classified by their main raw materials as soda lime (containers and windows), lead (house ware and decorations), borosilicate (industry, lamps, cookware) and special (optical, electronics) (Almirall, 1999).

The main raw materials utilized for the manufacture of soda lime glasses are sand (SiO_2), soda ash (Na_2CO_3) and limestone (CaO). Borosilicate glass also contains Boron in order to provide heat resistance, and "leaded" glasses, as its name implies uses lead as an extra raw material (Almirall, 1999). Glass manufacturers in North America use over 20 million tons of raw materials per year. The main component of glass is the silica obtained from sand. Although sand is abundant on earth, only reduced numbers of sources have

the proper quality to be employed in the manufacturing of glass. Table 1.1 summarizes some of the common impurities in sand that could provide undesired properties in the final product of glass (Koons, 2002).

Table 1.1. Common contaminants in quartz sand

Contaminant	Chemical Formula	Effect on glassmaking
feldspars	$[(K, Na)AlSi_3O_8\text{-}CaAl_2SiO_8)$	color glass and alter furnace temperatures
iron	Fe	color glass and alter furnace temperatures
Ilmenite	$(FeTiO_3)$	nonglassy impurities
Corundum	Al_2O_3	nonglassy impurities
Chromite	$FeCr_2O_4$	nonglassy impurities
Spinel	$MgAl_2O_4$	nonglassy impurities

The components of glass can be classified according to their function as: formers, fluxes, modifiers, stabilizers, colourants, decolourants, acceleranting, refining and opalisers agents. Former agents are products that generally form the framework of the glass structure and when cooled quickly after melting will solidify without crystallizing. Fluxes are components that are added to the formers to lower the melting temperature and therefore are used to reduce cost of production. Stabilizers are added to offer chemical resistance to the glass and decoulorants are used to clarify the glass. Refining agents are also an important component of glass that is used help to remove bubbles from the

molten glass during its production. Table 1.2 shows some of the main components of glass and their principal function (Almirall, 1999; Koons, 2002).

Table 1.2. Classification of components of glass according to their principal manufacturing function

Function	Common components
Formers (primary)	SiO_2, B_2O_3
Intermediate formers	Al_2O_3, ZrO_2, V_2O5, Sb_2O_5, PbO, ZnO, TiO_2
Modifiers	Na_2O, CaO, MgO, Li_2O, BaO, SrO
Colourants	Fe_2O_3, Cr^+, Se^+
Decolourants	As_2O_3, MnO_2, CoO, CeO_2
Refining Agents	As_2O_3, $CaSO_4$

The use of recycled glass or cullet is also commonly employed in the manufacture of glass to decrease the melt temperature and to reutilize the broken glass, reducing the cost of the manufacturing process. Most of the cullet used in sheet glass is recycled within the plant while some container plants use recycled consumer glass, which adds some heterogeneity between batches originated from the same plant. That is favorable from a forensic point of view because the elemental profiling will differ widely amongst different sources.

Although technological advances in the manufacture of glass has led to standardized products, minor variations in the physical properties and chemical

composition of the glass remain between and within batches due to the natural trace contaminations of raw materials. In addition, for float glass, as the furnace inner surfaces get older, the tendency of some elements to leach into the molten glass is greater. Some trace contaminants that could leach from the furnace are aluminum and zirconium. (Koons, 2002). These minor contaminants are the ones that allow the forensic chemists to discriminate between glass fragments that came from different sources and to associate glass fragments that originate from the same source.

1.2.3. Manufacture of glass

The manufacturing of glass usually follows five steps: a) manipulation of raw materials (storage, weighing and mixing), b) melting (refining and homogenizing), c) forming, d) annealing and e) warehouse or secondary processing. The melting process takes place at furnaces that are resistant to high temperatures (>1500°C), where a continuous flow of the melted glass is fed into automatic forming machines (Copley, 1999). During the refining process, the elimination of bubbles from the molten glass takes place and thermal and mechanical stirring ensures homogenizing of the glass, which is very important to offer uniform refractive index in the product. The forming procedure is then followed by gradual changes in viscosity that allows molten glass to be converted in different products; the process will depend on the final product of interest (container, blowing, flat glass, glass fiber). After the forming step, the annealing stage takes place and the glass is cooled at the proper rate to solidify without crystallization.

Within the flat glass manufacture there are two main glass-forming processes: the float process and the rolled process. Float glass is the main method employed for

glassmaking where the homogenized molten glass is placed into a float chamber that contains a bath of molten tin in a chemical controlled atmosphere free of oxygen. At the entrance of the chamber the tin is approximately at 1000 °C and at the exit the temperature is cooled at 600 °C. There are rollers at the exit that pull the glass. The speed of the rollers will determine the thickness of the glass. On the other hand, the rolled process is mainly employed for manufacture of patterned glass and is based on pouring the molten glass between water-cooled rollers to give the preferred texture (Copley, 1999).

Some glass products require a secondary processing such as tempering, coating and coloring or decolorizing. Tempered glass is ordinary glass that has followed a tempering process to provide additional strength and more safety breakage pattern and is widely employed in the manufacturing of automobile windows. During the tempering process the surfaces of the glass cool more rapidly than the center, and that forces the edges into a state of compression. This process can be used for flat glass or some curved screens, however it cannot be applied for containers.(Copley, 1999).

The coating method is used for decoration, protection or strengthening of the glass. This is a usual method in the manufacture of containers to improve the handling of the material. The coatings are applied by spray or as vapor two times, first between the forming step and the annealing step (hot end) and then just after the annealing (cold end). Hot end coatings are mainly made of titanium or tin and the cold ends are organic waxes or fatty acids. Some flat glass products are also coated.

As mentioned before, some impurities from the raw materials can produce a color in the glass. For some products, a clear appearance is desirable and therefore additional

14

amounts of elements such as selenium and cobalt are added to counterbalance the green or yellow color caused by iron. On the other hand, some products are colored intentionally for decorative or technical reasons. Common colorants are iron (green, brown or blue), manganese (purple), cobalt (blue, green, pink), titanium (purple, brown), cerium (yellow) and gold (red) (Copley, 1999).

1.2.4 Transfer and persistence of glass

The understanding of phenomena of transfer and persistence of glass fragments is important for the interpretation and significance of the evidence. For instance, some glass fragments, such as broken containers, are more commonly found in streets than fragments originated from architectural windows; and glass is more commonly found on footwear than on clothing of the general population. For this reason, it is important to evaluate the findings in a specific framework to assess the correct value to the evidence.

Numerous studies have been conducted in order to investigate these aspects. These studies have been widely used in Europe to enable estimations of the likelihood ratio (LR) of obtaining glass fragments on a suspect that matches a control of glass (Daéid, 1999). The likelihood ratio is estimated using the Baye's theorem given by the probability of the evidence "if prosecution proposition is true" divided by the probability of the evidence "if defense proposition is true". (Cook, 1998) In the United States, classical statistical methods are more commonly employed in courtrooms rather than the Bayesian method; nonetheless, the implications of transfer and persistence of glass fragments are also taken into account to judge the value of the findings.

When glass is broken, fragments are expelled not only with the direction of the breaking force but also backward. According to experimental data, the number and size of fragments transferred to the recipient is related to several factors such as type of cloths and garments, distance from the breaking window (Allen, Scranege 1998), wet versus dry clothing (Allen, Hoefler, 1998), type and thickness of glass, the breaking force and the number of blows and the object that broke the window. (Allen, Locke, 1998). Some of those studies found that glass fragments are more likely to transfer to wet clothing than to dry cloths and garments such as jumpers and socks retain more fragments than trousers.

Other authors have estimated the frequency of occurrence of glass based on surveys of some populations. In general, most of the studies showed that few glass fragments, if any, were found in clothing and footwear of randomly selected population not involved in breaking of glass (Petterd, 1999; Roux, 2001; Lau, 1997; Lambert, 1995). It was also reported that prevalence of glass is higher in the sole of shoes than in the upper area (Roux, 2001). Therefore for real casework, it is also important to document the areas where the glass was collected as well as its appearance (fresh vs scratched and dirty pieces).

It has also been determined that glass fragments usually range from 0.25 to 1mm in size and that large fragments (>5mm) are most likely to be lost easily. Although glass tends to fall out from clothing, hair and shoes over time, it was demonstrated that glass fragments could persist on the recipient at least 8 hours after the breaking event (Allen, Hoefler, 1998; Hicks, 1996).

Finally, it has also been confirmed that secondary transfer of glass fragments between objects and people may occur (Allen, Cox, 1998). All these findings about

16

transfer and persistence could support the scientific conclusions to strengthen either the prosecution or the defense proposition.

1.2.5. Glass Analysis: from physical to elemental analysis

Automobile hit and runs, burglaries, assaults, drive-by shootings and bombings may produce glass fragments that could be used as evidence of association in glass transfer cases. Broken glass can be transferred from the source of the glass to a suspect or to a crime scene. This information can be used to associate an individual to an event or to another person (Almirall, 1999).

Glass examiners often measure the physical and optical properties of glass such as color, thickness, density, refractive index (RI) and also, if necessary, they conduct elemental analysis to enhance the value of an association. Figure 1.1 shows the typical scheme for the forensic analysis of glass fragments.

1.2.5.1. Physical Examinations

The first step in any glass analysis is to identify the glass by physical and optical properties such as hardness, amorphous structure and isotropism. Physical observations such as color, thickness and fluorescence are made in the preliminary stages of the analysis. For comparison purposes, the fragments are inspected visually in order to determine whether or not there is a "fracture match" between any of the recovered fragments to any of the source fragments. Such a match requires the edges of one fragment to perfectly fit into an edge of another, much like a jig-saw puzzle, and is rarely found in real cases (Almirall, 2001).
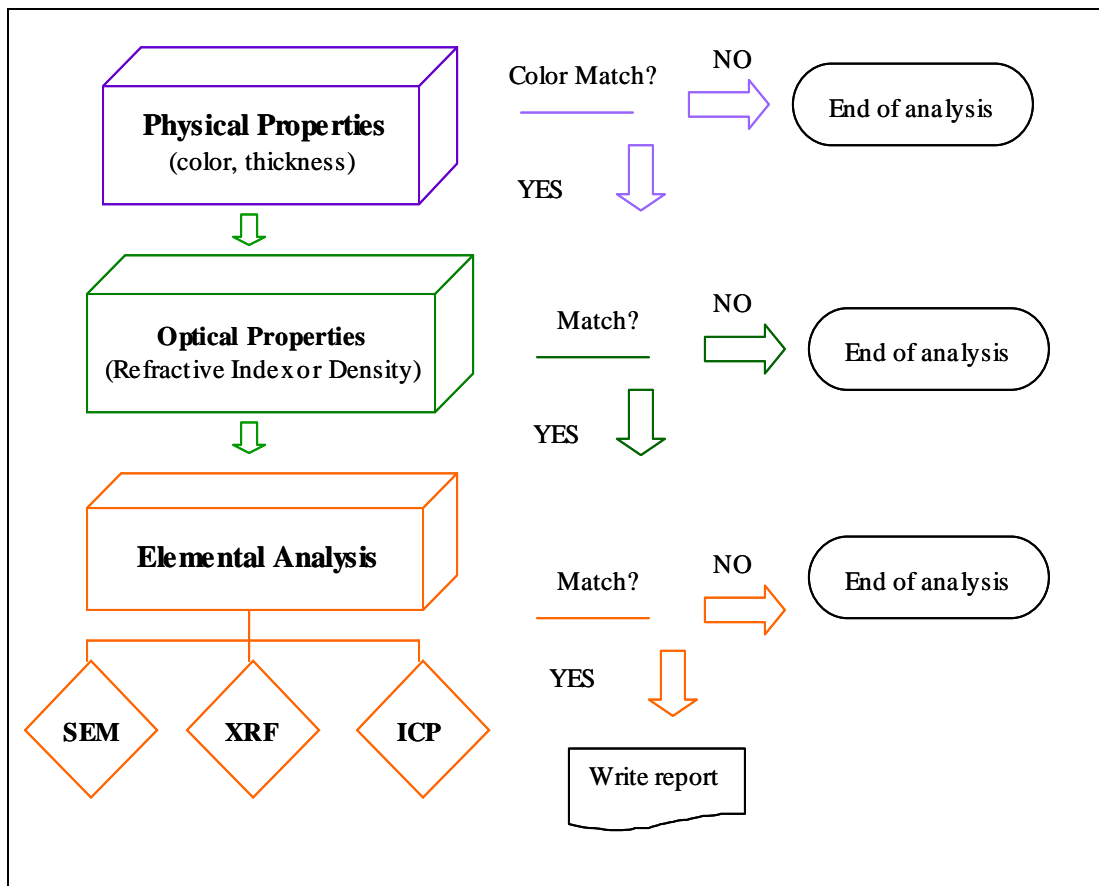
Figure 1.1. Basic scheme of forensic examination of glass

1.2.5.2. Density

Density of glass can be determined using the sink-float method. Nevertheless, the determination of density has the disadvantages of involving toxic liquids and requiring at least 5 mg of sample. Another limitation of density measurements is that measurements of small, irregular or dirty fragments of glass may be inaccurate (Koons, 2002). Nowadays, density measurements have been mostly replaced by refractive index measurements that provide similar information with the advantage of being faster, more accurate and more precise.

1.2.5.3. Refractive Index

Refractive index (RI) has been the most commonly used method in forensic laboratories for examination of glass. The first method employed for measuring RI was the immersion method that was based on the technique described in 1926 by Winchell and Emmons. In this method, a fragment of glass is immersed in a suitable oil and heated until the glass observed under a microscope disappeared. At this temperature, the refractive index of the glass is the same than the refractive index of the oil. The refractive index of the oil at that temperature is measured providing an indirect measurement of the refractive index of the glass (Hamer, 1999). The method is still in use in some laboratories but it has been almost replaced since the 80's by an automated method referred usually as GRIM, due to the model name given by the company that produces the instrument which stands for "Glass Refractive Index Measurement". Over the years, the original model GRIM1 has been replaced by newer models such as GRIM2 and the newly available GRIM3, which have some technical improvements but still the fundamentals behind the technique remain the same. ASTM has recently published a method for this automated determination of RI for the forensic comparison of glass fragments. (ASTM, 2001). Advantages of this method are that it is faster, is less tedious for the operator and provides more precise and accurate data.

1.2.5.4. Elemental analysis

Improvements in the quality control during the manufacture of glass have reduced the range of variation for refractive index values of glass as a population (Buscaglia, 2001) thereby reducing the "informing power" of refractive index as a discrimination tool

19

for glass fragments. As a consequence, it has become necessary to use additional
techniques, such as elemental composition analysis, to enhance the informing power of
the comparison between fragments (Almirall, 2001; Duckworth 2002).

Extensive research has been carried out on the use of elemental analysis of glass
by radiochemical, spectroscopic and mass spectrometric techniques (Stoecklein, 2001).
These include atomic absorption (Hughes, 1976; Catterick, 1978), x-ray fluorescence
(Buscaglia, 1994; Koons, 1991) neutron activation (Coleman, 1973; Coleman, 1968),
scanning electron microscopy (Kuisma-Kursula, 2000), inductively coupled plasma
atomic emission spectrometry (ICP-AES) (Koons, 1991) and ICP-MS (Zurhaar, 1990;
Parouchais, 1996; Duckworth, 2000). Each technique has its own advantages and
shortcomings but ICP-MS has been shown to be the most effective analytical method for
the comparison of trace elements in small glass fragments (Duckworth, 2002). Some of
the advantages of ICP-MS over the other analytical techniques include its multi-element
capability, excellent sensitivity, high sample throughput and the capability to provide
isotopic information. (Montero, 2003)

The isotope dilution (ID) method, when coupled to an ICP-MS analysis, usually
provides the best accuracy and precision when the sample size is limited (Smith, 2000).
The isotope dilution analysis method offers a technique that does not depend on the
comparison to external calibration standards. The method is analogous to the standard
addition technique in that the sample is spiked with a known quantity of analyte material,
and resembles the internal standardization procedure, with the exception that the analyte
itself is the internal standard. To use this method, two or more isotopes of the analyte
must be available for the measurement since one of the isotopes is in the added spike.

This approach can compensate for biases caused by instrumental drift as well as for sample loss during the preparation (Smith, 2000).

Although conventional solution ICP-MS (external calibration, EC and isotope dilution, ID) have been proven to be excellent tools for elemental analysis of glass, they have the disadvantage of requiring the dissolution of the sample, thereby destroying the sample prior to introduction into the ICP-MS. Newer sample introduction techniques, such as LA, provide additional advantages over solution analysis such as a reduction in time of sample preparation and a reduction of the amount of sample used for the analysis (Russo, 1998; Watling, 1997; Watling, 1999).

LA enables the introduction of the products from the direct sampling of solids into the plasma, with the advantages described above and also minimizing the risks of contamination and the use of hazardous reagents. Laser ablation has other added advantages and also limitations that are going to be covered in detailed in this work and is becoming the technique of choice for solid sampling of forensic casework samples of glass when elemental analysis by ICP-MS is required.

1.3. FORENSIC EXAMINATION AND COMPARISON OF PAINTS

1.3.1 Chemical composition of paint

Paints are used to protect and decorate diverse types of substrates such as metals, concrete, plastics, glass, wood and paper.

Higher demand for quality together with increasing competition between the paint manufacturers has led to a continuous development of new paint components that offer process simplification, savings and improved designs. For forensic purposes, this

represents an advantage because this allows the identification of paints from different
plants from different makers, different years or different models. The scope of this
research is delimited to automobile paints and therefore only this type of paint will be
discussed in detail.

1.3.1.1. Automotive paint

Paint consists mainly of three components: the vehicle, the pigments and
extenders, and the solvent. Pigments provide color and coating, vehicles provide final
film properties, adhesion and resistance; and solvents are added to aid manufacture and
application of the paint. The vehicle polymer resins include acrylic, alkyd, epoxy,
urethane, amino, vinyl, phenolic and cellulose. (Brun-Conti, 2000).Automobile paints are
invariably multi-layer because it is impossible to provide adhesion, anticorrosion and
environmental resistance in a single layer. Table 3 shows the typical multi-layer system
of an automobile paint and its characteristic thickness. (Bentley, 1999).

The steel pretreatment or galvanized consist in the electro-deposition of zinc as an
anticorrosive layer and it is applied to metallic body parts of the vehicle with the
exception on the roof, were water does not tends to accumulate and therefore corrosion is
not expected (Thornton, 2002). After this treatment, the primer or "E-coat" is applied
mainly by electrodeposition in big tanks, which permits the precise control of the
thickness of the layer. Once the primer layer is deposited in the metal body the metal
parts are rinsed with water and baked. Currently, the epoxy resin-cross linked with a
blocked isocyanate has almost replaced the use of acrylic resins for primers.
Nevertheless, primers were applied for old automobiles with the spray method instead of

electrodeposition and therefore alkyds and styrene resins may be detected. The resins of

the primers are usually mixed with titanium dioxide, talc and anticorrosive pigments.

Primer surfacers are applied over the primer to improve adhesion of the color coat. They

may be epoxy, polyester or acrylic powders. The topcoat is then placed above the primer

surfacer and the variety of resin used for topcoats is very extensive and have changed

dramatically over time. The topcoat can be solid monolayer color, solid multilayer color

followed by clear coat or metallic color with clear coat (Thornton, 2002).

It is important to notice that the above scheme of layers is referred to original

equipment manufacture (OEM) and that millions of vehicles on the road may have been

repaired or repainted and the chemical composition and sequence of layers may be very

unique, which is useful for forensic purposes.

Table 3. Typical laser sequence (from bottom to top) for automobile paints. (Bentley,
1999)

Type of automobile finishing			
Solid Color		**Metallic appearance**	
Substrate steel	_	Substrate steel	_
Pretreatment	2 µm	Pretreatment	2 µm
Electrocoat primer	20 µm	Electrocoat primer	20 µm
Primer surfacer	35 µm	Primer surfacer	35 µm
Topcoat	40 µm	Metallic basecoat	15 µm
		Clear coat	40 µm

1.3.2. Comparison of Analytical Methods for Paint Examinations: Strengths and Limitations

Forensic laboratories perform routine analysis of paint by different analytical techniques. Figure 1.2 presents the basic scheme of analysis for paints.
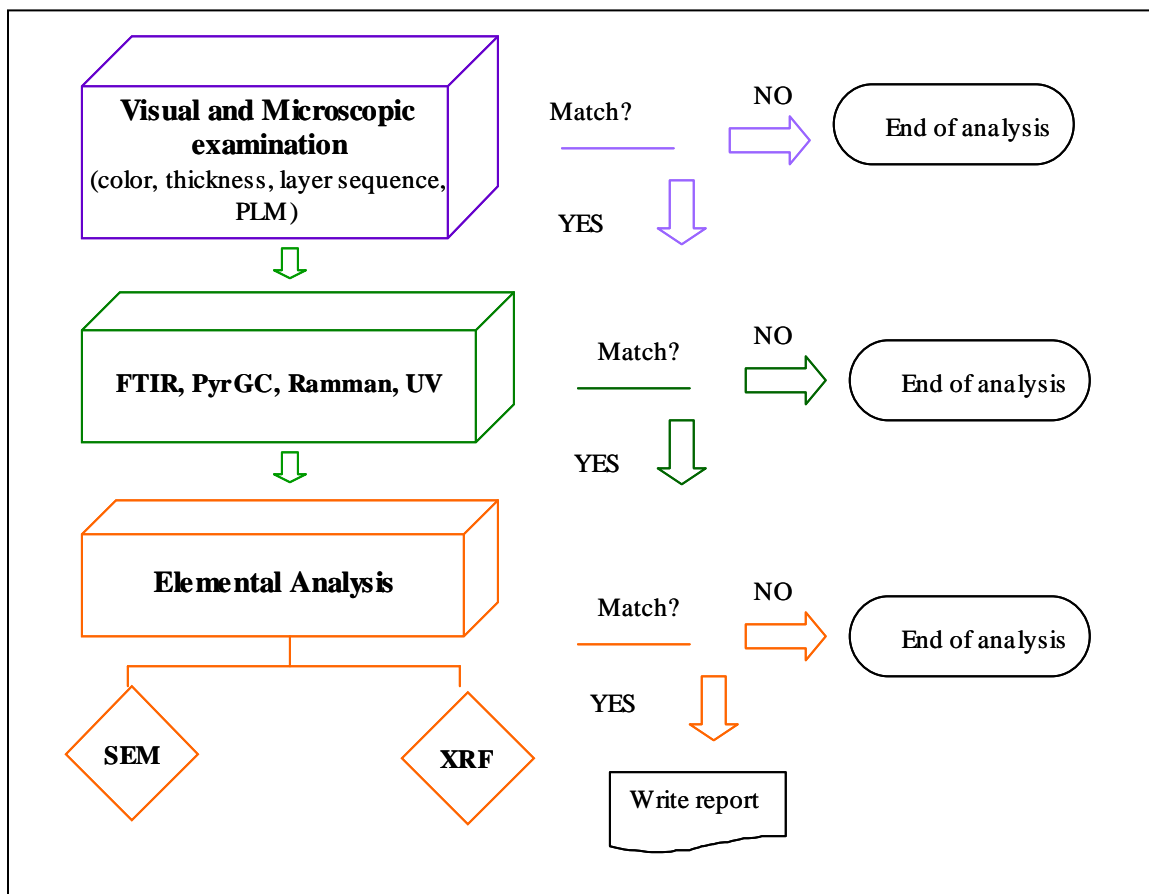
Figure 1.2. Typical scheme of forensic examination of paints.

1.3.2.1. Visual and microscopic examination

The first step for forensic analysis of paint is the visual and microscopic examination for color, shape, appearance, surface details and sequence of layers. Some layers in a paint chip are easily identified under the microscope, nonetheless, definitive paint layer identification require that the individual layers are carefully separated with a scalpel or a microtome to make precise cuts of the layers. Examination of cross sections under Polarized Light Microscope (PLM) may also provide additional information for comparisons (Thornton, 2002).

1.3.2.2. Infrared and GC- Pyrolisis

Infrared spectroscopy (IR) is very useful to provide identification of binders, additives and pigments. IR coupled with microscope accessories has the benefit of allowing the analysis of very small samples with minimum sample preparation. The major limitation of IR is that some polymers can be masked by strong bands of inorganic pigments making difficult the identification and comparison of some organic components. Pyrolysis gas chromatography (PyGC) with FID or MS detectors provides complementary information of polymer composition with the advantage of do not been affected by inorganic interferences (Challinor, 2001). The main limitation of PyGC is that it is destructive of the sample (5-10 µg), which is usually restricted for forensic examinations (USDOJ-FBI-SWGMAT, 2000). Ramman spectroscopy and UV-Visible spectroscopy can be utilized for the comparison of paints as well.

1.3.2.3. Elemental analysis

The inorganic components of paint and glass samples can be also analyzed by SEM-energy dispersive X-ray spectrometry (EDX) and X -ray fluorescence (XRF), but they have the disadvantage of not been very sensitive, in fact, these techniques can only detect elements present at concentrations over 0.1% and 0.01%, respectively (Henson, 2001). Furthermore, the sample requires additional manipulation in order to conduct the analysis by these methods and data is qualitative and not quantitative. Other limitations of SEM include the difficulty to remove coating and embedding materials from the sample after analysis. (USDOJ-FBI-SWGMAT, 2000).

Although XRF is more sensitive than SEM, it has the limitation of penetrating deep into several layers at once complicating the analysis of individual layers. (USDOJ-FBI-SWGMAT, 1999).

1.3.3. New developments in forensic analysis of paints

A recent study in our research group explored the application of LA-ICP-MS to complement commonly used techniques in a crime laboratory for paint examinations. The results showed that LA-ICP-MS is a viable tool for forensic analysis of these materials. Optimization and validation studies were conducted for analysis of automotive and architectural paints, and were taken as a starting point for the present research (Hobbs, 2003). The main advantage of LA-ICP-MS over the conventional techniques employed for elemental analysis is its lower detection limits that permit the analysis of trace elements in addition to the major and minor ones. Consequently, the discrimination power of the technique is superior to SEM or XRF. (Hobbs, Almirall, 2003).

26

Hobbs demonstrated that qualitative differences between samples originating from different sources could be visualized. Nevertheless, for semi-quantitative or quantitative analysis of paints, the major limitations of this technique are the lack of availability of matrix matched standards and the complexity of quantifying multi-layer systems of only a few microns in thickness. Additionally, other authors (Watling, 1999; Mason, 2001) have also recognized the potential of LA for the analysis of paint samples.

In order to bring this technique into courts, a match criterion has to be established as well as further investigation of the natural heterogeneity of automobile paints and the discrimination capabilities of the technique.

1.4. ELEMENTAL ANALYSIS OF TRACE EVIDENCE AND ITS SIGNIFICANCE IN COURT

1.4.1. Statistical Tools for the evaluation of evidence comparisons

Several methods for data analysis are used in many areas of forensic science to assist the interpretation of evidence. This section will be limited only to those statistical tools that were employed in this research.

Some examinations in the identification and comparison of glass and paints may generate discrete or qualitative data such as color, appearance, polymer type, number and sequence of layers. By contrast, examinations such as elemental analysis and refractive index generate quantitative data that may permit the application of statistical tools for a better characterization of evidence, measure associations between variables, calculate

27

confidence intervals, estimate systematic or random errors, assign discrimination values and present the data in a more understandable manner. (Almirall, 1999)

There are many statistical software packages such as SYSTAT, Excel and Minitab, to mention some, which greatly simplify the statistical analysis of data.

1.4.1.1. Descriptive Statistics

For data reduction, it is very useful to describe the sample sets by the arithmetic mean, the standard deviation and relative standard deviation. The arithmetic mean for a set of data can be estimated using the equation (Miller, 2000):

$$\overline{x} = \frac{\sum_{i=1}^{n} xi}{n} \qquad (1)$$

The standard deviation for the entire set or population is calculated as:

$$s = \sqrt{\frac{1}{n} \sum (xi - \overline{x})^2} \qquad (2)$$

For practical reasons a small representative sample is used instead of the entire population and the standard deviation is approximated using the following equation:

$$s = \sqrt{\frac{1}{n-1} \sum (xi - \overline{x})^2} \qquad (3)$$

The variance is another important value that measures the dispersion of the data about the mean; it is defined as the squared of the standard deviation:

$$s^2 = \frac{1}{n} \sum (x_i - \overline{x})^2 \qquad (4)$$

The relative standard deviation and the percentage of relative standard deviation is a value commonly employed to estimate the precision of a set of measurements and is calculated using the standard deviation and mean values. The only difference between RSD and %RSD is that 100 multiply the latter:

$$\% \ \text{RSD} = \frac{s}{\overline{x}} \times 100 \quad (5)$$

1.4.2. Match criterion for comparisons

The expert testimony and opinion of an association or discriminations between suspect and control samples may be supported by statistical match criterion. Individual comparisons of a pair of glass or paint samples can be performed using different approaches. A simple match criteria criterion would determine if the overall range of the control and recovered samples overlap. If so, the samples cannot be distinguished. Another method consist in calculating mean and standard deviations of both control and recovered samples, if the mean value of the recovered sample is within the mean value of the control plus or minus 2 or 3 standard deviations they are considered to match or originate from a common source.

A further statistical criterion consists in using Student t- statistic not assuming equal variances according to the equation (Miller, 2000):

$$t = \frac{(\overline{x}_1 - \overline{x}_2)}{\sqrt{\dfrac{s_1^{\,2}}{n_1} + \dfrac{s_2^{\,2}}{n_2}}} \quad (6)$$

29

With the degrees of freedom estimated as:

$$df = n_1 + n_2 - 2 \qquad (7)$$

Whenever the calculated t value is larger than the critical value, the null hypothesis states that the equivalence of the means is rejected and it can be stated that the control and recovered fragments does not originated from a common source. One advantage of the t test comparison is that the statement of match or not match can be supported with a significance or probability value.

When more than two samples (or two means) need to be compared, a pair-wise comparison (multiple pairs) should be carried out. A method used for multiple comparisons is the analysis of variance (ANOVA) (Miller, 2000).

The results of an ANOVA, however, only indicate whether these multiple means differ significantly without identifying which of the means are significantly different. The Tukey's post hoc test is useful to determine which pairs of means differed significantly. This test is very useful for estimating the discrimination power of a technique, where sets of large number of pair comparisons are required. The Tukey's test defines confidence values based on the mean square error (MSE) within "k" groups of "n" replicates. A further explanation of this statistical tool can be encountered in the literature (Almirall 1998; Kleinbaum 1978).

1.4.3. Discrimination potential of elemental analysis

As mentioned before, sophisticated manufacture processes and stringent quality control in glassmaking has led to less variability of refractive index of glasses produced within a single plant or even between different plants. As a result, the evidential value of

RI measurements has been limited and glass examiners have found it necessary to complement physical and optical measurements with elemental analysis.

An effective way of estimating the discrimination potential of elemental analysis is using ANOVA together with Tukey's tests. Duckworth et al (Duckworth 2000, Duckworth 2002) have investigated the overall discriminating power of ICP-MS and the individual discriminating potential of elements with the purpose of using them for development of glass databases.

An interesting survey of the variation of RI and elemental composition in a single plant for a period of 4.5 years as well as variation between 36 different manufacturing plants within the United States showed that the variation of RI is very limited while elemental analysis can distinguish small differences in glass composition even from glass originating from the same plant over short periods of time. (Montero, 2002)

Another recent study has shown that for a set of 45 headlamps and 46 vehicle windows originating from different sources, refractive index was able to discriminate only 90% and 52% of the headlamps and auto-windows respectively, while the combination of RI with elemental analysis enhanced those values to 100% and 99.9%. (Trejos, 2003)

There are many other papers that support the fact that the elemental profile of glass offers a very discriminating tool for comparison of glass fragments. (Buscaglia, 1994; Koons, 1991; Koons, 2002; Montero, 2003; Parouchais, 1996).

The elemental analysis of paints for forensic examinations is still novel and therefore there is less documentation of its overall discriminating power, nevertheless,

recent reports have shown that this application could be also promising (Hobbs, 2003;

Mason 2001)

1.5. LASER ABLATION INDUCTIVELY COUPLED MASS SPECTROMETRY

1.5.1. Laser Ablation Systems

1.5.1.1 History of Lasers

The world "laser" was is an acronym for Light Amplification by the Stimulated

Emission of Radiation. Stimulated emission occurs when an atom or molecule holds onto

excess energy until it is "stimulated" to emit it as light. (Silvfast, 1996)

Albert Einstein was the first to suggest the existence of stimulated emission in

1917. However it was not until after World War II that physicists began trying to make

stimulated emission dominate. In 1954 C.H Townes and co-workers developed a

microwave amplifier based on stimulated emission of radiation. It was called a maser.

Shortly thereafter, they adapted the principle of masers to light in the visible region and

in 1960, T.H. Mainman built the first laser device that incorporated a ruby crystal for the

laser amplifying medium which emitted deep red light at a wavelength of 694.3 nm. A.

Javan developed the fist gas laser, the helium –neon laser, which emitted light in both the

infrared and the visible spectra regions. Other laser devices followed in rapid succession,

each with a different laser medium and a different wavelength emission (Taylor, 2000).

Since that moment, lasers have been used for many areas, for example reading and

writing information, measurement and inspection, medicine, geology, environmental

science and others.

1.5.1.2 Laser Principles

A laser should be characterized by many important properties, such as wavelength, output power, beam size and divergence. Each type of laser emits a characteristic wavelength or range of wavelengths. The wavelength depends on the type of material that emits the laser light, the lasers optical system and the way the laser is energized. Table 1.4 summarizes some important laser types and their respective wavelengths. (Hecht, 1992).

Table 1.4. Important laser types and their wavelengths

Type	Wavelenght /nm
Argon-Fluoride excimer	193
Xenon chloride excimer	308
Nitrogen gas	337
Argon ion	450-530
Helium neon	543, 632.8, 1150
Semiconductor (GaInP)	670-680
Ruby	694
Neodymium YAG	1064
Carbon dioxide	900-11000

Output power measures the strength of a laser beam, which differs widely among lasers. Some lasers produce beams containing less than a thousandth of watt (mW), others produce thousands of watss (KW). Lasers could emit a continuous beam of light or pulses of light. Pulses come in various duration and repetition rates.

Laser beams are not completely straight, once they go far enough from the laser they actually spread out slightly with distance. The spreading angle is called the beam divergence. The diameter of this beam will determine the size of the spot in a material.

A laser has to have a population inversion in order to produce the stimulated emission. If the population distribution is at equilibrium, with more atoms or molecules in the lower level of transition than in the upper level, absorption will soak up any stimulated emission because there are more absorbers than emitters. However, if there are more atoms in the upper level, there are more emitters than absorbers. Thus, a photon with the transition energy is likely to encounter an excited state and stimulate emission before it is absorbed.

In order to produce population inversion, energy should be put into the laser medium to selectively excite atoms or molecules to certain higher levels. The most commons laser excitation techniques are light and electricity. However, these excitation techniques won't work unless atoms have the right type of energy-level structures. Normally excited states have short lifetimes and will release their excess energy by spontaneous emission very rapidly, so this state doesn't last long enough to be stimulated to emit their energy, most of it emerges as spontaneous emission. Fortunately, there are species that have longer-lived excited states that are called "metastable" and make possible the stimulated emission for lasers (Hecht, 1992).

In addition, to extract energy efficiently from a medium with a population inversion and make a laser beam, it will be necessary to have a resonant cavity that helps build up (or amplify) stimulated emission by feedback-reflecting some of it back into the laser medium.

Stimulated emission can amplify light. One photon with energy corresponding to a laser transition can stimulate the emission of a cascade of other photons at the same wavelength. The amount of amplification increases sharply with the distance light travels through the laser material.

Generally, the shape of a laser beam comes from the reflection of stimulated emission back and forth between a pair of mirrors at opposite ends of the laser cavity. The amount of stimulated emission grows on each pass through the laser medium until it reaches an equilibrium level and then will be a constant outside laser beam (Hecht, 1992).

There are different types of lasers. The three main families of lasers are a) gas lasers, b) semiconductor lasers and c) solid state lasers

The laser ablation works mainly with the last type of lasers, so we will cover some details about them bellow.

1.5.1.3 Solid State Lasers

In solid- state lasers, light is emitted by atoms immersed in a crystal or glassy material. The crystal is shaped into a rod, with mirrors placed at each end. Light from an external source enters the laser rod and excites the light-emitting atoms. The cavity mirrors from a resonant cavity provide the feedback needed to generate a laser beam that emerges through the output mirror (Silfvast, 1996)

The atoms that emit light are embedded in a glass or crystalline matrix. The laser characteristics will depend both on the light-emitting species and on the host. The light emitting species must have a set of suitable energy levels that let it absorb pump light to populate a metastable upper laser level. The best light emitters for solid state lasers are:

chromium, neodymium, erbium, holmium, cerium, cobalt and titanium. Chromium is the specie used in ruby lasers. Usually the laser ablation of glass relies on the emission from neodymium (Hecht, 1992).

Potential host media must meet several requirements. The most important is that the host should be reasonably transparent to the pump light, and absorb very little light at the laser wavelength. The thermal properties are also important, they should conduct away waste heat left over from laser action because excess heat can damage the laser material itself, causing it to warp, crack or soften and besides, temperature could changes influence population distributions and gain characteristics of the emitting atoms. (Hecht, 1992).

The light-emitting species interact with the host crystal in subtle ways that influence its energy level structure. Crystalline bonds and effects on adjacent atoms slightly shift energy levels in the light emitting species. This can change the laser wavelength, usually by a small amount. For example, Nd emits at 1054nm when it is doped into phosphate based glass and at 1064nm when in a crystalline host known as YAG (Ytrium Aluminum Garnet).

A final factor in considering solid- state laser materials is the ease of producing rods of the required size with adequate optical properties, such uniform refractive index that allows light oscillates smoothly back and forth in the laser cavity.

1.5.1.3.1. Neodymium-YAG lasers

In neodymium-YAG, the neodymium is an impurity that takes the place of some yttrium atoms in the YAG crystal. YAG's chemical formula is $Y_3Al_5O_{12}$, its crystalline structure

is similar to that of garnet. The crystal has good thermal, optical and mechanical properties, but its hard to grow. The crystal is grown in blocks called boules from which rods are drilled (7). The laser could use accessories that change lasers wavelength and pulse duration. The near- infrared wavelength of Nd-YAG lasers is fine for some purposes, but visible or UV light is better for many others (as for LA-ICP). Using a harmonic generator the frequency could by changed and therefore these lasers could emit light at 532, 355 or 266nm for different applications (Hecht, 1992).

Another useful accessory employed in these lasers is the Q switching mode that allows the changing of pulse length and could emit short pulses with high peak power.

1.5.1.4. Principles of LA-ICP-MS

A typical LA-ICP-MS setup consists of a laser, an ablation cell and the ICP-MS, which is used as an ionization source and analyzer. A solid sample is placed inside the ablation cell and a laser beam is focused on the surface of the sample (See figure 3). When the laser is fired, the high-energy interaction between the laser and the sample surface produces a cloud of very small particles and micro-droplets. These particles are removed from the sampling cell by a carrier gas, usually argon or helium, and are swept into the ICP plasma for atomization, ionization and subsequent analysis (Russo, 1998).

The ablation cell is provided with a quartz window. The sampling cell is mounted in a translation stage, providing X-Y positioning control for laser targeting on the sample and is under computer control. The Z axis of the translation stage is used to focus the laser via a CCD camera viewing system.
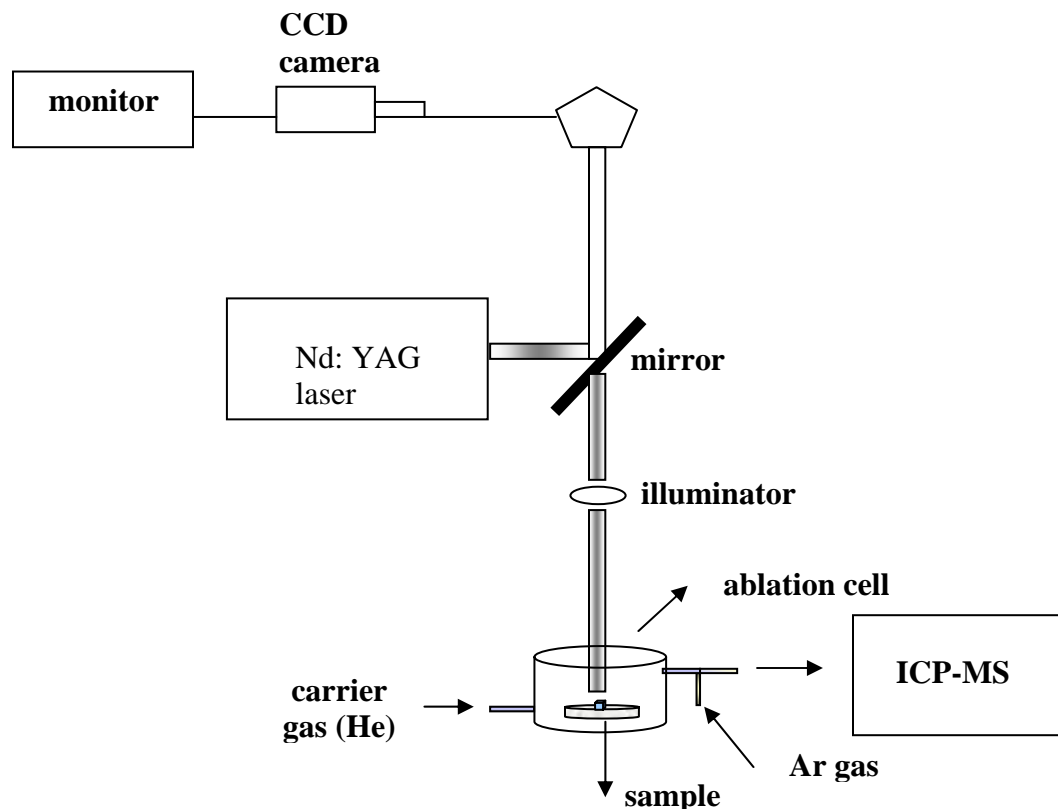
Figure 1.2. Diagram of a typical LA-ICP-MS set up.

Since air is unavoidably admitted into the sampling cell when changing samples, removing the air from the carrier gas flow path prior to switching back to the ICP is required to prevent plasma collapses. Most models of laser ablation provide a purge valve to solve this problem.

This approach enables the introduction of the products from the direct sampling of solids into the plasma, with the advantages described before and also minimizing the risks of contamination and the use of hazardous reagents. Laser ablation has the added advantages of providing excellent absolute detection limits due to the small amounts of sample required for a single determination. LA sampling removes a total of ~ 300

nanograms of glass for analysis instead of 2-5 milligrams needed for solution work, rendering the technique as essentially non-destructive.

The disadvantages to LA sample introduction include the fact that the optimization of laser parameters changes depending on the matrix, making the method development matrix dependent. The quantification is less straightforward than with solution analysis due to the lack of solid calibration standards, particularly matrix-matched standards. Matched standards are necessary for elemental analysis because the amount of mass ablated may vary according to the sample matrix. Another well-known disadvantage to LA is elemental fractionation, which is going to be discussed in detail later.

1.5.3 Optimization and quantification strategies

Several calibration strategies have been suggested for quantitative analysis of solid samples by LA (Mank, 1999; Mason, 2001; Raith, 1996; Shroeder, 1998; Stix, 1995; Tibi, 2001; Pearce, 1996). The quantification of glasses by LA-ICP-MS, could be performed by 3 different methods:

a) Internal Standardization

b) Calibration Curves

c) Single Standard Calibration

1.5.3.1 Internal standardization

External calibration alone has the disadvantage that large differences in ablation yields can result from laser output fluctuations due to small differences in the target

matrix therefore requiring a closely matched matrix. A combination of the use of an external reference standard with internal standardization corrects for differences in ablation yield between the sample and the reference material. Internal standards can also correct for matrix effects and instrumental drift. A major component of the material of known concentration should be used as the internal standard.

The internal standard is generally a major element whose concentration has been previously determined by electron-microprobe (EMP), x-Ray Fluorescence (XRF), or Solution ICP-MS. Ideally, a rule of thumb to follow in selecting an internal standard is to use the lowest-abundance isotope of the most abundant element in the material to be analyzed. Since glass has a high concentration of silicon ($\sim$70% as SiO_2), the lowest abundance isotope is usually selected in order to avoid saturation of the detector.

For silicates, one would thus use ^{30}Si, which has the lower relative abundance (3.09 %). However, nitrogen oxide produces a high background at mass 30, such that is preferable to use ^{29}Si, with an abundance of 4.7 %.

In practice, other major elements (e.g. Ca) may serve as well or better than Si, depending of the type of matrix, and chemical similarity between sample and standard. When analyzing an unknown material initially, it is good practice to use two or more internal standard to check consistency, precision and accuracy. For paint analysis, the elemental composition varies significantly between paints and between layers of a single paint, making the selection of an internal standard a difficult task.

1.5.3.2. Calibration curves and single standard calibrations

Quantitative LA-ICP-MS analysis can be accomplished using well characterized chemical reference standards whose major element composition is similar to those of the unknown material to be analyzed. The resulting calibration curves are ideally linear.

When analyzing standards it is recommendable to do 3 or 4 replicates in order to obtain homogeneous results. Background interference has to be substracted by running a blank of gas before analyzing each sample.

Raith et al (Raith, 1996) proposed the use of a 5 point calibration curve using solid standards and ^{139}La as an internal standard. Those standards have certified values that could be used to perform the quantitation and at the same time the certified value could be checked by an alternative technique like solution ICP-MS.

Calibration using a single standard can be advantageous because it saves time during analysis. However, a single point standard for the calibration of unknown samples may require prior establishment of a calibration curve, involving this standard and others. This curve must be linear and must pass through the origin. The standard and unknowns also should have similar composition in terms of major elements.

For glass analysis there are many solid standards available such as the NIST standards (National Institute of Standards and Technology, MD, USA), the P & H Glass Standard Series (Pulles and Hanique Ltd, UK) and recently, the European group NITECRIME has distributed to its members a new series of glass standards. On the other hand, paints represent once more a complicated sample for LA application due to the lack of matrix match standards available at the moment.

1.5.4. Elemental fractionation

Ideally, the ablation process should eject particles from the glass only by mechanical means. Nevertheless, the ablation process could be accompanied by undesirable processes such as melting and vaporization, which cause fractionation. Fractionation is defined as the process that produces a stoichiometry of laser products that is not representative of the sample composition (Beauchemin, 2000). Its effects on glass and other matrices have been investigated. Some authors have attributed fractionation to several factors including: laser wavelength (Figg, 1997; Montelica-Heino, 2001), depth of the craters (Borisov, 2000), mineralogical, crystallographic and chemical compositions of the matrix (Montelica-Heino, 2001), mode of ablation, laser densities and energy profiles (Borisov, 1998; Mao, 1998), transport system, carrier gas and the ionization in the plasma (Chen, 1999; Eggins, 1998; Figg, 1998; Guillong, 2002; Horn, 2003). The effect of this event is element-dependent and appears to be related to thermal properties of a particular element in different matrices and needs to be determined for individual matrices.

This phenomenon has long been recognized as a potential problem in laser ablation-ICP-MS that could impact the results of semi-quantitative and quantitative analyses and therefore it presents a concern to the forensic application of LA for comparisons of glass and paint evidence.

Fractionation index is a measure of the time-dependent variation of elemental ratios during an ablation and it is defined as (Chen, 1999; Guillong, 2002):

$$FI = \frac{\left[I_e / I_{int\,std}\right]_{t_2}}{\left[I_e / I_{int\,std}\right]_{t_1}} \qquad (8)$$

Where FI is the fractionation index, I_e is the intensity of the element of interest, $I_{int\ std}$ is the intensity of the internal standard, t_1 is the first half of the ablation signal and t_2 is the second half of the ablation signal.

Under optimal conditions, the index should be close to 1 because no changes in the signal over time are expected. Some authors have associated significant fractionation to index values of 1.5 to 2.0 while others have reported fractionation as index values as high as 3.5 (Russo, 2002).

1.6. LA-ICP-MS OF GLASS AND PAINTS: OBJECTIVES

While direct solid sampling of materials by laser ablation has increased in popularity as an analytical method, only a few studies have been published describing the application of LA-ICP-MS to the forensic analysis of glass and paint. The general objective of this work is to evaluate the technique of LA-ICP-MS and provide enough scientific support to facilitate the incorporation of this technique into the judicial system.

The specific objectives of this project are divided into three main sections:

1. LA-ICP-MS for glass analysis:

a) Develop and optimize a LA-ICP-MS method for the analysis of the each of the glasses of interest (float glass, headlamps and containers). Three different Nd:YAG lasers will be compared through this research (Cetac LSX 200, Cetac LSX 200 plus and New Wave 213). Parameters of interest will be: sample preparation, spot size, carrier gas, ablation mode, ablation time, internal standard, quantification strategies and elemental menu for characterization of samples.

b) Analyze sets of glasses typically found at crime scenes including automobile windows (windshields and side windows), containers and headlamps

c) Evaluate the advantages of LA-ICP-MS over ICP-MS solution methods for glass, including external calibration and isotope dilution methods. The subsets will be compared with solution work in terms of time of analysis, precision and accuracy.

d) Conduct a homogeneity study of glass samples in order to evaluate the discrimination power of the technique as well as sampling strategies.

e) Analysis of LA-ICP-MS of glass matrices without matrix match standards

f) Discrimination studies to evaluate the discrimination power of this technique

2) LA-ICP-MS for paint analysis:

a) Optimize a LA-ICP-MS method for the analysis of automotive paint samples and conduct a homogeneity study for these matrices. The study will be focused in the optimization for the ablation of each layer of an automobile paint.

b) Conduct a discrimination study of automotive paint samples that are not distinguishable by any other conventional method used for the examination of paints in forensic laboratories.

c) Evaluate and develop new quantification strategies and match criterion.

d) Develop an analytical technique for the elemental analysis of latex paints by LA-ICPMS and evaluate its discrimination power compared to other techniques commonly utilized in forensic examinations: SEM/EDS and micro FTIR.

3) Fundamentals of LA-ICP-MS:

a) Evaluate the effect of fractionation on the quantification of glass by LA-ICP-MS

Perform studies on the size and distribution of particles generated by the lasers in order to better understand and optimize the laser ablation process.

While direct solid sampling of materials by laser ablation has increased in popularity as an analytical method, only a few studies have been published describing the application of LA-ICP-MS to the forensic analysis of glass and paint. The general objective of this work is to evaluate the technique of LA-ICP-MS and provide enough scientific support to facilitate the incorporation of this technique into the judicial system.

SECTION II.   LA-ICP-MS for GLASS ANALYSIS

2.1 COMPARISON OF THREE DIFFERENT Nd:YAG LASER SYSTEMS: LSX 200 AND LSX 200+ AND NEW WAVE UP213

2.1.1 Instruments description

2.1.1.1 Cetac LSX-200 Plus and LSX 200

The CETAC LSX-200+ and LSX 200 (Cetac Technologies, Omaha, NE, USA) lasers are a 6 mJ Nd:YAG lasers with a 1064 nm primary wavelength, which frequency is quadrupled to 266 nm using optical components. The main differences between these laser systems are that the LSX 200+ has a flat beam profile instead of a Gaussian beam profile. This shape of the beam helps to keep a better focusing over time of the laser with the target surface and therefore the morphology of the crater is more symmetric.

The signal intensity can be optimized by adjusting power, laser focus, step rate, and laser frequency through the LSX-200 DigiLaz software. This instrument has the capability of ablating in different modes such as rastering, single line, depth profile, and single spot, which spot sizes range from 10 μm up to 200 μm. This laser ablation system generates particle aerosols from a solid material by pulsing a laser beam onto a target surface. Ablated material is then swept into the ICP-MS by a helium flow.

2.1.1.2 New Wave UP213

A Nd:YAG laser New Wave UP213 (New Wave Research, Fremont, CA, USA) laser unit was coupled to the ICP-MS system for the analysis of glass. The UV-light source from the laser is focus onto the sample surface in an ablation chamber that is purged with helium. The high power, short-wavelength 213 nm laser couples directly with the sample matrix, with high absorption efficiency, reducing or eliminating plasma induced fractionation. The resultant laser-induced aerosol of particles is then transported to the inductively coupled plasma in a helium carrier gas stream, where it is decomposed, atomized and ionized before extraction into the mass spectrometer vacuum system for analysis.

Instrumental conditions for the experiments include single spot ablations of 55 µm, scan rate of 10 Hz operated at 100% laser energy for 60 seconds dwell time using helium as carrier gas through cell and argon as make-up gas after the cell.

2.1.1.2 ICP-MS System

A Perkin Elmer, model ELAN DRC II (Perkin Elmer-SCIEX, Boston, MA, USA) was coupled to the different laser systems mentioned above for laser ablation analyses of glass. A typical ICP-MS system includes a sample introduction port that is connected to the ICP torch, where the plasma is formed as consequence of an electrical discharge that is sustained by a radio frequency (RF) field in a flowing stream of argon. The extremely high temperatures in the plasma, ranging from 7000-10,000 K, are responsible for the

atomization, ionization, and excitation of the sample particles. A cloud of these ionized particles is extracted with low vacuum in the skimmer cone and the sampling cone. The ions are then focused in the lenses, where the pressure is even lower, before they can be analyzed in the quadrupole zone.

The mass spectrometer detects each element based on their mass/charge ratio, and gives signal intensities according to their relative concentrations. The two vacuum pumps assure the rapid pass of the ions to the next part of the instrument by creating changes in pressure.

2.1.2. Methodology

2.1.2.1 LA-ICP-MS Optimization

2.1.2.1.1 Optimization of LSX 200+ and New Wave UP 213 lasers

The LA system was connected to the torch intake of the ICP-MS. A plasma mainly sustained by argon was lit and equilibrated for about 30 minutes before starting the analysis. The tubing was arranged such that helium could be used as the carrier gas flowing through the laser cell to transport the ablated particles to the ICP-MS. Argon was also added as a make-up gas prior to the introduction of the sample into the ICP.

The optimum flows for argon and helium were determined on a daily basis during the instrument tuning. A combination of high signals for certain elements present in the

glass standards with low percentages of oxides and doubly charged interferences were required for the optimization.

NIST 612 was the standard most frequently used for laser tuning. When doing so, it was important to take into account that the doubly charged percentage calculated using barium was affected by gallium interferences. Equation 2.1 was used to correct for this gallium contribution.

Equation 2.1 Percentage of barium doubly charged interferences corrected for the presence of gallium in NIST 612

$$\% \text{ Doubly charged (Ba)} = \frac{\left[Ba^{++}\right] - \left([Ga]*1.51\right)}{[Ba]} * 100$$

Where Ba^{2+} is monitored as $^{138}Ba^{2+}$ equating to an AMU of 69 . The correction is based on ^{71}Ga being corrected by the $^{69/71}Ga$ ratio (1.51).

The percentage of doubly charged interferences were below 3%, while the level of oxides calculated using the ratio of ThO to Th were below 1%. When checking for fractionation effects, a ratio between uranium and thorium ranging from 0.7 to 1.3 was acceptable.

Glass standard FGS02 was also used for tuning purposes. In this case, the oxide ratio was indicated using $^{140}Ce^{16}O/^{140}Ce$ and the doubly charged ions with barium as percentage of Ba^{2+}/Ba^{+}. Since gallium is not present in this standard, no corrections were needed. The levels of both interferences were lower than 3% for an accurate analysis.

49

Table 2.1 lists the optimized parameters for the analysis of glass by LA-ICP-MS using two different laser systems. They include the laser working at 100% energy, 10 Hz repetition rate, and single spot ablations with 50 μm or 100 μm diameter. No pre-ablation was needed.

Table 2.1 Parameters for laser ablation using two laser systems

LA-Parameters	Cetac LSX-200+	New Wave UP213
Spot size (round shape) (μm)	50 & 100	55 & 100
Power (% Energy)	100	100
Energy output (mJ)	~ 4.8	~ 0.598-1.98
Repetition rate (Hz)	10	10
Helium flow into the cell (L/min)	0.95	0.90-0.95
Argon makeup gas flow after the cell (L/min)	0.94-0.95	0.82-0.95
Plasma gas flow (L/min)	17	16.5
Time of ablation (seconds)	60	60
ICP RF power (V)	1500	1500-1550

2.1.2.1.2 Optimization of LSX 200+ and LSX 200

The method was first optimized using reference standard materials NIST 612, 610 and 614 as well as matrix-related standards that simulate the composition of some glasses

such as NIST 1831(for float glass), NIST 621 (for containers) and NIST 1411 (for headlamps). Once the preliminary optimization was set up, real set of samples were analyzed in order to obtain the best possible selection of elemental menus and other specific parameters.

Parameters studied during this step were: ablation mode, spot size, energy output, frequency, number of shots per sample, carrier gas, pre-ablation and surface pretreatment, tubing length, internal standards and quantification strategies. The optimization was performed in order to obtain the best response in terms of: a) signal shape, b) ion intensity and c) low relative standard deviation between runs ($< 10\%$).

2.1.2.2 LA-ICP-MS Quantification

The variation in measured properties of different glass objects constitutes the basis for discrimination among sources (Koons *et al.*, 2002). Therefore, quantitative information is crucial for forensic comparisons of glass fragments. Several calibration strategies have been suggested for quantitative analysis of solid samples by LA-ICP-MS (Stix, 1995; Schroeder, 1998; Raith *et al*., 1996; Pearce *et al.*, 1997; Mank *et al*., 1999; Mason *et al.*, 2001; Tibi *et al.*, 2001) In summary, the elemental quantification of glass by LA-ICP-MS can be achieved by three different methods: internal standardization, calibration curves, and single standard calibration.

Since different amounts of materials could be ablated within the samples, it was not recommended to use absolute intensities of signals for calibrations purposes. Instead, the intensity was usually normalized relative to the intensity of another isotope, the internal standard, whose concentration was known. The internal standardization, together with the external standard, allowed correcting for matrix effects, instrumental drift, and for the differences in the amount of particles ablated and transported into the ICP-MS.

The lowest abundant isotope of the most abundant element in the matrix to be analyzed was selected as the internal standard. The reason for this was that the major element is supposed to be present at detectable concentrations in all the samples, and the lowest abundant isotope was preferred to avoid saturation of the detector.

Most glasses have about 70% of silica as SiO_2. ^{30}Si has the lowest relative abundance (3.09%), but nitrogen oxide produces high interferences at mass 30. That is why ^{29}Si, with an abundance of 4.7%, was the chosen isotope for the internal standard. However, other major elements, like ^{42}Ca with relative abundance of 0.647%, may serve as an internal standard as well as ^{29}Si, depending on the type of matrix and chemical similarity between sample and standard (Trejos, 2003).

SRM NIST 612, was used as a single point external calibration standard. In order to control for temporal bias, SRM 612 was also run as a control sample. This external calibrator glass (NIST 612) was analyzed in two replicates at the beginning and at the end of the sequence. Another SRMs, specifically matrix-related to the samples were included

as an internal control to check the bias. SRM 1411 was used as another control standard for the headlamp set, SRM 621 for containers and SRM 1831 for the automobile set due to their very similar matrix with the samples of interest. Samples were normally analyzed in three to four replicates in order to be able to do statistical analysis to evaluate accuracy and precision. Figure 2.1 shows the order in which the glass standards and samples should be arranged for the quantitative analysis of glass by LA-ICP-MS.

SRM 612
SRM 612 } External calibrator

SRM 1831
SRM 1831 } Internal control (matrix-related)
SRM 1831

Sample A (3-5 replicates)
Sample B (3-5 replicates) } # of samples depends on time (no longer than 4 hours per sequence)

SRM 612
SRM 612 } External calibrator
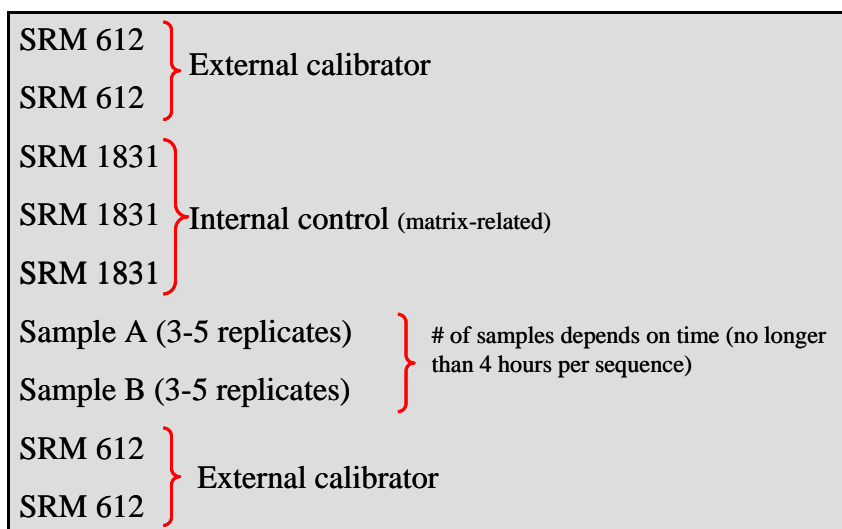
Figure 2.1 Sequence for quantitative analysis of glass samples by LA-ICP-MS

The element menu used for these analyses was previously selected based on the presence and detectability in each type of glass studied (Trejos, 2003) and based on research activities of the EU-funded network NITECRIME and published protocols product of this joined collaboration (Latckocy at al, 2005). The list of elements most commonly used in this work comprise ^{7}Li, ^{25}Mg, ^{27}Al, ^{29}Si, ^{39}K, ^{42}Ca, ^{49}Ti, ^{55}Mn,

^{57}Fe, ^{85}Rb, ^{88}Sr, ^{90}Zr, ^{118}Sn, ^{137}Ba, ^{139}La, ^{140}Ce, ^{146}Nd, ^{178}Hf, ^{206}Pb, ^{207}Pb, and ^{208}Pb.

The concentration of each element was calculated using the Glitter Software (GEMOC v4.4, Macquarie University, Australia), which integrated the signal of the sample after background subtraction. Figure 2.2 shows a bidimensional representation of the signal produced by the LA-ICP-MS in terms of intensity (CPS) vs. time (seconds). The vertical lines represent the signal selection for the data reduction using Glitter. The counts per second (CPS) were converted into concentration units based on the known relationship between the CPS and the concentration of each element in the external standard (NIST 612).
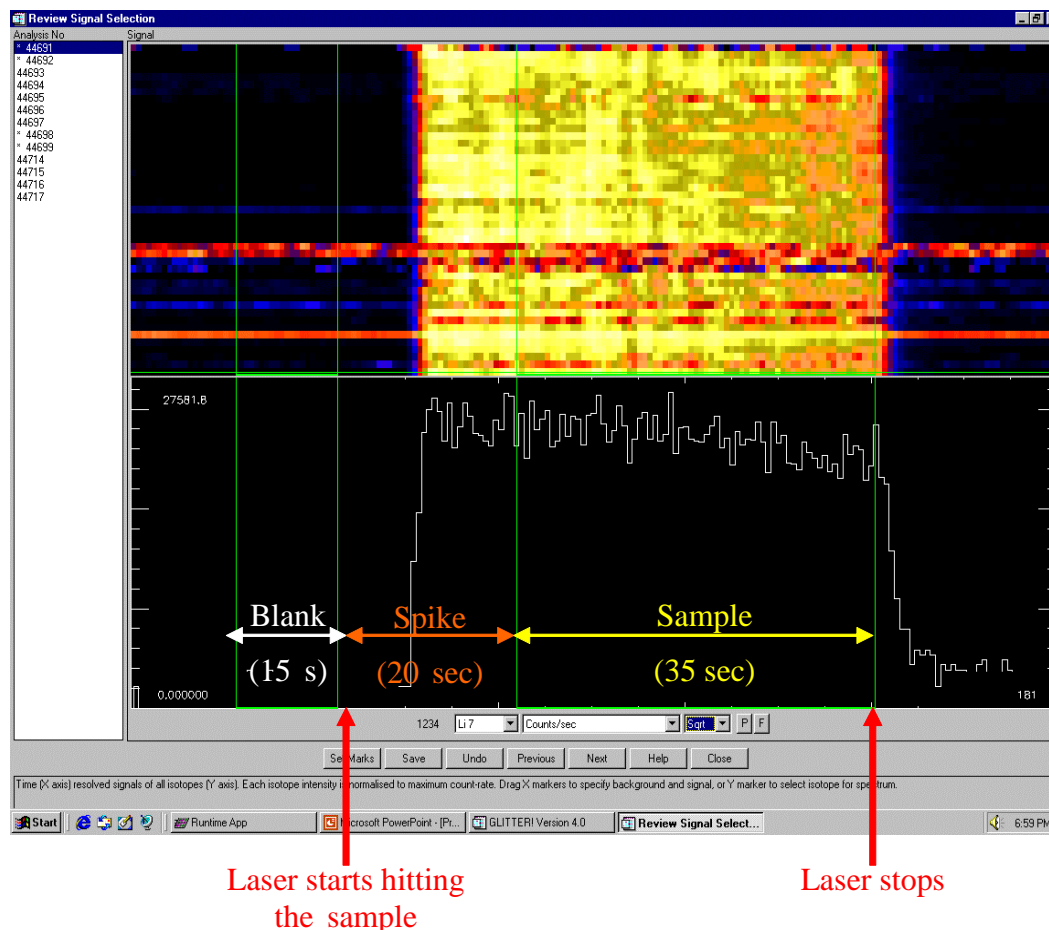
Figure 2.2 Bidimensional representation of the transient signal produced by one element
by LA-ICP-MS

For the comparison of LSX 200 and LSX 200+ laser systems the limits of
detection were estimated as 3 times the signal to noise ratio obtained for NIST 612 and
NIST 610 standards. The background signal was estimated from the 30 seconds of blank
that is acquired prior the ablation when only helium is passed through the cell. Absolute
detection limits were calculated by estimating the total mass removed from the glass. The
ablated mass was calculated as the product of the volume of the crater and the density of
the glass. Volume of the ablated craters was estimated using SEM images of the lateral
view of the craters. Since SEM is a "surface" technique and cannot "see through" the

55

glass, the lateral view of the craters needed to be exposed in order to get an image of its morphology. Craters were drilled into the edge of glass pellets and then the edges were polished with fine sand paper until half of the crater was exposed.

When the two laser systems New Wave UP213 and LSX 200+ were compared the background signal was collected setting a 30 second delay as one of the laser parameters. The laser was not hitting the sample during this time; only helium was passing through the ablation chamber. The integration of the signal acquired during these 30 seconds determined the background signal. Limits of detection (LOD) were calculated by the following equation via the Glitter software.

$$LOD = 2.3 * \sqrt{2(\text{mean}_{\text{blank}})}$$

Where mean $_{\text{blank}}$ is the mean value of the signal of the background.

2.1.3. Results and Discussion

2.1.3.1 Comparison of the two laser systems LSX 200 vs. LSX 200+

The main difference between the lasers used for this study is that the new model LSX 200+ has a flat beam profile instead of a Gaussian beam profile. This shape of the beam helps to keep a better focusing over time of the laser with the target surface and therefore the morphology of the crater is more symmetric. Figure 2.3 shows that the top view of the crater produced by LSX 200+ is more circular and the lateral view more cylindrical than the crater produced by the LSX 200. This enhancement in symmetry facilitates a more steady removal of particles from the ablation chamber, so depth profile mode is no longer required to generate a stable signal over time.

LSX 200 top view   **LSX 200 + top view**

LSX 200 lateral view   **LSX 200+ lateral view**
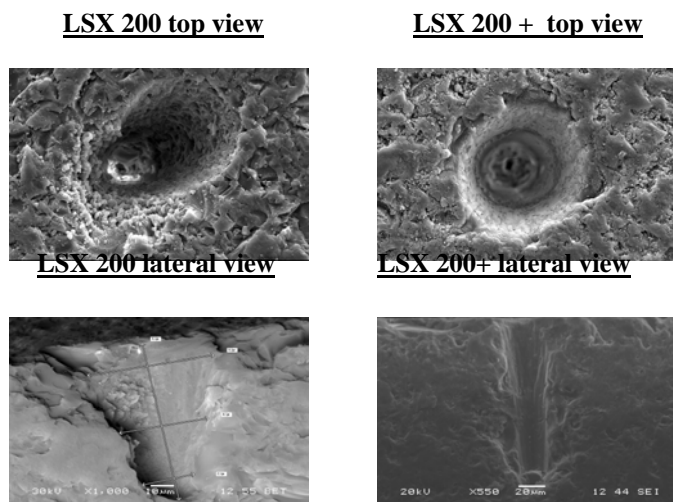
Figure 2.3 SEM images for the comparison of crater shape of 50 µm spot size ablations using LSX 200 (left) and LSX 200+ (right)

The newer laser has also a larger energy output, and therefore about double amount of glass is removed during each ablation increasing the intensity of the signals. The gain in sensitivity together with the improvement in symmetry of the crater translated also in better precision within replicates as is shown in Table 2.2

Due to the increase in the amount of glass removed using the flat beam profile laser (~280 ng for LSX 200+ vs 150ng for LSX 200), the limits of detection were improved. However, the absolute limits of detection are very similar because they take into account the total mass removed for the ablation (see Table 2.3).

Table 2.2 Comparison of precision obtained for SRM 612 using LSX 200 and LSX 200+

Element	LSX 200	LSX 200+	Element	LSX 200	LSX 200+
Li7	8.5	1.6	Ba137	11.3	1.4
B11	10.5	2.7	La139	11.2	1.0
Mg25	6.7	1.4	Ce140	10.5	0.5
Al27	3.3	1.0	Sm147	n/a	0.6
Ca42	3.3	0.5	Eu151	11.5	0.3
Ti49	10.5	4.4	Tb159	10.5	0.6
Mn55	9.0	1.3	Ho165	9.8	0.8
Fe57	16	4.7	Tm169	9.0	0.5
Co59	6.5	0.7	Lu175	9.7	1.0
Ga71	6.2	2.2	Hf178	9.6	2.1
Rb85	9.9	1.1	Ta181	11.2	1.1
Sr88	8.8	1.5	W182	9.3	1.7
Zr90	9.9	1.0	Au197	9.4	2.2
Nb93	7.6	1.0	Pb208	9.7	2.6
Sn118	12.2	1.8	Bi209	10.6	2.5
Sb123	9.7	1.4	Th232	11.5	1.0
Cs133	9.6	0.8	U238	11.1	1.1

Table 2.3 Limits of detection and absolute limits of detection of LSX 200+ and LSX 200

Laser	LSX 200	LSX 200	LSX 200+	LSX 200+
Element	LOD ug/g	LOD /pg	LOD ug/g	LOD /pg
Ti	38	5.4	24	5.5
Mn	16	2.3	8.5	2.0
Ga	3.8	0.5	2.5	0.6
Sr	4.0	0.6	0.7	0.2
Zr	6.3	0.9	1.4	0.3
Ce	1.5	0.2	0.6	0.1
Hf	0.9	0.1	2.8	0.7
Pb	4.5	0.6	1.9	0.4

2.1.3.1 Comparison of the two laser systems New Wave UP213 vs. LSX 200+

2.1.3.1.1Cetac LSX-200 Plus

This is a 6 mJ Nd:YAG laser with a 1064 nm primary wavelength, which frequency is quadrupled to 266 nm using optical components. Figure 2.4 shows an SEM-EDS image of the resulting crater caused by a single spot ablation of 50 μm diameter and 90 μm deep in glass using the Cetac LSX-200+.
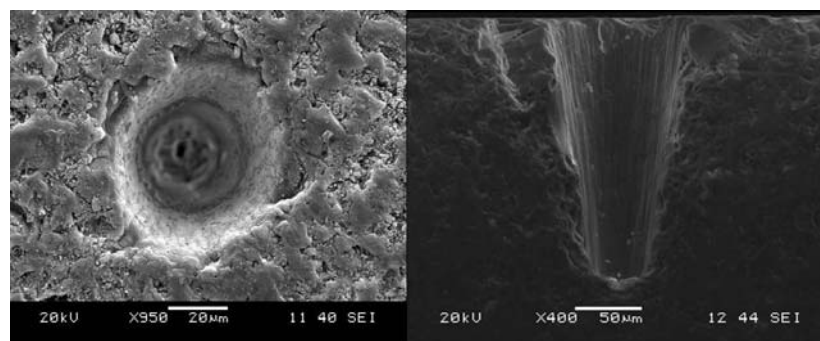
Figure 2.4 SEM-EDS image of the crater resulting from the laser ablation sampling in glass: top view (right) and cross section view (left) (Trejos *et al.*, 2004).

59

Table 2.4 shows some of the results obtained for the elemental analysis of FGS02 using the Cetac LSX-200+ laser system compared to the information values for this standard. The percentages of relative standard deviation were lower than 5% for nearly all the elements analyzed and lower than 15% for the rest of the elements, indicating a good precision. The comparison by t-tests of the experimental results to the certified values for glass standard reference materials permitted the evaluation of the accuracy. The utilization of this laser system led to accurate results with percentages of bias lower than 5% for most of the elements.

Table 2.4 Comparison of the results obtained for the elemental analysis of FGS02 by LA-ICP-MS using the LSX-200+ laser system and the information values for this glass standard

FGS02	^{55}Mn	^{85}Rb	^{88}Sr	^{90}Zr	^{137}Ba	^{139}La	^{140}Ce	^{146}Nd	^{178}Hf
Certified values	221	35	253	223	199	18	23	25	15
LA-ICP-MS (ppm)	218	37.6	246	218	191	17.8	22.5	24.8	14.3
Std. Dev (ppm)	1.6	0.33	2.2	2.1	2.9	0.49	0.29	1.1	0.51
%RSD	0.7	0.9	0.9	1.0	1.5	2.7	1.3	4.5	3.6
% Bias	1.6	7.6	2.8	2.3	4.0	1.4	2.1	0.8	4.5

Table 2.5 shows the minimum detection limits of some elements as the Glitter software automatically calculated them. Based on these values, nearly all the elements can be detected at concentrations lower than 1 ppm, meaning that the sensitivity achieved using this laser system was very good.

Table 2.5 Limits of detection (at 99% confidence) achieved with the Cetac LSX-200+

laser system for the elemental analysis of NIST 612 and NIST 1831

Glass Standard	^{25}Mg	^{55}Mn	^{85}Rb	^{88}Sr	^{90}Zr	^{137}Ba	^{139}La	^{140}Ce	^{146}Nd	^{178}Hf
NIST 612 (ppm)	4.54	1.2	0.11	0.078	0.17	0.47	0.072	0.081	0.30	0.23
NIST 1831 (ppm)	2.86	0.90	0.14	0.10	0.11	0.42	0.091	0.057	0.40	0.34

Several experiments for the analysis of glass standards by LA-ICP-MS using the

Cetac LSX-200+ were performed, revealing a good reproducibility.

2.1.3.1.2 New Wave UP213

The New Wave UP213 Nd:YAG laser ablates at 213 nm. Its performance was

evaluated in terms of precision, reproducibility and accuracy using glass standard

reference materials such as NIST 612, NIST 1831, FGS01, and FGS02. The RSD values

were lower than 5% for most of the elements except for those with concentrations very

close to the detection limits, for which the RSD values were lower than 10%. Its accuracy

was measured by comparing the results using this laser to the true values for the element

concentrations that NIST certified for each standard. Table 2.6 illustrates an example of

results obtained for the elemental analysis of FGS02 compared to the certified values for

this standard. The comparisons performed by t-test showed no significant differences

between the means and the "true" values, which accounted for an excellent accuracy. The

bias resulted lower than 5% for the majority of the elements analyzed and lower than

10% for those elements in concentrations close to the detection limits.

Table 2.6 Comparison of the results obtained for the elemental analysis of FGS02 by LA-ICP-MS using the New Wave UP213 laser system and the information values for this glass standard

FGS02	^{55}Mn	^{85}Rb	^{88}Sr	^{90}Zr	^{137}Ba	^{139}La	^{140}Ce	^{146}Nd	^{178}Hf
Certified values	221	35	253	223	199	18	23	25	15
LA-ICP-MS (ppm)	221	38.1	258	224	200	19.1	24.1	26.2	14.2
Std. Dev (ppm)	1.4	0.23	4.7	5.4	3.2	0.42	0.27	1.1	0.67
%RSD	0.6	0.6	1.8	2.4	1.6	2.2	1.1	4.2	4.7
% Bias	0.05	8.8	2.2	0.4	0.4	6.4	4.9	4.7	5.5

The limits of detection achieved using this laser system for the elemental analysis of different standard reference materials are shown in Table 2.7. Most of the elements exhibited limits of detection bellow 1 ppm. Judging by those results, the sensitivity of the method using the New Wave UP213 laser system was excellent.

Table 2.7 Limits of detection (at 99% confidence) achieved with the New Wave UP213 laser system for the elemental analysis of NIST 612, NIST 1831, and FGS02

Glass Standard	^{25}Mg	^{55}Mn	^{85}Rb	^{88}Sr	^{90}Zr	^{137}Ba	^{139}La	^{140}Ce	^{146}Nd	^{178}Hf
NIST 612 (ppm)	2.2	0.32	0.11	0.062	0.094	0.30	0.061	0.075	0.19	0.22
NIST 1831 (ppm)	2.1	0.32	0.10	0.072	0.10	0.24	0.053	0.065	0.17	0.21
FGS02 (ppm)	3.4	0.31	0.093	0.060	0.083	0.23	0.040	0.052	0.15	0.21

These analyses were repeated several times and the outcomes were reproducible.

2.1.3.1.3. Comparison of the two laser systems

The performance of laser ablations in the single spot mode using spot sizes of 50 or 55 µm and 100 µm made possible the comparison of the Cetac LSX-200+ and the New Wave UP213. The analytical conditions for these ablations using each laser unit were previously listed in Table 2.8.

Table 2.8 Optimal parameters for the LA-ICP-MS without matrix-matched standards experiments

Laser Parameters	
Spot size (round-shape)	100 µm
Power (% Energy)	100%
Energy output	1.88 mJ
Fluence	24.00 J/cm^2
Repetition rate	10 Hz
Helium flow into the cell	0.90 L/min
Argon makeup gas flow after the cell	0.92 L/min
Plasma gas flow	15.6 L/min
ICP RF power	1550
Time of ablation	60 sec
Delay time	30 sec
ICP-MS Parameters	
Solution intake flow	6 rpm

The elemental concentrations resulted from the analysis of NIST 612 and NIST 1831 by LA-ICP-MS using each of the laser systems in comparison with the certified values of each glass standard are shown in Tables 2.9 and 2.10, respectively. In both cases, the experimental results were very close to the "true" values, meaning that very good accuracy was achieved when using any of the lasers.

Table 2.9 Results of the analysis of NIST 612 by LA-ICP-MS comparing the accuracy achieved by each laser system

NIST 612	^{25}Mg	^{55}Mn	^{85}Rb	^{88}Sr	^{90}Zr	^{137}Ba	^{139}La	^{140}Ce	^{146}Nd	^{178}Hf
Certified values (ppm)	77.63	38.44	31.64	76.18	36	37.79	35.78	38.36	35.26	34.81
LSX-200+ (ppm)	76.60	37.80	31.47	75.98	35.87	37.51	35.79	38.24	35.35	34.86
New Wave UP213 (ppm)	77.46	38.44	31.65	76.19	36.05	37.76	35.78	38.36	35.26	34.82

Table 2.10 Results of the analysis of NIST 1831 by LA-ICP-MS comparing the accuracy achieved by each laser system

NIST 1831	^{25}Mg	^{55}Mn	^{85}Rb	^{88}Sr	^{90}Zr	^{137}Ba	^{139}La	^{140}Ce	^{146}Nd	^{178}Hf
Certified values (ppm)	21166	12.54	6.11	89.11	43.35	31.51	2.12	4.53	1.69	1.09
LSX-200+ (ppm)	25030	13.03	5.65	73.86	30.06	29.22	2.18	4.32	1.24	0.89
New wave UP 213 (ppm)	24841	13.08	6.03	78.52	32.67	30.39	2.21	4.43	1.63	0.89

The flat beam profile present in both laser systems provided good focusing over time that led to a symmetric morphology of the crater. The main difference between them is that the Cetac LSX-200+ ablates at 266 nm, while the New Wave UP213 does it at 213 nm. Since the New Wave laser ablates at a shorter wavelength, its higher energy allowed a better interaction with the sample by reducing the possibility of melting the solid surface and creating smaller particles that are typically better ionized. Nevertheless, the limits of detection and precision achieved by both laser systems were very good. RSDs ranged around 5% and LODs were lower than 1ppm for most of the elements analyzed.

As it can be appreciated in Figure 2.5, the crater that resulted from the New Wave UP213 laser ablation looks like a perfect cylinder whiles the crater resulted from using the Cetac LSX-200+ is conical. This difference in the shape of the crater is translated into a different amount of material being removed from the sample. In the case of the Cetac LSX-200+, the conical crater was probably produced due to less uniform energy distribution along the focus of the sample during the ablation, which might cause lower signal reproducibility. Contrary to expectations, the difference in the amount of material removed by each laser system did not impact considerably the quantification of elements in glass.

65
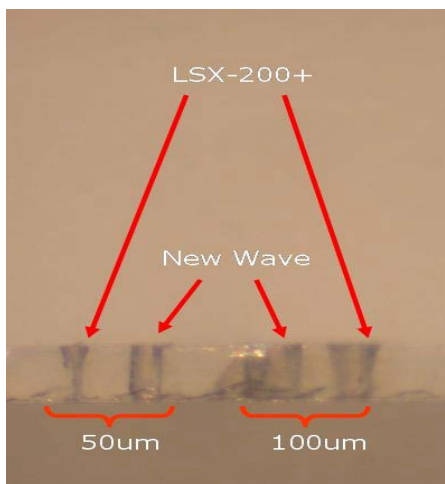
Figure 2.5 Lateral view of the craters (50µm and 100µm spot size) produced by laser ablation using two laser systems: Cetac LSX-200+ and New Wave UP213

In summary, it was determined that the dissimilarities between the New Wave UP213 and the Cetac LSX-200+ laser systems did not affect significantly the quantitative analysis of elements in glass samples by LA-ICP-MS. The use of each of these laser systems led to excellent sensitivity (LOD <1 ppm), great precision (RSD <5%), and very good accuracy (Bias <5%).

2.1.4. Conclusions

2.1.4.1 LSX 200 vs. LSX 200+

Fundamental studies on particle sizes allowed the determination that the interaction of the 266 nm laser systems LSX 200+ and LSX 200 with the glass surface produced small particles with a dominant diameter of 0.1 µm under the reported parameters, however, the LSX200+ flat top beam profile provides better precision (<5% RSDs).

66

The flat beam profile increases the sensitivity and the symmetry of the crater, which translated in better precision and lower detection limits.

2.1.4.2 New Wave UP213 vs. LSX 200+

As expected, the higher energy at which the New Wave laser system ablates resulted in a better coupling with the solid through non-thermal mechanisms that minimize undesired effects such as melting and fractionation. The ablation with this laser produced a cylindrical crater, while the ablation with the Cetac LSX-200+ created a conical crater indicating that the amount of material removed from the solid using each laser was different. Despite all those dissimilarities, the signal reproducibility seemed not to be affected significantly by the laser system used. Likewise, the final results utilizing both lasers were very precise and very accurate, presenting less than 5% of RSDs and LODs lower than 1 ppm for most of the elements analyzed. Hence, it was demonstrated that the New Wave UP213 and the Cetac LSX-200+ laser systems are equally useful for their application to the elemental analysis of glass by LA-ICP-MS.

2.2. ANALYSIS OF GLASSES TYPICALLY FOUND IN CRIME SCENES (AUTOMOBILE, CONTAINERS AND HEADLAMPS)

2.2.1. Methodology

2.2.1.1. Sampling Sets

A total of 239 glass fragments were selected to conduct the evaluation of the application of LA to glass analysis. A set of 131 glass samples were selected from the glass database existent in our laboratory for their use in the evaluation of the analytical performance of the method. Quantitative analysis on all samples was conducted by both EC and LA methods. Isotope Dilution analysis was performed only on those samples that were not distinguishable by the reported EC method. In addition, another set of 108 glass fragments was used for the homogeneity studies, these set was comprised of 56 fragments originated from glass containers, 28 fragments from automobile windshields and 20 fragments from architectural windowpanes. Finally a subset of four tempered glasses was also studied for homogeneity determinations. Figure 2.6 shows the distribution of sampling sets.

2.2.1.1.1. Automobile windows and windshields: CFS set

The automotive windows subset consisted of 46 auto window samples provided by the Centre of Forensic Sciences (CFS), Toronto Canada from actual casework samples that were submitted to the laboratory. The set consisted of 18 windshields and 28 windows (side or rear).

68
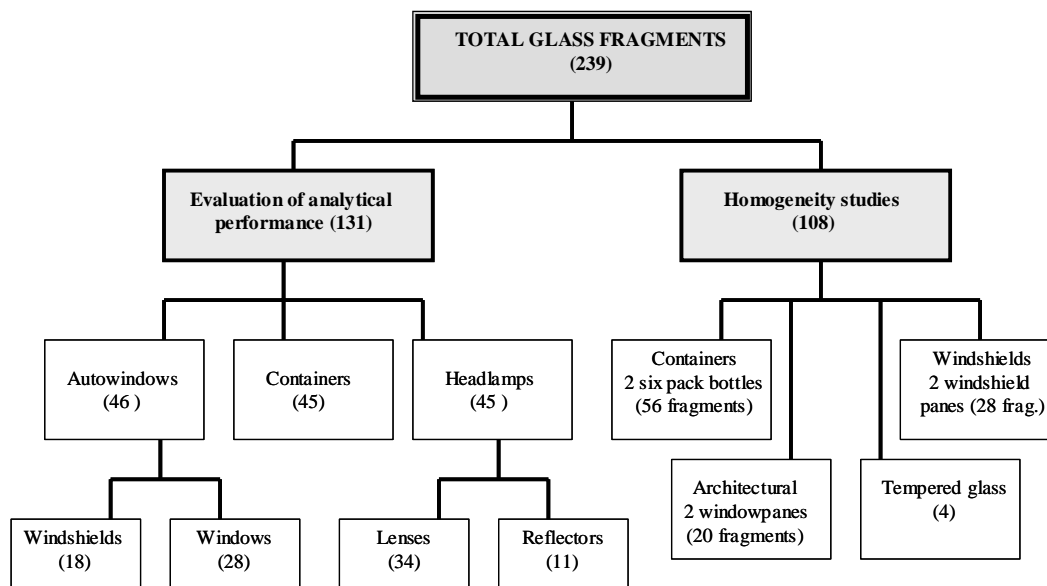
Figure 2.6 Description of sampling sets used for the evaluation of the method of analysis of glass fragments by LA-ICP-MS.

2.2.1.1.2 Headlamps

The headlamp subset consisted of a total of 45 headlamp samples collected from a variety of automobiles in a junkyard representing 20 years of manufacturing dates and included 34 lenses and 11 reflectors.

2.2.1.1.3. Containers

A total of 45 fragments originated from containers were selected from the existing glass database at our laboratory.

2.2.1.2. Samples for homogeneity studies

A total of 108 fragments were used for the homogeneity evaluation, all of them were selected $< 2mm^2$ in size in order to be typical of those glass fragments transferred from the crime scenarios.

The homogeneity of the architectural windows subset was comprised of two sheet of glass, each one of 19 by 26 inches long. One of the sides of each sheet was covered with tape, enclosed in clean cardboard and broken with a hammer. Ten fragments from each sample were randomly selected for analysis. During LA-ICP-MS analysis, a single fragments was measured ten (10) times in order to account for method variation (see A2 in Figure 2.7a), and ten (10) different fragments were measured once by LA-ICP-MS in order to account for variations in the sheet of interest (see A1 in Figure 2.7a). A total of 20 different fragments from both windowpanes were used for this set.

The windshield set consisted of two windshields originating from different sources, one from a Chevy vehicle, year 1985 and the other from a vehicle Jeep Wrangler, year 1988. Each windshield consisted in a two window panels separated by a plastic film. One of the sides of each windshield was covered with tape, enclosed in clean cardboard and broken with a hammer. Seven (7) fragments were randomly selected from each panel for a total of 14 fragments from each windshield. During LA-ICP-MS analysis seven measurements were performed on a single fragment in order to account for method variation. Seven different fragments were measured once by LA-ICP-MS in order to account for variations in the panel of interest. The analysis was done independently for each panel of the windshields (inner and outer sides) (see Figure 2.7b).
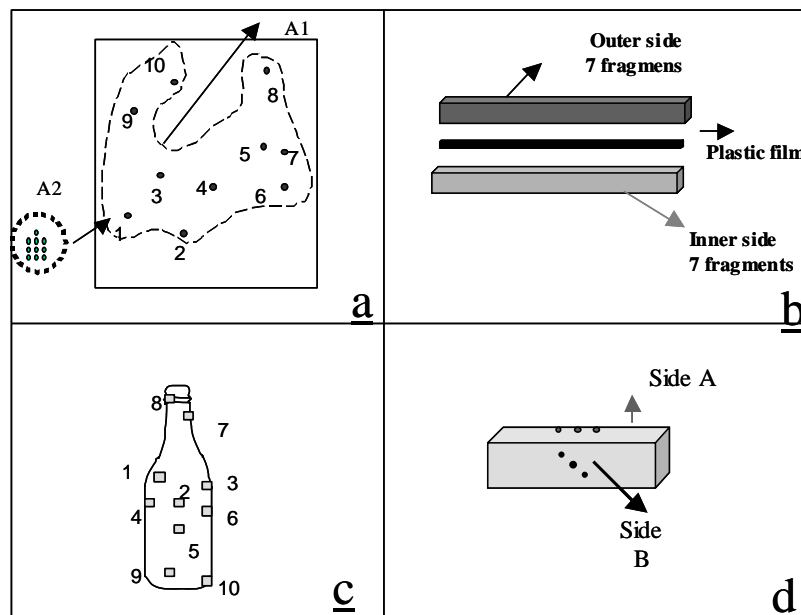
Figure 2.7 Sampling diagram used for the homogeneity study of a) architectural glass, b) windshields, c) containers and d) tempered glass

The container set was comprised of a four pack of green bottles, wine Bella Sera 2001, Merlot vinted and bottled in Italy (Villalta, Italy), and a six pack of brown bottles, beer Michelob 2003, brewed and bottled in USA (Anheuser-Bush Inc, MO, USA). All bottles from the same pack contained the same bar code number. The homogeneity study of containers was divided in two subgroups: a) homogeneity within a single bottle and b) homogeneity between bottles from the same six (or four) pack. For the homogeneity within a single bottle ten fragments were selected as shown in Figure 2.7c. Each fragment was measured in triplicate. A total of 56 fragments were analyzed for this set. In addition,

71

to assess the homogeneity between the bottles from the same pack three fragments from each bottle were measured by triplicate.

The tempered subset consisted of four window samples provided by the Centre of Forensic Sciences (CFS), Toronto Canada from actual casework samples that were submitted to the laboratory. The elemental composition of the fragment was measured in the top surface by triplicate and compared with the side composition at different depths among the thickness of the fragment.

2.2.1.3. Evaluation of the analytical performance of LA-ICP-MS

In order to evaluate the analytical performance of LA-ICP-MS for glass analysis, the method was compared with the well-known techniques of solution-ICP-MS: external calibration (EC) and isotope dilution (ID). The results for glass sets of automobile windows, containers and headlamps were compared in terms of precision, accuracy, repeatability and discrimination power. Precision was calculated as %RSD and accuracy was estimated by comparison with reported values for known standards. In order to assess the discrimination potential of LA, refractive index was also included for comparisons, using analysis of variance (ANOVA) and pairwise comparisons with Tukey's HSD test.

2.2.1.3.1. Sample preparation for EC-ICP-MS

The samples were washed, first in methanol for 10 minutes, then with 1.6molL^{-1} HNO_3 for 30 minutes followed by rinsing with high purity water. After rinsing, they were

left to dry overnight. The samples were crushed and weighed to approximately 2mg $\pm$ 1µg into 5mL polypropylene tubes. The glass dissolution procedure was adapted from the work of Parouchais *et al* (Parouchais, 1996). The digestion was performed by adding 600µL of a freshly-prepared mixture containing HF:HCl:HN0$_3$ 2:1:1 to each test tube before capping them. After 2 hours of ultrasonication, the tubes were uncapped and set into a dry heater block (80 $\pm$ 5°C) until the samples were completely dry (24-36 hours). The samples were then reconstituted using 0.8ml of 4molL^{-1} HN0$_3$, 20µL of 10mgL^{-1} Rh in 0.8molL^{-1} HN0$_3$, and 680µL of deionized water, then left capped overnight. An additional volume of 2500µL of deionized water was added and vigorously mixed. Prior to measuring these solutions, an aliquot of 50µL from each sample was diluted by transferring it to an 8mL test tube (Falcon, New York, USA) and mixing it with 30µL of 10.00µgL^{-1} Sc in 0.8molL^{-1} HNO$_3$ and 4920µL of 0.8molL^{-1} HNO$_3$. The undiluted samples and the 1:100 dilutions were measured using different calibration curves.

2.2.1.3.2. Sample preparation for ID-ICP-MS

The samples were washed and weighed using the same procedure as EC. Four replicates for each sample were digested by adding a 600 µL solution of a digestive mixture containing (HF:HCl:HNO$_3$, 2:1:1) to each test tube before capping them. After 2 hours inside an ultrasonic bath, the spikes were added to three of the samples as described in Table 2.11, vigorously mixed and all four replicates per sample were set into a dry bath (80 °C $\pm$ 5 °C) until dryness (24-36 hours). The unspiked replicate for each sample was used to calculate the mass bias. The samples were then reconstituted using 0.800 mL of

4.000 molL^{-1} HNO$_3$, and 0.700 mL of deionized water and left to equilibrate overnight. An additional volume of 2500 μL of deionized water was added and vigorously mixed. Prior to measuring these solutions, an aliquot of 50 μL from each sample was diluted by transferring it to an 8 mL test tube (Falcon, New York, USA) and mixing it with 4950 μL of 0.8 molL^{-1} HNO$_3$. These 1:100 dilutions were used in the case that the detector mode would change from pulse to analog for one of the isotopes in any of the isotopic pairs.

2.2.1.3.3. Sample preparation for LA-ICP-MS

The surface of the glass fragments were slightly scratched with a sand paper of 3600 mesh and then washed three times with deionized water followed by washing with 0.8 molL^{-1} HNO$_3$ for 30 minutes under the ultrasonic bath. The samples were rinsed with deionized water and then let dry. The dried fragments were mounted under the microscope into a small piece of "tacky blue" mounting medium of ~ 1cm^2 square. For the float windows subset, the samples were observed under UV-lamp (365nm and 254nm) and the non-fluorescent side was selected for the ablation to avoid the introduction of Sn from the surface of glass manufactured by the manufacturing process.

Table 2.11 Approximate mass in ng of the spikes added to different samples in ID

Spike	SRM 612	SRM 614	SRM621	SRM 1831 or float glasses
^{26}Mg	18	10	398	5088
^{86}Sr	177	120	251	232
^{91}Zr	69	17	87	69
^{137}Ba	47	2	3.1	0.47
^{123}Sb	118	25	2712	74
^{179}Hf	16	0.25	0.15	0.15
^{149}Sm	36	0.84	0.97	0.55
^{206}Pb	48	48	9.5	4.75

2.2.1.3.4. Quantitative analysis for EC-ICP-MS

Multi-element standards and calibration verification standards (CCV) were prepared with single element 1000 mgL^{-1} stock solutions from different vendors. One calibration curve for trace elements was prepared with six standards using rhodium as an internal standard (final concentration 50.0 mgL^{-1}) with the following elements: Mg, Mn, Ce, Ti, Zr, Sb, Ga, Ba, Rb, Sm, Sr, Hf, La and Pb. A second calibration curve was prepared for the analysis of minor elements and consists of four standards (Mg, Al, Ca, Ba) and Sc as an internal standard with a final concentration of 60.0 mgL^{-1}.

2.2.1.3.5. Quantitative analysis for ID-ICP-MS

The isotope dilution quantification is based on the precise addition of an accurately known quantity of an enriched stable isotope of the analyte element to the unknown

sample. After equilibration, the modified analyte isotope ratio is measured and the concentration of the analyte in the original sample can be calculated by Equation 2.3 (Beary, 1994) where C_x is the concentration of the analyte in the sample, C_s is the concentration of the analyte in the spike solution, W_s is the weight of the spike, W_x is the weight of the sample, A_s is the abundance of the reference isotope in the spike, B_s is the abundance of the spike isotope in the spike, A_x is the abundance of the reference isotope in the sample, B_x is the abundance of the spike isotope in the sample and R_t is the mass-bias corrected ratio between reference and spike isotope in the sample after spiking.

Equation 2.3 Equation to calculate the concentration of the analyte in the original sample in ID-ICP-MS analysis

$$C_x = (C_s W_s / W_x)\ (A_s - R B_s) / (R_t B_x - A_x)$$

In ID-ICP-MS, the isotopes measured were: ^{25}Mg, ^{26}Mg, ^{137}Ba, ^{138}Ba, ^{149}Sm, ^{152}Sm ,^{86}Sr, ^{88}Sr, ^{179}Hf, ^{180}Hf, ^{90}Zr, ^{91}Zr, ^{204}Pb, ^{206}Pb ^{207}Pb, ^{208}Pb and ^{121}Sb, ^{123}Sb. The elements used in this experiment were selected based on the discrimination power of the elements for glass analysis, concentration present in the sets of glass of interest and availability.

The concentrations of the spike solutions were determined by reverse isotope dilution ICP-MS, using elemental standards prepared from single element 1000 mgL^{-1} stock solutions (GFS Chemicals, Columbus, OH, USA) diluted to 10.00 mgL^{-1} with HNO$_3$ acid 0.8 molL^{-1}. The common lead isotopic standard reference material SRM 981

(NIST, Gaithersburg, MD) dissolved in HNO_3 acid 0.8 $molL^{-1}$ was used for Pb determinations, since the Pb isotopic composition is not constant in nature.

2.2.1.3.6. Quantitative analysis for LA-ICP-MS

In this study, ^{29}Si was used as an internal standard and the standard reference material, SRM NIST 612, was used as a single point external calibration standard. In order to control for temporal bias, SRM 612 was also run as a control sample. In addition, SRM 1411 was used as another control standard for the headlamp set, SRM 621 for containers and SRM 1831 for the automobile set due to their very similar matrix with the samples of interest.

2.2.1.3.7. Ruggedness test

The ruggedness test was performed after the standardization and optimization of the method in order to find which variables strongly influence the measurements provided by the procedure, and to determine how closely these variables need to be controlled. A Plackett-Burman design was used following the design recommended by ASTM method E 1169-89 for 7 parameters (ASTM, 2001). Eight experiments using SRM NIST 612 was conducted in two different days in order to evaluate the selected factors. Table 2.12 depicts the design of the experiment, where the "plus (+)" represents the higher values and "minus (-)" represents the lower values. The identification of the factors is showed in Table 2.13.

Table 2.12 Placket - Burman design for eight experiment (n=8) used in the ruggedness test for glass analysis by LA-ICP-MS.

Experiment	Factor						
	A	B	C	D	E	F	G
1	+	+	+	-	+	-	-
2	-	+	+	+	-	+	-
3	-	-	+	+	+	-	+
4	+	-	-	+	+	+	-
5	-	+	-	-	+	+	+
6	+	-	+	-	-	+	+
7	+	+	-	+	-	-	+
8	-	-	-	-	-	-	-

Table 2.13 Identification of the factors selected for the ruggedness test.

Factor	Description	Low value	High value
A	spot size (µm)	50	100
B	Energy output (%)	80	100
C	frequency (Hz)	5	10
D	Ar gas flow	0.95	1.00
E	He gas flow	0.95	1.00
F	ablation time (s)	40	50
G	defocus	no	yes (5µm)

2.2.1.3.8. Optimization and method development

The first step in this work was the development and optimization of a method for the analysis of glass by LA-ICP-MS. The method was first optimized using reference standard materials NIST 612, 610 and 614 as well as matrix-related standards that simulate the composition of some glasses such as NIST 1831(for float glass), NIST 621 (for containers) and NIST 1411 (for headlamps). Once the preliminary optimization was set up, a real set of samples was analyzed in order to obtain the best possible selection of elemental menus and other specific parameters.

Parameters studied during this step were: ablation mode, spot size, energy output, frequency, number of shots per sample, carrier gas, pre-ablation and surface pretreatment, tubing length, internal standards and quantification strategies. The optimization was performed in order to obtain the best response in terms of: a) signal shape, b) ion intensity and c) low relative standard deviation between runs ($< 10\%$).

In addition, studies of particle size distribution were also performed in order to better understand the process occurring during the ablation of glass samples. The effect of different ablation parameters on the distribution of the size of the laser aerosol particles was monitored with the simultaneous acquisition of transient signals. Parameters of interest during these studies were the ablation mode, ablation time, beam profile, carrier gas and pulse rate. The best parameters were selected for events that produced the smallest particles, best precision and best transport of particles into the plasma.

2.2.2. Results and Discussion

2.2.2.1 Sampling and Sample Homogeneity studies

The homogeneity studies presented in this work are intended to prove that even when very small amounts of sample are removed from a recovered fragment from a crime scene, the elemental composition could be representative of the original glass material, i.e. a whole window from a house, a windshield or side window from a vehicle or a container. Each of the distinct class of glasses has a different manufacturing process providing different opportunities to include contamination of trace elements into the final product.

2.2.2.1.1 Set of architectural glass

For the architectural set, a t-test for n=10 was done to compare the mean value given by the instrument variation (10 replicates from a single fragment) and the mean value of the ten fragments randomly selected from the sample, which represents the variation given by the natural heterogeneity within the whole piece of glass. The t-statistical analysis was performed for each of the elemental ratios of interest and in all cases they were not significantly different with a 99% of confidence (p >0.01). Table 2.143 shows the elemental ratios obtained from the replicates of one of the architectural glasses. The statistical results demonstrated that the elemental composition within a single sheet of architectural window is homogeneous. Figure 2.8 shows an example of the distribution of the values of Mn/Rb of 10 replicates from a single fragment versus 10 replicates made on different fragments among one of the architectural windowpanes.
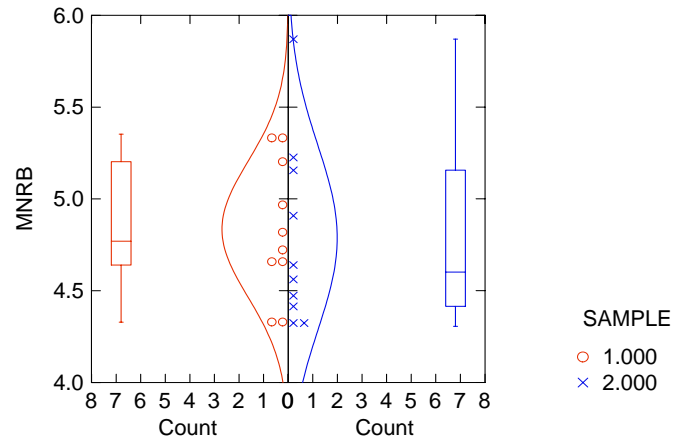
Figure 2.8 Distribution of values and standard deviation of the replicates within a single fragment (1) and replicates within the whole piece of architectural window (2)

Table 2.14 Elemental ratios obtained for the homogeneity evaluation of architectural windowpane (sample #1). Set 1 contains 10 replicates within a single fragment and set 2 contains ten measurements among the architectural pane.

set 1 fragment #	Th/U	Pb/Ce	AlK	AlCa	SrZr	ZrSn	Mg/Li	TiMn	MnRb	BaLa	CeLa
1-1	1.629	1.348	1.258	0.041	2.014	4.032	5887	1.515	4.329	5.924	2.229
1-2	1.476	1.678	1.351	0.042	1.696	3.732	6110	1.000	5.203	8.505	2.602
1-3	1.750	2.212	1.304	0.041	1.851	3.511	5065	1.507	5.353	6.024	1.638
1-4	1.143	1.621	1.507	0.042	1.623	3.961	6303	1.272	4.662	18.736	2.019
1-5	1.548	1.398	1.379	0.043	1.700	3.373	5345	1.252	4.722	7.181	2.034
1-6	1.500	1.308	1.370	0.042	1.678	2.867	6754	1.350	4.967	5.295	1.837
1-7	1.031	1.315	1.408	0.043	1.559	3.844	6705	1.345	4.340	4.823	1.490
1-8	1.133	1.301	1.614	0.043	1.630	3.113	5802	1.568	5.314	5.864	2.000
1-9	1.286	1.537	1.599	0.042	1.700	3.120	6430	1.272	4.818	7.482	1.813
1-10	1.054	1.239	1.613	0.046	1.706	3.218	5204	1.346	4.640	6.398	1.737
mean 1	1.355	1.496	1.440	0.043	1.716	3.477	5961	1.343	4.835	7.623	1.940
stdev 1	0.258	0.292	0.133	0.002	0.129	0.402	608	0.164	0.370	4.052	0.317

set 2 fragment #	Th/U	Pb/Ce	AlK	AlCa	SrZr	ZrSn	Mg/Li	TiMn	MnRb	BaLa	CeLa
2-1	1.294	1.301	1.522	0.043	1.812	3.704	6693	1.602	4.473	6.538	1.849
2-2	0.789	1.127	1.350	0.042	1.908	3.938	5945	1.362	4.909	5.482	1.789
2-3	1.353	1.460	1.265	0.041	1.773	3.232	5154	1.253	4.562	6.982	1.752
2-4	0.892	1.169	1.038	0.030	1.762	3.466	4218	1.681	4.306	6.524	1.905
2-5	1.237	1.316	1.265	0.041	1.845	3.337	5075	1.407	4.326	7.424	2.033
2-6	0.845	1.101	1.373	0.041	1.899	3.045	4415	1.321	4.415	7.118	2.039
2-7	1.123	1.231	1.217	0.040	1.868	3.189	6079	1.204	4.640	6.663	1.931
2-8	1.350	1.051	1.557	0.042	1.825	3.185	5452	1.464	5.870	7.788	2.438
2-9	1.409	1.178	1.554	0.046	1.621	4.096	5678	1.579	5.156	7.746	1.772
2-10	0.987	1.062	1.519	0.040	1.764	3.351	5206	1.331	5.226	4.747	1.500
mean 2	1.128	1.200	1.366	0.041	1.808	3.454	5392	1.420	4.788	6.701	1.901
stdev 2	0.233	0.129	0.173	0.004	0.084	0.348	751	0.158	0.502	0.967	0.245

2.2.2.1.2. Set of windshields

The individual panels (outer and inner sides) for two windshields were also evaluated for micro-homogeneity. Figure 2.9 shows the elemental composition of fragments from the outside panel of the Chevy's windshield. According to the t-test performed the replicates from a single fragment were not significantly different from the replicates from different fragments within the panel ($p > 0.01$), showing also good homogeneity within the sample. The same results were obtained for the other individual sheet of windshields analyzed. Nevertheless, when the elemental composition of the inside and the outside sheet of glass from the Chevy's windshield were compared versus each other, they were significantly different with a confidence level of 99% ($p > 0.01$). Figure 2.10 shows in color the ratios that were significantly different between the side sheets of the windshield (Sn/Ba, Co/Sr and Ti/Mn). These results stress the importance of employing a good sampling strategy during collection of windshield fragments in a real casework. A good practice will be to collect, whenever possible, glass fragments from both sides of the windshield and identify them properly because the recovered fragment from victim(s) and suspect(s) could originate from a different side of the windshield or from a mixture of them. Hence, a proper identification of the "known" samples is definitive in providing a conclusion about the existence of a common origin between glass fragments.
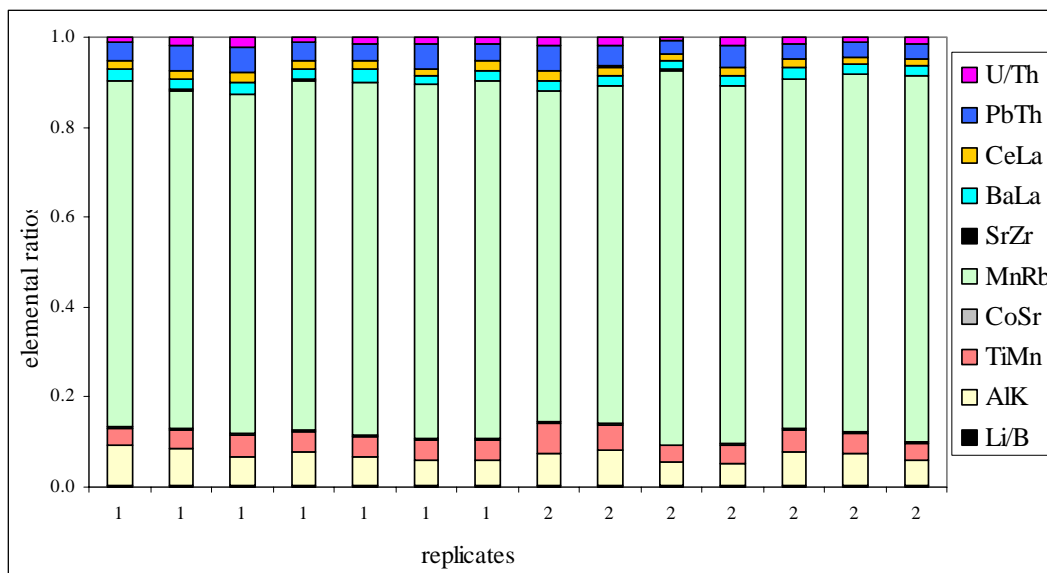
Figure 2.9 Comparison of elemental profile of seven replicates from a single fragment (1) and seven measurements of different fragments within the outside Chevy's windshield.
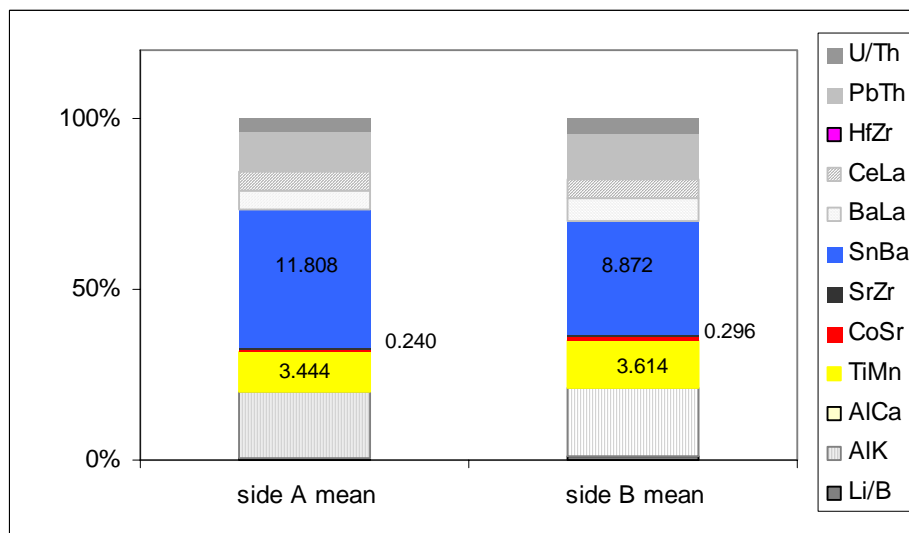
Figure 2.10 Comparison of elemental profile of outside (A) and inside (B) sheets of the Chevy's windshield

2.2.2.1.3. Set of containers

Both set of containers (wine and beer bottles) showed a natural heterogeneity in the elemental composition within a single bottle that can be caused by the manufacturing process of the containers, which involves the use of molding parts that allows more contamination of trace elements. Analysis of variance (ANOVA) was performed to ten fragments within the bottle, each one analyzed by triplicate. The variation due to heterogeneity in the sample was bigger than the instrumental variation given by LA-ICP-MS and therefore different matching criteria were employed to process the data from containers. The mean squared error within the replicates from the fragments (MSEw) and the mean squared treatment between the fragments (MST) were provided by the output of the ANOVA. Each MST was used as a fixed mean squared error parameter in the general linear model (GLM) for further comparisons of containers samples.

Once this correction was done, three fragments from each of the beer bottles from the six-pack were analyzed by triplicate and ANOVA was performed. All six bottles were indistinguishable by elemental composition (p>0.01). The same conclusion was obtained for the four wine bottles after the statistical analysis. Figure 2.11 shows the mean values for the elemental composition of the bottles that comprises these two sets.

Furthermore, a pairwise comparison was run for the two set of bottles and also the data analysis was reprocessed for the set of 45 containers originated from different sources, using the general linear model with the fixed MSE. The six-pack can produce total of 15 comparison pairs, the four pack set 6 comparison pairs and the set of 45 containers can produce a total of 990 pairs. All of the possible 990 pairs originated from the 45-container set were distinguishable (p >0.01) using the fixed match criteria while

the bottle sets that came from the same source were indistinguishable by LA-ICP-MS (see Table 2.15), demonstrating that the MSE correction allowed the association of samples known to come from a common source and the discrimination of samples that came from different sources without including type I or II errors.
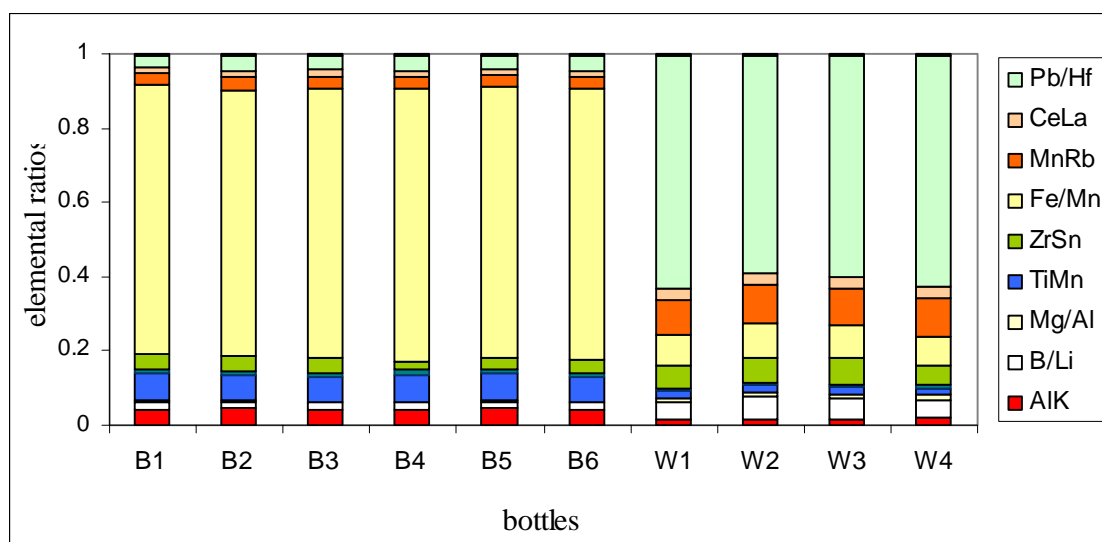
Figure 2.11 Comparison of elemental profile of six pack of beer bottles (B1 to B6) and four pack of wine bottles (W1 to W4).

Table 2.15 Relative association capabilities of LA-ICP-MS determined by pairwise comparisons of fragments originated from 6 beer bottles from the same pack and 4 wine bottles from the same pack.

Elemental Ratios	No. of undistinguishable pairs (p < 0.01) six pack beer bottles (n=6) Number of possible comparison pairs: 15	No. of undistinguishable pairs (p < 0.01) four pack wine bottles (n=4) Number of possible comparison pairs: 6
Ce/La	15	6
Fe/Mn	15	6
U/Th	15	6
Zr/Sn	15	6
Pb/Hf	15	6
Sr/Zr	15	6
B/Li	15	6
Rb/Sr	15	6
Mg/Al	15	6
Mn/Rb	15	6
Ti/Mn	15	6
All elements	15 (100% of association)	6 (100% of association)

2.2.2.1.4. Set of tempered glass

Tempered glass is another class of glass that has a tremendous importance for forensic analysis, and this study evaluated if there were differences in the elemental composition within the thickness of the fragment, especially in areas where different stages of tension were applied during the manufacturing. Four well-known and

previously characterized samples were selected from the glass database at IFRI and the elemental concentration of the top surface of each sample was compared with the elemental composition among the thickness of the fragment using student t-statistic. Table 2.16 presents the summary of results for the t-test where p values above 0.01 show no significant difference at 99% confidence level. No significant difference was found within the single fragments analyzed.

Special care should be taken when analyzing tin (Sn) in tempered glass and any other glass that has been manufactured using the "float" process, because the side that is exposed directly to the tin pool could have 25 to 50 times more content of tin than the rest of the three faces of the fragment. For example, in the tempered glass sample CFS 143 the mean value of Sn in the "float" side was 1735 μg mL^{-1} while the mean value for the other three sides was 36.90, 37.05 and 36.70 μg mL^{-1}, respectively. When the fragments recovered are big enough that they can be observed under a UV light, the non-fluorescent side should be used for analysis, if not the interpretation of tin content should be addressed carefully or not included at all.

Table 2.16 Output from t-test analysis (p values) for the comparison of elemental composition of different surface areas in the tempered glass samples CFS145, CFS 167, CFS 165 and CFS 594

Sample / ratio	CFS 143	CFS 167	CFS165	CFS 594
TiMn	0.210	0.391	0.116	0.991
CoSr	0.230	0.599	0.353	0.101
RbSr	0.288	0.628	0.241	0.551
SrZr	0.871	0.560	0.072	0.119
BaLa	0.987	0.489	0.895	0.448
CeLa	0.327	0.306	0.540	0.159
PbHf	0.060	0.060	0.611	0.014
MgAl	0.152	0.191	0.377	0.232
AlK	0.194	0.381	0.545	0.086
UTh	0.292	0.327	0.747	0.946

2.2.2.2. Evaluation of the analytical performance of LA-ICP-MS for glass analysis

2.2.2.2.1. Time and ease of analysis

According to experience in our laboratory, the analyses in triplicate of a batch of seven glass samples by conventional solution external calibration methods require at least one week from the sample preparation to the analysis and interpretation of the data. On the other hand, the same 7 glass samples can be analyzed in triplicate in only one day, including the data processing. The overall saving of time of analysis is close to 80% and that definitively represents one of the biggest advantages of using laser ablation instead of solution methods. Figure 2.17 compares the time required to complete each of the main parts of the analysis. For example, while LA sample preparation is minimum, sample preparation by solution-digestion methods involves complex steps that consume at least three days because the glass needs to be digested with a mix of acids (including HF) and later, those acids have to be slowly evaporated until dryness avoiding the loss of volatile elements as well as the contamination of the sample. The time of instrumental measurements by LA is also much faster because it only requires 50 seconds for each ablation to take place and no calibration curve is required at all. By contrast, with solution methods the whole set of samples is analyzed twice with two different calibration curves in order to be able to analyze trace and major or "high concentration" elements. In addition to that, the carry over between samples is a problem in solution methods and therefore, rinses with nitric acid are necessary after each replicate. Reagent blanks are also essential to corroborate that the batch of samples were free of contamination sources during the digestion and solution steps.
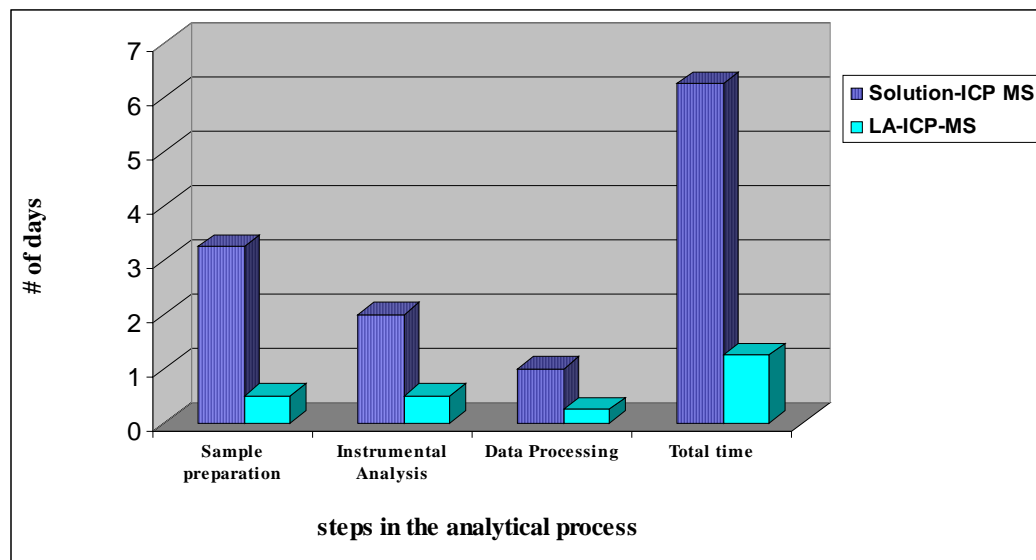
Figure 2.17 Comparison of time of analysis of glass by laser ablation and solution ICP-MS methods.

Furthermore, there are available different software packages to facilitate the data reduction of LA or even better, some of them allow on-line data reduction (i.e. GLITTER). Sometimes a bad coupling of the laser with the sample, or a random heterogeneity can cause a bad transient signal, but this can be monitored immediately and the sample analysis can be repeated, if necessary. In the case of solution methods, if for some reason one of the samples gets ruined the whole "week-based" method need to be repeated to reprocess the data. It has been also demonstrated that once the samples are into solution they have to be analyzed as soon as possible because an increase in the time elapsed between the sample preparation and the sample analysis produce a significant negative effect in some elements (Montero, 2002).

2.2.2.2.2. Repeatability, precision and accuracy

The repeatability of LA was tested in two samples of the auto window sets identified as CFS 355 and CFS 116. Five different fragments of each sample were selected randomly and each fragment was measured in triplicate. Figure 2.18 shows that good repeatability was obtained from the analysis of different pieces of glass originating from the same source.

The temporal variation was also studied by monitoring the intra and inter-day variations of the mean value for NIST 612 standards used as control samples. Four sets, each consisting in duplicates of NIST 612, were analyzed two hours apart from each other to correct for instrument drift. This experiment was performed in three consecutive days giving a total of 12 sets and 24 samples.

The mean concentration values for the NIST 612 presented inter day variation but this variation follows in a systematic fashion, therefore it can be corrected for by normalization using elemental ratios. Isotopic ratios were then used to compare between glass samples instead of single isotope concentration comparisons between samples. Figure 2.19 shows the effect in standard deviation using the ratios for ^{88}Sr and ^{90}Zr as an example of this correction by ratio. The isotopic ratios for each subset of samples were selected based on the relative standard deviation for each isotope measured as well as the detectability and discrimination power that they presented.
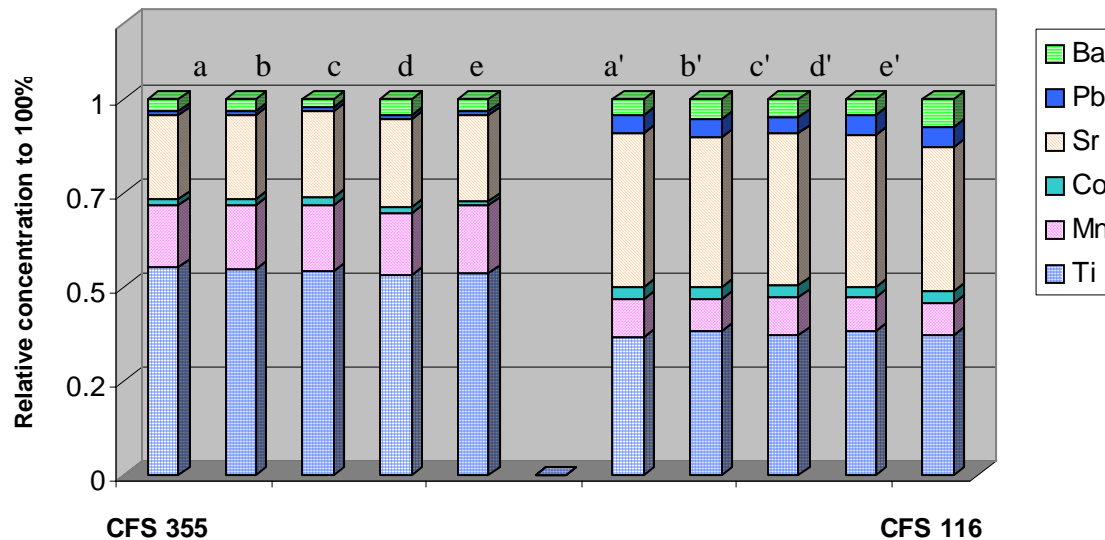
Figure 2.18 Comparison between 5 replicates of 2 different glass samples analyzed by LA-ICP-MS. Left to right, samples CFS 355 (a to e) and CFS 116 (a' to e')Comparison between 5 replicate measurements of two different glass samples analyzed by LA-ICP-MS. Left to right, samples CFS 355 (a to e) samples CFS 116 (a' to e').

Laser ablation presented good precision and accuracy when compared to EC and ID. Figure 2.20 presents the precision obtained for NIST 612 and NIST 1831 for Zr and Pb, respectively and Table 2.21 presents the comparison for all 8 of the common elements measured by the three methods.
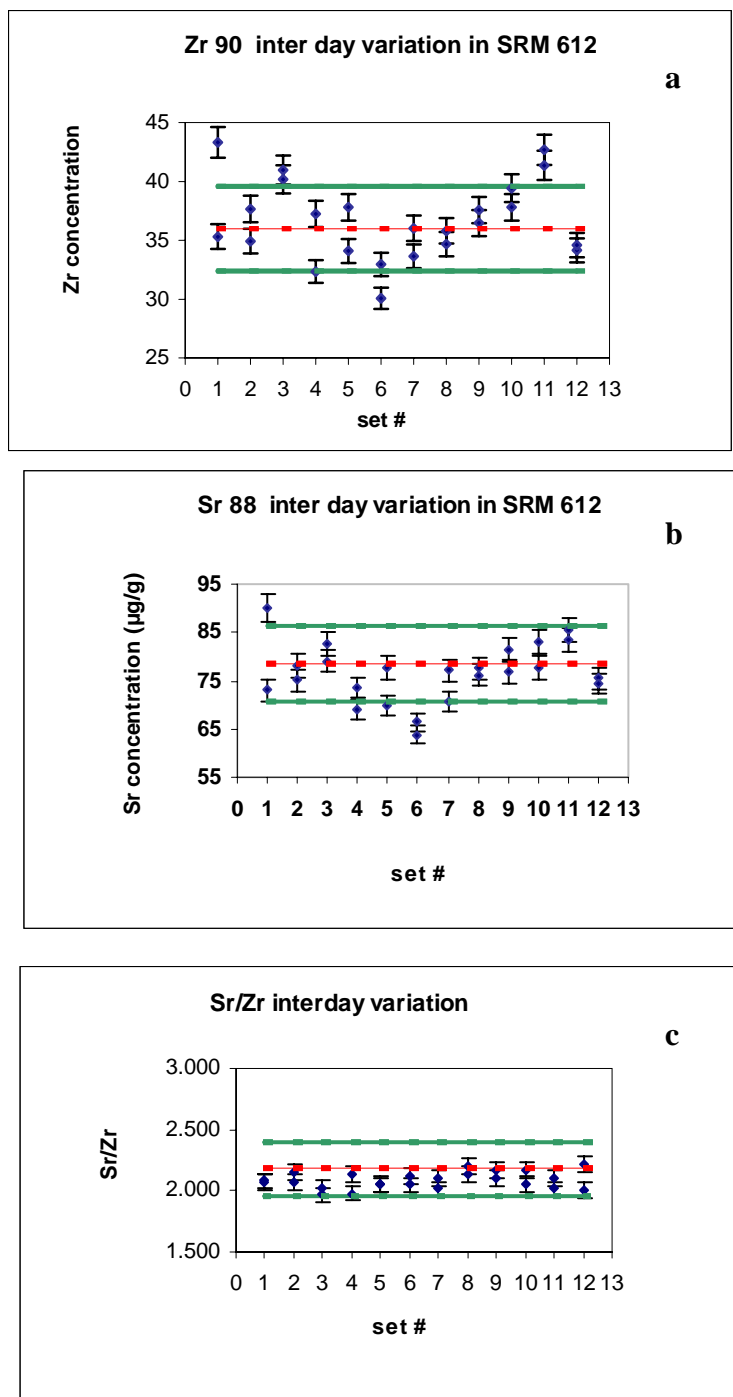
Figure 2.19 Normalization of temporal variation in SRM 612 by elemental ratios. a) [88]Sr variation, b) [90] Zr variation and c) ratio correction.

a

b
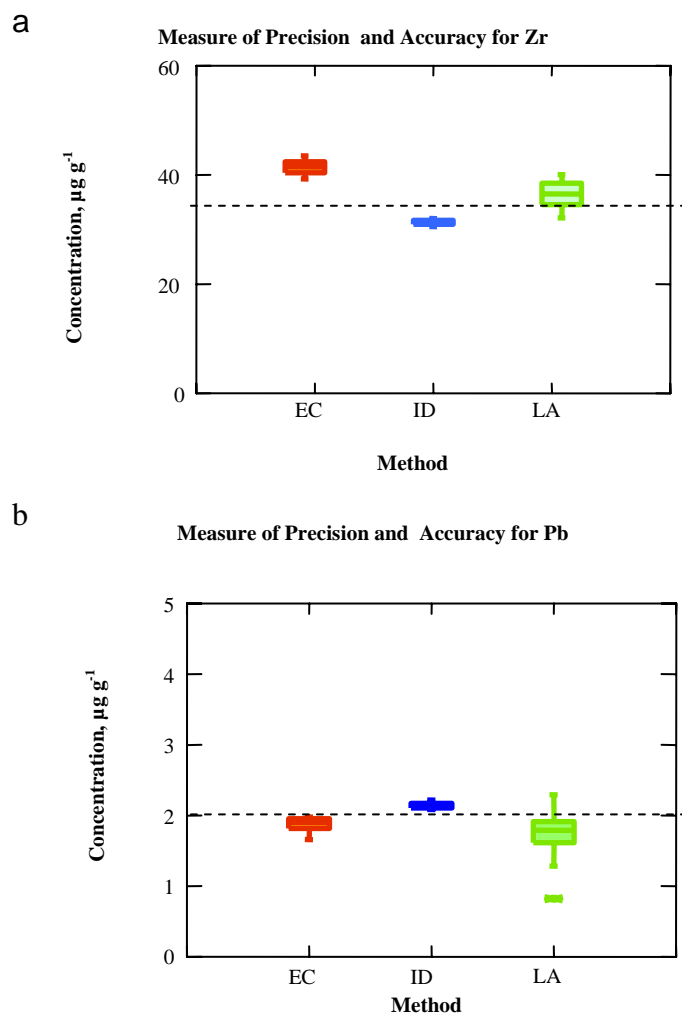
Figure 2.20 Comparison of precision and accuracy for EC, ID and LA-ICP-MS. Figure 2.20a) Zr in NIST 612 (reported value 35.99μgg^{-1} in glass Figure 2.20b) Pb in NIST 1831 (reported value 35.99 μg g^{-1}).

Table 2.21 Concentrations in μgg^{-1} for 8 elements in NIST 612 measured by EC, ID and LA-ICP-MS methods

Element	Reported value $\mu g\,g^{-1}$	EC- ICP-MS Average $\mu g\,g^{-1}$	%RSD	ID- ICP-MS Average $\mu g\,g^{-1}$	%RSD	LA- ICP-MS Average $\mu g\,g^{-1}$	%RSD
Mg	77.44[a]	60.49	3.8	66.48	4.2	78.35	7.4
Sr	78.4[b]	80.25	1.4	77.60	0.2	76.53	5.2
Zr	35.99[a]	41.32	4.2	31.68	1.1	36.66	1.3
Sb	38.44[a]	37.83	2.5	34.54	0.9	38.81	6.2
Ba	41[c]	41.76	1.7	39.44	1.6	39.22	9.3
Sm	39[c]	41.23	1.8	38.06	0.6	-	-
Hf	34.77[a]	41.32	4.9	38.28	1.0	36.27	7.3
Pb	38.57[b]	39.73	4.8	39.57	2.1	38.69	7.2

[a] reported in Geostandard Newsletter (Pearce, 1996)

[b] certified by NIST

[c] values given by NIST for information only

2.2.2.2.3. Limits of detection and sensitivity

Scanning Electron Microscopy imaging (SEM) as well as photomicrography were used to estimate the ablated mass in the standard NIST 612 calculating the volume of the ablated material. Figure 2.21 shows the SEM image of a crater resulting from the analysis of the NIST 612 using ablation parameters described before. The ablated mass in the standard was ~150 ng when the laser LSX 200 was used and this value was used to estimate the absolute detection limit values. In the case of ablations with LSX 200+ the amount of material removed per ablation was ~280 ng.

The laser ablation technique was shown to provide very low detection limits for elements of forensic interest permitting the quantitative analysis on the order of sub-picogram detection and quantification (see Table 2.22). The relative standard deviations on Table 2.22 represent the deviations for the measurements of the elements at the concentration level present in the reference material NIST 612 (~ 40 µgg^{-1}). All the selected elements presented relative standard deviations below 10%.
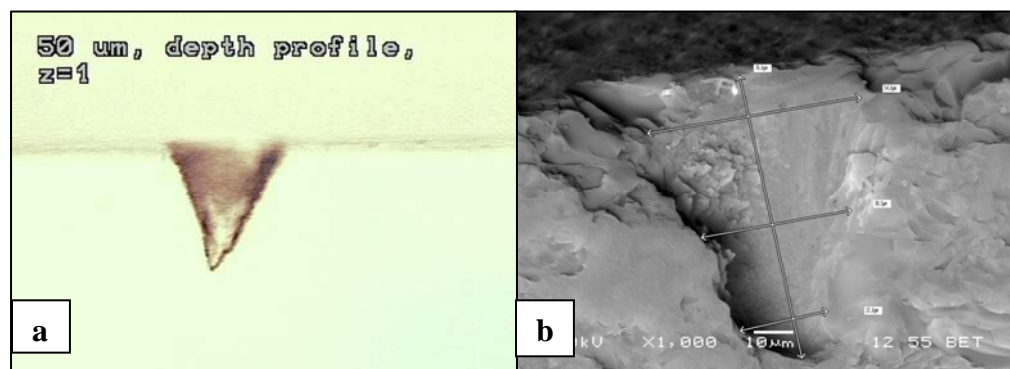
Figure 2.21 From top to bottom, a) Light microscope image of crater from ablation of NIST 612 (100x magnification). b) SEM of NIST 612 (1000x magnification)

Table 2.22 LA-ICP-MS limits of detection for SRM 612 using LSX 200.

Isotope measured	Element	LOD (µg/g)	LOD (pg)	%RSD (~ 40 µg/g in glass)
^{49}Ti	Ti	4.1	1.1	5.3
^{55}Mn	Mn	0.8	0.2	3.4
^{71}Ga	Ga	0.4	0.1	7.6
^{88}Sr	Sr	0.2	0.05	3.9
^{90}Zr	Zr	0.4	0.1	6.9
^{118}Sn	Sn	1.1	0.3	7.6
^{133}Cs	Cs	0.1	0.03	7.2
^{137}Ba	Ba	1.2	0.3	6.2
^{140}Ce	Ce	0.1	0.04	5.8
^{178}Hf	Hf	0.6	0.2	3.0
$^{\mathrm{sum\ (204,\ 206,\ 208)}}$Pb	Pb	0.2	0.06	7.6

2.2.2.2.4. Discrimination power: evaluation of subsets of glass samples

The set of forty-five headlamp samples was characterized by elemental analysis using 20 isotopes and 14 isotope ratios. The automotive glasses were characterized using 12 isotope ratios consisting of the analysis of 20 isotopes and the container glasses were studied using 19 isotopes and 13 isotope ratios.

In order to test the discrimination power (or informing power) of LA-ICP-MS, a total of 131 different glass samples were used for the comparison study. The informing power of the LA-ICP-MS technique was compared to the informing power of refractive index and to that of the solution-ICP-MS results, using analysis of variance (ANOVA), pair-wise comparisons and Tukey's HSD test. The combined discrimination power of two or more elements was found by sequentially applying Tukey's test to the subset of samples. The number of indistinguishable pairs in the glass samples was used to evaluate the discriminating power of each technique. The lower the number of indistinguishable pairs found in the headlamp and automobile sets, the better the informing power of the elemental composition measured by the technique.

The number of indistinguishable pairs of glass samples using the elemental composition by EC and the values from RI measurements is shown in Tables 2.23 to 2.28. Each reported refractive index value was the result of the mean of the measurements from five subsets/portions of a given fragment. Three of the forty five-samples of headlamps had a refractive index that could not be measured by the oils used. The remaining forty-two samples would form 861 possible comparison pairs or $n(n-1)/2$ pairs where n is the number of samples. When only refractive index is used, 102 of those pairs cannot be distinguished (11.9% of the pairs) for a $p=0.05$. For the CFS set, the number of possible comparison pairs was 1035, and 471 from those pairs (45%) were indistinguishable by RI. In the case of containers, 328 of 990 possible comparison pairs were indistinguishable by RI (33%).

The combination of elemental analysis and refractive index enhanced the informing power. In the CFS and containers subset only 1 and 2 of the possible pairs respectively were undistinguishable (0.01% and 0.02% of the pairs). In the headlamp subset all 990 pairs were distinguished. A summary of the results for the discrimination power of each of the elements is presented in Tables 2.23 to 2.28.

Four of the CFS samples (2 pairs) were selected from the casework automotive windows to be analyzed by the ID-ICP-MS method. The ID-ICP-MS method showed better precision than that obtained with EC-ICP-MS for most of the elements. One of the pairs was distinguished by EC and ID methods but the other was not discriminated even with the improved precision of the ID-ICP-MS method. The glass samples that comprised that indistinguishable pair were collected from very similar sources, from automobiles of make "Oldsmobile", manufactured by General Motors during 1987 and assembled in the same plant combination (Detroit, MI / Oshawa #1, Canada, suggesting a common source of origin of the glass (Montero, 2002). For the headlamps subset all samples were distinguished by EC, ID and LA. Laser ablation also provided discrimination power comparable to the external calibration and isotope dilution methods. Using only elemental composition by laser ablation, 7 of the CFS pairs, 5 of the containers and 21 of the headlamps were not distinguishable (0.7%, 0.5% and 2.1% of the pairs, respectively). When the results of elemental composition were combined with refractive index, just 3 of the 1035 pairs of automobile windows were indistinguishable by laser ablation (0.3%) and all the headlamp and container possible comparison pairs were distinguished.

Table 2.23 Relative discrimination capabilities of RI and EC-ICP-MS determined by pairwise comparisons of 45 headlamp glasses (990 comparisons) using Tukey's test.

Number of Samples: 45 Number of possible comparison pairs:990	No. of undistinguishable pairs ($p < 0.05$)
Mg	947
Ga	904
Pb	903
Sr	903
Ba	903
Sb	864
Mn	852
Ce	796
La	624
Sm	545
Ti	440
Hf	199
Zr	130
RI	102 *
All elements	44 (4.4 %)
All elements + RI	8 (0.8%)
All elements + RI after t-tests	0

* 102 pairs out of 861 possible pairs were not distinguished when compared by the RI measured.

Table 2.24 Relative discrimination capabilities of RI and LA-ICP-MS determined by pairwise comparisons of 45 headlamp glasses (990 comparisons) using Tukey's test.

Number of Samples: 45 Number of possible comparison pairs:990	No. of undistinguishable pairs($p < 0.05$)
Pb/Hf	941
Ca/K	898
Ba/La	856
Sr/Ce	856
Al/Mg	777
Fe/Ga	652
Zr/Hf	642
Ti/Mn	601
Sr/Rb	576
B/Mn	496
Zr/Sr	327
B/Li	264
RI	102 *
All elemental ratios	21 (2.1%)
All elemental ratios + RI	0

* 102 pairs out of 861 possible pairs were not distinguished when compared by the RI measured.

102

Table 2.25 Relative discrimination capabilities of RI and EC-ICP-MS determined by pairwise comparisons of 46 automobile glasses (1035 comparisons) using Tukey's test.

Number of Samples: 46 Number of possible comparison pairs:1035	No. of undistinguishable pairs $(p < 0.05)$
Rb	903
Sm	868
Ba	769
Ti	691
Pb	673
Ce	537
Mn	427
Sr	416
Hf	214
Zr	100
RI	494
	(49.9%)
All elements	43
	(4.2%)
All elements + RI	27
	(2.6%)
All elements + RI after t-tests	1 (0.01%)

Table 2.26 Relative discrimination capabilities of RI and LA-ICP-MS determined by pairwise comparisons of 46 automobile glasses (1035 comparisons) using Tukey's test.

Number of Samples: 46 Number of possible comparison pairs:1035	No. of undistinguishable pairs ($p < 0.05$)
Ti / Mn	985
U / Th	861
Ce / La	821
Rb / Sr	819
Zn / La	741
Pb / Hf	673
Hf / Ba	598
Ba / La	504
Al / K	365
Ca / K	357
Co / Sr	336
Fe / Mn	335
Mg / Al	309
Sr / Zr	132
RI	494 (49.9%)
All elemental ratios	7 (0.7%)
All elemental ratios + RI	3 (0.3%)

Table 2.27 Relative discrimination capabilities of RI and EC-ICP-MS determined by pairwise comparisons of 45 container glasses (990 comparisons) using Tukey's test.

Number of Samples: 45 Number of possible comparison pairs:990	No. of undistinguishable pairs ($p < 0.05$)
Ba	944
Hf	518
Rb	478
Sm	417
Zr	332
Mg	265
Pb	264
La	260
Cu	185
Mn	127
Sr	97
Ti	82
RI	328
	(33.1%)
All elements	7
	(0.7%)
All elements + RI	2 (0.2%)

Table 2.28 Relative discrimination capabilities of RI and LA-ICP-MS determined by pairwise comparisons of 45 containers (90 comparisons) using Tukey's test.

Number of Samples: 45 Number of possible comparison pairs: 990	No. of undistinguishable pairs ($p < 0.05$)
Ba/La	892
Ce/La	672
U/Th	655
Zr/Sn	587
Sr/Zr	539
Mn/Rb	488
Fe/Mn	484
B/Li	458
Pb/Hf	407
Ti/Mn	335
Rb/Sr	251
Mg/Al	160
Al/K	153
RI	328
	(33.1%)
All elements	5 (0.5%)

2.2.2.2.5. *Ruggedness test*

The final step for the evaluation of the analytical performance of the method was the ruggedness test. Ruggedness tests are used to find the variables that could strongly influence the measurements provided by the test method and should precede an interlaboratory study (round robin). Without a ruggedness test the precision of a round robin may be poor because the critical values are not properly restricted or controlled.

Eight experiments using SRM NIST 612 were conducted in two different days to evaluate the seven factors described on section 2.2.1.4.7 taking into account any variability within days. The statistical calculations defined by the ASTM method (ASTM 2001) estimate a "t" statistical value for each of the isotopes of interest and for each of the selected factors individually. Each t value can be compared to the t critical value, which is equal to 3.50 for n=8 and 7 degrees of freedom (p<0.01) so if the t estimated is lower than the t critical the factor is rugged with a 99% of probability. In other words, if t estimated is lower than 3.50 for a selected factor, it does not represent a variable that should be strictly controlled during the experiment in order to acquire reproducible data.

Table 2.29 shows the "t" estimated values for all isotopes and factors selected for this study. All values were lower than 3.50 and therefore the method proposed for glass analysis demonstrated to be rugged.

Table 2.29 Statistical "t" values estimated for the factors and isotopes of interest

t values obtained from the ruggedness test study									
Factor	Li	B	Mg	Al	K	Ti	Mn	Ga	Rb	Sr
A (spot size)	0.11	0.29	-1.47	0.96	0.81	-0.66	0.20	-0.57	-0.65	0.58
B (Energy)	1.19	-1.97	-0.41	-0.91	-0.24	1.22	-0.38	-0.63	-0.38	0.14
C (Frequency)	0.50	-0.49	1.01	-0.06	0.28	-0.93	-3.15	-1.58	-0.66	-0.59
D (Ar flow)	-0.33	-0.41	2.37	0.39	-0.17	0.15	-2.70	-1.72	-1.19	-0.48
E(He flow)	0.20	-0.43	-2.19	0.04	-0.60	0.38	1.31	1.38	1.37	1.53
F(ablation time)	1.35	-2.15	-0.61	-1.46	-0.30	0.08	-0.88	-0.48	-0.74	-0.19
G(defocus)	-0.85	0.37	0.56	-0.25	-0.94	-1.62	1.24	1.33	1.53	1.44

t values obtained from the ruggedness test study									
Factor	Zr	Sn	Sb	Ba	La	Hf	Ce	Pb	Th	U
A (spot size)	0.50	0.86	1.03	2.24	0.13	2.08	0.30	-0.07	0.53	0.40
B (Energy)	0.80	1.02	1.21	-0.16	-0.38	0.94	0.44	0.37	0.47	0.04
C (Frequency)	-0.36	0.34	-0.08	-1.16	-0.62	-1.02	-0.54	-1.29	0.06	-1.40
D (Ar flow)	-0.08	0.08	-0.17	-0.09	-0.13	0.21	0.40	-0.97	0.51	1.29
E(He flow)	1.08	1.49	1.51	1.69	0.52	0.95	0.37	1.44	0.26	0.49
F(ablation time)	0.49	0.33	0.75	-0.56	-0.77	0.06	0.18	-1.09	-0.36	0.27
G(defocus)	0.83	0.87	2.14	1.29	0.57	0.54	0.69	1.93	-0.09	0.71

2.2.3. Conclusions

Laser ablation has been thoroughly evaluated in the last decade; more than 150 papers have been published, including applications as well as improvements in designs of the laser systems. Nevertheless, the technique is fairly new in the forensic arena and therefore a good analytical performance, as well as a great capability of offering good discrimination between samples that originated from different sources, are desirable to assist its acceptance in court. The core objective of this work was to evaluate LA-ICP-MS and provide enough scientific support to facilitate its incorporation into the judicial system.

The strategy designed to accomplish this objective for glass analysis consisted in the comparison of LA-ICP-MS with other well accepted techniques for forensic examination of glass, such as solution ICP-MS (external calibration and isotope dilution). A total of 131 different samples, originating from glass types typically collected at crime scenes, were used for the comparison study. Results showed that LA-ICP-MS provided good precision, accuracy and discrimination power comparable to those obtained with the conventional solution ICP-MS methods.

Sampling methodologies and match criterion were proposed based on careful evaluation of the homogeneity of elemental composition of glass within single sources, including containers, windshields, architectural and tempered glasses. In general terms, a good characterization of the "known" source is very important to perform comparisons versus the recovered fragments from scenes, suspects, and/or victims. This is particularly significant for containers due to their high variation within a single source that could lead to a false discrimination if the proper statistical tools are not applied.

It was also found that some of the glass panes from a windshield (outside vs. inside) could have a different elemental profile. Hence, it is essential to sample fragments from both windowpanes in order to avoid misinterpretation of the results. Tempered glass was found to have an even distribution of the elemental composition within the thickness of the fragment, even though some differences in refractive index have been reported as a result from the manufacturing process. Glass samples that have been processed using the "float" method have a higher content of tin on the float side, an aspect that needs to be considered for comparison purposes. As a rule of thumb, as many fragments as practical need to be collected at the crime scene and analyzed in order to facilitate a good characterization of the "known" source and provide a comparison of the elemental "fingerprint" of glass supported by statistical tools.

In brief, it was demonstrated that LA-ICP-MS of glass has enough tools to support its integration to the forensic field. It offers a simpler, faster and a less destructive sample introduction to the forensic examiner than conventional digestion methods and also offers a high discriminating power.

2.3. DISCRIMINATION STUDIES TO EVALUATE THE DISCRIMINATION POWER OF LA-ICP-MS

2.3.1. Methodology

2.3.1.1. LA-ICP-MS with matrix-match standard

A laser ablation (LA)-ICP-MS method for elemental analysis of glass was developed with the use of standard reference materials (SRMs) NIST 612 (National

Institute of Standards and Technology, Gaithersburg, USA) and FGS02 (Bundeskriminalamt, Forensic Science Institute/Germany). Five sample sets were analyzed with two different LA-ICP-MS systems to determine the utility of the method for the association /discrimination of glass samples. Sample set # 1 is composed of 37 sheet glass samples with a range of refractive index values between 1.5184 and 1.5185 from an FDLE collection of casework samples (Table 2.32), the sample set # 2 is composed of 49 samples of clear float glass with a range of refractive index values between 1.51817 to 1.51905 that were manufactured in Cardinal, one of the plants in the United States (Table 2.33), sample set # 3 includes 69 samples of glass with refractive indices between 1.51734 – 1.52327 manufactured in seven different plants in the United States (Table 2.34), sample set # 4 includes a total of 52 samples collected from 41 different vehicles that were manufactured between 1984 and 1994 (Table 2.35) and sample set # 5 is composed by 41 samples of glass collected from 14 crashed vehicles in junkyards in Miami (Table 2.36). The first 21 samples of sample set #1 were analyzed to do a comparison of different analytical techniques. Sample set #2 was collected May 1997 to September 2001 to assess the variability of elemental composition within a same manufacturing plant. Sample set #3 was collected from October 1994 to May 1996 to do a study of the seven different manufacturing plants. Sample sets #4 and #5 were used to update the FIU glass database.

Table 2.32 Sample Set # 1: FDLE Samples

Sample	Color	Thickness	Float	Temper	Source
W 23	Blue-Green	5.95	Yes	Yes	Vehicle side window
W 33	Green	4.75	Yes	Yes	Vehicle side window
W 49	Colorless	2.40	Yes	No	Store window
W 62	Colorless	2.15	Yes	No	Hardware store window
W 79	Light green	5.79	Yes	No	Store plate glass (J.C. Penny Winter
W 83	Blue-Green	3.95	Yes	Yes	Vehicle side window
W 95	Blue-Green	3.95	Yes	Yes	Vehicle side window
W 103	Green	4.81	Yes	Yes	Vehicle side window
W 107	Green	4.93	Yes	Yes	Vehicle side window
W 129	Brown	4.87	No	Yes	Sliding glass door
W 132	Colorless	5.61	Yes	No	Display case
W 142	Colorless	2.69	Yes	No	Laminated windshield (outside of
W 143	Colorless	2.69	Yes	No	Laminated windshield (inside of
W 152	Light green	5.82	Yes	No	Bathroom window (outer pane)
W 153	Colorless	4.75	No	No	Bathroom window patterned (inner
W 165	Brown	4.73	Yes	Yes	Store window
W 174	Blue	4.89	Yes	Yes	Vehicle side window
W 193	Blue-Green	4.08	Yes	Yes	Vehicle rear window
W 204	Gray	5.68	Yes	No	Store window
W 206	Light blue	5.69	Yes	No	Store window
W 232	Light blue	5.63	Yes	No	Business window
W 248	Colorless	2.20	Yes	No	Residence window
W 255	Brown	5.68	Yes	Yes	Business window
W 259	Brown	4.72	Yes	Yes	Business window
W 266	Colorless	4.68	Yes	No	Business window
W 285	Brown	5.74	Yes	Yes	Business window
W 319	Colorless	2.64	Yes	No	Laminated store window
W 320	Colorless	2.64	Yes	No	Laminated store window
W 323	Blue-Green	4.17	Yes	Yes	Vehicle side window
W 340	Blue-Green	4.90	Yes	Yes	Vehicle side window
W 350	Blue	3.97	Yes	Yes	Vehicle side window
W 351	Blue	3.55	Yes	Yes	Vehicle rear window
W 352	Colorless	3.19	No	No	Business window (garage door)
W 360	Colorless	2.29	Yes	No	Laminated business door (outside)
W 368	Colorless	2.64	Yes	No	Residence window
W 383	Colorless	2.16	Yes	No	Residence window
W 399	Gray	5.80	No	Yes	Business door

Table 2.33 Sample Set # 2: Cardinal Plant Study

Sample	Glass Type	Sub Type	Source	Sample Description	Color	RI
970516	Float	Window	Cardinal	5/16/1997	Clear	1.51848
970715	Float	Window	Cardinal	7/15/1997	Clear	1.51817
970718	Float	Window	Cardinal	7/18/1997	Clear	1.51841
970817	Float	Window	Cardinal	8/17/1997	Clear	1.51840
970916	Float	Window	Cardinal	9/16/1997	Clear	1.51837
971015	Float	Window	Cardinal	10/15/1997	Clear	1.51838
971115	Float	Window	Cardinal	11/15/1997	Clear	1.51840
971215	Float	Window	Cardinal	12/15/1997	Clear	1.51841
980114	Float	Window	Cardinal	1/14/1998	Clear	1.51835
980215	Float	Window	Cardinal	2/15/1998	Clear	1.51817
980415	Float	Window	Cardinal	4/15/1998	Clear	1.51878
980517	Float	Window	Cardinal	5/17/1998	Clear	1.51897
980614	Float	Window	Cardinal	6/14/1998	Clear	1.51880
980717	Float	Window	Cardinal	7/17/1998	Clear	1.51870
980812	Float	Window	Cardinal	8/12/1998	Clear	1.51869
980920	Float	Window	Cardinal	9/20/1998	Clear	1.51881
981114	Float	Window	Cardinal	11/14/1998	Clear	1.51902
990115	Float	Window	Cardinal	1/15/1999	Clear	1.51882
990315	Float	Window	Cardinal	3/15/1999	Clear	1.51901
990414	Float	Window	Cardinal	4/14/1999	Clear	1.51894
990520	Float	Window	Cardinal	5/20/1999	Clear	1.51895
990611	Float	Window	Cardinal	6/11/1999	Clear	1.51905
990710	Float	Window	Cardinal	7/10/1999	Clear	1.51898
990819	Float	Window	Cardinal	8/19/1999	Clear	1.51895
990914	Float	Window	Cardinal	9/14/1999	Clear	1.51884
991018	Float	Window	Cardinal	10/18/1999	Clear	1.51902
991124	Float	Window	Cardinal	11/24/1999	Clear	1.51889
991213	Float	Window	Cardinal	12/13/1999	Clear	1.51901
991213	Float	Window	Cardinal	12/13/1999	Clear	1.51878
000101	Float	Window	Cardinal	1/1/2000	Clear	1.51887
000118	Float	Window	Cardinal	1/18/2000	Clear	1.51879
000201	Float	Window	Cardinal	2/1/2000	Clear	1.51865
000224	Float	Window	Cardinal	2/24/2000	Clear	1.51892
000301	Float	Window	Cardinal	3/1/2000	Clear	1.51890
000327	Float	Window	Cardinal	3/27/2000	Clear	1.51877
000401	Float	Window	Cardinal	4/1/2000	Clear	1.51878
000416	Float	Window	Cardinal	4/16/2000	Clear	1.51882
000501	Float	Window	Cardinal	5/1/2000	Clear	1.51876
000601	Float	Window	Cardinal	6/1/2000	Clear	1.51875
001001	Float	Window	Cardinal	10/1/2000	Clear	1.51870
001101	Float	Window	Cardinal	11/1/2000	Clear	1.51862
001201	Float	Window	Cardinal	12/1/2000	Clear	1.51874
010101	Float	Window	Cardinal	1/1/2001	Clear	1.51880
010201	Float	Window	Cardinal	2/1/2001	Clear	1.51886
010301	Float	Window	Cardinal	3/1/2001	Clear	1.51866

Sample	Glass Type	Sub Type	Source	Sample Description	Color	RI
010401	Float	Window	Cardinal	4/1/2001	Clear	1.51870
010501	Float	Window	Cardinal	5/1/2001	Clear	1.51875
010601	Float	Window	Cardinal	6/1/2001	Clear	1.51885
010701	Float	Window	Cardinal	7/1/2001	Clear	1.51857
010801	Float	Window	Cardinal	8/1/2001	Clear	1.51876

Table 2.34 Sample Set # 3: Different Manufacturing Plants Study

Sample	Glass Type	Sub Type	Source	Sample Description	Color	RI
107	Float	2.5 mm	PPG	Oct/94, Line 1, Right, Wks #6	Clear	1.51845
108	Float	2.5 mm	PPG	Oct/94, Line 1, Center, Wks #6	Clear	1.51855
109	Float	2.5 mm	PPG	Oct/94, Line 1, Left, Wks #6	Clear	1.51849
110	Float	.125 inches	PPG	Oct/94, Line 2, Right, Wks #6	Clear	1.51857
111	Float	.125 inches	PPG	Oct/94, Line 2, Center, Wks #6	Clear	1.51857
112	Float	.125 inches	PPG	Oct/94, Line 2, Left, Wks #6	Clear	1.51860
113	Float	6.0 mm	PPG	March/95, Line 1, Right, Wks #6	Clear	1.51865
114	Float	6.0 mm	PPG	March/95, Line 1, Center, Wks #6	Clear	1.51866
115	Float	6.0 mm	PPG	March/95, Line 1, Left, Wks #6	Clear	1.51871
116	Float	2.5 mm	PPG	March/95, Line 2, Right, Wks #6	Clear	1.51850
223	Float	Window	Guardian	AFG, 3/32	Clear	1.51881
224	Float	Window	Guardian	Carelton, 3/16	Green	1.52087
225	Float	Window	Guardian	Crepe, 1/8	Bronze	1.52195
226	Float	Window	Guardian	Carelton, 1/4	Green	1.52164
227	Float	Window	Guardian	Crepe, 1/8	Clear	1.52309
228	Float	Window	Guardian	Spraylite, 3/16	Clear	1.52246
229	Float	Window	Guardian	AFG, Crepe, 3/16	Clear	1.51898
230	Float	Window	Guardian	AFG, Crepe, 3/16	Clear	1.52276
231	Float	Window	Guardian	SSB	Floreffe	1.52052
232	Float	Window	Guardian	AFG, 1/8	Clear	1.51858
233	Float	Window	Guardian	Nazareth, 1/8	Clear	1.52009
234	Float	Window	Guardian	Floreffe, 1/8	Green	1.52066
235	Float	Window	Guardian	SSB, Richborg	Clear	1.52013
236	Float	Window	Guardian	AFG, 1/8, Crepe	Clear	1.51874

Sample	Glass Type	Sub Type	Source	Sample Description	Color	RI
237	Float	Window	Guardian	SSB, Crepe	Clear	1.52233
238	Float	Window	Guardian	AFG, 3/16	Gray	1.51740
239	Float	Window	Guardian	PPG, 3/16	Bronze	1.51943
240	Float	Window	Guardian	CGM, 7/32, Laminated	Clear	1.52016
241	Float	Window	Guardian	AFG, 1/4	Bronze	1.51823
242	Float	Window	Guardian	AFG, 1/4	Gray	1.51826
243	Float	Window	Guardian	LOF, 1/8	Gray	1.51834
244	Float	Window	Guardian	AFG, 1/8	Gray	1.51826
245	Float	Window	Guardian	AFG, 1/4	Gray	1.51824
247	Float	Window	Guardian	PPG, 1/4	Bronze	1.51975
248	Float	Window	Guardian	PPG, 1/8	Bronze	1.51980
249	Float	Window	Guardian	AFG, 1/8	Bronze	1.51955
250	Float	Window	Guardian	SSB, Richborg, 1/8	Bronze	1.51814
281	Float	Window	PPG, 3.3mm	Owensound Plant (4/95)	Clear	1.51828
283	Float	Window	PPG,	Fresno Plant (4/95)	Clear	1.51771
285	Float	Window	PPG	Mt 210N Illinois Plant	Clear	1.51883
515	Float	Window	PPG	6-2c 01-08-96	Clear	1.51864
522	Float	Window	PPG	L/wks#6 Tk2 05-30-96	Clear	1.51868
605	Float	Window	Ford	Dearborn, Michigan, 11/95	Clear	1.52014
606	Float	Window	LOF	Laurinburg, North Carolina, 1/9/96	Clear	1.51894
607	Float	Window	LOF	Ottawa, IL 1/4/96	Clear	1.51908
608	Float	Window	LOF	Rassford, Ohio, 1/3/96	Clear	1.52324
609	Float	Window	LOF	Lathrop, California 5/14/96	Clear	1.51918
610	Float	Window	PPG	Perry, Georgia, 1995	Clear	1.52269
611	Float	Window	PPG	Carlisle, Pa AP-11/95	Clear	1.51858
612	Float	Window	PPG	Carlisle, Pa AQ-11/95	Clear	1.51865
613	Float	Window	PPG	Mt.Zion, IL AV-11/95	Clear	1.51874
614	Float	Window	PPG	Mt. Zion, IL AY-11/95	Clear	1.52258
615	Float	Window	PPG	Meadville, Pa BB-8/95	Clear	1.52253
616	Float	Window	PPG	Meadville, Pa BG-9/95	Clear	1.52327
617	Float	Window	PPG	Crestline, Oh 11/95	Clear	1.51785
618	Float	Window	Guardian	Richburg, S.C 1-New	Clear	1.52058
619	Float	Window	Guardian	Richburg, S.C 2-Old	Clear	1.52023
620	Float	Window	AFG	Cinnaminson, NJ 9/95	Clear	1.51899
621	Float	Window	LOF	Ottawa, Canada 8/95	Clear	1.51782
622	Float	Window	Guardian	Rogers, Ark. 8/95	Clear	1.51874
623	Float	Window	AFG	Greenland, Tx 10/95	Clear	1.51734
624	Float	Window	HGP	Tampa, Fl 9/95	Clear	1.51849
625	Float	Window	Guardian	Corsicana, Tx 9/95	Clear	1.52045

Sample	Glass Type	Sub Type	Source	Sample Description	Color	RI
626	Float	Window	HGP	Houston Tx 8/95	Clear	1.51957
627	Float	Window	LOF	Laurinburg, N.C 8/95	Clear	1.51904
628	Float	Window	LOF	Lathrop Ca. 9/95	Clear	1.51854
629	Float	Window	LOF	Lathrop Ca.8/4/94	Clear	1.51906
630	Float	Window	HGP	Phoenix, Arizona 8/95	Clear	1.51771
631	Float	Window	PPG	Wichita Falls, Tx 98-11/95	Clear	1.51887

Table 2.35 Sample Set # 4: Vehicles 1984-1994 Dataset

Sample	Glass Type	Subtype	Source	Description	Color	RI
427	Float	Automobile	'90 Civic	Rear	Clear	1.51901
435	Float	Automobile	'93 Nissan Sentra	Windshield	Clear	1.51889
445	Float	Automobile	'88 Cadillac Seville		Clear	1.51903
492	Float	Automobile	'91 Cadillac Seville		Clear	1.51911
127	Vehicle Window	Tempered	Camaro	Junk Yard	Slightly Green	1.51929
128	Vehicle Window	Tempered	Ford Mustang	Junk Yard	Slightly Green	1.51993
129	Vehicle Window	Tempered	'89 Ford Mustang	Junk Yard	Slightly Green	1.51972
415	Float	Automobile	'91 Accord (a1)	Back	Clear	1.51916
419	Float	Automobile	'90 Isuzu Pick-Up	Side	Clear	1.51931
425	Float	Automobile	'91 Accord	Back	Clear	1.51925
426	Float	Automobile	'90 Civic	Windshield	Clear	1.51994
431	Float	Automobile	'89 Mazda 626	Side	Clear	1.51977
434	Float	Automobile	'85 Toyota Celica		Clear	1.52004
437	Float	Automobile	'94 Mazda MX3	Rear	Clear	1.51978
439	Float	Automobile	'87 Nissan Stanza	Windshield	Clear	1.51973
441	Float	Automobile	'93 Toyota Corolla	Outside	Clear	1.51935
443	Float	Automobile	'90 Isuzu Pick-up		Clear	1.51931
456	Float	Automobile	'91 Mercury Capri		Clear	1.52003
462	Float	Automobile	'93 Toyota Corolla	Inside	Clear	1.51937
466	Float	Automobile	'90 Buick Century		Clear	1.51958
471	Float	Automobile	'94 Dodge Minivan		Clear	1.52001
483	Float	Automobile	'94 Dodge Van		Clear	1.52000
485	Float	Automobile	'90 Pontiac APV Van		Clear	1.51991
424	Float	Automobile	'91 Accord	Windshield	Clear	1.52016
442	Float	Automobile	'84-'87 Honda Civic	Replace	Clear	1.52016
448	Float	Automobile	'91 Subaru XT		Clear	1.52021
458	Float	Automobile	'90 Honda Prelude		Clear	1.52009

115

Sample	Glass Type	Subtype	Source	Description	Color	RI
460	Float	Automobile	'94 Mercury Villager		Clear	1.52025
467	Float	Automobile	'91 Ford Thunderbird		Clear	1.52013
472	Float	Automobile	'90 Mitsubishi Mirage		Clear	1.52023
474	Float	Automobile	'95 Dodge Van		Clear	1.52024
476	Float	Automobile	'95 Dodge Daytona		Clear	1.52033
478	Float	Automobile	'90-'93 Subaru Legacy	Replace	Clear	1.52016
481	Float	Automobile	'92 Ford F-150 Pick-up		Clear	1.52012
494	Float	Automobile	'91 Toyota Previa		Clear	1.52018
496	Float	Automobile	'89 Ford Mustang		Clear	1.52032
497	Float	Automobile	'92 GMC Yukon		Clear	1.52007
446	Float	Automobile	'89 Ford Mustang		Clear	1.52044
457	Float	Automobile	'94 Ford Crown Victoria		Clear	1.52052
465	Float	Automobile	'90 Ford Mustang		Clear	1.52040
470	Float	Automobile	'90 Buick Century		Clear	1.52046
480	Float	Automobile	'94 Dodge Neon		Clear	1.52048
490	Float	Automobile	'94 Mazda 626		Clear	1.52037
493	Float	Automobile	'92 Ford F150 Pick-up		Clear	1.52047
495	Float	Automobile	'93 Ford Astro Van		Clear	1.52044
450	Float	Automobile	'94 Dodge Van		Clear	1.52058
454	Float	Automobile	'90 Dodge Daytona		Clear	1.52058
459	Float	Automobile	'89 Mazda Pick-up		Clear	1.52056
468	Float	Automobile	'88-'91 Honda CRX	Replace	Clear	1.52091
473	Float	Automobile	'89 Cadillac Deville		Clear	1.52052
486	Float	Automobile	'91 Honda Accord		Clear	1.52053
489	Float	Automobile	'94 Ford Thunderbird		Clear	1.52087

116

Table 2.36 Sample Set # 5: Vehicles 1995-2004 Dataset

Sample	Make	Model	Year	Source	Glass type	Glass color
1	GMC	Jimmy	1998	Inner windshield	Float	Green
2	GMC	Jimmy	1998	Outer windshield	Float	Green
3	Mitsubishi	Galant ES	2000	Front window	Tempered	Green
4	Mitsubishi	Galant ES	2000	Outer windshield	Float	Green
5	Mitsubishi	Galant ES	2000	Inner windshield	Float	Green
6	Chevrolet	Cavalier	2004	Outer windshield	Float	Green
7	Chevrolet	Cavalier	2004	Inner windshield	Float	Green
8	Chevrolet	Cavalier	2004	Side window	Tempered	Green
9	Chevrolet	Cavalier	2004	Rear window	Tempered	Green
10	Oldsmobile	Intrigue	1998	Rear window	Tempered	Green
11	Oldsmobile	Intrigue	1998	Outer windshield	Float	Green
12	Oldsmobile	Intrigue	1998	Inner windshield	Float	Green
13	Dodge	Neon	2000	Outer windshield	Float	Green
14	Dodge	Neon	2000	Inner windshield	Float	Green
15	Dodge	Neon	2000	Front window	Tempered	Green
16	Dodge	Neon	2000	Rear window	Tempered	Green
17	KIA	Spectra GS	2002	Outer windshield	Float	Green
18	KIA	Spectra GS	2002	Inner windshield	Float	Green
19	Chevrolet	Cavalier	2003	Rear window	Tempered	Green
20	Chevrolet	Cavalier	2003	Outer windshield	Float	Green
21	Chevrolet	Cavalier	2003	Inner windshield	Float	Green
22	Chevrolet	Cavalier	2003	Front window	Tempered	Green
23	Dodge	Stratus	1998	Outer windshield	Float	Green
24	Dodge	Stratus	1998	Inner windshield	Float	Green
25	Dodge	Stratus	1998	Rear window	Tempered	Green
26	Ford	Explorer Sport	2000	Outer windshield	Float	Green
27	Ford	Explorer Sport	2000	Inner windshield	Float	Green
28	Ford	Expedition Eddie Bauer	2004	Inside windshield	Float	Green
29	Ford	Expedition Eddie Bauer	2004	Outer windshield	Float	Green
30	GMC	Envoy	2004	Outer windshield	Float	Green
31	GMC	Envoy	2004	Front window	Tempered	Green
32	GMC	Envoy	2004	Inner windshield	Float	Green
33	Ford	Ranger XLT (pick up)	2001	Outer windshield	Float	Green
34	Ford	Ranger XLT (pick up)	2001	Front window	Tempered	Green
35	Ford	Ranger XLT (pick up)	2001	Inner windshield	Float	Green
36	Ford	Ranger XLT (pick up)	2001	Rear window	Tempered	Green

117

Sample	Make	Model	Year	Source	Glass type	Glass color
37	Jeep	Grand Cherokee	2001	Outer windshield	Float	Green
38	Jeep	Grand Cherokee	2001	Inner windshield	Float	Green
39	Jeep	Grand Cherokee	2001	Front window	Tempered	Green
40	Jeep	Grand Cherokee Laredo	2001	Outer windshield	Float	Green
41	Jeep	Grand Cherokee Laredo	2001	Inner windshield	Float	Green

The laser ablation system, a 213 nm Nd:YAG New Wave laser (New Wave Research, Fremont, CA, USA), was coupled to an ELAN DRC II ICP-MS system (PerkinElmer, LAS, Shelton, CT, USA). The ICP-MS acquisition parameters included an RF power of 1500 W, plasma gas flow rate of 17.5 L/min, and total dwell time of 8.3 ms. Both LA-ICP-MS systems were optimized with SRM NIST 612 in terms of doubly charge ($Ba^{++}<3\%$) and oxides (ThO/Th ~1%) which are inherently present during the ablation process due to the glass matrix composition. The optimized instrumental parameters for the LA-ICP-MS setup are shown in Table 2.37.

Table 2.37 Parameters for laser ablation using two laser systems

LA-Parameters	New Wave UP213
Spot size (round shape) (μm)	55 & 100
Power (% Energy)	100
Energy output (mJ)	~ 0.598-1.98
Repetition rate (Hz)	10
Helium flow into the cell (L/min)	0.90-0.95
Argon makeup gas flow after the cell (L/min)	0.82-0.95
Plasma gas flow (L/min)	16.5
Time of ablation (seconds)	60
ICP RF power (W)	1500-1550

118

The capability on detecting differences and/or similarities in terms of elemental composition of different sources of glass is the basis for a good discrimination among sources. Quantitative information provides crucial information for comparison of glass fragments. The most known calibration strategies for quantitative analysis of solid samples by LA-ICP-MS are: internal calibration, calibration curves and single standard addition. By combining internal standardization with external standard it is possible to correct for matrix effects, instrumental drift and for differences in the amount of particles ablated and transported into the ICP-MS. In this study ^{29}Si and SRM NIST 612 were used as internal standard and external calibrator respectively. The SRM NIST 612 was analyzed in two replicates at the beginning and at the end of the sequence. SRMs NIST 1831 and NIST 612 were used to evaluate the figures of merit for each of the methods. Other standards such as FGS01 and FGS02 were used as internal control when doing quantitative elemental analysis of float glass. Glass samples were analyzed in three to four replicates to do statistical analysis in terms of accuracy and precision.

The elements selected for discrimination of glasses by ICP-MS have been assessed in terms of accuracy, precision and discrimination potential in previous studies (Duckworth, 2002; Latckoczy 2005). The element menu used for LA-ICP-MS analyses included: ^{7}Li, ^{25}Mg, ^{27}Al, ^{29}Si, ^{39}K, ^{42}Ca, ^{49}Ti, ^{55}Mn, ^{57}Fe, ^{85}Rb, ^{88}Sr, ^{90}Zr, ^{118}Sn, ^{137}Ba, ^{139}La, ^{140}Ce, ^{146}Nd, ^{178}Hf, ^{206}Pb, ^{207}Pb, and ^{208}Pb.

The LA transient signal of the ICP-MS analysis was collected and analyzed using the Glitter Software (GEMOC v4.4, Macquarie University, Australia). A background signal was collected during the first 20 seconds of analysis without firing the laser. After 20 second the laser was fired for 60 seconds to collect the signal produced from the

ablation process. Another 20 of background were recorded after the ablation was completed to ensure the signal dropped to background levels and to clean up prior the next analysis. Only the middle 30 seconds of the total ablation signal were integrated for each element avoiding the initial spike created when the laser interacts with the sample for the first time. The signal integration in count per second (cps) is converted using the Glitter Software to concentration units (ppm).

The discrimination potential of the LA-ICP-MS analysis was determined by comparing statistically the elemental profile of the samples using t-test assuming unequal variances and the Estimate Model of the Analysis of Variance (ANOVA) with the Tukey's test as post hoc test. For this study both tests were used to determine if there were significant differences between the means of two or more samples with a 95% limit of confidence.

2.3.2 Results and Discussion

2.3.2.1. LA-ICP-MS with matrix-match standard

2.3.2.1.1. FDLE Samples Set

A 99.6 % of discrimination was obtained from the elemental analysis of these 37 float glass samples by LA-ICP-MS. Three indistinguishable pairs of samples out of 666 possible pairs were found. The discrimination by element of this data set is presented in Table 3.38. Discrimination by element only decreases the discrimination power of the elemental analysis. Zirconium showed to provide the best discrimination with an 80% differentiation of the sample set.

Glass fragments W142 and W143 were one of the indistinguishable pairs. These two fragments came from the two laminates of the same windshield. The other indistinguishable pair was W103 and W107 coming form the side windows of two different cars manufactured in different plants the one year apart. W103 originated from the side window of a 1978 Buick Riviera manufactured in GM's Flint, Michigan plant, while W107 originated from the side window of a 1977 Cadillac DeVille manufactured in GM's Linden, New Jersey plant. Since this pair could not be discriminated by micro-XRF either, it is possible that their elemental composition is similar. The third indistinguishable pair corresponds to W319 and W320, which actually originated from the same laminated store window.

Table 2.38 FDLE Dataset: Discrimination by element

Element	Indistinguishable pairs (out of 666)
^{49}Ti	152
^{55}Mn	294
Rb85	253
^{88}Sr	144
^{90}Zr	122
^{137}Ba	167
^{139}La	317
^{140}Ce	199
^{146}Nd	396
^{178}Hf	259
Pb mean	282
^{25}Mg	286
^{27}Al	147
^{42}Ca	489
All (14 elements)	3

### 2.3.2.1.2. Within Manufacturing Plant Study: Cardinal Dataset

For these analyses NIST 1831 was used as control to determine the precision and accuracy of each analysis. Excellent accuracy was obtained when the experimental isotopic concentration were compared to the certified values. The precision of the analyses was better than 5% RSDs.

From the 49 Cardinal's plant samples there were 1176 possible pairs for comparison. These amount of samples were compared with ANOVA with the Tukey's test using Systat 11 since there amount of samples to analyze. The ANOVA results showed 157 indistinguishable pairs which means 86.65% discrimination. Figure 2.22 shows the indistinguishable pairs arranged by dates. In Figure 2.22 is clearly the separation of these indistinguishable pairs in 5 different groups. More indistinguishable pairs are in the 2000-2001 period possible due to the similarities in elemental composition of glass samples that come from the same manufacturing plant as time progress.
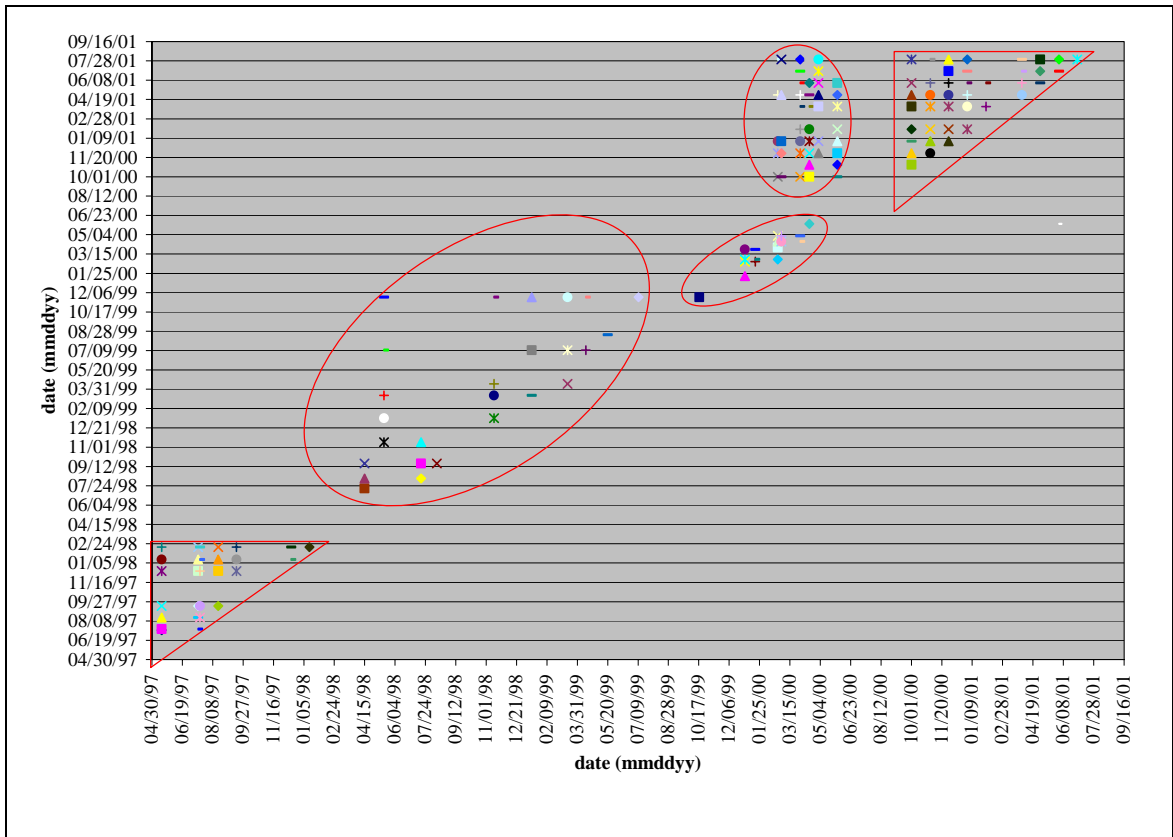
**Figure 2.22** Cardinal indistinguishable pairs using ANOVA

Additional statistical analysis (t-test) of the 157 indistinguishable pairs made the discrimination of 118 pairs corresponding to a 96.7% discrimination of the Cardinal plant sample set. The 39 indistinguishable pairs were arranged by date in Figure 2.23. The indistinguishable pairs were groped by samples collected within a few months.

123
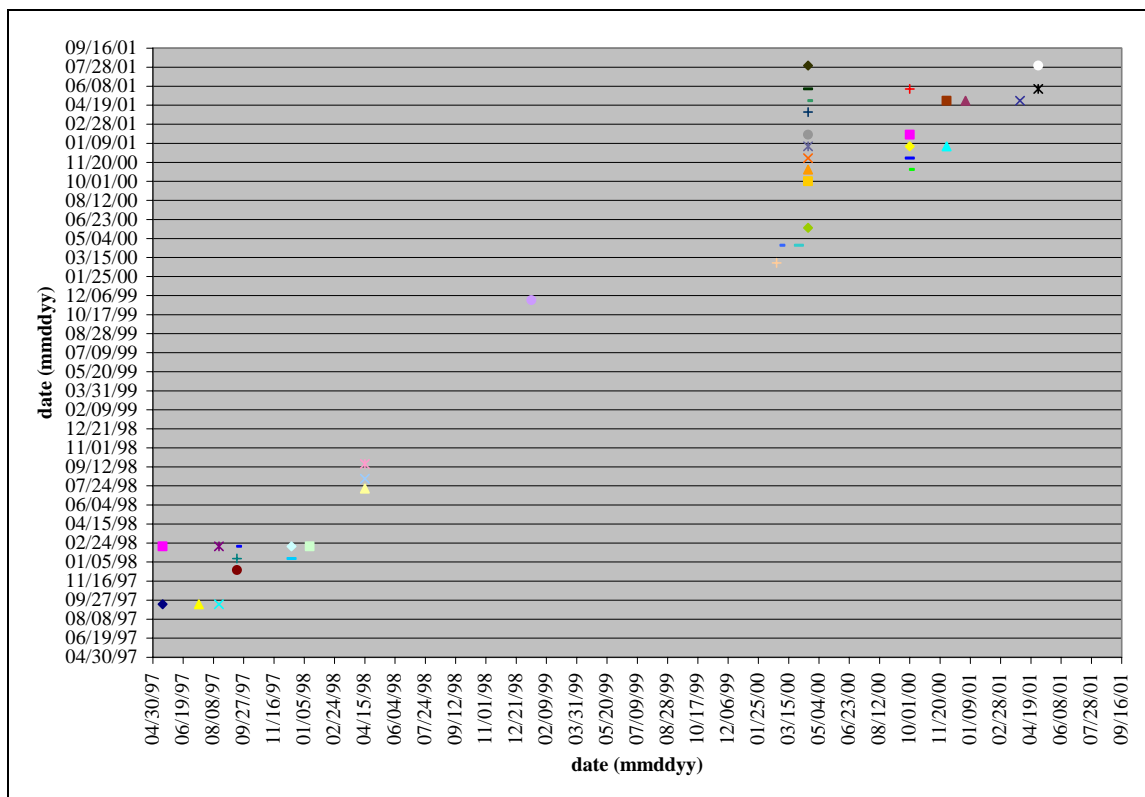
Figure 2.23 Cardinal indistinguishable pairs using t-tests after ANOVA

The discrimination achieved in this analysis was achieved due to the variability of

the elemental composition among the samples. The best discriminating elements for this

analysis were Zr, Sr, Mn and Ti. Figure 2.24 show the variability of Sr, Mn and Ti

elements within the samples collected at the Cardinal plant from 1997-2001. The change

in formulation of the glass manufacture process on 1998 and 1999 resulted in a high

discrimination of the samples collected during these years. From the 1176 total possible

pairs for comparison, 1137 pairs could be differentiated even though they share the same

color and many of them have the same RI.
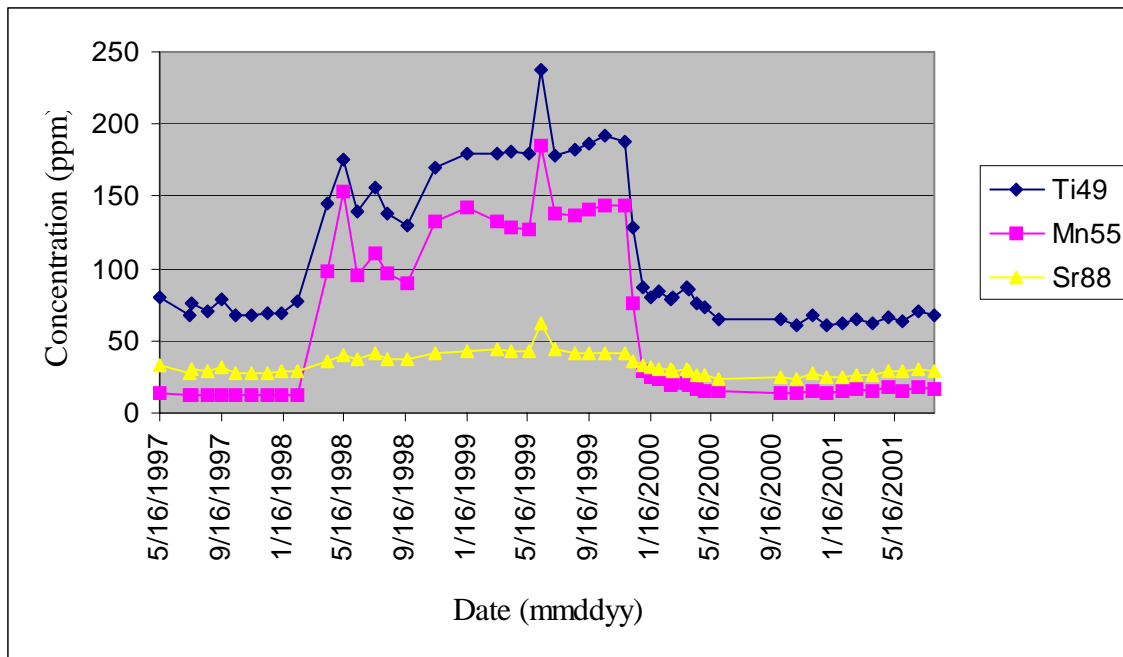
Figure 2.24 Glass elemental composition variability within Cardinal manufacturing plant

2.3.2.1.3. Different Manufacturing Plants Samples Set

A total of 2346 possible pairs were compared with ANOVA using the Tukey's test. Analysis with t-test was done to the indistinguishable pair resulted from the ANOVA analysis. The analysis of this dataset showed excellent discrimination with only three indistinguishable pairs. Pair 110-111 came from the right and center positions of the same ribbon of glass at the PPG manufacturing plant. The second pair (224-226) came from the same plant (Guardian), have the same color (green) and have very similar refractive index 1.52087 and 1.52164 respectively. The third pair is 285-613 came from the same plant (PPG), have the same color (clear) and have similar refractive index 1.51883 and 1.51874 respectively.

LA-ICP-MS showed its capabilities on the discrimination of samples with similar origin, refractive index and colors although some samples were discriminated even

though they came from different areas of the same glass ribbon. To assess the discrimination of the samples coming from different areas of the same glass ribbon, three glass ribbons were sampled three times each (right, left and center positions). Figure 2.25 shows the elemental profile of these samples. Eight out of 9 possible pairs from the three groups resulted to be distinguishable leading to an 88.9% discrimination of sources with common origin. Glass fragments from the same glass ribbon showed to be discriminated by LA-ICP-MS. A wide collection of fragments different areas of each glass should be sampled to have a better representation of the whole sample and to prevent false discriminations/associations.
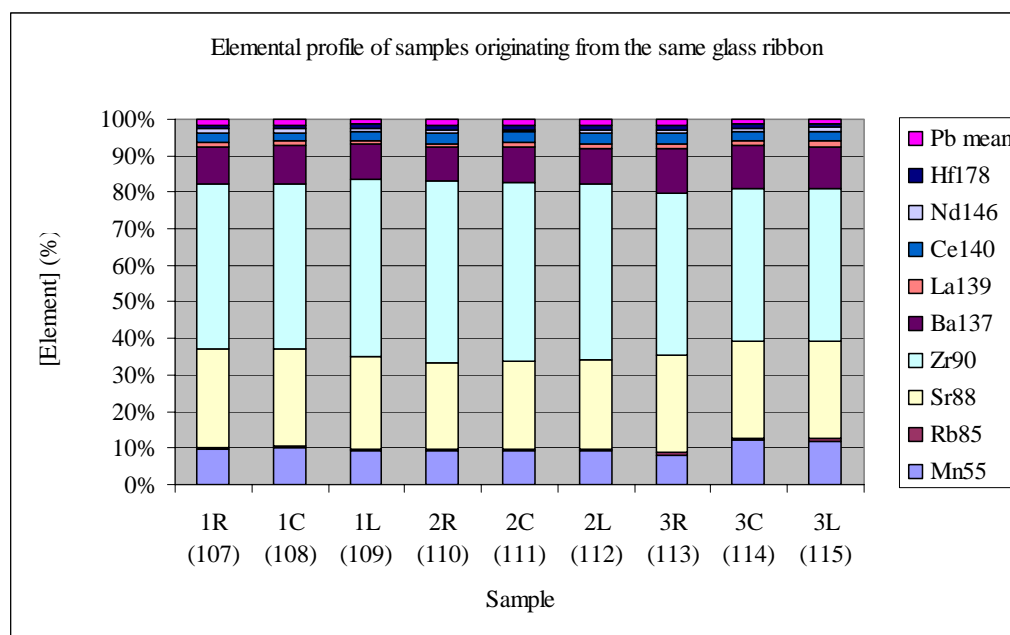
Figure 2.25 Elemental profile of fragments from three different areas (Right, Center and Left) of three different glass ribbons

126

2.3.2.1.4. Vehicles 1984-1994 Dataset

A total of 1326 possible pairs were compared with ANOVA and t-test in which 1305 sample pairs resulted to be distinguished. Out of the 1305 distinguished pairs12 pairs came from common sources. Twenty one sample pairs were found to be indistinguishable and four pairs were composed by samples originating from the same source: 424-425 (Honda Accord 91'), 441-462 (Toyota Corolla 93' outer and inner windshield layers), 471-483 (Dodge Minivan 94') and 128-129 (Ford Mustang 89' tempered glass, vehicle windows).

The elements that provided better discrimination with the lower numbers of indistinguishable pairs are showed in Table 2.39. For this analysis Sr and Zr showed to be the best discriminators.

Table 2.39 Vehicles 1984-1994 Dataset: Discrimination by element

Element	Indistinguishable pairs (out of 1326)
^{49}Ti	279
^{85}Rb	466
^{88}Sr	210
^{90}Zr	239
^{137}Ba	515
All (12 elements)	21

2.3.2.1.5. Vehicles 1995-2004 Dataset

Eight out of 820 possible pairs compared were indistinguishable even though this dataset was composed of many samples with common sources.

Even though this dataset was composed by many samples with common sources, 99% discrimination was achieved. Only 8 out of 820 possible pairs for comparison were found to be indistinguishable. Their descriptions are summarized in Table 2.40.

Table 2.40 Summary of the 8 Indistinguishable Pairs Resulted from the Analysis of the Vehicles 1995-2004 Dataset by LA-ICP-MS

Pair	Sample Number	Vehicle Make	Vehicle Model	Year	Sample collected from
1	6	Chevrolet	Cavalier	2004	Outer windshield
1	7	Chevrolet	Cavalier	2004	Inner windshield
2	8	Chevrolet	Cavalier	2004	Side window
2	9	Chevrolet	Cavalier	2004	Rear window
3	11	Oldsmobile	Intrigue	98	Outer windshield
3	12	Oldsmobile	Intrigue	98	Inner windshield
4	13	Dodge	Neon	2000	Outer windshield
4	14	Dodge	Neon	2000	Inner windshield
5	20	Chevrolet	Cavalier	2003	Outer windshield
5	21	Chevrolet	Cavalier	2003	Inner windshield
6	23	Dodge	Stratus	98	Outer windshield
6	24	Dodge	Stratus	98	Inner windshield
7	28	Ford	Expedition Eddie Bauer	2004	Inner windshield
7	29	Ford	Expedition Eddie Bauer	2004	Outer windshield
8	37	Jeep	Grand Cherokee	2001	Outer windshield
8	38	Jeep	Grand Cherokee	2001	Inner windshield

Seven of the indistinguishable pairs were formed by glass fragments originating from the outer and the inner panes of the same windshield, which explains why LA-ICP-MS was not able to separate them. In just one case, the fragments came from the side window and the rear window of the same automobile. Therefore, it is possible that the glass from those samples could have been manufactured in the same plant.

The number of samples differentiated by the analysis of each element can be seen in Table 2.41. Again, strontium and zirconium showed to be the best discriminator elements.

Table 2.41 Vehicles 1994-2004 Dataset: Discrimination by element

Element	Indistinguishable pairs (out of 820)
^{49}Ti	142
^{85}Rb	176
^{88}Sr	76
^{90}Zr	127
^{137}Ba	191
All (14 elements)	8

2.3.3. Conclusions

It was proven that LA-ICP-MS is the best technique for the quantitative analysis of elements in glass. Accuracy, precision and discrimination power were evaluated by means of the analysis of 248 glass samples originating from various sources. Detection limits lower than 1 ppm were achieved for most of the elements, indicating an enhanced sensitivity that provided better discrimination than the attained by the other analytical techniques. The percentages of relative standard deviation found were lower than 5% for nearly all the elements and lower than 10% for the remaining elements, giving good precision.

The sensitivity of LA-ICP-MS made the quantification of trace elements possible, allowing the differentiation of glass samples with similar origin. The variation of the elemental composition in glass manufacturing, detected by this technique, permitted the discrimination of samples within and between manufacturing plants.

It was determined in eight cases out of nine possible pairs that glass shards originating from the same glass ribbon could be distinguished by elemental analysis when doing LA-ICP-MS. Therefore, more than one fragment from different areas of each glass sample should be collected in order to have better representation of the whole sample.

This would help avoiding false discriminations/associations when doing glass comparisons for forensic purposes.

2.4. LA-ICP-MS ANALYSIS OF GLASS WITHOUT MATRIX-MATCHED STANDARD

2.4.1. Methodology

2.4.1.1. LA-ICP-MS without matrix-match standard

This method includes the use of a solution as standard of some elements of known concentrations introduced into the plasma via a nebulizer flow producing a constant background signal. This signal is the "blank" of the standard addition experiments in which a "spike" of the ablation signal is produced during certain amount of time. By using a T-connector the volume of the ablated solid was spitted before reaching the ICP-MS. To measure on-line the amount of solids entering into the plasma a piezoelectric microbalance was used allowing the calculation on the concentration values fore each element. A modified spray chamber was developed for the introduction of the solution at the same time as the ablated particles prior the ICP-MS measurement. The setup of this analytical method is based on the Aeschliman method for the quantification of elements in glass by LA-ICP-MS without the need for matrix-matched standards. Our approach used a dry aerosol from a standard solution to calibrate the laser ablation response. The calibration solution was introduced into the ICP-MS by a using a Meinhard nebulizer and by reducing the speed of the intake flow to simulate a micronebulizer flow. In this way the introduction of the disolvated particles was similar to the ablation products. A solid

standard was used for the calculation of particles transported from the nebulizer. Since this procedure was used only to characterize the nebulizer, the solid standard needed not match the matrix of the unknown samples, as long as the mass of solid removed was measured for each unknown material (Aeschliman *et al.*, 2003). Therefore, the measurement of mass from the solid transported into the ICP was measured online via a piezoelectric balance to provide normalization of the signal due to variations of laser performance over time. The equations used to calculate the concentration of each element in the solid are described in Aeschliman et al. 2003 article.

The same instrumentation used to run and evaluate the LA-ICP-MS technique was utilized for the LA-ICP-MS without matrix-match standard method. The instrumental parameters used for the analyses of LA-ICP-MS without matrix matched standard method are describes in Table 2.42.

Table 2.42 Optimal parameters for the LA-ICP-MS without matrix-matched standards experiments

| Laser Parameters	
Spot size (round-shape)	100 μm
Power (% Energy)	100%
Energy output	1.88 mJ
Fluence	24.00 J/cm^2
Repetition rate	10 Hz
Helium flow into the cell	0.90 L/min
Argon makeup gas flow after the cell	0.92 L/min
Plasma gas flow	15.6 L/min
ICP RF power	1550
Time of ablation	60 sec
Delay time	30 sec
ICP-MS Parameters	
Solution intake flow	6 rpm
Piezoelectric Balance Parameters	
Intake flow	1 L/min
Measurement time	120 sec

131

2.4.3. Results

2.4.3.1 Results Using Reference Standard Materials

The quantitative analysis of glass standards was successfully achieved. The use of standards was advantageous because it permitted the comparison of the experimental results to the available certified values for each element. The concentration of elements such as magnesium, lead, manganese, titanium, rubidium, strontium, cerium, barium, and zirconium in NIST 612 was determined with excellent precision and accuracy. In the case of NIST 1831, the quantification of Ba, Mn, Ti, Sr, and Zr gave good results, while the analysis of elements in concentrations close to the detection limits such as Rb and Ce came up inconsistent and inaccurate.

All the connections in the set up were checked at the beginning of each experimental section to guarantee that there were no gas leaks. The functioning of the ICP-MS instrument coupled to the laser system was properly optimized using the solid glass standard NIST 612. The operation of the ICP-MS using only solution was also optimized using tuning solution. In both cases, the signals produced for selected elements were greater than the required values. The percentages of oxides and the percentages of doubly charged were bellow the minimum limits, ensuring the presence of negligible interferences during the analyses.

Figure 2.26 illustrates typical calibration curves obtained for each element in NIST 612 using LA-ICP-MS without matrix-matched standards. The slope and the intercept of the equation of each line were used in the quantification of the corresponding element in the solid.
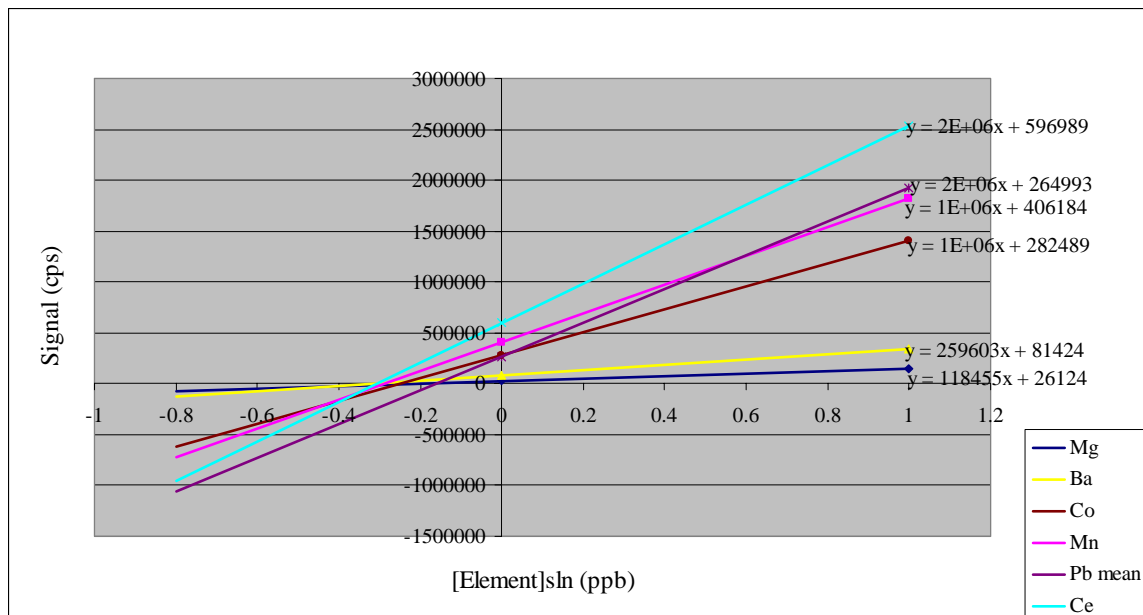
Figure 2.26 Calibration curves obtained from the analysis of NIST 612 by LA-ICP-MS without matrix-matched standards

Several tests were performed in order to improve the LA-ICP-MS without matrix-matched standards method. The speed of introduction of the calibration solution, the laser ablation spot size, the time of signal acquisition, and the conditions of mass measurements were modified. In Table 2.43 can be seen the results obtained for the elemental analysis of NIST 612 when introducing a calibration solution of 1 ppb of Mg, Mn, Ba, Ce and Pb at a speed of 4 rpm simultaneously with the particles from the laser ablation of a 65 μm single spot of the solid standard.

133

Table 2.43 Results of the quantitative analysis of NIST 612 by LA-ICP-MS without matrix-matched standards using 65 um LA spot size and 4 rpm solution introduction speed

Element	^{25}Mg	^{55}Mn	^{137}Ba	^{140}Ce	Pb mean
[X] $_{solid}$ (µg/g)	81.12	38.06	37.04	37.93	38.00
Standard Deviation (µg/g)	9.36	3.70	2.94	2.85	4.72
%RSD	11.54	9.73	7.94	7.52	12.43
Certified values (µg/g)	77.63	38.44	37.79	38.36	38.54
%Bias	4.49	0.99	1.97	1.12	1.41

With the purpose of enhancing the precision of the analysis, the volume of the calibration solution entering the plasma was adjusted by increasing the speed of the peristaltic pump to 6 rpm. The laser ablation spot size was also enlarged to 100 µm in order to raise the signal of the solids and stabilize the mass of particles measured online. A new list including more discriminator elements was selected. Table 2.44 shows the subsequent results gathered under the new experimental conditions.

Table 2.44 Results of the quantitative analysis of NIST 612 by LA-ICP-MS without matrix-matched standards using 100 um LA spot size and 6 rpm solution introduction speed

Element	^{55}Mn	^{85}Rb	^{88}Sr	^{90}Zr	^{137}Ba	^{140}Ce
[X] $_{solid}$ (µg/g)	38.41	31.64	89.11	36.00	37.77	40.08
Standard Deviation (µg/g)	1.46	1.87	7.98	2.01	0.931	1.63
%RSD	3.80	5.91	8.95	5.59	2.47	4.07
Certified values (µg/g)	38.44	31.64	76.18	36.00	37.79	38.36
%Bias	0.10	0.013	16.9	0.00	0.032	4.5

As can be seen in the table above, strontium and cerium did not exhibit good accuracy. Since LA-ICP-MS without matrix-matched standards works with a two-point calibration curve per element, the big difference between the high signal produced by

134

strontium or cerium in the solid compared to the low signal produced by the solution containing 1 ppb of this element may cause bad quantification.

Figure 2.27 illustrates a plot of signal vs. time obtained from processing the data in GeoPro. The differences in signal yielded by strontium and barium during the same experiment were obvious. The signal produced by barium was taken as a reference for a good quantification. A calibration solution that could provide about the same ratio between S_{solid} and $S_{solution}$ that was obtained for barium was desired for all the elements.
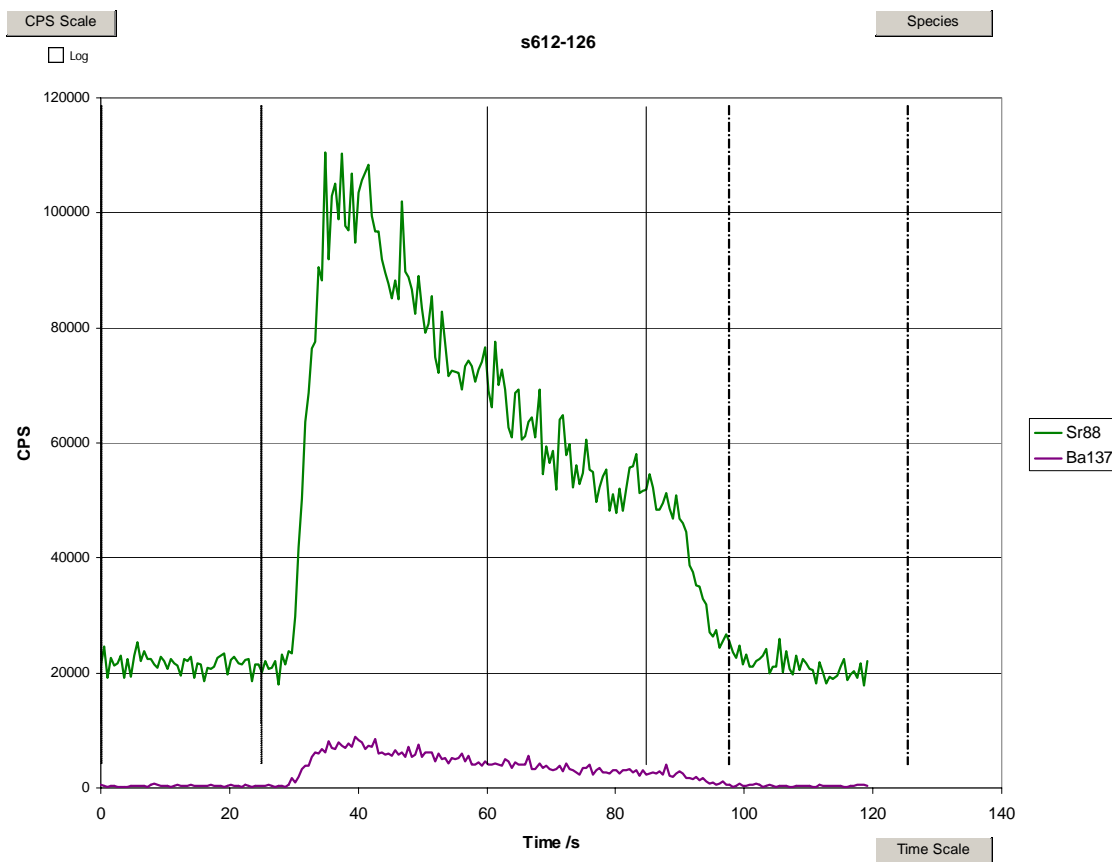
Figure 2.27 Analysis of barium and strontium in NIST 612 by LA-ICP-MS without matrix-matched standards

Further experiments were conducted using different concentrations of Ce and Sr in the calibration solution ranging from 0.5 to 10 ppb. Unfortunately, none of these

changes improved the accuracy. Ambiguous results were obtained, indicating that Sr and Ce were the least stable elements among the elements analyzed. Freshly prepared solutions of 1 ppb of those elements led to the better results but no good reproducibility was achieved.

Since the elemental concentrations in NIST 1831 glass standard are intended to reproduce the typical elemental profile of float glasses, the quantitative analysis of this SRM by LA-ICP-MS without matrix-matched standards was required. Treating NIST 1831 as a sample, the results obtained using NIST 612 for the volume calibration were poor compared to those measured using the NIST 1831 volume calibration. Therefore, it is clear that the difference in concentrations of the elements in the solid affects the response factor of each of them, which consequently affects the calibration of the volume of each element in solution being introduced into the ICP-MS. A direct comparison between the two volume calibrations is shown in Table 2.45.

Table 2.45 Comparison between the volume calibrations achieved using NIST 612 and NIST 1831 for the analysis of NIST 1831 by LA-ICP-MS without matrix-matched standards

Element	Certified Values (ppm)	Volume calibration using NIST612			Volume calibration using NIST1831		
		$[X]_{solid}$ (ppm)	Std Dev	%Bias	$[X]_{solid}$ (ppm)	Std Dev	%Bias
^{55}Mn	12.54	17.61	0.80	40.45	13.16	0.45	4.91
^{85}Rb	6.11	7.10	0.32	16.17	6.48	0.39	6.06
^{88}Sr	89.11	175.21	7.97	96.62	102.94	17.90	15.52
^{90}Zr	43.35	42.63	1.94	1.65	49.28	2.98	13.67
^{137}Ba	31.51	42.98	1.96	36.40	31.91	1.93	1.26
^{140}Ce	4.53	7.43	0.34	63.98	5.80	0.35	28.00

As in typical float glasses, the concentrations of cerium and rubidium in NIST 1831 are close to the detection limits. Hence, their quantification is difficult. This fact suggested that Rb and Ce be replaced by another element that were normally present in higher concentrations and still provided good discrimination among glass samples such as titanium.

Figure 2.28 shows the signal produced by rubidium and cerium in contrast to the signal yielded by titanium. Titanium presents a less dramatic difference between $S_{solution}$ and S_{solid}, which provides better calibration for this experiment.
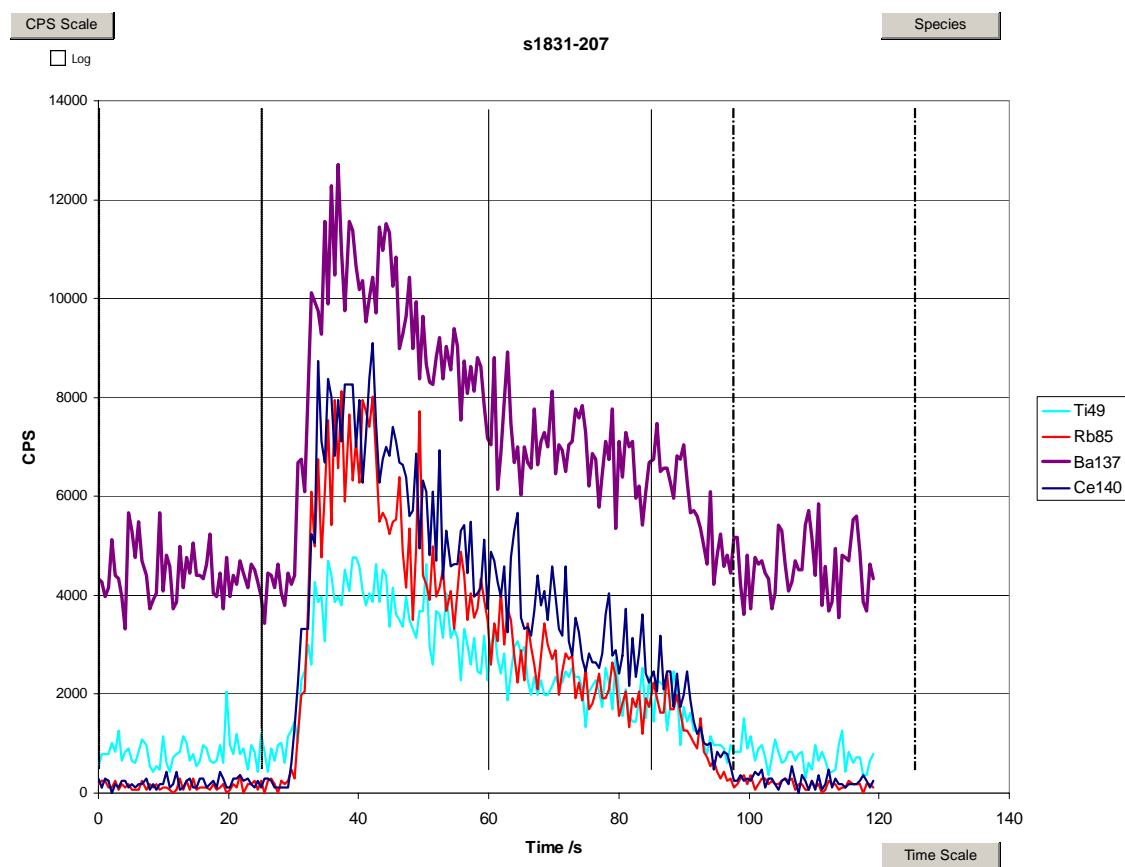
Figure 2.28 Analysis of barium, titanium, cerium, and rubidium in NIST 1831 by LA-ICP-MS without matrix-matched standards

Table 2.46 shows some of the results obtained for the quantitative analysis of NIST 1831 by LA-ICP-MS without matrix-matched standards using the same glass standard for the volume calibration. In this case, more precise and more accurate quantification of the elements was achieved.

Table 2.46 Results of the quantitative analysis of NIST 1831 by LA-ICP-MS without matrix-matched standards

Element	^{49}Ti	^{55}Mn	^{88}Sr	^{90}Zr	^{137}Ba
[X] $_{solid}$ (µg/g)	114.17	12.70	92.44	40.06	27.98
Standard Deviation (µg/g)	11.24	1.86	7.88	2.29	1.60
%RSD	9.85	14.63	8.52	5.72	5.72
Certified values (µg/g)	113.80	12.54	89.11	43.35	31.51
%Bias	0.33	1.29	3.74	7.60	11.20

In general, the online measurement of the mass of ablated particles ensured the normalization of the signal produced by the elements in the solid. The volume of the calibration solution introduced into the ICP-MS was effectively calibrated using the certified elemental concentrations of the same glass standard. All this allowed very low percentages of relative standard deviation as well as almost unbiased results for most of the elements analyzed.

2.2.4.3.2. Results Using Samples

Five glass samples from the FDLE samples set were quantitatively analyzed by LA-ICP-MS without matrix-matched standards. The samples were selected based on their relationship according to the results obtained by LA-ICP-MS in order to determine the discrimination power of the new method. This subset included samples W103 and W107, which could not be distinguished by LA-ICP-MS, neither by micro-XRF, even though these samples have different sources. It also incorporated W83 and W95, which were

138

easily distinguished by LA-ICP-MS but barely distinguished by micro-XRF. The fifth glass sample was randomly added and it was discriminated from the rest of the samples by both techniques.

NIST 1831 was employed in the volume calibration because it is the standard that best resembles the elemental profile of float glasses. However, the results were not as precise or as accurate as expected. Table 2.47 illustrates an example of the elemental profile obtained for W103 using this method in contrast with the results previously gotten using the validated LA-ICP-MS.

Table 2.47 Results of the quantitative analysis of W103 by LA-ICP-MS without matrix-matched standards

Element	^{49}Ti	^{55}Mn	^{88}Sr	^{90}Zr	^{137}Ba
[X] $_{solid}$ (µg/g)	121.58	11.60	61.24	231.99	21.41
Standard Deviation (µg/g)	16.09	1.53	8.10	30.70	2.83
%RSD	13.23	13.23	13.23	13.23	13.23
LA-ICP-MS values (µg/g)	133.70	12.80	37.10	140.09	24.38
%Bias	9.07	9.44	65.07	65.61	12.18

As a result of the statistical analysis of the quantitative information gathered for five elements in these glasses using LA-ICP-MS without matrix-matched standards, only one pair out of ten possible pairs of glass samples was found to be indistinguishable. W83 and W95 were the samples that could not be differentiated; meaning that the discrimination achieved using this method disagrees with the discrimination accomplished using the validated LA-ICP-MS and micro-XRF.

One factor that could have affected the elemental quantification in real samples is inconsistency in the mass measurements acquired with the piezoelectric balance. Despite the fact that the piezo balance was continuously cleaned and the tubing transporting

139

particles was purged after every exchange of sample in the ablation chamber to avoid carry over, the acquisition of the mass of particles resulting from replicates of the same solid ablated under the same conditions varied significantly. The use of helium as carrier gas might be in part responsible for this inefficiency because the piezoelectric balance is less sensitive to the small particles ablated in the presence of this gas. However, helium was selected for this application because it has been previously shown that it provides better analytical results for the elemental quantification of glass than when using argon.

Another fact affecting the results could be the use of a 400 µL-nebulizer instead of a 20 µL-nebulizer as Aechliman suggests. As a consequence of the introduction of an excess of calibration solution, the wet droplets aid in the condensation of the wet plus dry particles together. A wet aerosol containing a mix of solution and solid particles is then formed. The atomization and ionization of this wet aerosol is not as efficient as occurs for the solid particles.

2.4.4. Recommendations

The development of the LA-ICP-MS without matrix-matched standards method encountered limitations in its application to certain standards and samples that have elements in very low concentrations, which suggests the performance of further studies on different standard reference materials. The analysis of float glasses using FGS01 or FGS02 could be of help in the volume calibration taking into account that their elemental concentrations are similar to the ones in common float glasses. A recent study over the forensic analysis of glass by LA-ICP-MS established an improved analytical protocol in which these standards were used (Latkoczy *et al.*, 2005). However, this new method is

not intended to promote the use of matrix-matched standards. Hence, modifications to the actual methodology are preferably suggested.

The utilization of a different piezoelectric balance or another system able to provide consistent measurements of mass of particles is strongly recommended. Without the information that accounts for the differences in amount of material ablated and transported to the ICP-MS, the normalization of the signal produced by each element in the solid material cannot be achieved.

In order to test whether the piezoelectric balance is working properly, the size of the particles produced by the laser ablation of the solid should be increased. The use of argon instead of helium as carrier gas in the ablation cell usually helps generate larger particles that can be easily weighted. A less energetic laser ablation process can also produce larger particles, which represent an advantage for the mass measurements but, on the other hand, may affect the analytical results of the experiment. The use of the Cetac LSX-200+ laser system may help fulfill this objective since it provides a less energetic ablation without affecting the quantitative analysis of elements in glass.

The use of a low flow micronebulizer (20 µL/min or 50 µL/min) for the introduction of the calibration solution is adviced. This would aid reduced the wet droplets that are formed in the spray chamber, making the solution to behave like a dry aerosol. Ideally, the aerosol introduced should be as dry as possible in order to achieve nearly the same atomization and ionization as for the laser ablation particles.

A solution calibration using more than two points might also provide better quantification results. Since the calibration solution should be introduced simultaneously with the LA-particles, a way of introducing different concentrations of the same element

141

in the same solution could be using different isotopes for each element. In this case, the abundance of each isotope should be taken into account for the calculations.

Since the use of the modified spray chamber might affect the amount of sample being introduced into the ICP-MS, it would be worthwhile to explore another set up for this experiment.

2.4.5. Conclusions

The proposed development of the LA-ICP-MS method that does not need matrix-matched standards was not accomplished in its entirety. The elemental analysis of glass standards, specifically of NIST 612 and NIST 1831, resulted in very precise and accurate quantitative information for the majority of the elements of interest. However, the analysis of real samples, which elemental concentrations are unknown, was accurate, precise, or reproducible.

There are certain limitations that need to be addressed before this technique can become a common place in a forensic laboratory. These include the inconsistency in the mass measurements acquired with the piezoelectric balance and the excess of calibration solution introduced into the spray chamber.

The generation of larger particles was recommended to enhance the mass measurements. Low-energy laser ablations or the use of argon as carrier gas in the ablation cell could help create bigger particles. The use of the Cetac LSX-200+ laser system was suggested since it provides a less energetic ablation without affecting the quantitative analysis of elements in glass. The introduction of calibration solution through

a low-flow nebulizer (20-50 µL/min) would facilitate the formation of a drier aerosol that provides nearly the same atomization and ionization as for the laser ablation particles.

LA-ICP-MS without matrix-matched standards represents a promising technique for the quantitative analysis of elements in materials. The validation of this method is required before it can be applied to the analysis of other matrices.

SECTION III. LA-ICP-MS for PAINT ANALYSIS

3.1. MATERIALS AND METHODS

3.1.1. Analysis of automotive paint

The flow chart of the strategy of analysis employed for the study on automotive paint samples is shown in figure 3.1.
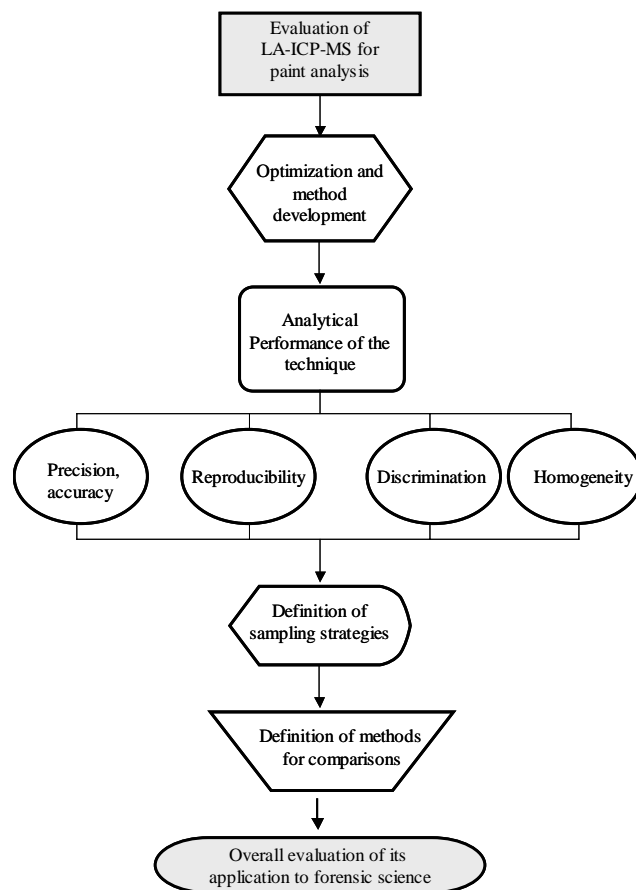
Figure 3,1. Flow chart of the strategy of analysis of paints by LA-ICP-MS.

3.1.1.1. Sample preparation

Paint samples that were already on steel or plastic substrates were cut into ~3cm squares so they can fit into the ablation chamber and the surface was cleaned with a kimwipe. Other than that the samples did not required further manipulation.

3.1.1.2. Optimization and method development

The method suggested by Hobbs (Hobbs, 2003) was used as the start point of this work. The optimization was focused on the improvement of precision and reproducibility of the method as well as the development of quantification strategies.

3.1.1.3. Sampling sets

3.1.1.3.1. Homogeneity studies

Homogeneity studies on paint were performed for two different sets of paints. The first set consisted of five blocks of red automobile paint purchased from ACT Laboratories, each block was ~ 15 cm x 10cm. The five blocks originated from the same batch of paint and had four layers. The second set was comprised of a piece of green paint of ~ 15 x 10 cm, provided by the Royal Canadian Mounted Police (RCMP), Toronto, Canada). The sample was part of the Paint Database Query (PDQ), it was identified as UVWC00023 and the structure of the paint consisted of six layers. For a homogeneity study within a single block the piece was cut into 15 squared pieces of ~ 2 cm and then 7 of those pieces were randomly selected for analysis. Four replicates were analyzed in each square for further statistical comparisons.

For the red set an additional study was done to determine heterogeneity between the 5 blocks of paint. Four replicates were measured on each block.

3.1.1.3.2. Discrimination study of automobile paints

In order to determine if LA-ICP-MS was capable of further discrimination as compared to the currently used techniques in forensic laboratories, three sets of paints that originated from different sources and were not distinguishable by conventional techniques were selected. The first set consisted of three (3) red paints, the second consisted of three (3) white paints and the third one was comprised of two (2) black paints. The characteristics of each set are detailed on table3.1. Each subset was analyzed in four replicates by the LA-ICP-MS method and comparison was done by looking at elemental ratio profiles for each layer.

Table 3.5. Description of the set of paints for discrimination study.

Sample ID	Main color	Manufact-urer	Plant	Manufact-uring year	Make	Line	Model
UAZP 0166	Red	Chevrolet	Saint Louis	1999	Dodge	RAM	R15
UAZP00181	Red	Chevrolet	Saint Louis	2000	Dodge	RAM	R15
UAZP00198	Red	Chevrolet	Saint Louis	2000	Dodge	Dakota	
UAZP00147	White	Chevrolet	Saint Louis	1998	Dodge	RAM	R15
UAZP00167	White	Chevrolet	Saint Louis	1999	Dodge	RAM	R15
UAZP00189	White	Chevrolet	Saint Louis	2000	Dodge	RAM	R15
UAZP00096	Black	Chevrolet	Saint Louis	1999	Dodge	RAM	R35
UAZP 0190	Black	Chevrolet	Saint Louis	2000	Dodge	RAM	R35

3.1.1.4. Methods for comparison of paints

3.1.1.4.1. Qualitative comparison of paints

Qualitative comparison of paints was done by comparison of the transient signal or time-resolved signal obtained during ablation for all layers. It was also expressed in element ratio plots, where elements are displayed in the bar graphs for each layer and the total signal is normalized to 100%.

#### 3.1.1.4.2. Semi-quantitative analysis using glass standards

Semiquantitative analyses were conducted using SRM 612 as a calibrator. Two replicates of the standard were run at the beginning and at the end of each run in order to account for drift corrections. Each layer was integrated individually and ^{29}Si was used as an internal standard.

3.1.1.4.3. Quantitative characterization of paints without matrix matched solid standards

In order to calibrate the response of the laser ablation system without the use of matrix match standards the procedure reported by Aeschliman et al (Aeschliman, 2003) was modified and applied to paint samples. Figure 3.2 depicts a scheme of the set up of the experiment. The meinhard nebulizer (PE, Boston, MA, USA) with a 1.3 mL/min intake flow rate was adapted to a flow of ~ 100 μL/min using a reduction of the internal diameter of the tubing and a speed of 6rpm. The flow of particles coming from the ablation chamber was split with a T connector and 25% of it was directed into the piezoelectric balance where on-line measurement of mass transport of the ablated

material was acquired. The remaining laser ablation products (75%) were mixed with 15% of the particles originated from a calibration solution (after exit the spray chamber).

The solution contained 1pbb of Mg, Al, Cr, Mn, Cu, Ce and Pb and 10 ppb of Ba. The solution left over (85%) was sent to waste. This solution produced a constant background signal and worked as the "blank" for a standard addition experiment and the "spike" was produced by the ablation signal that was generated by 50 seconds.   The percentage of flow that was split in each "T" connection was optimized and calibrated using a digital flow meter ADM 1000 (J & W Scientific, CA, USA).
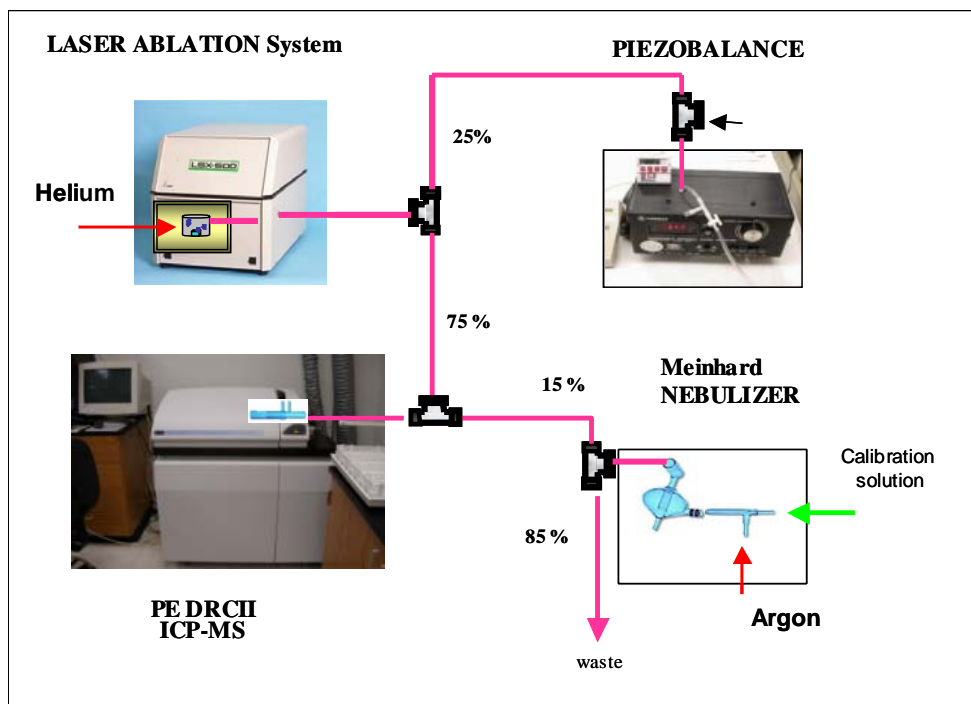
Figure 3.3. Set up diagram for the experiments of quantification of paints without matrix match standards

148

Since a mass needed to be registered individually for each of the paint layers, the ablation mode was optimized to ablate each layer for 50 seconds using single line at 10μm/sec, 100μm spot size, 70% energy output and 2Hz of frequency. At the end of the ablation of each layer, a blank was acquired for ~100 seconds and then the subsequent layer was ablated from the same start point. The calculation of the concentration of elements in each layer was estimated by using the following equation:

$$S_{total} = Rx * V * [Cn_{solution}] + Rx * m * [Cn_{solid}]$$

Where S_{total} is the total signal produced by the background solution and the ablation of the solid, Rx is the isotope response factor, V is the volume of solution that reaches the ICP, m is the mass entering the plasma from the LA, $Cn_{solution}$ is the concentration of the isotope in the standard solution and Cn_{solid} is the concentration of the isotope in the solid (unknown). A thorough explanation of the calculations will be covered in the results and discussion chapter.

3.1.2. Analysis of Latex Paints

3.1.2.1. Sample Collection/Preparation:

All samples collected were classified as white latex architectural paint. All samples were purchased from various stores, in their liquid form, which allowed for more control over sample preparation and manipulation, Table 3.2 lists and describes all latex paint samples obtained for this research. The preliminary experiments consisted of three paint samples were collected and prepared from three different manufacturers; Behr

Premium Plus, Ralph Lauren, and Glidden Evermore, labeled as samples 3, 5 and 6, respectively.

Table 3.2: List of all white latex paint samples collected for this study

Sample #	Brand Name	Color	Product #	Int/Ext.	Notes
1	*Glidden Evermore*	Deep tint Base	HD-6980	EXT	
2	*Ralph Lauren*	Brilliant White	RL 1291	INT	SATIN
3	*Behr Premium Plus*	Deep Base	3300	INT	SEMI-GLOSS
4	*Behr Premium Plus*	Ultra Pure White	8050	INT/EXT	HI-GLOSS
5	*Glidden Evermore*	White	HD-6224	INT	SATIN
6	*Quik Hide*	White	26960	EXT	FLAT
7	*Weatherbeater*	White	30 37804	EXT	PRIMER
8	*Easy Living*	White	30 58754	INT/EXT	PRIMER SEALER
9	*ColorPlace*	White	5407	INT	SEMI-GLOSS
10	*KILZ2 LATEX*	White	NONE	INT/EXT	
11	*McCloskey: Multiuse*	White/Light base	7445	EXT	PAINT & PRIMER
12	*Martha Stewart Everyday Colors*	Bright White	24-02	INT	SEMI-GLOSS
13	*Dutchboy: Home*	Brilliant White	WM.0D7400	INT	SEMI-GLOSS
14	*Krylon Color Creations*	Gloss White	KDH5001	INT/EXT	GLOSS
15	*Decotime: Cabinet Rescue*	White	DT43	INT	LOW-LUSTER SEMI-MATE
16	*Zinsser: Permawhite*	Eggshell	2774	INT	MOLD/MILDEW PROOF
17	*Rust oleum: Painter's Touch*	Gloss White	1992	INT/EXT	
18	*Behr Premium Plus*	Ultra Pure White	1050	INT	FLAT
19	*Behr Premium Plus*	Ultra Pure White	8050	INT/EXT	HIGH GLOSS
20	*Behr Premium Plus*	Pastel Base	4560	EXT	FLAT
21	*Martha Stewart: Everyday Colors*	IronStone White	22-04	INT	SATIN
23	*Martha Stewart: Everyday Colors*	IronStone White	74-04	INT	SEMI-GLOSS
24	*Martha Stewart: Everyday Colors*	Magnolia White	24-06	INT	SEMI-GLOSS
25	*Behr Premium Plus*	Ultra Pure White	1050	INT	FLAT: TINTED

Several substrates were initially tested to determine which would provide the greatest ease of sample handling and analysis. The substrates investigated were wood, glass, metal, and Teflon strips. The samples were prepared on the given substrates and allowed to air dry. They were then examined to determine uniformity of thickness, potential for interaction with substrate and ease of removal from substrate. It was concluded that the Teflon strips allowed for the easiest sample handling and labeling and

provided the least substrate interaction compared to the others, see Figure 3.2. Therefore, all sample preparation described from this point was completed on Teflon coated strips.
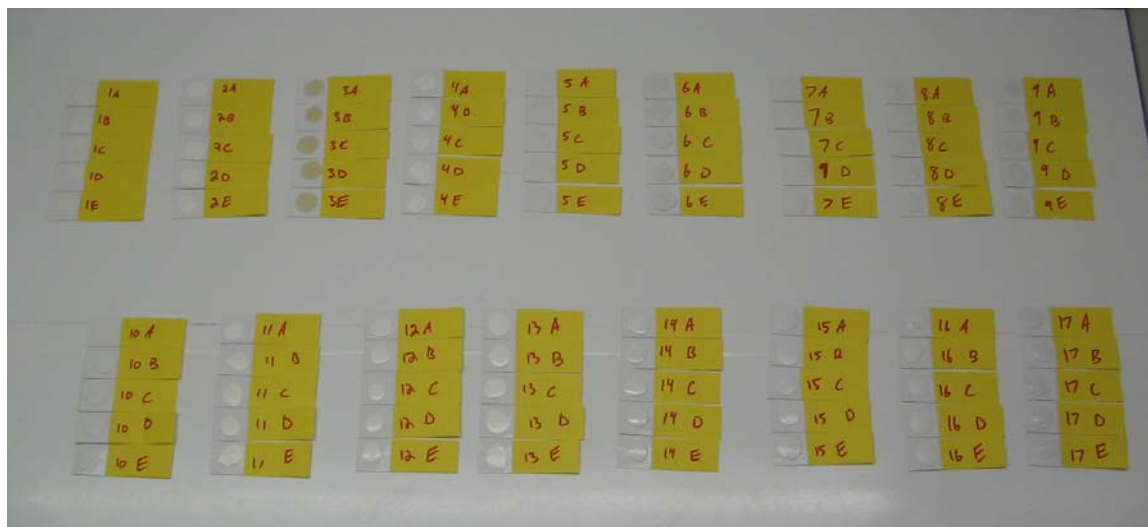
Figure 3.2. White latex paint samples prepared on Teflon coated strips.

All samples were prepared using the following method. The individual cans were vigorously shaken manually for approximately two minutes. The lids were then carefully removed. A separate disposable pipette was used for each sample and disposed of prior to the preparation of the following sample to minimize risk of cross contamination. The samples were pipetted onto the center of the labeled Teflon strip. The samples were then dried in an oven at approximately $50 - 60\,^{\circ}C$. If necessary, several coats of sample were applied to ensure adequate quantities for analysis. After drying in the oven, the samples were allowed to sit in a hood for at least 24 hours at room temperature to ensure adequate drying.

3.1.2.2. Laser Optimization:

The parameters to optimize were spot size (100 µm and 55 µm), the percent power (70%, 60%, and 40%), the pulse frequency (2, 5, and 10 Hz) and ablation mode (line vs spot).

The optimum parameter combination was determined to be a line with spot size of 100 µm, power at 60% and the pulse frequency of 5 Hz.

3.1.2.3. Element Menu:

A sample of Behr Premium (8050) was analyzed by LA-ICP-MS, with NIST 612 as an external standard, to determine a menu of possible discriminating elements. Also during this experiment four different areas of the same paint chip were measured in triplicate to determine the homogeneity of the sample. A list of 37 potential elements includes: Mg, Rb, Sr, Zr, Pb, As, Na, Al, P, K, Sc, Ti, V, Cr, Fe, Ni, Cu, Zn, Ga, Y, Nb, Mo, Cd, In, Sn, Sb, Cs, Ba, Hf, Ta, W, and Bi.

3.1.2.4. Within Can Variation:

The original three brands of paint were prepared and analyzed to determine the variation that exists in a single can. The cans were manually shaken for approximately 2-3 min. prior to sampling. A small amount of paint was pipetted, via disposable polyethylene transfer pipettes, onto Teflon strips. Ten samples were prepared per can. The samples were taken from random points in an attempt to ensure proper representation of the homogeneity of the paint can. The Teflon strips were then dried as detailed before. The average standard deviation and the relative standard deviation were calculated for

each of the 10 samples to assess the variation within each can as well as the potential variation between cans.

The results of the within can variation study were used to determine the sampling and analysis method that would optimally represent the natural heterogeneity of the paint matrix, while providing a practical analysis time. The data analysis method was also adjusted to provide a means for acquiring an accurate value, which would represent the relative concentration of the target elements and allow the heterogeneity of the sample to be taken into account for sample comparisons.

It was determined that the best way to accomplish this was to sample five paint chips, each in triplicate. This will provide enough variation within a sample to be representative of the heterogeneity in the calculation. Also, several element ratios were utilized to determine which ratio would provide the most consistent values for one can. The element ratios that were investigated were ratios to titanium, aluminum, potassium and sodium. It was determined that when the elements were used as a ratio to sodium they had the lowest percent relative standard deviation. Therefore, all element ratios, discussed from this point on, refer to a ratio to the sodium signal.

3.1.2.5. Latex Paint Discrimination Study:

For the first paint discrimination experiment, fourteen (14) additional paints were collected and combined with the original three paint sources. In all seventeen (17) samples, there were only two cases of duplicate brands, nevertheless they were different types of white latex paint. The new samples were prepared in the same fashion as for the within can variation study, except only five samples were prepared per can instead of ten.

The collected data were processed by Glitter to obtain raw background subtracted signals. These element signals were then analyzed using Systat to determine the mean squared error for each element pertaining to each sample of paint. The highest value for each element was then used to compare the individual samples by a General Linear Model pairwise comparison with Tukey as the post hoc test.

3.1.2.6. Reproducibility Study:

Four samples were chosen and analyzed to determine the reproducibility within day and between days. Two of the samples analyzed for this study were the two cans of Behr Premium Plus Ultra Pure White 8050, which consisted of different lot numbers. They were previously distinguishable when analyzed during the twenty-four sample discrimination study. The remaining samples were the samples of Behr Premium Plus Ultra Pure White 1050, one of which was tinted in the store, again, with different lot numbers. These samples were previously indistinguishable during the twenty-four sample discrimination study. The five samples pertaining to each can were analyzed in triplicate. The Behr Premium Plus 8050 samples were run at the beginning and at the end of each run to determine reproducibility within a run. The sample set was analyzed once

154

in the morning and was repeated in the afternoon to assess within day reproducibility. This process was repeated the following day to determine day-to-day reproducibility.

The data were processed using element ratios and pairwise comparisons were performed using Systat and Excel.

3.1.2.7. Comparison of LA-ICP-MS with Micro-FTIR and SEM-EDS

3.1.2.7.1. SEM/EDS Instrumentation

The selected paint samples were analyzed on a Jeol JSM 5910LV SEM with an EDAX Phoenix Energy Dispersion Spectroscopy. The SEM/EDS system was operated under high vacuum and the target elements were chosen based on previous LA-ICP-MS data. The instrument parameters are given in Table 3.3.

Table 3.3. SEM/EDS operating parameters for Latex Paint analysis

Spot size	Accel. Voltage	Working Dist.	Signal	Magnification	Preset
43-46 µm	30kV	12mm	Secondary Electron Image	X100	100 sec.

For bulk sampling a raster pattern of approximately 400µm by 300µm was used. The position of analysis was chosen to avoid any foreign particulates that may have interfered with the recovered signal. The samples were not coated with gold or carbon, thereby allowing the semi-quantitative analysis of surface elements.

Three chips of each sample were analyzed in duplicate. Each chip was secured to the sample stage by copper double-faced tape. Due to time constraints only nine selected samples were analyzed over two days. The selected samples are displayed in Table 3.4.

The reported percent by weight values for each element was used to calculate element ratios. These element ratios were then analyzed using Systat and Excel to perform a general linear model pairwise comparison, using the same process as described for the data collected for the LA-ICP-MS results. These data were compared to the results obtained from the LA-ICP-MS analysis and the false positive and false negative errors were identified.

3.1.2.7.2. FTIR instrumentation

The instrumentation utilized for the infrared analysis was a Perkin Elmer Spectrum 2000 NIR FT-RAMAN coupled with a Perkin Elmer i-series FT-IR microscope. This allowed for precise micro-sampling of the collected paint samples. The analysis was run in mid IR range. The resolution was set at 2 with strong apodization and a gain of 8. Thirty-two scans were for each sample was found to be adequate. The spectra range analyzed was 750 to 4000cm^{-1}. Focusing of the sample was achieved manually with the assistance of a CCD camera and monitor attached to the microscope optics.

The samples were prepared by manually slicing thin cross sections of the samples with a clean scalpel, while viewing under a stereoscopic microscope. These cross sections were then placed in between two KBr crystals and positioned in the Carver

manual Pellet Press, with the 13mm die. A pressure of approximately 3-4 metric tons

was applied to the crystals and sample. This resulted in a solid transparent KBr pellet

with the collected cross section pressed into an extremely thin layer in the middle of the

pellet. These pellets were then analyzed by the micro-FTIR. A background was taken,

for each pellet, by focusing on, and sampling an area of the pellet that did not have the

paint sample present. The area sampled for background was always the same shape and

size of the area analyzed for the paint sample.

Table 3.4. Selected samples for SEM/EDS analysis

Sample #	Brand Name	Color	Product #	Int/Ext.	Notes
1	*Glidden Evermore*	Deep tint Base	HD-6980	EXT	
2	*Ralph Lauren*	Brilliant White	RL 1291	INT	SATIN
3	*Behr Premium Plus*	Deep Base	3300	INT	SEMI-GLOSS
4	*Behr Premium Plus*	Ultra Pure White	8050	INT/EXT	HI-GLOSS
5	*Glidden Evermore*	White	HD-6224	INT	SATIN
6	*Quik Hide*	White	26960	EXT	FLAT
9	*ColorPlace*	White	5407	INT	SEMI-GLOSS
19	*Behr Premium Plus*	Ultra Pure White	8050	INT/EXT	HIGH GLOSS
23	*Martha Stewart: Everyday Colors*	IronStone White	74-04	INT	SEMI-GLOSS

3.2. RESULTS AND DISCUSSION: AUTOMOTIVE PAINTS

### 3.2.1. Optimization of the method and evaluation of the analytical performance

Previous studies conducted in our research group (Hobbs, 2003) have demonstrated that LA-ICP-MS is a viable tool for forensic analysis of automotive paints, which provides better detection limits compared to SEM/EDS and XRF.

The scope of this work was to conduct further investigation of the precision, repeatability, homogeneity, discrimination power and sampling strategies. The use of internal standards and quantification methods were also explored. Moreover, statistical tools were applied to numerical data resulting from the semiquantitative and quantitative analysis in order to propose match criterion for the association and discrimination of paint samples.

3.2.1.1. Precision and repeatability

The first target objective during the optimization of the LA-ICP-MS method was to improve the precision. It was observed that by using the optimum parameters of spot size (100 µm), energy output (70%) and frequency (2Hz) the precision was poor particularly for those elements with low concentration levels. The paints used for this study have a metallic appearance (red and blue ACT sample) and consequently when the sample is observed under the microscope there are "flakes" of metallic components that make it heterogeneous in a micro-scale range. Figure 3.3 illustrates the microscopic

appearance of the red paint where the "flakes" are observed as yellow, brown and white dots. The whole length of the photograph is 800 µm and two dashed squares were draw to simulate the sampling area for a 100µm spot. It can be visually determined that the occurrence of flakes varies significantly between the sampling areas and therefore natural heterogeneity of the sample at a micro range may be the main source of poor precision between runs.
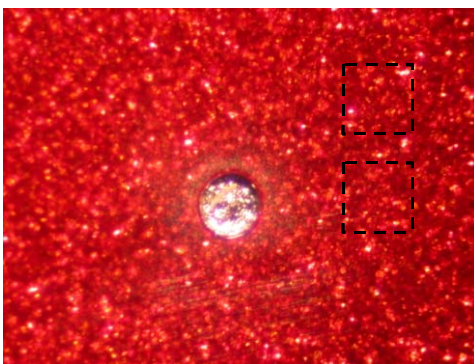
Figure 3.3 Microscopic photograph at 20x of a 100 µm spot size crater of the red ACT paint standard.

As a consequence, the sampling area was increased to 200µm spot size in order to evaluate if the precision could be enhanced. Figure 3.4 shows that this approach reduced the relative standard deviations for the vast majority of elements (< 12 %), except for lead and tin in the second layer and strontium in the fourth layer. Layers sampled with 200µm are shown as yellow bars while layers analyzed with 100µm are shown as blue bars.
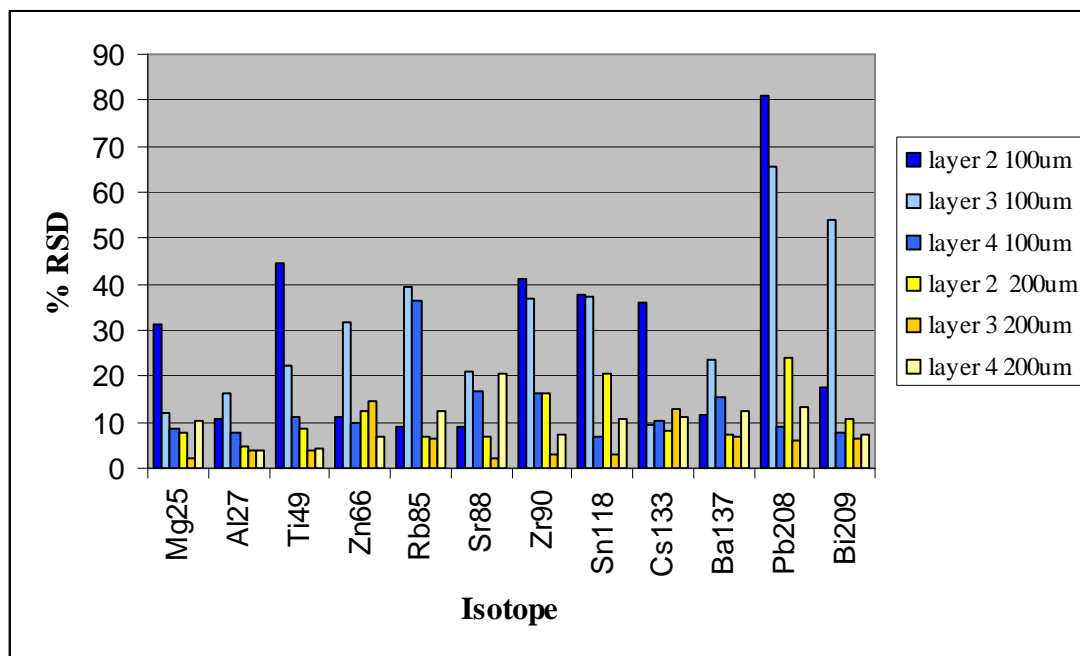
Figure 3.4. Comparison of precision between 200 µm (yellow bars) and 100µm

(blue bars) spot sizes for layers 2, 3 and 4 of paint red ACT.

The first layer was not included in the graph above on purpose because it

followed a different behavior due to the very low concentration of elements present on it.

As a consequence, the precision of the measurements even with 200µm spot size was

close to 20% for most of the elements. Some of the elements such as Cr, Rb, Ce and Bi

were not detected in the first layer using 100µm spot size. Bad precision in the first layer

was therefore a result of the low detection of elements rather than natural heterogeneity

of the paint.

Although for forensic purposes the minimum consumption of evidence is always

preferred, best results were achieved sampling 200 µm spot sizes because it takes into

account a representative area if the elemental composition of the paint. The experiments were repeated using a blue ACT paint and same conclusions were obtained.

3.2.1.2. Homogeneity studies and match criterion

Prior to defining match criteria for comparison of paints as well as to evaluate the discrimination power of the method, it was necessary to study the natural homogeneity of the matrix. The study was performed in two set of samples, the first consisted of five blocks of red automobile paint purchased from ACT Laboratories and the second one consisted of a piece of green paint provided by the Royal Canadian Mounted Police (RCMP).

The statistical evaluation of the homogeneity on the red paint was done using ANOVA for seven pieces of paint randomly selected from the original source of paint, each one was measured in four replicates. Figure 3.5 shows the elemental profile for the 7 pieces for the second, third and fourth layer.

Even if visual examination of the elemental profile on figure 3.5 seems to associate the seven fragments to the same source, when ANOVA was performed, the fragments were distinguishable by some elements. The total number of pairs that can be generated by pairwise comparison of this set of 7 sub-samples are 21, (n(n-1)/2), and all of them should not be distinguishable since they came from the same piece of paint. However, table 3.5 shows that the concentration of some elements was significantly different.

161

These results demonstrate that the variation due to heterogeneity in the sample is larger than the instrumental variation and therefore for forensic comparisons is essential to characterize the "known" or "control" sample before conduct any association or discrimination of samples recovered at the crime scene, from the suspect or victim.
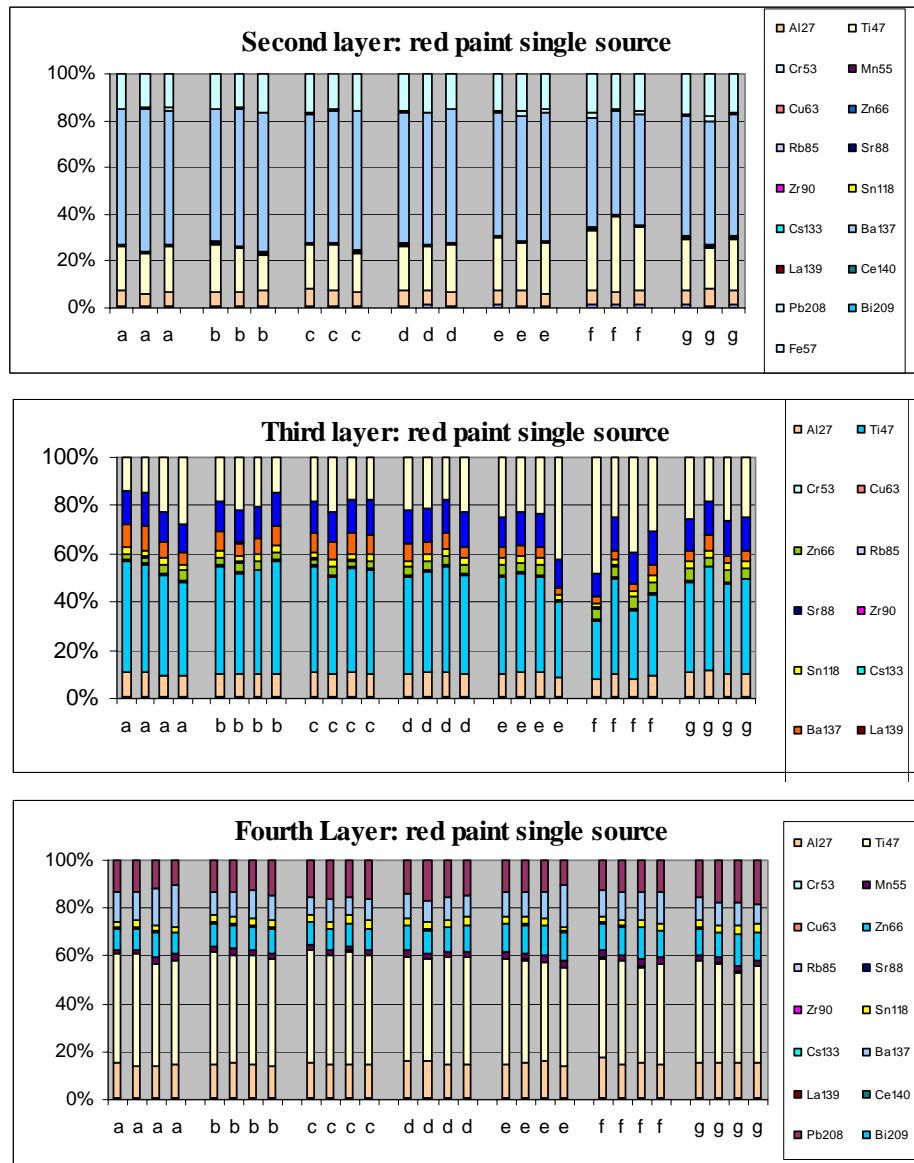
Figure 3.5. Comparison of elemental composition of 7 pieces of paint originated from the same source

One way of characterizing the known sample is to measure several replicates from the original source and perform an ANOVA to use the mean square error between the measurements (MSE) as an indicative of the natural variation of the elemental composition in the sample. This method therefore counts the real heterogeneity of the source sample as match criteria.

Another five blocks of the same batch of red paint, each one of ~ 15 x 12cm, were available at the laboratory and therefore an ANOVA comparison was performed with and without the MSE correction. When ANOVA was conducted without the correction all five blocks were distinguishable. On the other hand, when the statistical analysis was carried out with the correct characterization of the heterogeneity of the paint, all blocks were associated as originated from the same source. Figure 3.6 shows the comparison of elemental profiling between the five blocks for the fourth layer of paint.
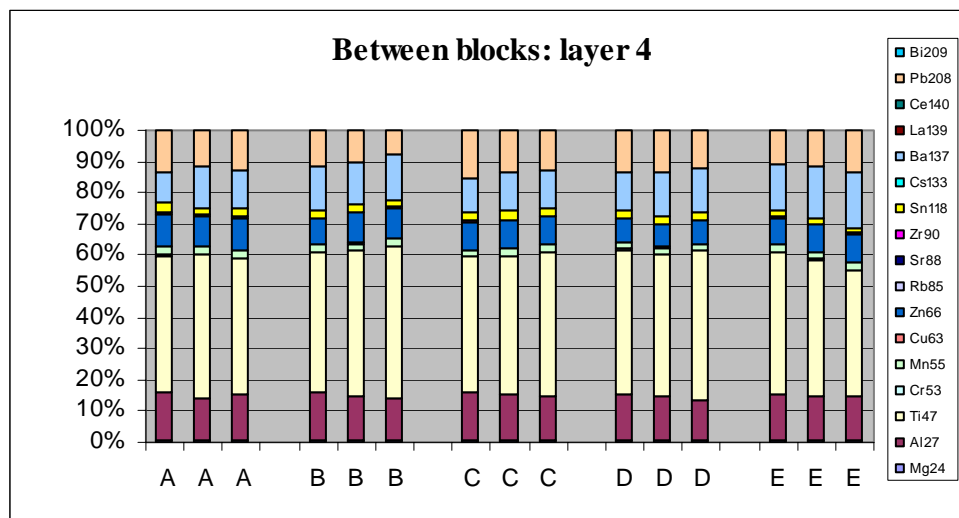
Figure 3.6. Comparison of elemental profiling between five blocks of red paint

Table 3.5. Summary of ANOVA results for the comparison of seven fragments originated from the same automobile paint.

LAYER	2		3		4	
Isotope	ndp[a]	dp[b]	ndp[a]	dp[b]	ndp[a]	dp[b]
^{24}Mg		2	x		x	
^{25}Mg		3	x		x	
^{27}Al	x		x		x	
^{47}Ti		2		5	x	
^{49}Ti		2	x		x	
^{53}Cr	x		x		x	
^{55}Mn	x		x			4
^{63}Cu	x		x		x	
^{66}Zn	x			1	x	
^{85}Rb	x		x			2
^{88}Sr	x			2	x	
^{90}Zr		4	x			1
^{118}Sn		4		2		4
^{133}Cs	x		x		x	
^{137}Ba		1		6		2
^{139}La		4	x		x	
^{140}Ce	x		x		x	
^{208}Pb	x		x			3
^{209}Bi	x		x		x	

ndp[a] : non distinguishable pairs

dp[b] : distinguishable pairs

Same conclusions were derived from the analysis of the second set of paint (green paint block). Nonetheless, it might be important to notice that both set of paints used for this study had a "metallic" appearance and therefore the inherent heterogeneity could be larger than that of solid coat paints. Additional studies of homogeneity on large samples of paints of this type should be conducted in a future.

3.2.2. Discrimination study for automobile paints

The discrimination study was conducted for a total of eight automobile samples to evaluate if LA-ICP-MS can distinguish samples that would otherwise be classified as indistinguishable. If LA-ICP-MS were not used in those instances, a false positive association could result.

The automobile paint samples were submitted by the RCMP and were obtained from their paint database query (PDQ). The sets were selected so they had a very similar color, layer structure and layer sequence. The sets were divided in three subsets that are discussed in detail in the following sections.

3.2.2.1 Set of white paints

The white set was comprised of three white paints that originated from vehicles that differ by the manufacturing year but otherwise they were manufactured by the same manufacturer, same plant, same make, same line and same model. All paints have the same color and appearance; they have the same layer sequence and are undistinguishable by visual and microscopic examination. Table 3.6 shows that the chemical composition amongst the four layers of paints 167 and 189 are identical. On the other hand, sample 147 is very similar to the others, except for the first and second layer that have polyurethane in addition to the other resin binders. Another difference between samples 147 and the rest is that the fourth layer does not contain silicate. Nonetheless, the infrared spectra for the fourth layer were undistinguishable between the 3 samples of interest as is shown in figure 3.7.
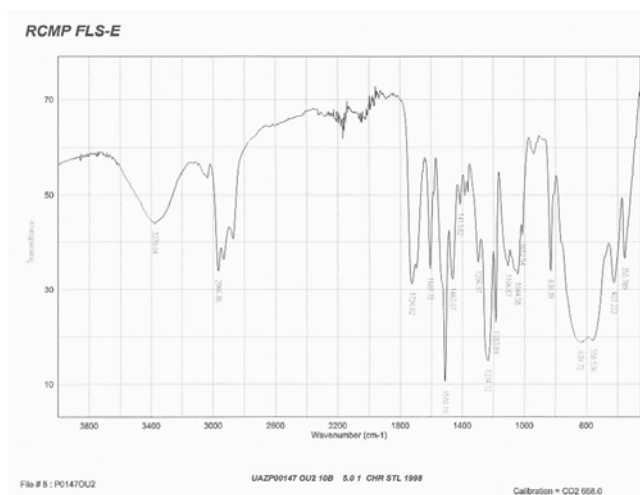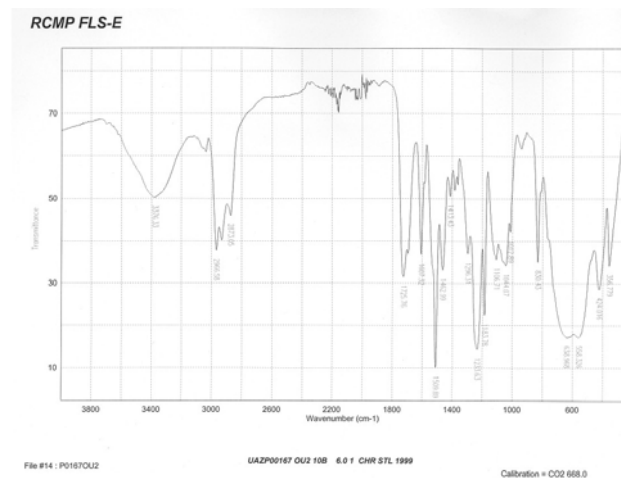
Figure 3.7. Comparison of infrared sprectra of fourth layer of white paint samples 147 and 167.

Comparison of the paints by LA-ICP-MS allowed for the discrimination of all 3 samples; as is shown in figure 3.8 they were distinguishable by the elemental profiling of the first and second layers. Is important to notice that since we only had a piece of paint from each sample, characterization of the natural heterogeneity of the source was not possible and consequently statistical ANOVA is not appropriate because it could generate false discrimination as explained during the homogeneities studies. A conservative approach was thereby applied and comparisons of paint relied on the visual examination of the elemental ratios and only profiles that were obviously different were considered distinguishable.

The results of this set demonstrate that LA-ICP-MS analysis provided additional information that can be useful for comparison of paints. Samples 167 and 189 were distinguishable by the elemental composition of the first layer; by their content of Ti, Zn and Fe. The proposed method added discrimination potential to the conventional methods used for examination of paints that were unable to discriminate between these two samples even though they were manufactured in different years. This is particularly important for forensic purposes because a false association could cause an innocent person to be associated to a crime that he/she did not commit.

Table 6.6. Chemical composition of the layers of the white paint set

Paint identification	UAZP00147	UAZP00167	UAZP00189
First layer	Acrylic	Acrylic	Acrylic
	Melamine Polyurethane	Melamine	Melamine
	Styrene	Styrene	Styrene
Second layer	Acrylic	Acrylic	Acrylic
	Isophthalic alkyd Epoxy	Isophthalic alkyd	Isophthalic alkyd
	Melamine Polyurethane	Melamine	Melamine
	Styrene	Styrene	Styrene
Third layer	Terephthalic alkyl	Terephthalic alkyl	Terephthalic alkyl
	Epoxy	Epoxy	Epoxy
	Titanium dioxide	Titanium dioxide	Titanium dioxide
	Barium sulphate	Barium sulphate	Barium sulphate
Fourth layer	Epoxy	Epoxy	Epoxy
	Titanium dioxide	Titanium dioxide	Titanium dioxide
	Zinc Phosphate	Zinc Phosphate	Zinc Phosphate
	Polyurethane	Polyurethane Silicate (Kaolinite)	Polyurethane Silicate (Kaolinite)
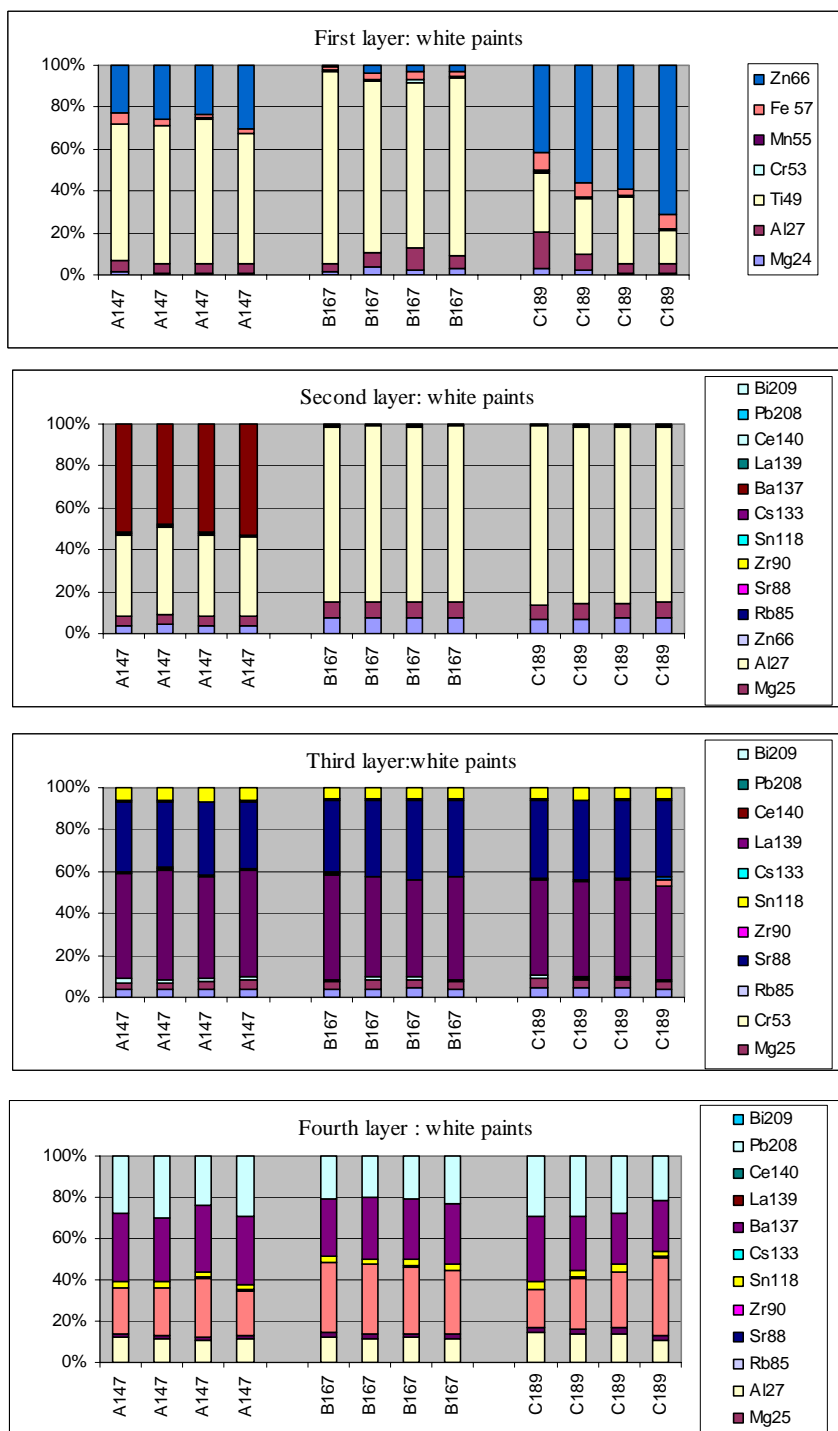
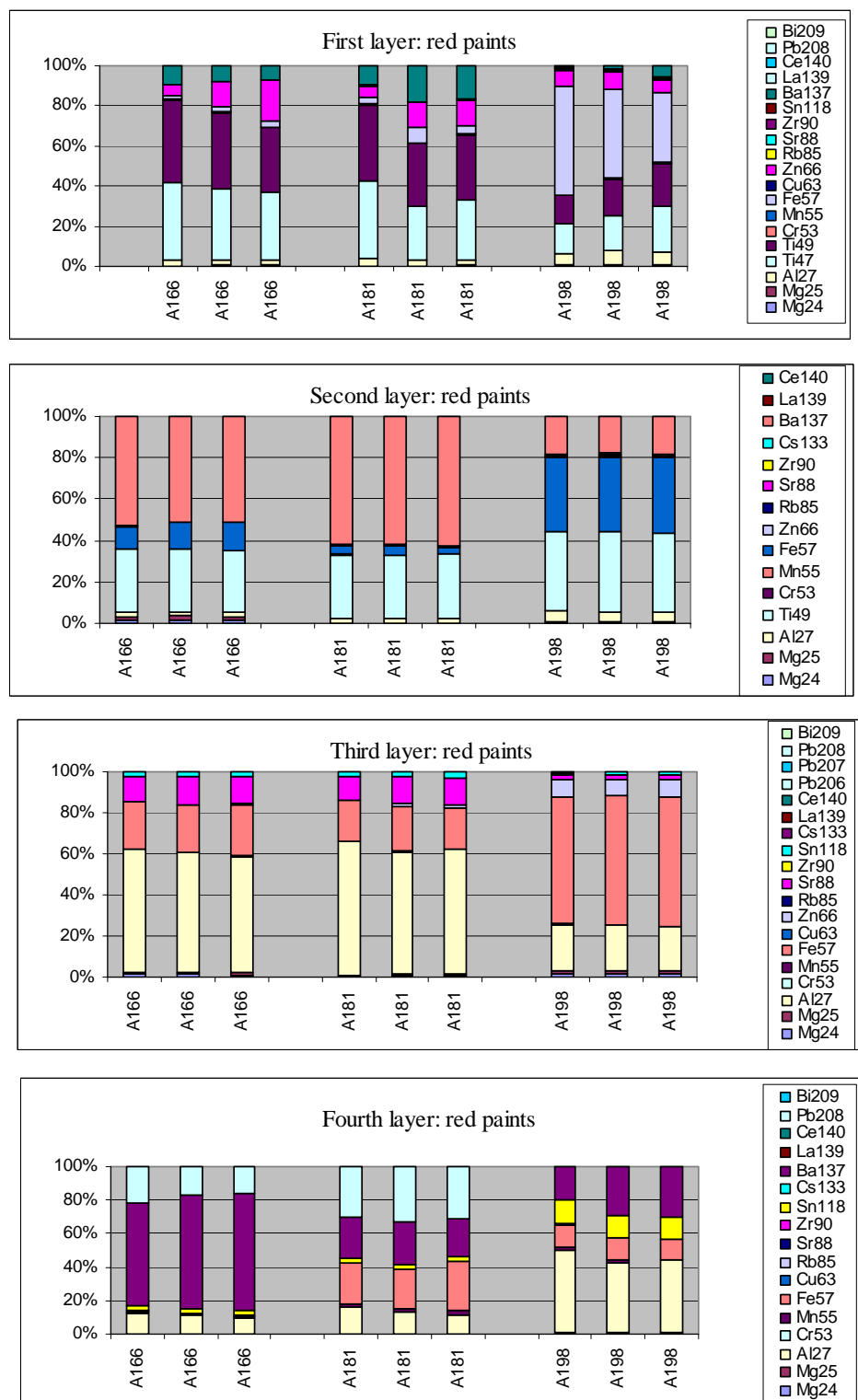**Figure 3.8**. Comparison of elemental profile of white paint set.

3.2.2.2. Set of red paints

The red set was comprised of three paints that originate from vehicles that differ by the manufacturing year or the line. This set has also same color, appearance and layer sequence. In terms of chemical composition of the layers, they were different by the second layer only (see table 3.7). Sample 181 has a different content of inorganic pigments than samples 166 and 198, but again that difference was not detected by conventional methods. Elemental analysis by LA-ICP-MS was able to discriminate all samples by their composition on the second, third and fourth layer. In addition, sample 166 presented also a different elemental profile than sample 198 (see figure 3.9).

Table 3.7. Chemical composition of the layers of the red paint set

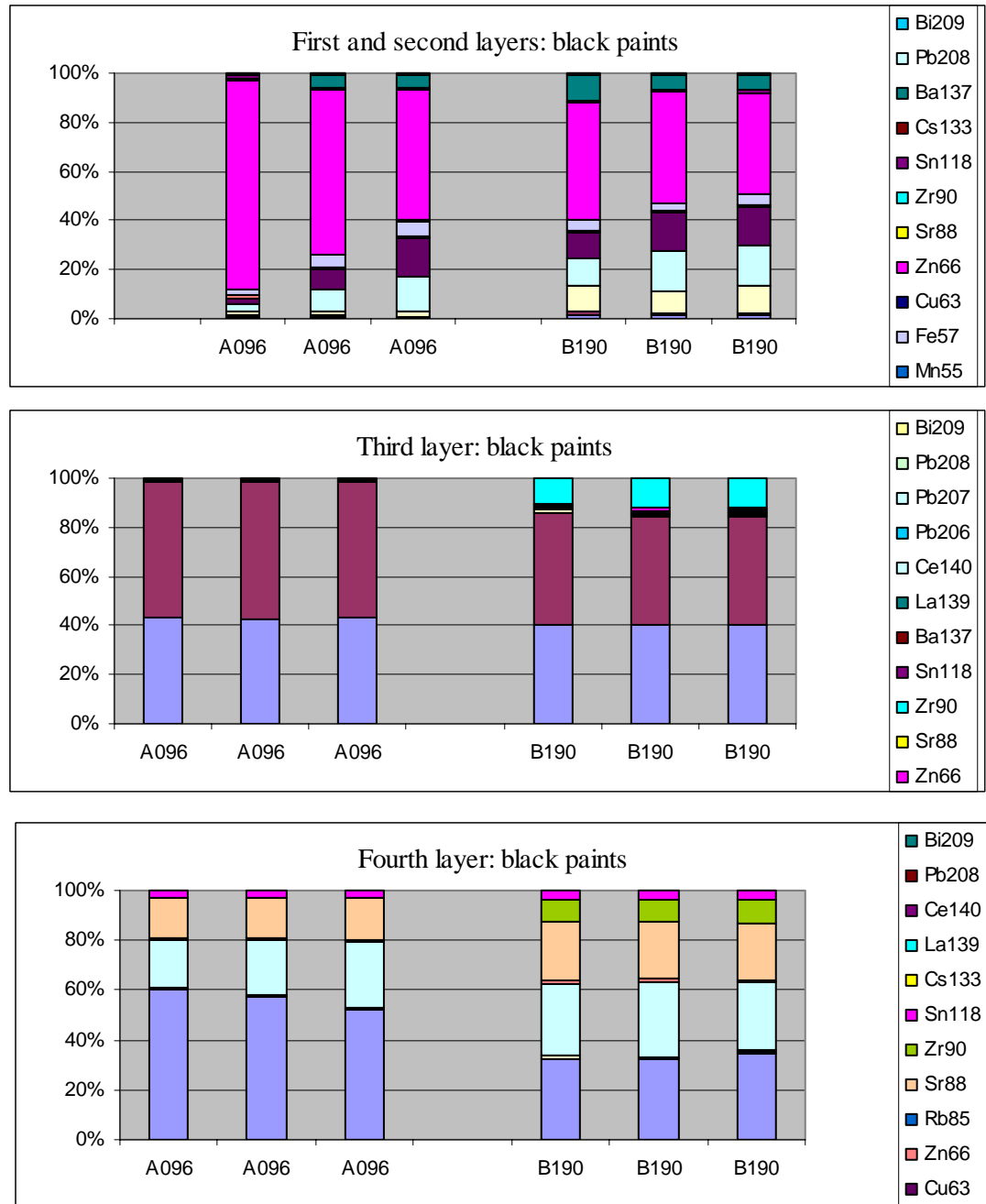| Paint identification	UAZP00166	UAZP00181	UAZP00198
First layer	Acrylic	Acrylic	Acrylic
	Melamine	Melamine	Melamine
	Styrene	Styrene	Styrene
Second layer	Acrylic	Acrylic	Acrylic
	Isophthalic alkyd	Isophthalic alkyd	Melamine
	Melamine	Melamine	Styrene
	Styrene	Styrene	
		Polyurethane	
Third layer	Terephthalic alkyl	Terephthalic alkyl	Terephthalic alkyl
	Epoxy	Epoxy	Epoxy
	Titanium dioxide	Titanium dioxide	Titanium dioxide
	Barium sulphate	Barium sulphate	Barium sulphate
Fourth layer	Epoxy	Epoxy	Epoxy
	Titanium dioxide	Titanium dioxide	Titanium dioxide
	Barium sulphate	Zinc Phosphate	Barium sulphate
		Polyurethane Silicate	
		(Kaolinite)	

171

Figure 3.9. Comparison of elemental profiles for the set of red paints

3.2.2.3. Set of black paints

This set was composed of two black paints that originate from vehicles that differ by the manufacturing year only. They were undistinguishable by visual and microscopic examination since they have the same color and layer sequence. Chemical composition differs between the samples only in the additional content of polyurethane for layers one and two (see table 3.8). When LA-ICP-MS analyses were conducted not only those two first layers were distinguished but also the third and fourth layers presented different elemental profile (see figure 3.10). In these particular paints the first and second layers were so close together that it was hard to integrate them individually so they were evaluated as a single layer.

Table 3.8. Chemical composition of the set of black paints

Paint identification	UAZP00096	UAZP00190
First layer	Acrylic	Acrylic
	Melamine	Melamine
	Polyurethane	Styrene
	Styrene	
Second layer	Acrylic	Acrylic
	Isophthalic alkyd	Isophthalic alkyd
	Melamine	Melamine
	Polyurethane	Styrene
Third layer	Terephthalic alkyl	Terephthalic alkyl
	Epoxy	Epoxy
	Titanium dioxide	Titanium dioxide
	Barium sulphate	Barium sulphate
Fourth layer	Epoxy	Epoxy
	Titanium dioxide	Titanium dioxide
	Zinc Phosphate	Zinc Phosphate
	Polyurethane Silicate (Kaolinite)	Polyurethane Silicate (Kaolinite)

174

Figure 3.10. Elemental profile of the set of black paints

For all sets studied, laser ablation ICP-MS was demonstrated to improve the discrimination power of samples that originated from different sources, particularly for those samples that were completely undistinguishable by their infrared spectra (167 and 189 white; 166 and 198 red). Furthermore, elemental analysis also discriminated between the under coat layers (layers 3 and 4) of the red and black sets (see figure 3.11). In these layers the differentiation given by the color coat is no longer present and it could be noticed from tables 3.7 and 3.8 that the chemical composition of these layers is undistinguishable by conventional techniques since they have the same IR and microscopic appearance; while LA offer a clear discrimination between the samples.
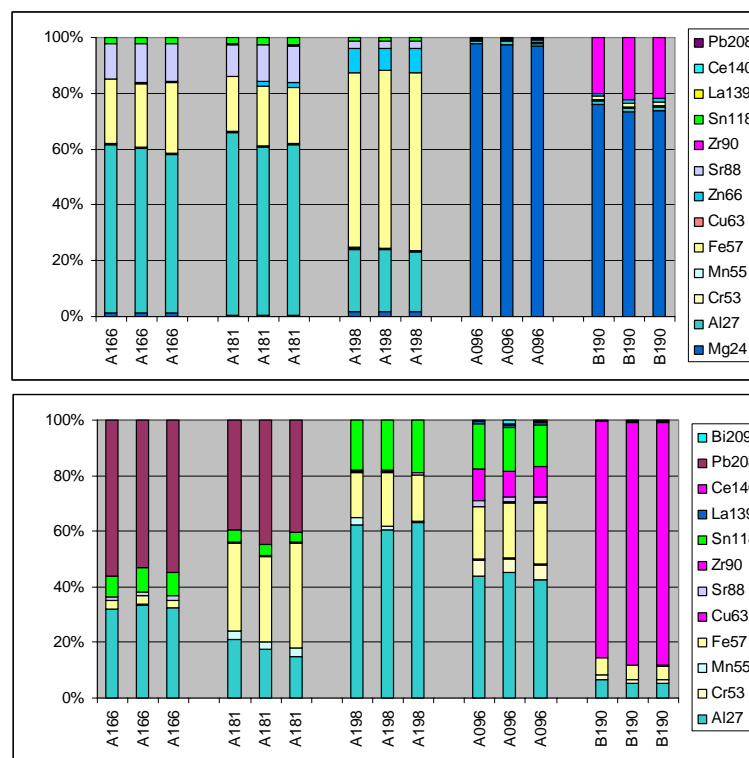
Figure 3.11. Comparison of elemental composition of the under coat layers for set of red and black paints

3.2.3. Strategies for the forensic comparison of elemental composition of automotive paints

The method of comparison of paints proposed by Hobbs (Hobbs, 2003) includes the display and processing of data in a variety of forms such as the time resolved plots and the elemental ratios plots. The time resolved plots represent the easier and faster way to compare two samples and visualize the separation between layers. They have the advantage of being displayed in real-time during the analysis and consequently they may be useful as a fast screening tool to discard two samples that have an obvious different profile. A practical application of the time resolved plots may be the screening of different suspect vehicles where only the vehicle that provide a close match with the recovered sample should be analyzed in more detail. This could save time and reduce backlogs in forensic laboratories. Nevertheless, this method is merely qualitative and is not accurate to make a definitive association of samples because the visual comparison of elements present at high concentration may mask the signals of elements present at lower levels, which in most cases are essential to discriminate samples.

The elemental ratios plots are still a qualitative comparison where the layers are integrated individually, and element profiles plots can be constructed based on the relative intensity of elements. The main advantage of these plots compared to the time resolved graphs is that the individual layers of the paint can be visualized more easily and the numeric ratios can be used to perform statistical treatment of the data.

In contrast with glass analysis, analysis of paints by LA-ICP-MS present a series of limitations such as: a) there are no available in the market matrix-match solid standards, b) the multi-layer system is more complex than glass, c) there are more heterogeneity in the matrix, and d) there is no element present at even concentration amongst the different paints and/or layers and therefore is very difficult to find an internal standard.

During this work two additional approaches to compare paint samples were investigated, the first one involves the use of a normalization with glass standards and the second one the quantification of paints without the need for solid match standards.

### 3.2.3.1 Semi-quantitative analysis of paint using glass standards

Although the ablation behavior of glass and paint samples is different, the use of glass NIST 612 as calibrator for paint analysis was investigated and some advantages were found, such as providing a way to correct for drift over time and performing a semi-quantitative estimation of the concentration of elements in the paint.

In addition to that, it was observed that the content of silicon was a good indicative of the separation between layers of paint and that opposite to the majority of elements, it does not suffered from drastic carry over effects between layers. It was also noticed from the samples under study that the signal of silicon remains steady within each layer of paint, which is a desirable characteristic for an internal standard (see figure 3.12, blue signals). However, because the content of ^{29}Si seems to vary between layers and

between different paints it cannot be used strictly as an "internal standard" but it could be used as a "normalization" factor to improve precision between runs. Figure 3.13 shows the improvement in precision achieved with the semi-quantitative approach using NIST 612 as calibrator and normalization with silicon versus the qualitative comparison of elemental ratios (count intensities). The relative standard deviation illustrates the precision between ten (10) replicates of the ACT blue automobile paint. Another important advantage of running the glass standard between samples is that data reduction can be easily performed with GLITTER software, which not only save time but also have an automatic tool to perform drift correction for the data.
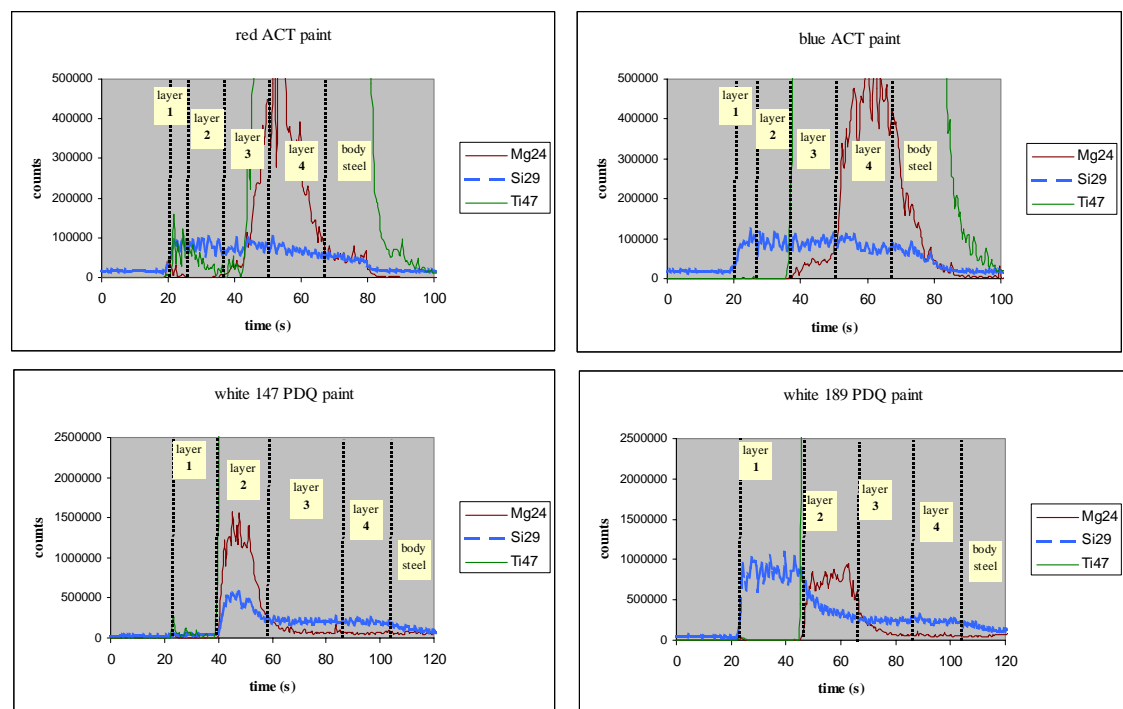
Figure 3.12. Time resolved signal for ^{29}Si in four different paints (red ACT, blue ACT, white 147 PDQ and white 189 PDQ)
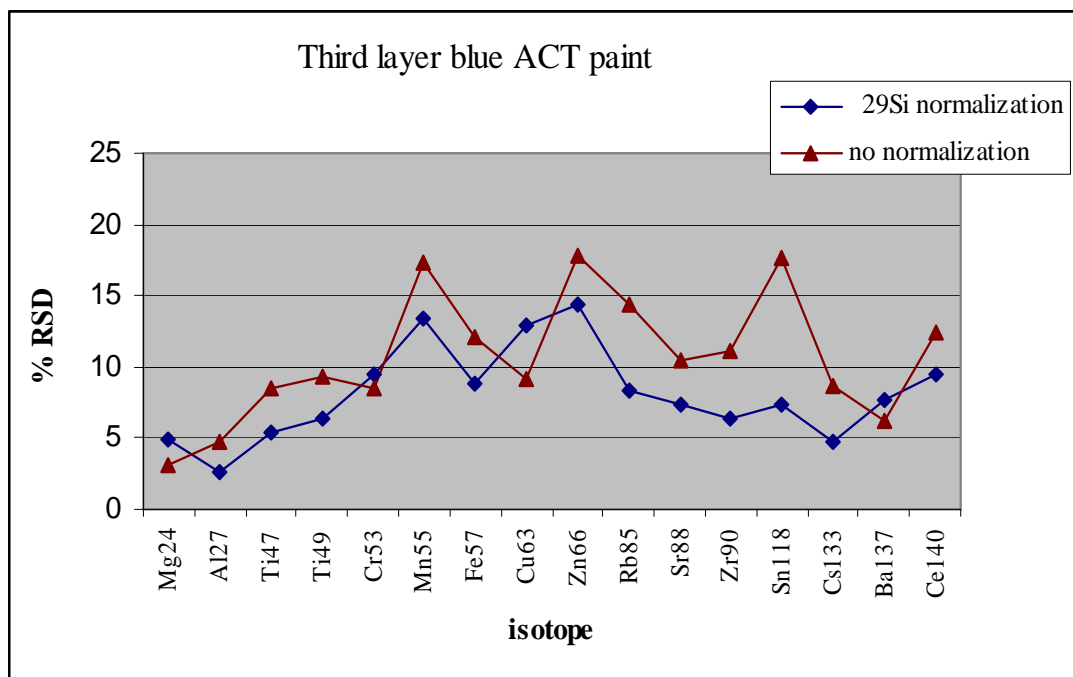
Figure 3.13. Comparison of precision (%RSD) between runs (n=10) with and without normalization with ^{29}Si.

Is necessary to point out that this approach improved precision but did not provide an accurate determination of the concentrations of the elements present in paints due to sources of systematic errors such as the dissimilar concentration of the "internal standard" between glass and paint, as well as differences in the ablation properties of the matrices. For these reasons, the best quantification of paints should be achieved if matrix matched standards were available.

An alternative way to overcome this limitation was explored and is discussed in the following section.

3.2.3.2 <u>Quantitative characterization of paints without matrix matched solid standards</u>

This method was adopted from the procedure suggested by Aeschliman et al (Aeschliman, 2003) who reported its application to glass and steel samples. The key benefit of this approach is not requiring matrix matched solid standards to perform quantification of laser ablation products. As described previously, the desolvated particles introduced from the nebulizer are mixed with the ablation aerosol of particles from the solid sample and then they are simultaneously introduced into the plasma. On the other hand, a portion of the particles from the ablation chamber are measured via online with a piezoelectric balance in order to provide normalization of the signal.

The authors suggested the use of a micronebulizer (Aeschliman, 2003) but since we did not count with one at the time of the experiments, the intake flow of the nebulizer was reduced from 1.3mL/min to 100 µL/min using a reduction of the speed of intake liquid (6 rpm) and a reduction of the diameter of the tubing. The purpose of that was to favor the natural evaporation of the solvent and provide a high percentage of desolvated particles that behave similar to the ablation products.

The laser ablation response was calibrated using a continuous "background signal" of dry aerosol from the standard solution, so when the laser ablation took place a "spike" was observed and it worked similar to a standard addition experiment.

Since glass is a much simpler matrix to work with laser ablation, the experiment was run first for the glass standard NIST 612 in order to optimize parameters and also to calibrate the volume of calibration solution that reached the plasma.

Figure 3.14 illustrates the signal obtained for two replicate "spikes" of two ablations of SRM 612, each one lasted 50 seconds. The figure also shows the "background" signal given by a 1ppb solution that contained eight elements; only signal of four of them is shown below, though.
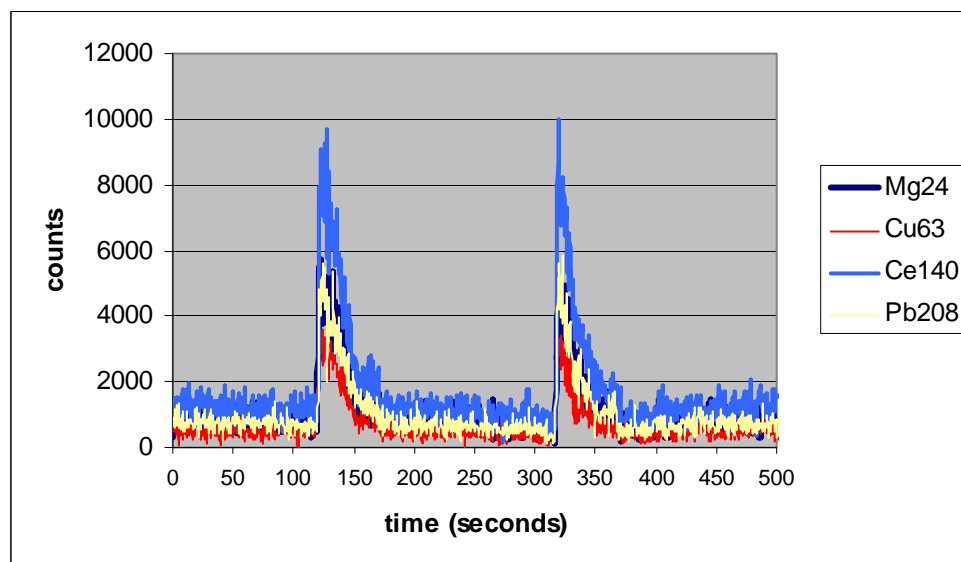
Figure 3.14. Replicate "spikes" from laser ablation of SRM 612 using single spot 500 shots (50 seconds ablation).

The calculation of the concentration of the solid was conducted using the equations:

$$S_{total} = S_{solution} + S_{solid}$$

$$S_{total} = Rx \times V \times [Conc_{solution}] + Rx \times m \times [Conc_{solid}]$$

Where S_{total} is the total signal produced by the background solution and the ablation of the solid together, Rx is the isotope response factor (counts/ng), V is the volume of solution that reaches the ICP (L), m is the mass entering the plasma from the LA (ng of solid), $Cn_{solution}$ is the concentration of the isotope in the standard solution (ng/L) and Cn_{solid} is the concentration of the isotope in the solid (ng/ng of solid, unknown).

The figure 3.15 represents the integration of the total signal (yellow) and the solution signal (blue), which was estimated right before the spike for a equivalent time of 50 seconds. The signal produced by the solid is then calculated subtracting the background signal from the total peak signal.
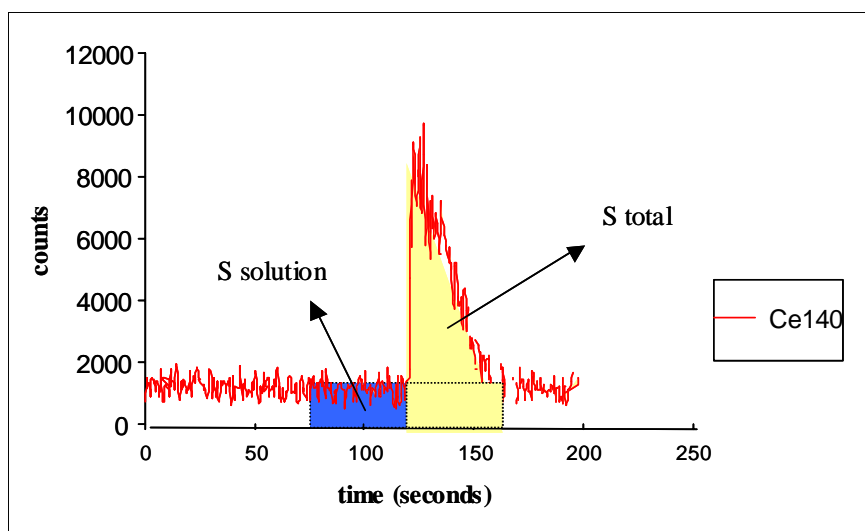
Figure 3.15. Typical integration ranges for the estimation of the total signal and the signal produced by the soution.

Once the signals were properly integrated, the subsequent step was to estimate the volume of solution transported from the nebulizer to the plasma. This calibration was performed with the ablation of a solid standard of known concentration (NIST 612) using the following equation:

$$S_{solid} = Rx \times m \times [Conc_{solid}]$$

Since the concentration of the solid NIST 612 was known and the mass of ablated particles was registered on the piezoelectric balance, the response factor for each isotope can be calculated as:

$$Rx = \frac{Ssolid}{m \times [Cn_{solid}]}$$

Then, the volume of aerosol from the liquid solution can be calibrated as:

$$V = \frac{S_{total} - Rx \times m \times [Conc_{solid}]}{Rx \times [Conc_{solution}]}$$

After the volume is calibrated, the experiment can be conducted to estimate the concentration of unknown solids using a two point calibration curve where the first pair of data points is given by the concentration of the solution equal to "zero" and the signal of the solid only ($x_1, y_1 = 0$, S_{solid}); the second pair is given by the value of the concentration used for the solution (1000 ng/L in this case) and the total signal (x_2, $y_2 = 1000$, S_{total}). The known values at this time were volume (V), total signal (S total), concentration of the standard solution (Conc $_{solution}$) and the mass acquired with the piezoelectric balance (m). The response factor can be estimated for each isotope from the

184

slope of the calibration curve and the concentration of the unknown sample can be derived from the intercept:

$$slope = Rx \times V$$

$$intercept = Rx \times m \times [Conc_{solid}]$$

The first attempt for quantification of solid samples without using matrix standards was conducted for glass NIST 612. Table 3.9 shows the results for the quantification of five replicates using 500 shots (50 s) for each ablation. Excellent precision and accuracy was obtained for the isotopes studied, except for barium. The poor results for barium were expected because the signal generated by the solution was too high in comparison with the signal generated by the ablation products and therefore that difficulties its quantification. This situation also reflects the importance of using a concentration at the calibrator solution that produces a "background" signal of similar intensity that the signal produced by the ablation of the solid only. Since only "two" points are used for this calculation a background signal too low or two high in comparison with the ablation signal will generate errors in the estimation of the slope and intercept. The signal produced by the solution was optimized diverting and discarding a large percentage of the nebulized particles to the waste (~85%) but in the case of barium the background signal was still high. For the rest of isotopes, these calibrations work out fine.

The estimation of the ablated mass with the piezoelectric balance was advantageous because it provided a very efficient way to normalize the signal between runs and made possible the correction for variations of laser performance over time.

Table 3.9. Results for quantification without using solid standards for five replicates of ablation of SRM 612

Replicate	Mg24	Al27	Mn55	Cu63	Ba137	Ce140	Pb208
1	79.29	9573	36.04	33.59	32.1	35.68	35.97
2	76.15	9529	38.91	36.3	33.61	37.58	35.03
3	73.57	10858	36.4	35.2	25.92	35.76	36.62
4	78.99	11163	34	38.4	19.89	36.64	35.87
5	68.35	10891	40.91	33.8	31.05	37.71	38.08
Mean	75.27	10403	37.25	35.46	28.51	36.68	36.32
stdev	4.51	787	2.69	1.98	5.62	0.96	1.14
%RSD	6.0	7.6	7.2	5.6	19.7	2.6	3.1
reported value	77.44	10580	39.60	37.70	41.0	39.00	38.57
% error	2.8	1.7	5.9	5.9	30.5	6.0	5.8

The application of this method to paint analysis was more complex because it was necessary to register the mass of each layer individually, which was impossible to achieve using single spot ablation, where the ablation of each layer last only 10-30 seconds and there is carry over of the elemental composition between layers. So in order to overcome that, single line rastering was used instead of drilling a hole through the layers and that way the signal was acquired during 50 seconds for each layer individually. The single line method was optimized for the red ACT paint in order to provide sequential ablation of each of the layers independently. Final conditions were set up at 70% energy output, 2Hz frequency, 100µm spot size and 10µm/s scan rate for a total of 50 seconds of acquisition. After the ablation of each layer, a blank of ~100 seconds was

run in order to avoid any carry over effect for the ablated mass between layers. Figure 3.16 shows the ablation profile, for magnesium only, for this four- layer paint using the single line mode.
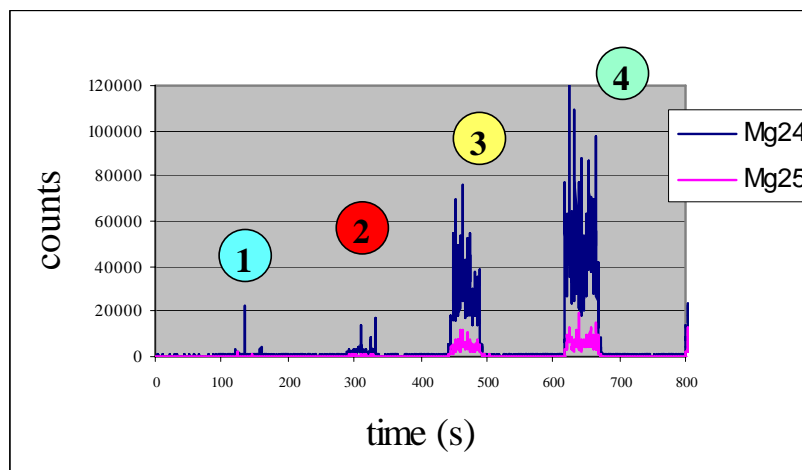
Figure 3.16. Transient signal for the 4 layers of red ACT paint using single line mode.

In order to calibrate the volume of the calibration solution that enters the plasma, glass 612 was employed to later estimate the known concentration of elements in paint using the same procedure as explained before for glass samples. Table 3.10 shows the preliminary quantification results obtained for three replicates measured on paint standard red ACT. The precision was not as good as for glass analysis because paints required a further optimization of the background levels given by solution. The limitation with paint analysis is that the levels of concentration of elements varied a lot between layers and therefore the solution of 1ppb did not work out fine for all of them.

From a practical point of view is very time consuming to "match" the signal produced by solution with the signal of each isotope produced by different layers of the paint. Nevertheless, it is worth it to perform the experiment for the red ACT standard in order to characterize the concentration values for elements of that sample with the purpose of using it in the future as a matrix match standard for the quantification of automobile paints. The experiment can be also used for characterization of standards designed at the laboratory.

Table 3.10. Quantification values obtained for red paint using the standardless experiment.

isotope	LAYER 1 Mean (ug/g)	%RSD	LAYER 2 Mean (ug/g)	%RSD	LAYER 3 Mean (ug/g)	%RSD	LAYER 4 Mean (ug/g)	%RSD
Mg24	250	13	262	26	4248	12	1739	20
Mg25	383	43	374	33	6221	15	2129	19
Al27	1996	34	16378	15	26210	7.1	33754	14
Cr 53	nd [a]		397	19	177	13	146	20
Mn55	296	12	1035	16	578	7.7	7657	23
Cu63	nd [a]		13.8	11	32.1	27	23.43	19
Ba137	750	14	11124	37	9166	30	2758	48
Ce140	nd [a]		nd [a]		nd [a]		nd [a]	

[a] not detected due to high concentration of solution vs ablated signal

188

3.3. RESULTS AND DISCUSSION: LATEX PAINTS

3.3.1. Preliminary LA-ICP-MS analysis for element menu determination:

The three initial samples of latex paint were analyzed by LA-ICP-MS, using the initial parameters: 100% power, 10Hz, and 55µm spot size. The collected raw signals were analyzed by GeoPro software and the resulting spectra were used to obtain a preliminary analysis of elemental content. The signal are illustrated below, Figures 17-19
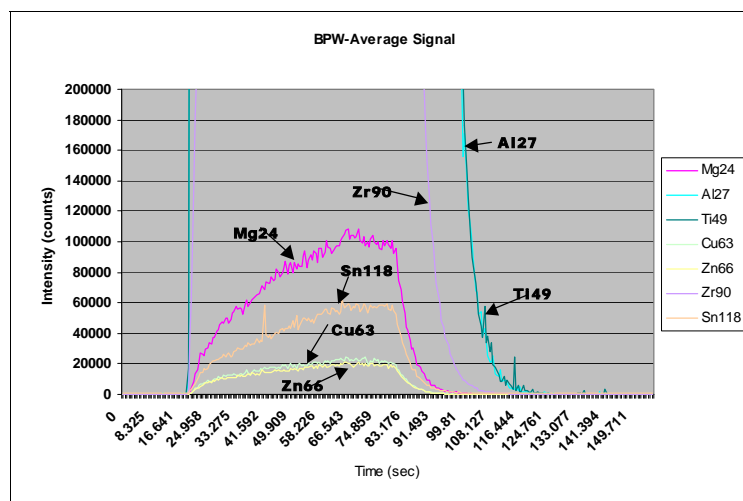
Figure 3.17. Average signal for Behr Premium Plus White 8050, LA-ICP-MS

189
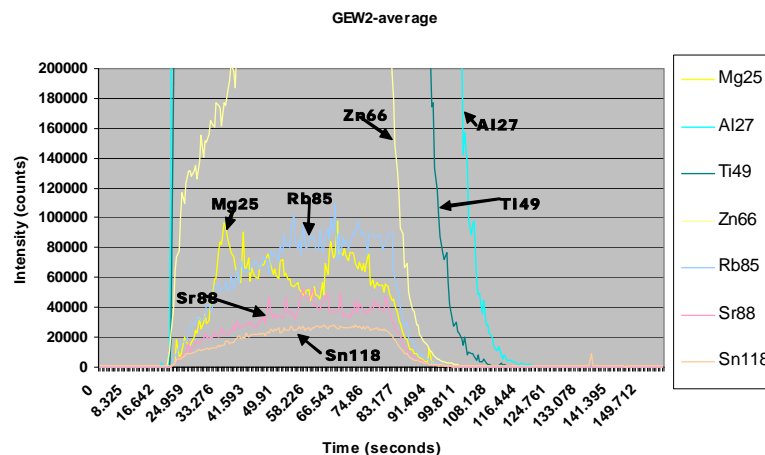
Figure 3.18. Average signal for Glidden Evermore White HD-6980, LA-ICP-MS.
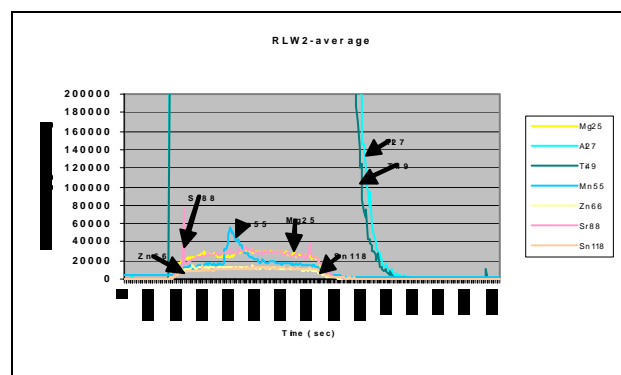
Figure 3.19. Average signal for Ralph Lauren RL 1291, LA-ICP-MS.

3.3.2. Laser Optimization

Dried paint samples were ground with a mortar and then pressed in a manual
press into 13mm pellets and used to attempt a preliminary optimization of the laser
parameters. The parameters explored were spot size, pulse frequency and power
intensity. It was observed that during the ablation of the pellets, the particle size was
highly irregular. The pellets were very fragile and during handling would be highly

190

susceptible to breaking. During the ablation process some of the larger particles were dislodged and would create an irregular shaped crater. This in turn would decrease the consistency of the signal and negatively affect the reproducibility.

Therefore, a new set of samples were prepared from liquid paint which were not ground. These samples were then used to repeat the optimization experiment. It was observed, during the optimization with the pellets, that the larger spot size generally increased the samples signal. It was also theorized that the larger spot size would aid in the accurate representation of the samples naturally heterogeneity. For the second optimization experiment the only variables optimized were frequency and percent power. The percent power was varied from 40, 60 and 70%, while the frequency was varied by 2, 5, and 10Hz. The resulting signals were more constant and provided more reproducible results. The final optimized parameters were determined by the general shape of the element signal as well as the signal strength.

3.3.3. Laser Ablation Element Menu

The new optimized LA-ICP-MS method was used to analyze a solid sample of Behr Premium Plus 8050 to determine a large menu of detectable elements. The concentrations were calculated using NIST 612 as an external calibrator and $Si29$ as an internal standard. The concentration of Si in the paint sample was set as 3% based on the range provided on the MSDS provided by the manufacturer. These calculations are not considered accurate representations of the concentration of the sample, but are relative to those concentrations and, in turn, were used to determine which elements were detectable. It was observed

that the relative standard deviation for several of the elements was significant. Therefore, the natural variation found within a single can of latex paint was determined by taking numerous measurements per can for the three original brands of paint.

3.3.4. Within can variation study:

The ten samples of paint collected were analyzed five times each. Several element ratios were calculated and analyzed to determine which resulted in the lowest variation within a sample and within a single can. The ratios were calculated using the elements titanium, aluminum, potassium, and sodium. For example, the results of the ratio comparison for Behr Premium Plus 8050 are displayed in Table 3.10

When the signals were ratioed to the sodium signal there was a larger number of elements with lower relative standard deviations. Consequently, the remaining results were calculated using the sodium ratio. A reduced element menu was created based on the observed variation in element ratios between the original three brands. The resulting variation within a single can is represented in Table 3.11.

Due to the reasonably high variation observed within a single can, a sampling method was devised to accurately represent this heterogeneity. It was determined that five samples from each source would be analyzed in triplicate. Also, to ensure accurate comparison, calculations the mean square error for each element in each sample were calculated. The largest mean square error for each element was used in calculating the pairwise comparisons.

192

Table 3.10. Comparison of elemental ratios for variation comparison

Al Ratio			Ti Ratio			K Ratio			Na Ratio		
Element	AVG	RSD	Element	AVG	RSD	Element	AVG	RSD	Element	AVG	RSD
Al27	1.0000	0.0000	Ti48	1.0000	0.0000	K39	1.0000	0.0000	Na23	1.0000	0.0000
I127	0.6398	12.9857	Sb121	0.0005	10.8834	W184	0.0003	8.8613	Ni58	0.0017	6.7941
Ti48	0.9556	13.1821	Cr52	0.0110	12.0621	Nb93	0.0352	9.0213	Zn64	0.1528	7.7501
As75	0.0007	13.5734	Ba138	0.0024	12.1717	Ta181	0.0011	9.1561	Cu63	0.0145	7.7848
P31	0.0544	14.9847	Si28	0.2999	13.1975	Zn64	0.0879	9.1581	Bi209	0.0031	8.0041
Si28	0.2747	17.7947	Hf180	0.0501	13.2774	Zr90	1.5157	9.1758	Sn120	0.0898	8.1405
Sb121	0.0004	19.9673	P31	0.0595	13.3749	V51	0.0068	9.4268	Nb93	0.0611	8.2951
Mg24	0.0358	20.0242	Cd114	0.0008	13.4152	Ni58	0.0010	9.4412	Ta181	0.0019	8.3901
Ba138	0.0022	20.2016	Sn120	0.0441	13.4548	Sn120	0.0517	9.5510	V51	0.0118	8.4518
Hf180	0.0462	20.5969	Mg24	0.0390	13.7848	Hf180	0.0587	9.6276	Ga69	0.0034	8.9591
Cr52	0.0101	20.6140	V51	0.0058	14.2159	Mg24	0.0458	9.7146	Zr90	2.6355	9.1861
Ta181	0.0009	20.6798	Nb93	0.0301	14.3555	Rb85	0.0003	9.8599	In115	0.0009	9.3115
Zr90	1.1960	22.0136	Ta181	0.0009	14.6377	Bi209	0.0018	10.0318	Hf180	0.1021	9.3585
W184	0.0003	22.0975	Zr90	1.2981	14.8422	Cr52	0.0129	10.0965	Cd114	0.0017	9.6679
Nb93	0.0278	22.2601	Bi209	0.0015	15.1044	Cu63	0.0083	10.1492	Mg24	0.0796	9.6949
V51	0.0054	22.2730	Zn64	0.0758	16.2012	Ga69	0.0020	10.8025	Ba138	0.0048	9.9206
Sn120	0.0409	22.3033	Cu63	0.0072	16.6224	Ba138	0.0028	10.9551	W184	0.0006	10.1169
K39	0.7950	23.2316	In115	0.0004	17.1985	Na23	0.5795	11.0359	Cr52	0.0224	10.3904
Sc45	0.0008	23.2629	Na23	0.4970	17.3902	Sc45	0.0011	11.0595	Sb121	0.0009	10.5707
Cd114	0.0008	23.8946	Ni58	0.0008	17.3956	In115	0.0005	11.3858	Pb208	0.0008	10.8651
S32	0.0376	24.0094	W184	0.0003	17.8218	Cd114	0.0010	12.3051	K39	1.7496	11.1895
In115	0.0004	24.5958	Ga69	0.0017	17.9831	Si28	0.3545	12.3327	Si28	0.6161	12.5456
Rb85	0.0002	25.1111	As75	0.0008	18.2097	Ir193	0.0001	13.0797	Rb85	0.0004	13.5955
Zn64	0.0704	25.3585	Pb208	0.0004	18.4189	Sb121	0.0005	13.3241	Pt195	0.0002	13.8380
Bi209	0.0014	25.7384	K39	0.8655	18.7611	Pb208	0.0004	13.6087	Sc45	0.0018	15.2049
Ga69	0.0016	25.9644	Pt195	0.0001	20.8157	P31	0.0710	15.1389	Sr88	0.0028	16.0408
Ni58	0.0008	26.0745	Rb85	0.0002	21.0907	Ti48	1.2545	15.3205	Ir193	0.0002	16.1047
Cu63	0.0067	26.1252	Ir193	0.0001	22.3124	Sr88	0.0016	15.3814	P31	0.1237	16.6867
Ir193	0.0001	26.4823	S32	0.0415	22.4369	As75	0.0009	17.2426	Ti48	2.1883	17.6009
Na23	0.4618	26.6208	I127	0.7132	22.8048	Pt195	0.0001	18.1113	Fe57	0.0006	18.2131

Table 3.11. Comparison of element ratios between three brands of paint, all above ratios are to Na.

BP 8050			HD 6224			RL 1291		
Element	AVG	RSD %	Element	Avg	RSD	Element	AVG	*RSD %*
Al27	2.5077	47.48	Al27	0.5943	18.85	Al27	0.8409	15.44
Cu63	0.0145	7.78	Cu63	0.0040	14.30	Cu63	0.0049	36.98
Hf180	0.1021	9.36	Hf180	0.0002	45.00	Hf180	0.0002	81.54
K39	1.7496	11.19	K39	0.7053	7.48	K39	1.3696	19.12
Mg24	0.0796	9.69	Mg24	0.1703	13.80	Mg24	0.0619	27.70
Na23	1.0000	0.00	Na23	1.0000	0.00	Na23	1.0000	0.00
Nb93	0.0611	8.30	Nb93	0.0022	18.35	Nb93	0.0002	43.32
Si28	0.6161	12.55	Si28	0.4145	29.72	Si28	1.1618	28.66
Sn120	0.0898	8.14	Sn120	0.0158	13.09	Sn120	0.0096	31.73
Ti48	2.1883	17.60	Ti48	0.5943	18.88	Ti48	0.8373	15.50
Zn64	0.1528	7.75	Zn64	0.0306	13.86	Zn64	0.0456	36.03
Zr90	2.6355	9.19	Zr90	0.0042	36.65	Zr90	0.0060	84.53

Using the devised sampling method, two samples of each brand of paint were processed and compared to demonstrate the discrimination power based on the selected element menu. The resulting pairwise comparison matrix is shown in Table 3.12

Table 3.12. Pairwise comparison of three brands of paint; Behr Premium 8050, Glidden Evermore HD-6224 and Ralph Lauren 1291

MATRIX	BP	BP2	HD	HD2	RL	RL2	
BP	1	0	0	0	0	0	
BP2	1	1	0	0	0	0	
HD	0	0	1	0	0	0	
HD2	0	0	1	1	0	0	
RL	0	0	0	0	1	0	
RL2	0	0	0	0	1	1	TOTAL
SUM	1	0	1	0	1	0	3

194

3.3.5. Paint Discrimination Study:

The first seventeen paints listed in table 3.2. were analyzed by LA-ICP-MS and submitted to pair wise comparisons using Siesta. This method was capable of discriminating all but 8 out of a total 120 possible pairs. Although this represents approximately a 93% discrimination power, it was not as accurate as suspected. Most likely, the inaccuracy was due to the relatively high mean square errors observed for some of the elements. Therefore, it was necessary to alter the laser ablation sampling method, such that it could allow for a better representation of sample heterogeneity within a single run. The proposed solution was to utilize a linear ablation pattern rather than a single spot, due to the increased surface area that can be analyzed.

These two ablation techniques were performed for samples identified as 13, 15, and 17 and the mean square errors for each method were compared, see Table 3.13. There was a clear decrease in mean square errors when the linear ablation was used, versus single spot ablation. This allowed for improved discrimination.

Table 3.13. Comparison of Mean Square Errors for two laser sampling methods, Linear and Spot Ablation

Spot MSE df=4				Line MSE df=4			
Element	7	13	15	Element	7	13	15
Mg 24	0.540	0.003	0.000	Mg 24	0.008	0.002	0.000
Zr 90	0.000	0.000	0.000	Zr 90	0.000	0.000	0.000
Al 27	0.370	0.358	0.886	Al 27	0.209	0.359	0.580
K 39	0.015	0.002	0.073	K 39	0.002	0.002	0.006
Ti 48	0.087	0.128	0.007	Ti 48	0.017	0.047	0.013
Zn 64	0.084	0.000	0.000	Zn 64	0.153	0.000	0.000
Nb 93	0.000	0.000	0.000	Nb 93	0.000	0.000	0.000
I 127	0.037	0.002	0.000	I 127	0.010	0.002	0.000
Hf 180	0.000	0.000	0.000	Hf 180	0.000	0.000	0.000
Si 29	0.011	0.000	0.003	Si 29	0.006	0.000	0.002

It was suspected that there may be some spectral interferences with the selected isotopes, using the quadrupole MS. Therefore a few samples were randomly selected and analyzed on the high resolution ICP-MS, in medium resolution mode to determine if any interference was present. There were several isotopes that were identified as having interference, Mg 24, K39, Zn 64, Hf 180, Ni 60, and Cu 63. To eliminate any problems this may cause, a new element menu was created using different isotopes that did not show any interference; the new menu included; Al 27, Zr 90, Ti 48, Nb 93, Mg 26, Si 29, K 41, Zn 66, Hf 178, Cu 65, and Sn 118.

The discrimination study was repeated using the linear laser sampling method. Additional samples of paint were obtained and prepared to be included in this analysis. Samples 18 – 25, from Table 1, were chosen to determine if it was possible to distinguish between samples of the same brand, but different types of white latex paint. For example samples 3, 4, 18, and 20 (Behr Premium) or samples 12, 21, 23, and 24 (Martha Stewart), see Table 3.2. Sample 19 was chosen because it is the same brand and type of paint as sample 4 (Behr Premium) except they originated from two different lots. Samples 18 and 25 originate from the same brand and type but they originate from different lots; sample 25 was tinted at the store. It should be noted that a paint chip was peeled from the can for sample 25 (given the ID CHIP) and analyzed. Since this sample was not subjected to the thorough and controlled sample collection method that the other samples were, it can more accurately represent an actual sample that may be found at a crime scene, which is why it is analyzed as well.

The twenty five samples were analyzed using the linear LA methodology and processed with Systat and Excel to create a pairwise comparison matrix. It should be noted that due to the large number of samples the LA-ICP-MS analysis was spread out over three days. A summary of the results of this analysis is shown in Tables 3.14 and 3.15, which shows that copper and tin appear to be the best elements for discrimination. Overall, it was possible to discriminate all but 6 pairs, out of a possible 300; three of these pairs can be explained. First, sample 25 was determined to be indistinguishable from sample CHIP which was collected from lid of the can for 25, therefore this conclusion is expected and accurate, given that they originate from the same source. Samples 25 and 18 were found to be indistinguishable, as were CHIP and 18. These two pairs can be explained because the samples were of the same brand and type, (different lots); moreover, samples 25 (and CHIP) were tinted, therefore it is suspected that the particular element that was used to tint the paint was not included in the menu. If these three indistinguishable pairs are removed this leaves only three unexplained pairs out of 300, which equates to a 99% discrimination.

Table3.14. Summary of Latex Paint discrimination by element, all elements are ratios to Na

Element	# of Indistinguishable pairs
Zr 90	236/300
Al 27	235/300
Ti 48	197/300
Nb 93	99/300
Mg 26	232/300
Si 29	206/300
K 41	289/300
Zn 66	232/300
Hf 178	128/300
Cu 65	75/300
Sn 118	93/300
Combined	6/300

Table 3.15. Description of Indistinguishable pairs

Indistiguishable pairs			
#	*Name*	*Name*	#
15	Decotime:White Int low luster	Behr Premium Plus: Base Ext. Flat	20
18	Behr Premium Plus: 1050	Behr Premium Plus:1050 tinted	25
18	Behr Premium Plus: 1050	Behr Premium Plus: 1050 tinted (chip from can)	CHIP
23	Martha Stewart: Ironstone white	Colorplace: White	9
25	Behr Premium Plus: 1050 Tinted	Behr Premium Plus: 1050 tinted (chip from can)	CHIP
20	Behr Premium Plus: Base Ext. Flat	Martha stewart: ironstone white satin	21

3.3.6. Reproducibility Study:

An experiment was designed and performed to determine if the data were consistent within a single day and between days. The samples selected for this study were 18, 19, 25, and 4. Samples 4 and 19 were run twice, once at the beginning and once at the end of the sequence. This sequence was repeated on two consecutive days and the results compared. The results show that the analyses are both consistent within a day and between days. However, samples 18 and 25 were previously determined to be indistinguishable and, during this experiment, were in fact distinguishable. This leads to

the conclusion that, when samples run on different days are compared, the accuracy of those comparisons may be limited, which could explain the three previously unexplainable indistinguishable pairs. In conclusion, to obtain comparisons of the highest accuracy, all samples should be run on the same day.

3.3.7. Comparison of LA-ICP-MS vs SEM and micro-FTIR

3.3.7.1. SEM/EDS results:

The nine samples analyzed by SEM/EDS were chosen to assess and compare the discrimination power of this technique. Samples 23 and 9 were chosen because these two samples were not able to be distinguished with previously mentioned LA-ICP-MS analysis. Samples 4 and 19 were chosen because they are the same sample of paint but are from different lots, and therefore would most likely be indistinguishable by SEM/EDS. A summary of the results of this analysis is presented in Tables 3.16 and 3.17.

The samples were separated into two groups and then compared to each other to determine if false negatives and false positives were present. There was one case where a false negative occurred. The two subsets of sample 1, Glidden Evermore 6980, were determined to be distinguishable when the data for all 12 elements was combined. It is important to draw attention to the fact that several of the elements chosen, Na, Mg, Si, Cl, and Sn, were not useful in distinguishing any of the samples. These elements were however, useful in the discrimination of the paint samples when analyzed by LA-ICP-MS. There were 44 reported indistinguishable pairs out of a total 171 possible pairs

using SEM/EDS. However, 10 of those were correctly identified as being indistinguishable; therefore there were actually 34 incorrectly identified indistinguishable pairs. The power of discrimination was estimated to be approximately 80% using this technique.

Table 3.16. Summary of SEM/EDS discrimination results

Element	# of Indistinguishable Pairs
Na	171/171
Mg	171/171
Al	92/171
Si	95/171
P	155/171
Si	171/171
Cl	171/171
K	137/171
Sn	171/171
Ti	49/171
Cu	137/171
Zr	147/171
Total	44/171

Table 3.17. List of indistinghishable pairs based on SEM/EDS analysis

Sample #	Description	Error	Description	Sample #
19	Behr Premium Plus 8050	False +	Behr Premium Plus 8050	4
19	Behr Premium Plus 8050	False +	ColorPlace 5407	9
2	Ralph Lauren 1291	False +	Glidden Evermore 6224	5
23	Martha Stewart: Everyday Colors	False +	ColorPlace 5407	9
23	Martha Stewart: Everyday Colors	False +	Behr Premium Plus 8050	19
24	Martha Stewart: Everyday Colors	False +	Behr Premium Plus 8050	4
9	ColorPlace 5407	False +	Behr Premium Plus 8051	5
1	Glidden Evermore 6980	False -	Glidden Evermore 6980	1

3.3.7.2. Micro-FTIR results

Twenty three out of the twenty four samples were analyzed via micro-FTIR. The omitted sample was sample #3 because it had physical characteristics that made it easily distinguishable through visual examination. The IR spectra for the remaining samples were analyzed based on the wavelength, relative shape and intensity of the observed peaks. In several situations, peak characteristics of multiple binder types were observed. A summary of the classification results can be seen in Table 3.18.

Table 3.18. Binder and extender classifications for architectural paint samples

| Sample	Binder	Extenders
1	Acrylic	unknown
2	PVA/Acrylic	unknown
4	Acrylic	n/a
5	PVA/Acrylic/acetate	Clay
6	Acrylic	Silica/ Calcium Carbonate
7	Acrylic	Talc
8	Acrylic	Talc
9	PVA/Acrylic	n/a
10	Unknown	Calcium Carbonate/Talc
11	Acrylic	unknown
12	PVA/Acrylic	Calcium Carbonate
13	PVA/Acrylic	Calcium Carbonate
14	Acrylic/Styrene butadiene	unknown
15	Acrylic/Styrene butadiene	unknown
16	Acrylic	Calcium Carbonate/Calcium Sulfate
17	Acrylic/styrene	n/a
18	Acrylic	Calcium Carbonate/unknown sulfate
19	Acrylic	n/a
20	Acrylic	Calcium silicate
21	PVA/Acrylic	Clay
23	Acrylic/Vinyl acetate	Calcium Carbonate
24	Acrylic/Vinyl acetate	Calcium Carbonate
25	Acrylic	Calcium Carbonate/unknown Sulfate

The majority of the observed binders were found to be either acrylic based or with an acrylic modification. There was one case where the binder was not able to be determined; in this situation, the signals for the observed extenders were too strong and broad to allow correct identifications.

The spectra were also used to identify some of the possible extenders present. This was not possible for all samples. The primary limiting factor for the identification of extenders was the limited range of the IR analysis; more specifically, the low end of the spectrum was 750 cm^{-1}. However the majority of the distinguishing signals for extenders fall below 700cm^{-1}. Therefore, in Table 25, the spectra that have evidence of extenders present but cannot be classified with the available information are thus listed as "unknown". The samples that did not have signal representative of any extender in the observable spectral range, were classified as "n/a".

There are several examples of spectra that cannot be distinguished based only on the IR classifications from Table 25. They are: 1/11, 4/19, 7/8, 12/13, 14/15, and 23/24. Of these indistinguishable classifications all are distinguishable when the relative intensities and ratios of the peaks were compared except for # 7/8, 4/19 and 12/13. An example of this can be seen in Figures 3.20 and 3.21.
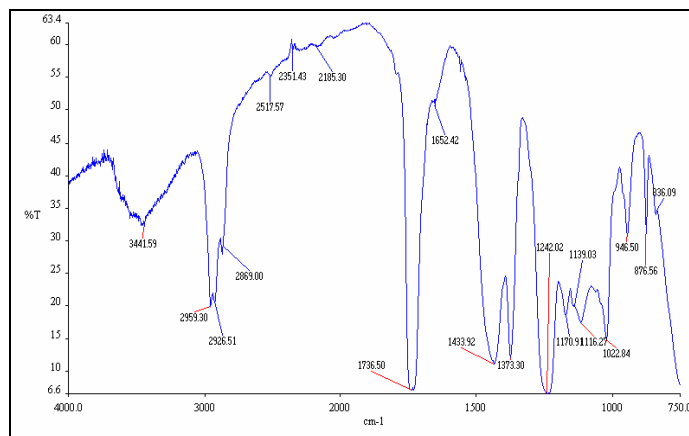
Figure 3.20. Micro-FTIR spectra for sample #12 (Martha Stewart Bright white)
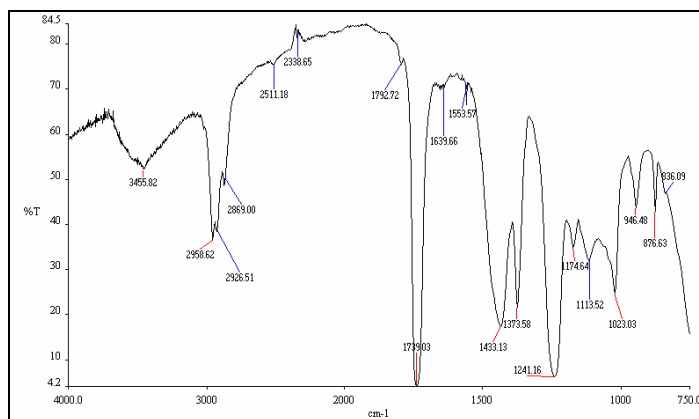
Figure 3.21. Micro-FTIR spectra for sample # 13 (Dutchboy Brilliant White)

Overall, the discrimination power of micro-FTIR for the analysis of white latex architectural paints is reasonably high. However, several of the discriminations are based on relative signal intensities. The reproducibility of these spectra and the effect of sample or pellet thickness should be investigated.

The estimated discrimination values, based on each set of samples, were ~80% for SEM/EDS, 97% for micro-FTIR and 99% for LA-ICP-MS. Despite the reasonably high power of discrimination, micro-FTIR was unable to discriminate samples from different lot numbers or similar composition, where as LA-ICP-MS was.

3.4. SUMMARY OF LA-ICP-MS RESULTS FOR THE ANALYSIS OF PAINTS

3.4.1. Automotive paints by LA-ICP-MS

Method optimization was performed during this work and alternative methods for comparison of paints are proposed. Drift correction over time was improved using normalization of the signals with ^{29}Si and glass standard 612 as calibrator. Precision of the method was enhanced using 200µm spots for ablation (<10% RSD).

The homogeneity studies permitted a better understanding of the natural heterogeneity of elemental composition of automotive paints and the application of statistical models that take that variation into account for match criterion. The homogeneity studies were conducted on sets of samples with a metallic appearance, which have shown to be more heterogeneous in a micro-scale range than solid coats and thereby it could be useful to find large samples of this type of paint in order to perform an additional study of their elemental composition variation.

The application of the quantification method without the need of matrix solid standards is a viable tool for characterization of automobile paint samples, such as the red and blue ACT samples, or "home" made standards, that can be used in a future as matrix-matched standards for paint analyses. The method is very effective since it provide normalization of the signal within runs by acquiring a mass of the ablated materials. In addition to that, the use of dry aerosols from calibration solutions facilitates the quantification of samples without the need of solid standards. Precision within runs needs to be improved in a near future by adjusting properly the concentration levels of solution for each of the layers present in the paint.

It has been proved that LA-ICP-MS is a promising tool for the elemental characterization of fragments of automotive paints, found as evidence in cases such as hit and run. This technique can complement conventional techniques used for forensic examination of paints since it does add discrimination power and allow the discrimination of samples that would otherwise be classified as indistinguishable.

For qualitative and semi-quantitative analysis the proposed methods can provide useful information for comparison of known and questioned samples. Nonetheless, paint is a very complex matrix for laser ablation and therefore further studies need to be completed before this technique can be applied in quantitative determinations.

The quantitative analysis of each layer of paint may be useful in databases, while qualitative and semiquantitative (ratios) comparisons are sufficient for comparison of elemental profiles to determine association between samples or discrimination.

3.4.2. Latex paints by LA-ICP-MS

One of the goals of this research was to develop and investigate a potential method for solid-state sampling and subsequent elemental analysis of architectural coatings. There has been significant amount of interest and research into the application of laser ablation as a sampling method of a wide variety of solid matrices. Automotive paints and latex paints differ not only in the chemical composition and manufacturing process but also in the application to the surfaces. Therefore, these two types of paints were studied separately as different matrices. Each matrix brings about its own advantages and challenges. In the case of architectural paint, the production processes and the different formulations provide variation between manufacturers; which equates

into discrimination. However, there is some inherent variation also found within a single manufacturer, as well as within a single can.

One of the preliminary experiments in this study analyzed the natural variation within a can and compared that to the variation found between manufacturers. It was found that even after thorough mixing, a significant relative standard deviation could be observed within a single can. Therefore, to statistically represent the full range of possible values for a source, effective sampling must be done. Based on the results for the within can study, a sampling method was developed where five samples from a single source were analyzed in triplicate. This method was found to be very effective in providing high discrimination while avoiding the false negatives that may be observed with inadequate sampling.

With a proper sampling method and element menu developed, it was necessary to optimize the laser ablation method to ensure that ample signal was being produced with minimal damage to the sample. After comparing the resulting signals and craters formed by various combinations of parameters, it was concluded that when analyzing latex architectural paint the power and pulse frequency should be reduced to 60% and 5 Hz, respectively. Also, it was found that, to further minimize the negative effect on discrimination caused by within sample variation, a linear ablation mode with a spot size of at least 100 µm should be employed. This sampling method is dually beneficial. First, the linear ablation, and, large spot size, allow for a better representation of natural deviation observed in the X-Y plane of the sample. This, in turn, lowers the observed mean square error and increases the power of discrimination. Secondly, the use of a

linear vs. single spot ablation is more conducive to the analysis of very thin samples, such as chips and smears that are more likely to be encountered as forensic evidence.

The discrimination ability of this method was evaluated by analyzing 25 samples of paint with known sources. These samples were run with the previously stated optimized parameters over the course of four days. This resulted in the discrimination of 3 out of 300 possible comparisons. Therefore, it is possible to conclude that this developed method for the elemental analysis of solid samples of architectural white paint has a discrimination power of at least 99%. It is suspected that the discrimination ability may be even higher if all the samples are able to be analyzed within a single day. This is supported by the observation that in the original four-day analysis, samples 18 and 25 were indistinguishable, despite the fact that they originated from two separate cans of Behr Premium Plus 1050 paint. In addition to having different lot numbers one of the samples was tinted in the store. In the first analysis these samples were analyzed on two consecutive days. When these samples were rerun during the reproducibility study, they were able to be distinguished. Therefore, it is essential that the samples being compared are analyzed during the same day. The disadvantages of this requirement are that it is difficult to analyze large numbers of samples for comparison. This also eliminates the potential for creating a database for future comparisons.

The developed LA-ICP-MS method was compared to the existing methods of forensic paint analysis, specifically SEM/EDS and FTIR. For the SEM/EDS the discrimination power was significantly lower than that for LA-ICP-MS; out of 171 possible pairs there were 44 that were indistinguishable. Ten of those were correctly identified and there was one example of a false negative, therefore there were 35

207

incorrect conclusions. This represents an 80% discrimination power, compared to 99% discrimination obtained via LA-ICP-MS.

The FTIR analysis exhibited greater discrimination than the SEM/EDS because it was possible to obtain information about the organic binders, as well as some of the extenders present. Another benefit of the use of micro-FTIR is the fact that, even though samples may have similar binder and extender classifications, their spectra may be able to be distinguished by the presence of additional peaks or the relative ratios of the peak intensities. The estimated power of discrimination for FTIR analysis of these samples was 97%. Despite the reasonably high power of discrimination, micro-FTIR was unable to discriminate samples from different lot numbers or similar composition, where as LA-ICP-MS was.

The positive results of these studies support the growing interest in the use of LA-ICP-MS for the elemental analysis of forensic materials.

SECTION IV. FUNDAMENTAL STUDIES of LA-ICP-MS

4.1. MATERIALS AND METHODS

4.1.1 Study of the effect of fragment size on the quantification of glass

In order to study if the size of the fragment used for laser ablation has any effect on the comparison of glass fragments, standard reference materials SRM NIST 612 and SRM NIST 610 were employed. The standards were individually crushed using a rubber-head hammer and disposable polypropylene weighing boats (Fisher, Pittsburg, PA, USA). Seven fragments from different shapes and sizes (6 mm to 0.1 mm length) were selected from each standard. The fragments were mounted under a microscope into a small piece of "tacky blue" mounting medium. During LA-ICP-MS each fragment was analyzed in triplicate. The sequence of analysis was randomly selected and the order of analysis was fragment number: 3, 5, 2, 7, 4, 1 and 6, being fragment 7 the smaller one. The calibrators SRM 612 or SRM 610 were run at the beginning and at the end of the sequence in order to account for any drift correction.

4.1.2. Single shot determinations

In order to evaluate the viability to conduct single shot determinations for glass analysis (one laser pulse per analysis), the experiments were performed on the standard SRM 612 measuring five replicates and recording simultaneously the particle size counts with the LASAIR system. The experiment was repeated in two different days evaluating sensitivity and precision.

4.1.3. Fractionation study

Two different approaches were used to evaluate the effect of fractionation on glass samples: a) the fractionation index and b) the U/Th ratio. The fractionation index was calculated using equation 8 (see section 1.5.4.). The U and Th ratio was estimated by monitoring the U/Th ratio for the transient signal of SRM 612, SRM 610 and SRM 1831. Further comparisons of laser ablation versus bulk analysis were used to evaluate its effect on the quantification of glass. For quantification purposes, ^{29}Si was used as an internal standard and the signals were normalized to this isotope to perform the calculation of fractionation index.

4.2. RESULTS AND DISCUSION

### 4.2.1. Study of the effect of fragment size on the quantification of glass

Glass fragments collected from the crime scene and from suspect(s) and victim(s) are random in size. Typically, the fragments recovered from clothing in casework are so small that require microscopic observation (0.1 - 1mm in length) for their initial examination while the "known" samples are usually larger, i.e. a broken fragment from a windshield (> 3mm) (Hammer, 1999). For bulk digestion analysis, the difference in fragment size does not represent a problem for elemental comparisons -other than requiring at least 6 mg- because sample is crushed and homogenized before been weighed. Nevertheless, for laser ablation small craters (~50µm) are drilled into the sample due to the interaction of the laser with the target.

The manner the laser interacts with the sample could be altered by the size of the glass fragment. The aim of this study was to evaluate if the elemental quantification of the LA method is affected by the size of the glass fragment due to differences in heat dissipation and surface–laser interaction.

The standards SRM 612 and SRM 610 were used for this work in order to account for differences in the opacity of the sample as well as differences in concentration levels. The standard SRM 612 is more transparent than SRM 610 and depending of the laser used for the ablation that could affect the efficiency of the coupling of the laser beam with the surface as well as loose of energy due to reflection. The set under study was comprised of 7 fragments originated from each standard at different sizes and shapes ranging from 6 mm to 0.2 mm length. The fragments were run randomly in the sequence and in triplicate. The sizes of the fragments were selected according to the typical sizes recovered from crime scenes. The smallest size of the fragments (#7) was limited by the minimum area that a glass fragment should have in order to perform the LA analysis of craters of 50µm spot size in triplicate and leaving at least 50µm of space between each ablation in order to avoid contamination due to depositions. Table 3.19 shows the size, mass and shape of the fragments used for the laser ablation analysis. The shape description is approximated because most of the fragments were amorphous. Figure 3.22 shows the comparison of size between the biggest and the smallest fragment sampled from SRM 610, in this example, fragment # 7 had a length that is ~25 times smaller than fragment # 1.

Table 3.19. Distribution of size and shape of the glass fragments selected for this study

|	SRM 612				SRM 610		
Fragment	Surface size /mm	mass /mg	Shape		Surface size /mm	mass /mg	Shape
1	6.39 by 2.98	99.024	triangular		3.6 by 3.5	45.020	quasi-squared
2	2.25 by 3.14	35.080	pentagonal		3.8 by 1.97	33.841	triangular
3	2.21 by 2.07	13.280	amorphous		1.32, 1.44 by 2.2	15.284	trapezoid
4	2.02 by 1.64	11.834	pentagonal		1.07 by 0.70	3.248	pentagonal
5	1.78 by 0.81	2.565	rectangular		1.31 by 0.6	2.280	triangular
6	0.91 by 0.66	1.025	rectangular		0.78 by 0.65	1.258	amorphous
7	0.13 by 0.72	0.616	rectangular		0.11 by 0.20	0.907	amorphous
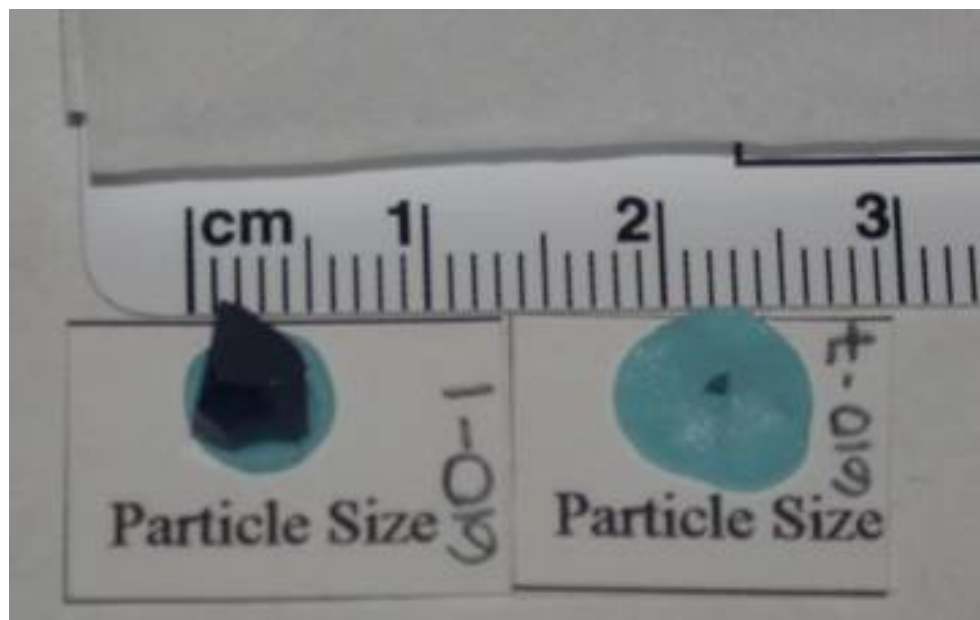
Figure 3.22 Comparison of the fragment size 1 and fragment size 7 of SRM 610

The SEM image on figure 3.23 shows the ablation of three craters on the fragment
6 of SRM 610, which are less than 1mm in length. This fragment #6 represents a good
example of the superiority of LA over digestion method because with the amount of
material ~ 1 mg it would be impossible to run the digestion method, that requires at least
6 mg to run the analysis in triplicate, while by laser ablation the analysis was performed
in triplicate and still there is enough glass left to conduct additional analysis if required
by a court, which may be critical for some forensic casework.

Analysis of variance (ANOVA) was conducted in order to find if there was a
significant difference in the elemental concentration of the fragments due to the size and
shape of the glass piece. With 99% confidence level (p=0.01) there was no significant
difference on the elemental concentration of any of the fragments originated from SRM

610 and SRM 612. Table 3.20 shows the elemental ratios for the different replicates in the fragments from both standards and good correlation between fragments originated from the same standard can be observed.
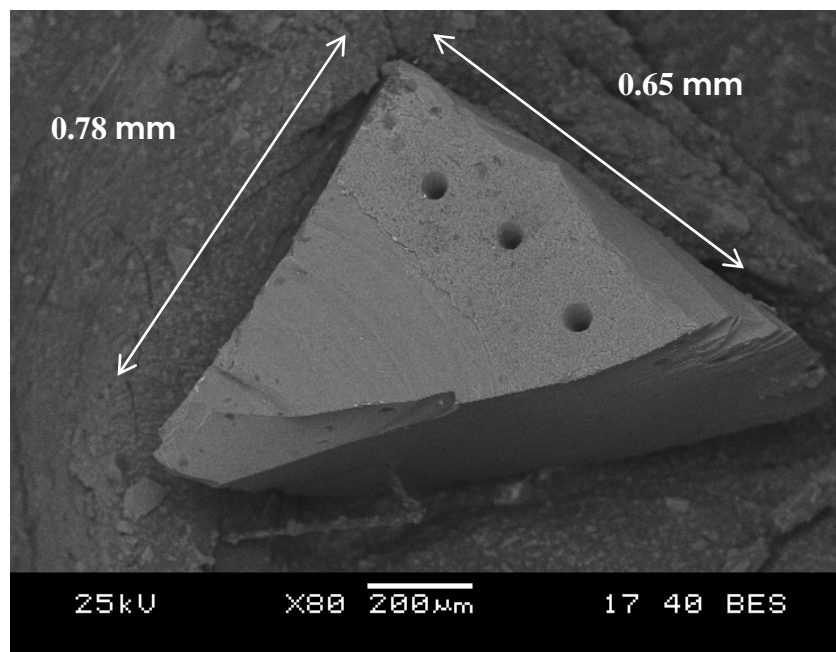
Figure 3.23. SEM image of fragment #6 of SRM 610 after ablation in triplicate

Figure 3.24 gives an example of the comparison of mean values and standard deviation of the elemental ratios between fragments originated from SRM 610. The precision for the vast majority of elements was determined less than 6% when NIST SRM 612 (~40 µg g^{-1}) and SRM 610 (~500 µg g^{-1}) were measured.

In addition to the good association between fragments of different sizes, figure 3.25 shows the good accuracy of the elemental ratios for SRM 612 fragments compared versus the reported values. Experiments conducted on the SRM 610 fragments showed also the same behavior.

**Table 3.20.** Mean values of the elemental ratios of fragments of SRM 612 and SRM 610
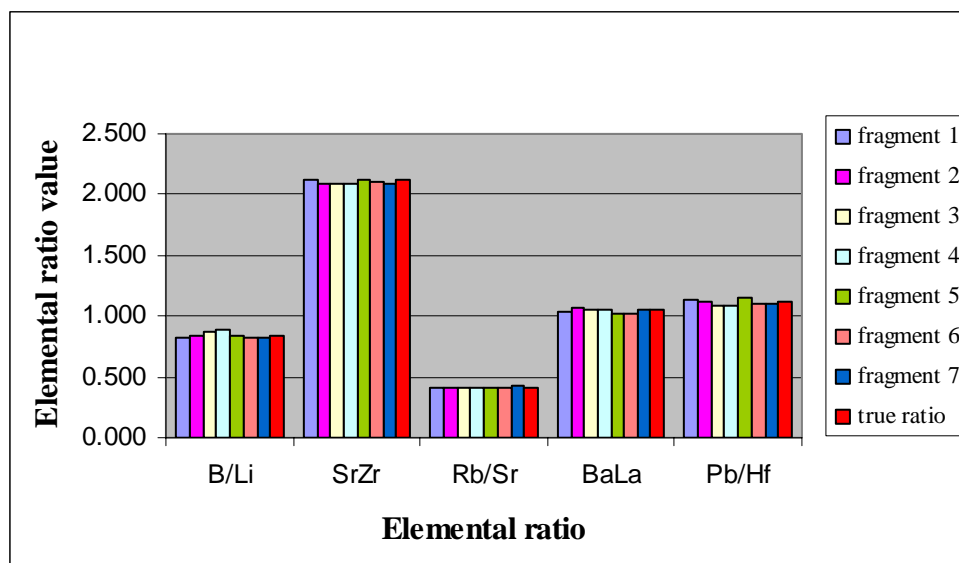
fragment #	SRM 612						
	1	2	3	4	5	6	7
B/Li	0.824	0.834	0.877	0.884	0.837	0.828	0.819
Mg/Al	0.007	0.007	0.007	0.007	0.007	0.007	0.007
TiMn	1.211	1.203	1.534	1.209	1.318	1.315	1.282
SrZr	2.129	2.09	2.092	2.093	2.117	2.097	2.081
Rb/Sr	0.413	0.415	0.416	0.415	0.418	0.418	0.422
Fe/Mn	1.691	1.498	1.529	1.495	1.696	1.696	1.721
MnRb	1.189	1.158	1.14	1.204	1.184	1.207	1.165
BaLa	1.044	1.065	1.057	1.059	1.014	1.024	1.047
CeLa	1.082	1.052	1.073	1.067	1.042	1.027	1.055
Pb/Hf	1.134	1.121	1.085	1.079	1.144	1.095	1.098
U/Th	1.078	1.071	1.026	1.043	1.096	1.025	1.04
ZrSn	0.907	0.979	0.97	0.931	0.907	0.933	0.951
AlK	168.2	162.9	157.3	178.9	168.1	177.1	180.7
CoSr	0.472	0.467	0.478	0.46	0.451	0.466	0.461

| fragment #	SRM 610						
	1	2	3	4	5	6	7
B/Li	0.787	0.793	0.784	0.728	0.792	0.795	0.779
B/Li	0.787	0.793	0.784	0.728	0.792	0.795	0.779
Mg/Al	0.048	0.049	0.048	0.049	0.048	0.049	0.047
TiMn	0.961	0.959	0.973	0.939	0.959	0.951	0.977
SrZr	1.176	1.161	1.146	1.175	1.147	1.187	1.140
Rb/Sr	0.894	0.911	0.894	0.902	0.876	0.928	0.875
Fe/Mn	1.043	1.055	1.038	1.064	1.042	1.04	1.048
MnRb	0.972	0.953	0.949	0.978	0.969	0.948	0.995
BaLa	0.953	0.929	0.942	0.946	0.948	0.95	0.923
CeLa	1.025	1.008	0.992	1.018	0.996	1.035	0.990
Pb/Hf	1.094	1.091	1.04	1.112	1.057	1.163	1.001
U/Th	1.086	1.08	1.045	1.129	1.026	1.144	1.053
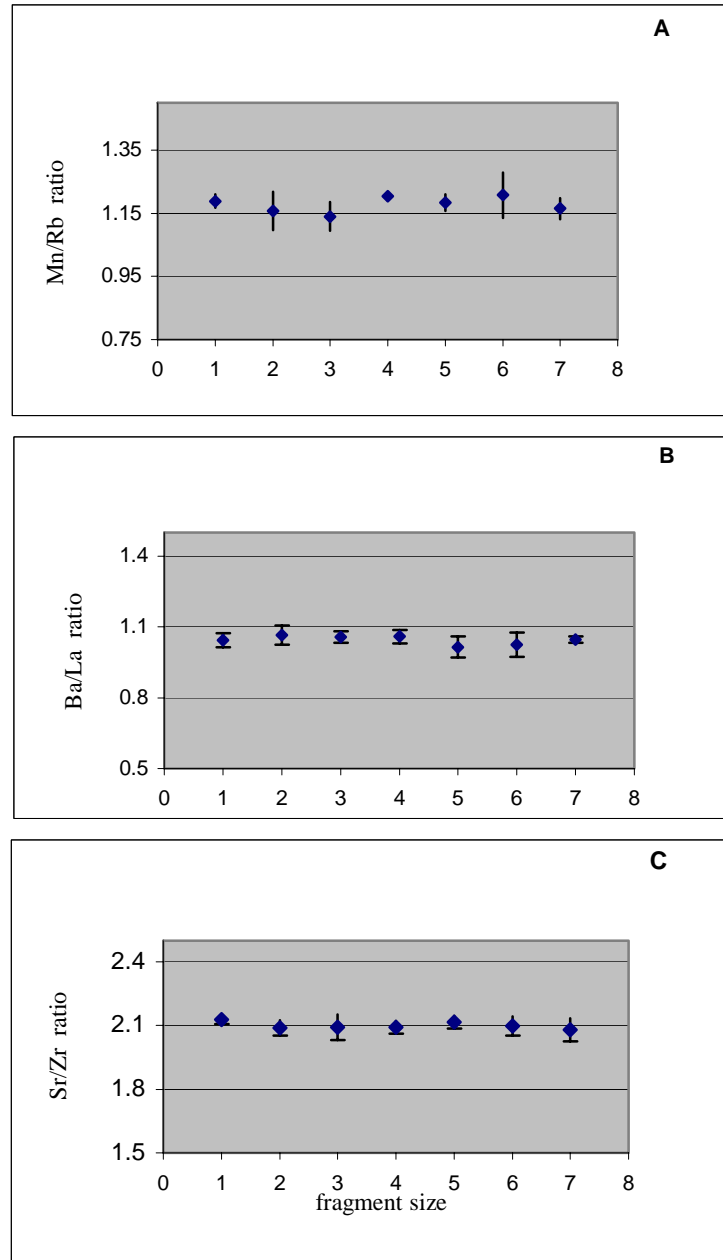
Figure 3.24. Mean values and standard deviation of the elemental rations of 7 different glass fragments from SRM 612. A) Mn/rb, B) Ba/La, C) Sr/Zr.
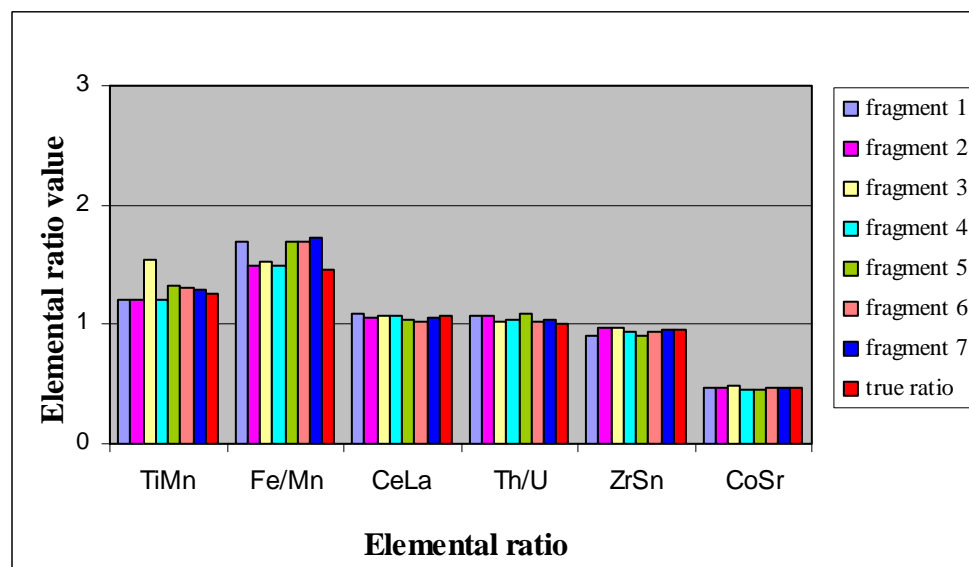
Figure 3.25. Comparison of true values and experimental ratios in glass fragments of different sizes originated from SRM 612 standard.

The SEM images demonstrated also that there was not a significant difference in the shape of the ablation craters and their immediate surrounding surface. Figure 3.26

shows the comparison of crater images obtained for the bigger and the smaller fragments of SRM 612, where no differences in crater shape or deposition of particles were observed.
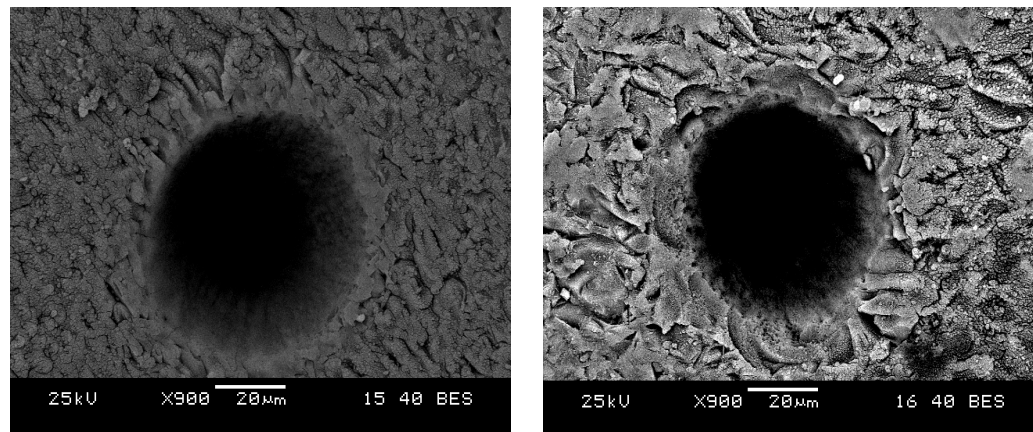
Figure 3.26. Comparison of SEM images of the crater of fragment #1 (left) and fragment #7 (right)

The experimental results demonstrated that the proposed LA-ICP-MS method is not affected by the variability in fragment size of the samples and it is reliable to perform routine forensic glass casework. The conclusions cannot be generalized for fragments below 0.1 mm in length.

## 4.2.2. Study of the effect of fractionation on the quantification of glass

4.2.2.1. Estimation of fractionation

Two different approaches were used to evaluate the fractionation on glass samples: a) the fractionation index and b) the U/Th ratio. Further comparison of laser ablation versus bulk analysis was used to evaluate its effect on the quantification of glass.

For quantification purposes, ^{29}Si was used as an internal standard and the signals were normalized to this isotope to perform the calculation of fractionation index. Under optimal conditions, the fractionation index (FI) should be close to 1 because no changes in the signal over time are to be expected. Some authors have associated significant fractionation to index values of 1.5 to 2.0 while others have reported fractionation as index values as high as 3.5 (Russo, 2002). The equation used for the estimation of FI is:

$$FI = \frac{\left[I_e / I_{int\,std} \right]_{t_2}}{\left[I_e / I_{int\,std} \right]_{t_1}}$$

The experiments performed for 29 different elements, using depth profile mode of ablation with the laser LSX 200 resulted in fractionation index values for SRM 610 between 0.9 and 1.0, for SRM 612 between 0.8 and 1.2 and for SRM 1831 between 0.7 and 1.2 (see Figure 3.27). The fractionation index of ^{133}Cs and ^{232}Th presented the major deviation from 1 in the fractionation index for the reference standard material SRM 1831. The low concentration levels (^{133}Cs: 0.2 µg g^{-1}, ^{232}Th: 0.5 µg g^{-1}) could affect these values as the signal associated with these analytes is close to the limit of detection. The index values for these isotopes are significantly improved when analyzing SRM 612 and SRM 610, where the concentrations are at ~40 µg g^{-1} and ~400 µg g^{-1} respectively.
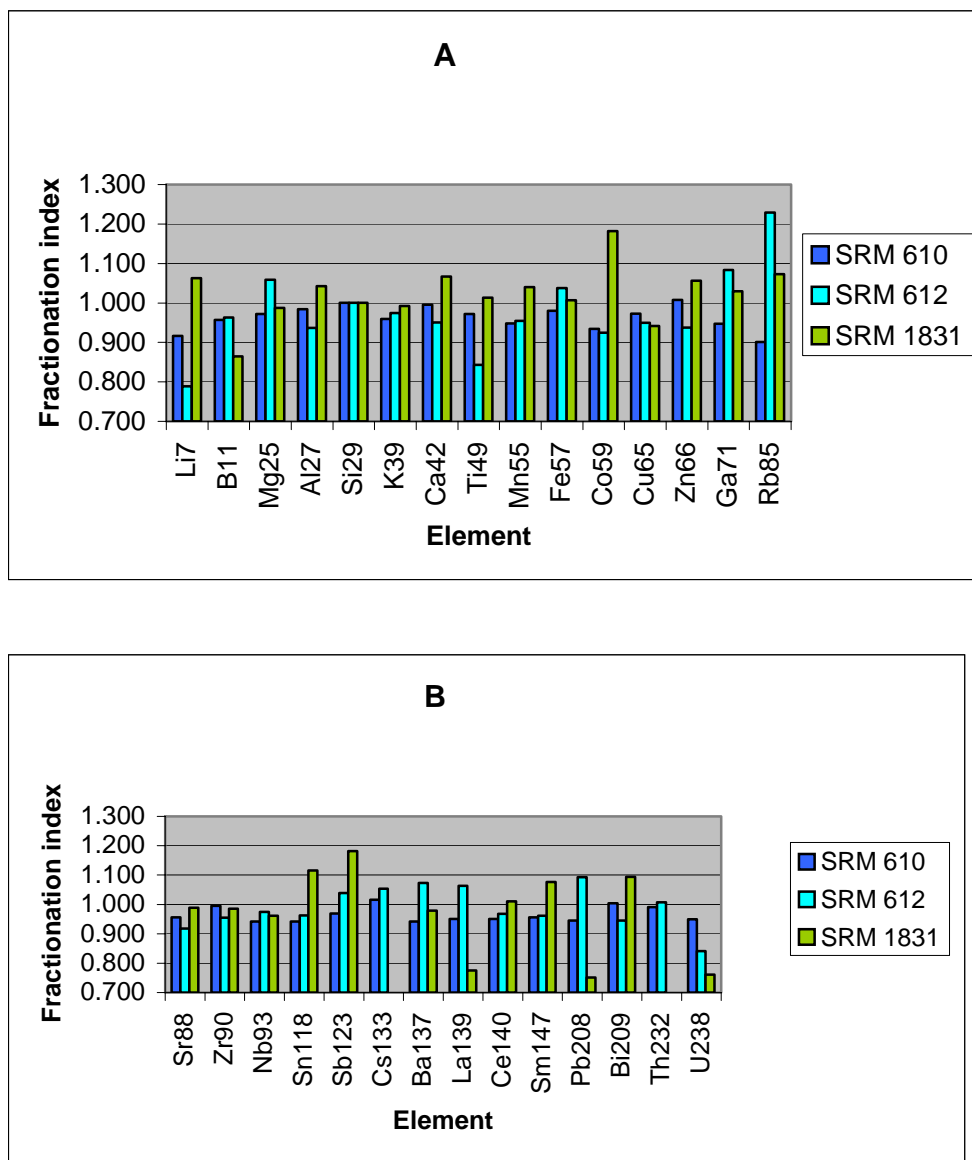
Figure 3.27. Fractionation values obtained for SRM 610, SRM 612 and SRM 1831 using LA-ICP-MS (LSX 200). Upper figure: isotope range from ^{7}Li to ^{85}Rb. Lower figure: isotope range from ^{88}Sr to ^{238}U.

The standards SRM 610, 612 and 1831 where chosen for this study because they have slightly different matrices, ranges of concentration and transparency/opacity characteristics. In addition, SRM 612 is the standard that is commonly used for quantification of glass samples while SRM 1831 is usually analyzed as a verification control for float glass sets, because of their similar elemental compositions. The signals where acquired for 29 isotopes to counter the effect on elements with different mass to charge ratios, ionization potentials and electronic configurations. The majority of the isotopes studied presented low fractionation values suggesting that the fractionation of these elements during glass analysis using the proposed method is not significant.

The fractionation index was also estimated using the laser LSX 200+; the main difference being that the LSX 200+ has a flat beam profile that improves the coupling of the laser with the surface of the glass. As mentioned before, in comparison with the LSX 200 the newer model offered better sensitivity, precision and symmetry of the crater. Approximately double the amount of material is removed using the LSX 500 for ablation. Even though the improvement in crater shape and symmetry is related to improve precision of the ICP-MS measurements, in terms of fractionation there isn't a significant difference between the two systems. The fractionation indices for SRM 610 using both lasers range from 0.8 to 1.2 (see figure 3.28).

The ratio of U/Th has been used as another indication of fractionation due to their similar concentrations within the glass reference materials SRM 610 (U: 461.5µgg^{-1}, Th: 457.2 µgg^{-1}) and SRM 612 (U: 37.38 µg g^{-1}, Th: 37.79 µg g^{-1}) and their similar

ionization potential (U:597 KJmol^{-1}, Th:587 KJmol^{-1}) (Russo, 1998). A stoichoimetric

U/Th ratio close to 1 is therefore expected if no fractionation occurs (theoretical ratio 1.1

for SRM 610 and 0.99 for SRM 612).
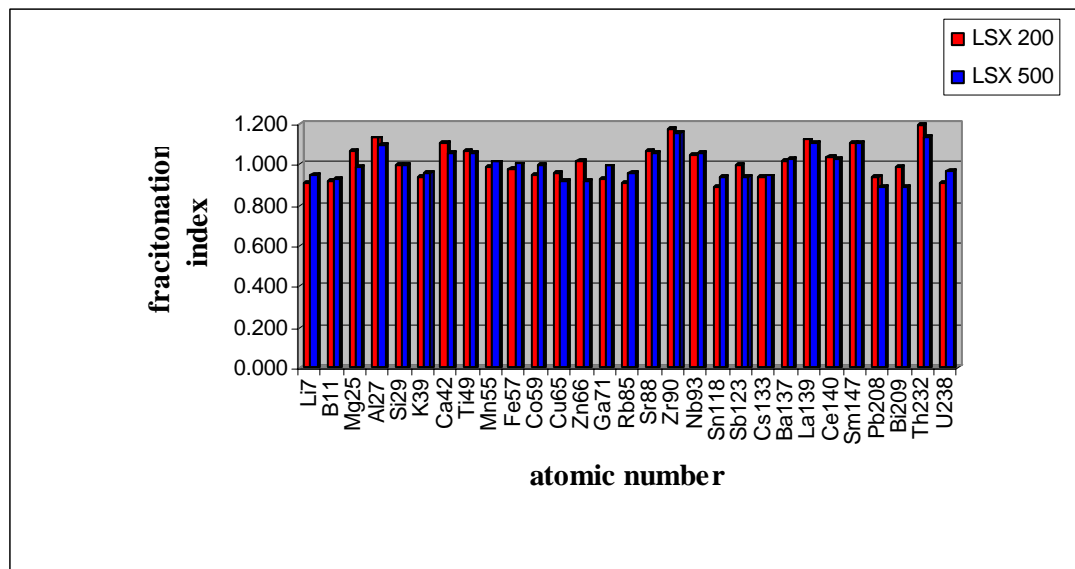
Figure 3.28. Comparison of fractionation index for 29 different isotopes using the laser

systems LSX 200 and LSX 500.

Figure 3.29 illustrates that the U/Th ratio for SRM 610 is close to 3 during the

first 10 seconds of ablation and then drops to ~1.5 for the rest of the ablation. Uranium

and Thorium then exhibit fractionation according to this definition. The first ten seconds

of ablation area are associated with a sharp increase in the signal that then stabilizes

during the last 40 seconds of ablation. As previously mentioned, that increase in signal is

due to the first interaction of the laser with the surface of the glass. Therefore, for

quantification purposes, is recommended that the integration of the signal should be

calculated from the signal in the "stable" area and avoid the portion of the signal that is

related to the higher fractionation value.
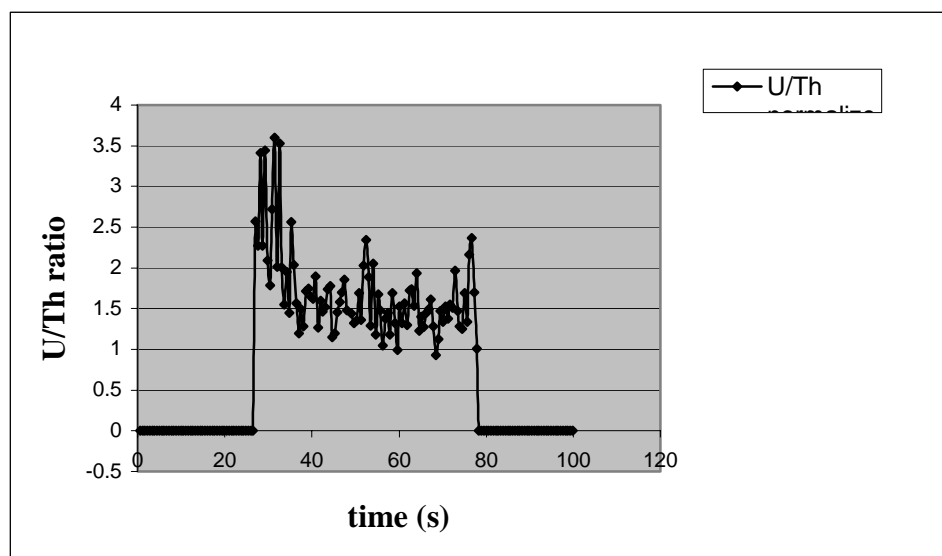
**Figure 3.29.** U/Th ratio obtained for SRM 610 during 50 seconds of ablation

4.2.2.2. Elemental profiling of glass

Since fractionation is also defined as a stoichiometric difference between the

laser products and the composition of the bulk sample, a direct comparison of bulk–

solution analysis versus laser ablation analysis was conducted in order to further evaluate

whether the fractionation phenomena affects the elemental quantification of glass. The

comparison was based on quantitative results of SRM 612 and SRM 1831 (n = 55

samples), as well as the comparison of the elemental profiles of ten casework samples.

Since solution work is more time consuming than laser ablation, the quantitative results

of the 55 replicates for each standard were collected over a period of 2 months for the solution method and over a period of one week for the laser ablation method.

Several calibration strategies have been suggested for the quantitative analysis of solid samples by LA. External calibration alone has the disadvantage that large differences in ablation yields can result from laser interactions with the sample due to differences in the target matrix and the standard matrix. A combination of the use of an external reference standard with internal standardization gives more accurate results. The internal standard corrects for differences in ablation yield between the sample and the reference material. In this study, the isotope ^{29}Si was used as an internal standard and the standard reference material, SRM NIST 612, was used as a single point external calibration standard. The quantification of the isotopes was calculated based on the integration of 30 seconds of the signal.

Figure 3.30 compares the concentrations reported for some elements in SRM 612 and SRM 1831 versus the values obtained with conventional solution ICP-MS and LA-ICP-MS. If fractionation were present in LA, a large difference between the concentration values obtained with this technique and the solution (bulk analysis) would be expected. However, the values obtained with LA and conventional solution ICP-MS were so close together that they overlap in most of the cases. For example, for ^{88}Sr in SRM 612, the reported value is 78.40 µg g^{-1}, the values obtained by LA and solution ICP-MS are 76.76 and 81.30 µg g^{-1} respectively; those values are plotted in Figure 34 at the ^{88}Sr axis and they overlap under the scale used.
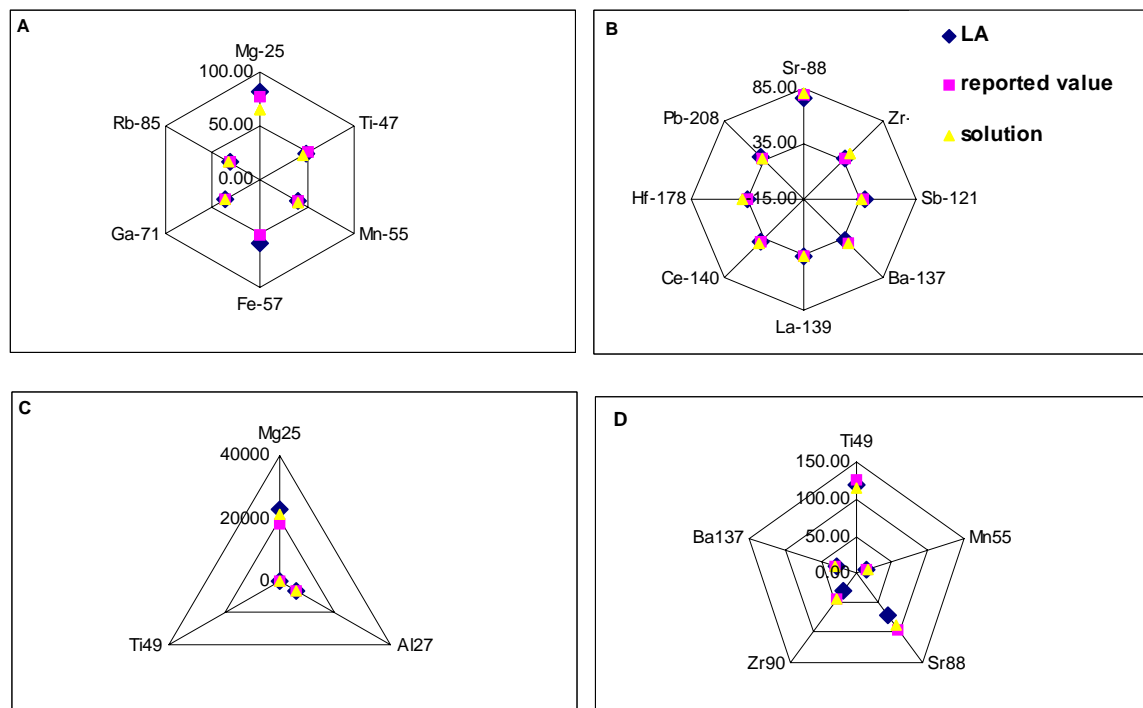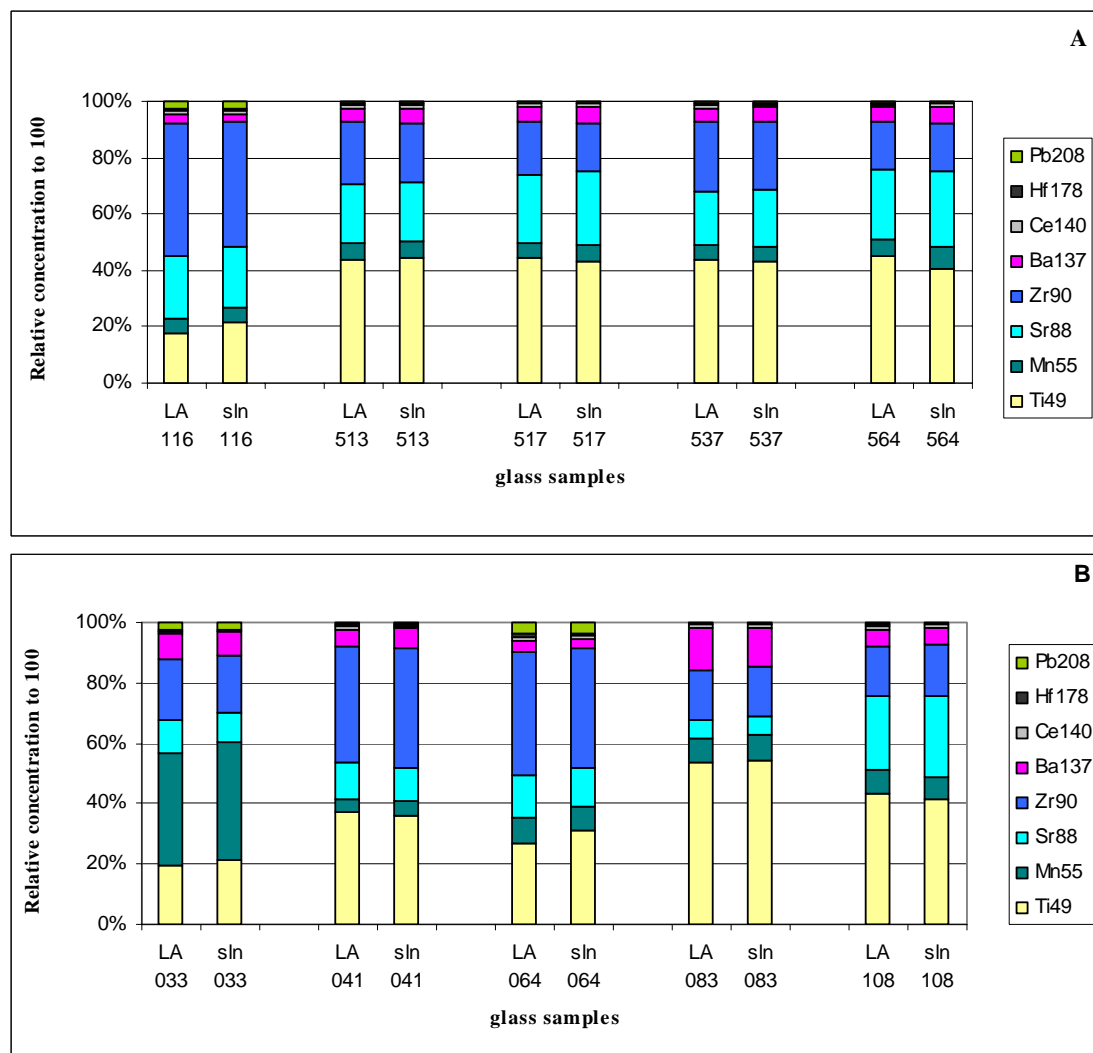
Figure 3.30. Comparison of the reported values versus the quantitative values obtained by LA-ICP-Ms and conventional solution ICP-MS. Upper graphs: results for SRM 612. Lower graphs: results for SRM 1831

The results obtained for ten glass samples originating from different vehicles are also shown in figure 3.31. Good correlation between the elemental profiles obtained using conventional solution and laser ablation ICP-MS was obtained for the set of samples studied.

No significant difference between the elemental concentrations obtained with LA and solution techniques was found and hence this approach supports the hypothesis that

even though some fractionation is still observed (by one definition) for the majority of elements evaluated, the quantification of glass by LA-ICP-MS is not significantly affected for forensic analysis using the optimized method described in this study.

Figure 3.31. Comparison of the elemental profiling of ten glass samples originated from different automobiles, using LA and solution ICP-MS methods.

4.2.2.3. Particle size studies

Some authors have reported that the carrier gas used to transport the particles from the ablation chamber to the ICP greatly influence the deposition of particles around the crater and the intensity of the signal (Eggings, 1998; Bleiner, 2001). Although this effect has been reported to be more significant on excimer lasers than in 266 nm lasers (Horn, 2003), our results showed that using helium instead of argon as carrier gas significantly improved the signal. The best sensitivity and precision were achieved using 100% of helium through the ablation cell at a flow of ~0.95 L/min and mixing the gas output with ~1L/min of argon after the ablation cell and before the introduction into the plasma.

Particle size studies are in good agreement with the observations of signal intensities and precision obtained by LA-ICP-MS analysis of glass standards. The particle size studies were performed for 5 replicates of SRM 612, and showed that using helium as carrier gas reduced the number of big particles entering the plasma, improved the precision of particles entering the ICP and enhanced the sensitivity as much as 3 times. (see table below).

Table 3.21. Comparison of particle size distribution and precision obtained for SRM 612 using helium and argon as carrier gases

Carrier gas	Helium			Argon		
Particle size	Count of particles (intensity)	% RSD	% particles	Count of particles (intensity)	% RSD	% particles
0.1 µm	440795	2.4	97.12	120165	4.5	75.10
0.2 µm	7611	5.2	1.68	19444	3.1	12.15
0.3 µm	1599	1.9	0.35	8188	8.5	5.12
0.4 µm	1087	3.6	0.24	5050	9.8	3.16
0.5 µm	899	3.7	0.20	3975	13.2	2.48
0.7 µm	744	3.3	0.16	1892	12.0	1.18
1 µm	1041	4.9	0.23	1231	9.9	0.77
2 µm	106	9.5	0.02	67	27.6	0.04
Sum of all sizes	453882			160013		

Figure 3.32 depicts the shift in particle size distribution towards smaller particle sizes when argon is replaced with helium. The production of smaller particles contributes to enhance the ionization into the plasma and can explain partially the enhance in sensitivity. This behavior could be a consequence of the higher thermal conductivity of

228

helium that could produce a faster dissipation of the thermal energy from the surface of

the glass reducing the condensation or agglomeration of bigger particles.
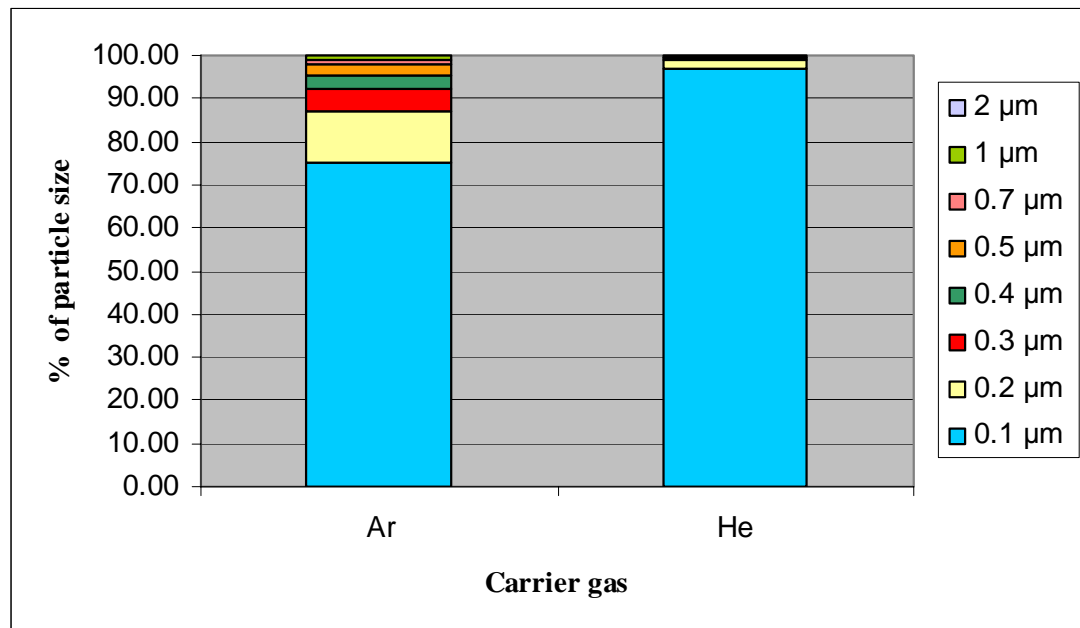
Figure 3.32. Particle size distribution of ablations of SRM 612 using helium or argon as

carrier gases

4.3. SUMMARY OF FUNDAMENTAL STUDIES

Single shot is an attractive sampling technique that could be used in a future glass analysis with even lower sample consumption than the proposed laser ablation method, however intensive research must be done before it can be reliable to do forensic glass examinations.

One of the concerns of the application of laser ablation to forensic evidence was if the surface interaction of the laser-target might be affected by the size and shape of the recovered material due to possible differences in heat dissipation. In spite of this, the quantification of glass with internal standardization does not reflect any significant effect on the analytical results and therefore fragment size is not a matter for forensic comparison of typical glass fragments.

The proposed method is limited to fragments bigger than 0.1mm in length, so the conclusions do not apply to sizes below that range nor other ablation techniques such as single shot.

On the other hand, fractionation on glass was also another aspect of interest for this work because the mechanism of the fractionation in LA-ICP-MS is not very well understood and it is still one of the major challenges for the application of this technique for *in-situ* trace elemental profiling of solid samples.

According to the fractionation index estimation, low levels of fractionation were found in the majority of the elements evaluated. There is, however, evidence of fractionation of U and Th that is more pronounced in the first ten seconds of ablation. There is still some fractionation , however, it would cost a lot of signal to adjust plasma conditions to further reduce this ratio, so fewer elements could be measured, which

would restrict the overall value of the technique. The small bias that can result from possible fractionation does not affect the precision, therefore not affecting comparisons of elemental profiling for forensic casework.

Fundamental studies on particle sizes allowed the determination that the interaction of the 266 nm laser systems LSX 500 and LSX 200 with the glass surface produced small particles with a dominant diameter of 0.1 µm under the reported parameters, however, the LSX500 flat top beam profile provides better precision (<5% RSDs).

Good correlation between the elemental analysis of glass by bulk solution methods and by the LA method was observed for the samples and standards of interest. These results lead to a better understanding of the fractionation phenomenon in glass matrices and its contribution to quantification of glass evidence. Fractionation is dependent on the matrix and therefore these conclusions cannot be applied to other matrices.

SECTION V. CONCLUSIONS AND RECOMMENDATIONS

Extensive effort has been devoted to this study to develop and optimize LA-ICP-MS methods for the analysis of glass and paint samples, as well as to evaluate its advantages and limitations for the application to forensic examinations.

Laser ablation ICP-MS is a technique that affords several key features that provide a tremendous potential for its application to forensic analysis such as, requiring minimum sample preparation and sample consumption (< 250 nanograms), eliminating the need of complex procedures and handling of hazardous materials for the digestion of samples, permitting the detection of major, minor and trace elements with high precision and accuracy, reducing the risk of contamination and polyatomic interferences associated with aqueous solutions; to mention some.

Laser ablation has been thoroughly evaluated in the last decade, with more than 150 papers published, including applications as well as improvements in designs of the laser systems, nevertheless, the technique is fairly new in the forensic arena. The technique provides excellent analytical performance, as well as an excellent discrimination between glass samples that originated from different sources. The objective of this work was to evaluate LA-ICP-MS as a forensic tool and to provide scientific support to facilitate its incorporation into the judicial system.

5.1. Laser ablation for glass analysis

The strategy designed to accomplish this objective for glass analysis consisted in the comparison of LA-ICP-MS with other well accepted techniques for forensic examination of glass, such as solution ICP-MS (external calibration) and refractive index measurements. Accuracy, precision and discrimination power were evaluated by means of the analysis of over 300 samples originating from various sources. Results showed that LA-ICP-MS provided good precision, accuracy and discrimination power comparable to those obtained with the conventional solution ICP-MS methods.

The sensitivity of LA-ICP-MS made the quantification of trace elements possible, allowing the differentiation of glass samples with different origins. The variation of the elemental composition in glass manufacturing, detected by this technique, permitted the discrimination of samples within and between manufacturing plants.

It was determined in eight cases out of nine possible pairs that glass shards originating from the same glass ribbon could be distinguished by elemental analysis when conducting LA-ICP-MS. Therefore, more than one fragment from different areas of each glass sample should be collected in order to have better representation of the whole sample as the analytical method can detect very small differences, even within the same large pane of glass. This would help avoiding false discriminations/associations when conducting glass comparisons for forensic purposes.

Sampling methodologies and match criteria were proposed based on careful evaluation of the homogeneity of elemental composition of glass within a single source(s), including containers, windshields, architectural and tempered glasses. In general terms, a thorough characterization of the "known" source is very important to perform comparisons versus the recovered fragments from scenes, suspects, and/or victims. This is particularly significant for containers due to their high variation within a single source that could lead to a false discrimination if the proper sampling and statistical tools are not applied.

It was also found that some of the glass panes from a windshield (outside vs inside) could have analytically different elemental profiles. Hence, it is essential to sample fragments from both windowpanes in order to avoid misinterpretation of the results. Tempered glass was found to have an even distribution of the elemental composition within the thickness of the fragment, even though some differences in refractive index have been reported as a result from the manufacturing process. Glass samples that have been processed using the "float" method have a higher content of tin on the float side, an aspect that needs to be considered for comparison purposes. As a rule of thumb, as many fragments as practical need to be collected at the crime scene and analyzed in order to facilitate a good characterization of the "known" source and provide a comparison of the elemental "fingerprint" of glass supported by statistical tools.

Investigation on fragments of different size and shape, representative of the sizes typically collected at crime scenarios, were also conducted to determine if the fragment

234

size really matters for comparisons. No significant differences were observed between fragments ranging from 7 mm to 0.1 mm in length.

5.2. LA-ICP-MS for paint analysis

For the application of LA-ICP-MS to paint analysis, different upgrades were proposed to the existing method of analysis, but still the technique is in its evaluation stages and more studies need to be completed before it can be satisfactorily examined in courtrooms.

The technique was found to be viable for the trace elemental analysis and comparison of paints with the advantages to offer much better limits of detection than SEM and XRF methods, with minimum sample manipulation and more discrimination potential.

Natural heterogeneity of the elemental profile of paints was determined to be decisive for the evaluation of the applicability of the technique because it directly affects the discrimination power of the method. The homogeneity is not a limitation for elemental comparisons but a characterization of the variation of each known source is required for association or discrimination of recovered chips.

Bigger sampling areas take into account the aforementioned micro-spatial variability within small paint samples, thereby spot sizes of 200 µm are required for LA-ICP-MS analysis. On the other hand, drift correction over time was acceptably accomplished using glass standards.

The application of the quantification method without the need of solid standards is an effective tool for the preliminary characterization of automobile paints that can be used in a future as matrix matched standards.

Since the manufacture of architectural paints and automotive paint differs significantly, latex paint was studied as a separate matrix and method development and optimization was conducted. One of the studies on architectural paint consisted on analyzing the natural variation within a can and compared that to the variation found between manufacturers. It was found that even after thorough mixing, a significant relative standard deviation could be observed within a single can. Therefore, to statistically represent the full range of possible values for a source, effective sampling must be done. Based on the results for the within can study, a sampling method was developed where five samples from a single source were analyzed in triplicate. This method was found to be very effective in providing high discrimination while avoiding the false negatives that may be observed with inadequate sampling

The discrimination ability of the method proposed for latex paint was evaluated by analyzing 25 samples of paint with known sources. These samples were run with the previously stated optimized parameters over the course of four days. This resulted in the discrimination of 3 out of 300 possible comparisons. Therefore, it is possible to conclude that this developed method for the elemental analysis of solid samples of architectural white paint has an accuracy of at least 99%. It is suspected that the discrimination ability may be even higher if all the samples are able to be analyzed within a single day.

It was demonstrated that is essential that the samples being compared are analyzed during the same day. The disadvantages of this requirement are that it is difficult to analyze large numbers of samples for comparison. This also eliminates the potential for creating a database for future comparisons.

Follow-up studies in this area are strongly recommended in order to facilitate the overall evaluation of the use of this technique in the forensic field. Suggested studies include continuing the characterization of paints with the "standardless" method; completing homogeneity studies for samples with a solid color coat; performing discrimination and homogeneity studies on paint samples originated from the same batch of a painting factory. Additionally, applicability to transfer evidence such as paint smears from hit and run cases would be an attractive focus of study. It might be also interesting to expand this study to household paints and sprays.

5.3. Fundamental Studies of LA-ICP-MS

Additionally, the optimization of the method was assisted with fundamental studies including determination of the size and distribution of particles leaving the ablation cell and fractionation of elements during the ablation process.

At the beginning of this work, fractionation was still a drawback attributed to laser ablation. Even though fractionation on glass was not eliminated or corrected, it was demonstrated with this investigation that the level of fractionation obtained with the proposed method of analysis was low and what is more important, that the presence of this phenomenon is negligible for the quantification of elements for forensic applications.

Single shot experiments were also evaluated and they were found to have several limitations for the application to forensic glass examinations, particularly with the LA and ICP-MS devices available at our facilities.

The results described in this study provide support that LA-ICP-MS analysis of glass can be used for accurate and precise determinations of the elemental

characterization of this material. LA-ICP-MS can also be used to compare fragments to determine whether the fragments share a common source of origin.

Finally, the completion of this project has lead to a better understanding of the theoretical fundamentals and practical application of LA-ICP-MS to trace evidence analyses, particularly glass and paint. Features of forensic interest such as discrimination power, accuracy, precision and reproducibility of LA-ICP-MS were determined for these samples. Laser ablation has the potential to be applied not only to glass and paint samples but also to a variety of trace evidence such as fibers, inks, polymers, gunshot residues, drugs, bones, soil, plastics and other matrices and constitute a promising technique that can be further explored.

LIST OF PUBLICATIONS DERIVED FROM THIS STUDY

Scientific papers

1. Umpierrez S, Trejos T, Neubauer K, **Almirall J**. Determination of Iron in Glass by Laser Ablation and Solution using a DRC-ICP-MS. Atomic Spectroscopy, 27 (3), May/june **2006**, p 76-79

2. Smith K, Trejos T, Watling J, **Almirall J**. A Guide for the quantitative elemental analysis of glass using LA-ICP-MS. Atomic Spectroscopy, 27 (3), May/june **2006**, p 69-75.

3. **J.R. Almiral**l and T. Trejos, Advances in the Forensic Analysis of Glass Fragments with a Focus on Refractive Index and Elemental Analysis, Forensic Science Review, **2006**,18(2) 73-96.

4. C. Latzchoczy, M. Dücking, S. Becker, D. Günther, J. Hoogewerff , **J. Almiral**l, J.A. Buscaglia, A. Dobney, R. Koons, S. Montero, G. van der Peyl, W. Stoecklein, T. Trejos, J. Watling, V. Zdanowicz, Evaluation of a standard method for the quantitative elemental analysis of float glass samples by LA-ICP-MS, *J. of Forensic Sciences*, **2005**, 50 (6), 1327-1341.

5. T. Trejos and **J.R. Almirall**, Sampling strategies for the analysis of glass fragments by LA-ICP-MS. Part II: sample size and sample shape considerations, *Talanta*, **2005**, 67(2) 396-401.

6. T. Trejos and **J.R. Almirall,** Sampling strategies for the analysis of glass fragments by LA-ICP-MS. Part I: micro-homogeneity study of glass and its application to the interpretation of forensic evidence, *Talanta*, **2005**, 67(2) 388-395.

7. **J.R. Almiral**l, Forensic Chemistry Education, *Analytical Chemistry*, **2005**, 77(3) 69A-72A.

8. **J.R. Almirall**, T. Trejos, A. Hobbs, J. Perr and K.G. Furton, Mass spectrometry in forensic science, in *Advances in Mass Spectrometry*, Vol 16, A.E. Ashcroft, G. Breton and J.J. Monaghan, Eds., Elsevier, **2004**, 167-187.

9. T. Trejos and **J.R. Almirall**, Effect of fractionation on the elemental analysis of glass using laser ablation inductively coupled plasma mass spectrometry (LA-ICP-MS), *Analytical Chemistry,* **2004**, 76(5) 1236-1242.

10. J.R. Almirall, T. Trejos, A. Hobbs and K.G. Furton, Trace elemental analysis of glass and paint samples of forensic interest by ICP-MS using laser ablation solid sample introduction**,** in *Sensors, and Command, Control, Communications, and Intelligence Technologies for Homeland Defense and Law Enforcement (5071)*, E.M. Carapezza, Ed.,

Proceedings of the SPIE - The International Society for Optical Engineering, **2003**, 193-204.

11. A. Hobbs and **J.R. Almirall**, Trace elemental analysis of automotive paints by laser ablation inductively coupled plasma mass spectrometry (LA-ICP-MS)**,** *Journal of Analytical and Bioanalytical Chemistry,* **2003**, 376: 1265-1271.

12. T. Trejos, S. Montero, and **J.R. Almirall**, Analysis and comparison of glass fragments by laser ablation inductively coupled plasma mass spectrometry (LA-ICP-MS), *Journal of Analytical and Bioanalytical Chemistry,* **2003**, 376: 1255-1264.

Oral and Poster Presentations

1. **May 2006**, "Forensic Science Research in the U.S.A.", Forensic Science Institute e-Symposium on Forensic Education, Edinburgh, Scotland (via web, **Invited Speaker**)

2. **May 2006**, "Innovative Technology at the IFRI of FIU", Florida Technology Transfer Conference, Sarasota, FL (**PA**)

3. **April 2006**, Advances in Forensic Sciences in the Americas, Organization of American States Meeting of Attorney Generals (REMJA VI), Santo Domingo, Dominican Republic **(Invited Keynote, PA)**

4. **April 2006**, Glass Analysis Workshop, Florida International University (**PA**)

241

5.   **February-March 2006**, "Glass as a Model Matrix for LA-ICP-MS and LIBS", in *Elemental Analysis of Forensic Evidence Workshop,* FIU/NIJ Workshop, Chemistry and Biochemistry, Florida International University, Miami, FL **(Workshop Organizer, PA)**

6.   **Feb. 2006**, Elemental Profiling of Paint Samples by ICP-MS and LA-ICP-MS, AAFS Meeting, Seattle WA (SP, Poster)

7.   **Feb. 2006**, Elemental Analysis of Glass by LA-ICP-MS, a Comparison of Various Laser Methods to Optimize Sensitivity, Precision and Accuracy, AAFS Meeting, Seattle WA (SP, Oral)

8.   **Feb. 2006**, Forensic Elemental Analysis of Glass by Laser Induced Breakdown Spectroscopy (LIBS), SEM-EDS, XRF and LA-ICPMS, NIJ Grantees Meeting AAFS Meeting, Seattle WA (PA, invited Poster Presentation)

9.   **Feb. 2006**, Elemental Analysis of Glass and Paint Materials by LA-ICP-MS NIJ Grantees Meeting AAFS Meeting, Seattle WA (PA, invited Oral Presentation)

10.   **January 2006**, Laser Ablation-ICP-MS for the Examination of Trace Evidence, NIJ Applied Technology Conference, Hilton Head, SC (PA, invited Oral Presentation)

11.   **January 2006**, Quantitative Determination of Elements in Forensic Float Glass Samples by LA-ICP-MS; Presentation of a Standard Routine Method, Winter Plasma Conference, Tucson, AZ (Poster)

12.   **January 2006**, A Comparison of Nanosecond Vs Femtosecond Laser Ablation for the Analysis of Glass, Winter Plasma Conference, Tucson, AZ (SP, Poster)

13.   **January 2006**, ^{57}FE and ^{56}FE Limits of Detection in Glass by HR-ICP-MS and DRC-ICP-MS, Winter Plasma Conference, Tucson, AZ (SP, Poster)

14.   **Nov. 2005**, Elemental Analysis of Glass and Paint Materials by LA-ICP-MS, NIJ Technical Working Group, Washington D.C. (PA, invited Oral Presentation)

15.   **Sept. 2005**, "Forensic Elemental Analysis of Glass by Laser Induced Breakdown Spectroscopy (LIBS), EMS LIBS, Aachen, Germany (PA, poster)

16.   **June 2005**, "Elemental Analysis of Glass and Paint Materials by LA-ICP-MS"*, in* ***Elemental Analysis of Forensic Evidence NITECRIME Workshop,*** Sitges, Spain (PA)

17.   **May 2005**, "Glass Examination and Comparison Workshop", NEAFS, Syracuse, NY (PA)

18.   **May 2005**, "Elemental Composition Variation of Glass Within and Between Manufacturing Plants", FAME, Orlando, FL (SP)

19.   **March 2005**, "Forensic Elemental Analysis of Materials by Laser Induced Breakdown Spectroscopy (LIBS)", SPIE Conference, Orlando, FL (PA)

20.   **March 2005**, "Elemental Characterization of Materials", in *Catching Criminals with Forensic Chemistry Symposium*, American Chemical Society Meeting, San Diego, CA (PA)

21.   **February 2005**, "Elemental Analysis of Glass and Paint Materials by LA-ICP-MS"*,* American Academy of Forensic Sciences, New Orleans, LA (PA, NIJ Grantees meeting)

22.   **February 2005**, "Forensic Elemental Analysis of Glass by Laser Induced Breakdown Spectroscopy (LIBS), Laser Ablation ICPMS and X-Ray Fluorescence"*,* American Academy of Forensic Sciences, New Orleans, LA (SP, Poster)

23.   **February 2005**, "LIBS: A new forensic tool for elemental analysis of materials"*,* American Academy of Forensic Sciences, New Orleans, LA (SP, Poster)

24.   **February 2005**, "Forensic Chemistry; Catching Criminals with Chemistry", Deakin University Dept. of Chemistry, Geelong, Australia (**Invited, PA**)

25. **February 2005**, "Elemental analysis of glass; SEM, XRF, Laser Induced Breakdown Spectroscopy (LIBS) and Laser Ablation-ICP-MS", South Australia Forensic Laboratory, Adelaide, Australia (**Invited, PA**)

26. **February 2005**, "Forensic Applications of Mass Spectrometry", Australian and New Zealand Mass Spectrometry Society, Adelaide, Australia (**Invited Plenary, PA**)

27. **November 2004**, "Análisis Forense de Vidrio por Espectroscopía de Degradación Inducida por Laser (LIBS), Espectrometria de Masas con Ablación por Laser con Plasma Inducidamente Acoplado (LA-ICP-MS) y Fluorescencia de Rayos X (XRF)", I Congreso de Ciencias Forenses, San Jose, Costa Rica (SP)

28. **September 2004**, "Forensic Elemental Analysis of Glass by Laser Induced Breakdown Spectroscopy (LIBS), Laser Ablation Inductively Coupled Plasma Mass Spectrometry, and X-Ray Fluorescence", SAFS/MAFS/CAFS Meeting, Orlando FL (SP)

29. **September 2004**, "Forensic Analysis of Paint by LA-ICP-MS", ENFSI Meeting, Prague, Czech Republic (PA)

30. **September 2004**, "Elemental analysis of glass; SEM, XRF, *Laser Induced Breakdown Spectroscopy (LIBS)* and Laser Ablation-ICP-MS, ENFSI Meeting, Prague, CR (PA)

31. **Sept. 2004**, "Analysis of Glass and Paint by LA-ICP-MS", NITECRIME Workshop, ENFSI Meeting, Prague, Czech Republic (Invited Speaker, PA)

32. **July 2004**, "Analysis of Glass and Paint by LA-ICP-MS", NITECRIME Workshop, Norwich, U.K. (Invited Speaker, PA)

33. **June 2004**, "Forensic Elemental Analysis of Glass by Laser Induced Breakdown Spectroscopy (LIBS)", 7th European Workshop on Laser Ablation, Sheffield, U.K. (PA)

34. **May 2004**, "Glass Analysis and Interpretation Workshop", Dept. of Chemistry and Biochemistry, Florida International University, Miami, FL (Workshop Organizer, PA)

35. **April 2004**, "Forensic Examination and Comparison of Glass Evidence with a Focus on Elemental Analysis by ICP-MS and LA-ICP-MS", NITECRIME Workshop, Wellington, NZ (PA, Invited Talk)

36. **March 2004**, "Forensic Elemental Analysis of Glass and Other Materials by Laser Induced Breakdown Spectroscopy (LIBS)", 17th International Symposium on the Forensic Sciences, ANZFSS, Wellington, NZ (PA, **Keynote Talk**)

37. **March 2004**, "Sampling considerations in the analysis of glass fragments by Laser Ablation Inductively Coupled Plasma Mass Spectrometry (LA-ICP-MS) ", 17th

International Symposium on the Forensic Sciences, ANZFSS, Wellington, NZ (PA, **Best Poster Award**)

38. **February 2004** "Laser Ablation Inductively Coupled Plasma Mass Spectrometry (LA-ICPMS) Elemental Analysis of Glass; Sampling, Instrumental and Database Considerations ", American Academy of Forensic Sciences, Dallas, TX (PA, NIJ Grantees Invited Oral)

39. **February 2004** "Elemental Analysis of Materials by Laser Ablation Inductively Coupled Plasma (LA- ICPMS) for Forensic Applications; Instrumental Considerations", American Academy of Forensic Sciences, Dallas, TX (PA, poster)

40. **February 2004** "Sampling considerations in the analysis of glass fragments by Laser Ablation Inductively Coupled Plasma Mass Spectrometry (LA-ICP-MS) ", American Academy of Forensic Sciences, Dallas, TX (SP,oral)

41. **February 2004** "Micro-homogeneity Considerations for the Forensic Analysis of Glass by LA-ICPMS", American Academy of Forensic Sciences, Dallas, TX (SP, poster)

42. **January 2004** "Micro-homogeneity considerations for the Forensic analysis of Glass by Laser Ablation-ICPMS", Winter Plasma Conference, Ft. Lauderdale (PA, poster)

43. **December 2003** "Forensic Glass Analysis Workshop", Colorado Bureau of

Investigation, Denver, CO (PA)

LIST OF REFERENCES

Aeschliman, D.B., Bajic, S.J., Baldwin, D.P, Houck, R.S. (2003) "Spatially-resolved analysis of solids by laser ablation inductively coupled mass spectrometry: trace elemental quantification without matrix-matched solid standards", Journal of Analytical Atomic Spectrometry, 18, 872-877.

Alexander, M.L.; Smith, M.R.; Hartman, A.; Mendoza, A.; Koppenaal, D.W. (1998) "Laser ablation inductively coupled plasma mass spectrometry", Applied Surface Science, 127-129, 255-261.

Allen, T.J., Cox, A.R., Barton, S., Messam, P., Lambert, J.A. (1998) "The transfer of glass- part 4- The transfer of glass fragments from the surface of an item to the person carrying it", Forensic Science International, 93, 201-208.

Allen, T.J., Hoefler, K., Rose, S.J. (1998) "The transfer of glass- part 2- A study if the transfer of glass to a person by various methods", Forensic Science International, 93, 175-193.

Allen, T.J., Locke, J., Scranage, J.K. (1998) "Breaking of flat glass- part 4- Size and distribution of fragments from vehicle windscreens", Forensic Science International, 93, 209-218.

Allen, T.J., Scranage, J.K. (1998) "The transfer of glass- part 1- Transfer of glass to individuals at different distances", Forensic Science International, 93, 167-174.

Almirall J. (1998) The Evaluation of Glass Evidence by the Statistical Analysis of Inductively Coupled Plasma-Atomic Emission Spectroscopy and Refractive Index data. [Ph.D. dissertation]. Glasgow: University of Strathclyde.

Almirall, J. (1999) Elemental Analysis of Glass Fragments. In: Forensic Examination of Glass and Paint. Caddy, B. Ed.; Taylor & Francis: London, 65-80.

Almirall J. (2001) Glass as evidence of association. In: Mute Witness; When Trace Evidence Makes the Case. Houck M. Ed.; Academic Press: San Diego, 139-155.

American Society for Testing and Materials (2000) "Standard terminology of glass and glass products" Annual Book of ASTM Standards. Vol. 15.02 ASTM: West Conshohocken

American Society for Testing and Materials (2001) "Standard guide for conducting ruggedness tests" (ASTM 1169-89) Annual Book of ASTM Standards. Vol. 14.04 ASTM: West Conshohocken, 416-421.

American Society for Testing and Materials (2001) "Standard test method for the automated determination of refractive index of glass samples using the oil immersion method and a phase contrast microscope" (ASTM 1968-98) Annual Book of ASTM Standards. Vol. 14.02 ASTM: West Conshohocken, 664-666

Beary, E.S., Paulsen, P.J., Fasset, J.D. (1994) "Sample preparation approaches for isotope dilution inductively coupled plasma mass spectrometric certification of reference materials", Journal of Analytical Atomic Spectrometry, 9,1363-1369.

Beauchemin, D.; Gregoire, D.C.; Günther, D.; Karanassios, V.; Mermet, J.M.; Wood, T.J. (2000). In Wilson and Wilson's Comprehensive Analytical Chemistry Series: Discrete Sample Introduction Techniques for Inductively Coupled Plasma Mass Spectrometry, Volume XXXIV. Barcelo, D, Ed., Elsevier, London, 445-501.

Bentley, J. (1999) Composition, Manufacture and Use of Paint. In: Forensic Examination of Glass and Paint. Caddy, B. Ed.; Taylor & Francis: London, 123-141.

Bleiner. D., Gunther, D. (2001) "Theoretical description and experimental observation of aerosol transport process in laser ablation inductively coupled plasma mass spectrometry", Journal of Analytical Atomic Spectroscopy, , 16, 449-456.

Borisov, O.V., Mao, X.L., Cioacan, A.C., Russo, R.E. (1998) "Time resolved parametric studies of laser ablation using inductively coupled plasma atomic emission spectroscopy", Applied Surface Science, 127-129, 315-320.

Borisov, O.V.; Mao X.L.; Russo, R.E. (2000) "Effects of crater development in fractionation and signal intensity during laser ablation inductively coupled plasma mass spectrometry", Spectrochimical Acta, 5, 1693-1704.

Brun-Conti, L (2000) Paints and Coatings. In: Encyclopedia of Forensic Sciences. Siegel, J.A. Ed.; Academic Press: UK, 2000; 1141-1148.

Buscaglia J, Koons R (2001) "Distribution of refractive index values in sheet glasses", Forensic Science Communications, January 3 (1), http://www.fbi.gov/hq/lab/fsc/backissu/jan2001/koons.htm

Buscaglia, J. (1994) "Elemental Analysis of small glass fragments in forensic science", Analytical Chimical Acta, 288, 17-24.

Catterick, T., Wall, C.D. (1978) "Rapid Analysis of Small Fragments by Atomic Absorption Spectroscopy", Talanta, 25, 573-577.

Challinor, J.M. (2001) In: Forensic Examination of Glass and Paint. Caddy B. (ed); Taylor and Francis: London, 165-182

Chen, Z.X. (1999) "Interelement fractionation and correction in laser ablation inductively coupled plasma mass spectrometry", Journal of Analytical Atomic Spectrometry", 14, 1823-1828.

Coleman, R.F., Goode, G.C. (1973) "Comparison of Glass Fragments by Neutron Activation Analysis", Journal of Radiological Chemistry, 15, 367-388.

Coleman, R.F., Weston, N.T. (1968) "A case concerning neutron activation analysis of glass", Journal of Forensic Science Society, 8, 1, 32-33

Cook, R., Evett, I.W., Jackson, G., Jones, P.J., Lambert, J.A. (1998) "A model for case assessment and interpretation," Science and Justice, 38, 3, 151-156.

Copley, G.J. (1999) The comparison and Manufacture of Glass and its Domestic and Industrial Applications. In: Forensic Examination of Glass and Paint. Caddy, B. Ed.; Taylor & Francis: London, 27-46.

Daéid, N.N. (1999) Statistical Interpretation of Glass Evidence. In: Forensic Examination of Glass and Paint. Caddy, B. Ed.; Taylor & Francis: London, 85-94.

Duckworth, D.C., Bayne, C.K., Morton, S.J., Almirall, J.R. (2000) "Analysis of Variance of Forensic Glass Analysis by ICP-MS: Variance Within the Method", Journal of Analytical Atomic Spectrometry, 15, 821-828.

Duckworth DC, Morton SJ, Bayne K, Montero S, Koons RD, Almirall JR (2002) "Forensic Glass Analysis by ICP-MS: a multi-element assessment of discriminating power via analysis of variance and pairwise comparisons", Journal of Analytical and Atomic Spectrometry, 17, 662-668.

Eggins, S.M.; Kinsley L.P.;, Shelley J.M. (1998) "Deposition and element fractionation processes during atmospheric pressure laser sampling for analysis by ICP-MS" , Applied Surface Science, 127-129, 278-286.

Figg, D.; Kahr, M.S. (1997) "Elemental fractionation of glass using laser ablation inductively coupled plasma mass spectrometry", Applied Surface Spectroscopy, 51, 1185.

Figg, D.; Cross, J.B.; Brink, C. (1998) "More investigations into elemental fractionation resulting from laser ablation-inductively coupled plasma-mass spectrometry on glass samples", Applied Surface Science, 129, 287-291

Fisher, B.A. (1993) Techniques of Crime Scene Investigation. 5 ed., CRC Press, Boca Raton, FL, 160-215.

Guillong, M.; Günther, D. (2002) "Effect of particle size distribution on ICP-induced elemental fractionation in laser ablation inductively coupled plasma mass spectrometry", Journal of Analytical Atomic Spectrometry, 17, 8, 831-837.

Hamer, P.S. (1999) Microscopic techniques for glass examination. In: Forensic Examination of Glass and Paint. Caddy, B. Ed.; Taylor & Francis: London, 47-63.

Hecht, J. (1992) Understanding Lasers an entry –level guide, The Institute of Electrical and Electronic Engineers, Inc., New York, chapters 1,3,4,7.

Hicks, T., Vanina, R., Margot, P. (1996) "Transfer and persistence of glass fragments on garments", Science and Justice, 36, 2, 101-107.

Hobbs, A.L, Almirall, J.R., (2003) "Trace elemental analysis of automotive paints by laser ablation inductively coupled plasma mass spectrometry (LA-ICP-MS)", Analytical and Bioanalytical Chemistry, 376,1265-1271.

Hobbs, A.L. (2003) "Elemental Analysis of Automotive Paints by Laser Ablation Inductively Coupled Plasma Mass Spectrometry (LA-ICP-MS) and Paint and Glass by Laser Induced Breakdown Spectroscopy (LIBS)" dissertation, Florida International University, Miami, FL

Horn, I. Gunther, D. (2003) "The influence of ablation carrier gasses Ar, He and Ne on the particle size distribution efficiencies of laser ablation-induced aerosols: implications for LA-ICP-MS", Applied Surface Science, 9710, 1-14.

Hughes, J.C., Catterick T., Southear, G. (1976) "The quantitative analysis of glass by atomic absorption spectroscopy", Journal of Forensic Science, 8, 217-227.

Kleinbaum DG, Kupper LL (1978). Applied Regression Analysis and Other Multivariate Methods. Duxbury: Belmont, California.

Koons, R.D., Buscaglia, J., Bottrell, M. and Miller, E.T. (2002) "Forensic glass comparisons". In: Saferstein R, ed. Forensic Science Handbook, Volume 1, 2nd ed. Upper Saddle River, NJ: Prentice Hall, 161-214

Koons, R.D., Peters, C.A., Rebbert, P.S (1991) "Comparison of Refractive Index, Energy dispersive X ray fluorescence and Inductively Coupled Plasma Atomic Emission Spectrometry for forensic characterization of sheet glass fragments", Journal of Analytical Atomic Spectrometry, 6, 451-456

Kuisma-Kursula P (2000) "Accuracy, precision and detection limits of SEM-WDS, SEM-EDS and PIXE in the multi-elemental analysis of medieval glass", X-Ray Spectrometry, 29, 111-118.

Lambert, J.A., Satterthwaite, M.J., Harrison, P.H. (1995) "A survey of glass fragments recovered from clothing of persons suspected of involvement in crime", Science and Justice, 35 4, 273-281.

Lau, L., Beveridge, A.D. (1997) "The frequency of occurrence of paint and glass on the clothing of high school students. Canadian Society of Forensic Science, 60, 4, 233-240.

Leach, A.M., Hieftje, G..M, (2000) "Methods for shot to shot normalization in laser ablation with an inductively coupled plasma mass time of flight mass spectrometer", Journal of Analytical Atomic Spectrometry, 15, 1121-1124.

Leach, A.M., Hieftje, G..M. (2002) "Factors affecting the production of fast transient signals in single shot laser ablation inductively coupled plasma mass spectrometry", Applied Spectroscopy, 56, 1, 62-69.

Mank, A.J, Masson, P.R. (1999) "A critical assessment of laser ablation ICPMS as an analytical tool for depth analysis in silica based glass samples", Journal of Analytical Atomic Spectrometry, 14, 1143-1153.

Mao, X.L.; Ciocan, C.; Russo, R.E. (1998) "Preferential vaporization during laser ablation inductively coupled plasma atomic emission spectroscopy", Applied Spectroscopy, 52, 7, 913-918.

Mason, P.R. Arjan, J. Mank, G. (2001) "Depth resolved analysis in multi-layer glass and metal materials using laser ablation inductively coupled plasma mass spectrometry", Journal of Analytical Atomic Spectrometry, 16,1381-1388.

Miller, J.N., and Miller, J.C. (2000) Statistics and Chemometrics for Analytical Chemistry, 4 ed., Pearson Education Limited, Essex, England.

Montelica-Heino, M. Le Coustumer, P.; Donard, FX. (2001) "Micro and macro scale investigation of fractionation and matrix effects in LA-ICP-MS at 1064nm and 266nm on glassy materials", Journal of Analytical and Bioanalytical Chemistry, 16, 542-550.

Montero, S. (2002) "Trace elemental analysis of glass by inductively coupled plasma-mass spectrometry (ICP-MS) and laser ablation-inductively coupled plasma-mass spectrometry (LA-ICP-MS)" dissertation, Florida International University, Miami, FL

Montero, S., Hobbs, A., French, T., Almirall, J.R. (2003) "Elemental analysis of glass fragments by ICP-MS as evidence of association: analysis of a case". Journal of Forensic Sciences, 48(5), 1101-1107.

Parouchais T, Warner IM, Palmer LT, Kobus H (1996) "The analysis of small glass fragments using inductively coupled plasma mass spectrometry", Journal of Forensic Science, 41, 351-360.

Pearce NJ, Perkins Wt, Westgate JA, Gorton MP, Jackson SE, Neal CR (1996) "A compilation of new and published major and trace element data for NIST SRM 610 and NIST SRM 612 glass reference materials", Geostandard Newsletter, 1,115-144

Petterd, C.I., Hamshere, J., Stewart, S., Brinch, K., Masi, T., Roux, C. (1999) " Glass particles in the clothing of members of the public in south-eastern Australia- a survey", Forensic Science International, 103, 193-198.

Raith A, Godfrey R, Hutton C (1996) "Quantitation methods using laser ablation ICP-MS", Fresenius' Journal of Analytical Chemistry, 354, 163-168

Roux, C., Kirk, R., Benson, S., Van Haren, T., Petterd, C.I. (2001) " Glass particles in footwear of members of the public in south-eastern Australia- a survey", Forensic Science International, 116, 149-156.

Russo, R.E.; Mao, X.; Lui, H.; Gonzalez, J.;   Mao, S. (2002) "Laser ablation in analytical chemistry: a review", Talanta, 57, 425-451.

Russo. R.E. (1998) Laser Ablation. In: Focus on Analytical Spectrometry: A compendium of Applied Spectroscopy Focal Point Articles (1994-1997). Holcome J, Hiefte, G, Majidi V. Ed.; Society for Applied Spectroscopy: MD, 41-55.

Saferstein, R. (1998) Criminalistics, An Introduction to Forensic Science. 6 ed., Prentice Hall, Upper Saddle River, NJ

Sapir, G.I. (2002) Legal Aspects of Forensic Science. In: Forensic Science Handbook. Saferstein R.Ed.; Prentice Hall: New Jersey, 18-24.

Schroeder E, Hamester M, Kaiser M (1998) "Properties and characteristics of a laser ablation ICP-MS system for the quantitative elemental analysis of glasses", Applied Surface Science, 127-129, 292-298.

Silfvast, W.T. (1996) Laser Fundamentals, Cambridge University Press, New York.

Smith, D.H. (2000) Isotope Dilution Mass Spectrometry. In: Inorganic Mass Spectrometry. Barshick.; Duckword DC.; Smith DH, Eds.; Dekker: New York, 223-239.

Stix J, Gauthier G, Ludden J (1995) "A critical look at quantitative laser ablation ICP-MS analysis of natural and synthetic glasses", The Cannadian Mineralogist, 33, 435-444

Stoecklein, W., Becker, S. (2001) Proceedings of the 13th INTERPOL Forensic Science Symposium, Lyon, France, October, 2001.

Taylor, N. (2000) Laser: the inventor, the nobel laureate and the thirty year patent war, Simon & Schuster, New York.

Thornton, J.I. (2002) Forensic Paint Examination. In: Saferstein R, ed. Forensic Science Handbook, Volume 1, 2nd ed. Upper Saddle River, NJ: Prentice Hall, 430-475.

Tibi M, Heumann KG (2001) "Determination of trace elements in quartz glass by use of LINA-Spark-ICP-Ms as a new method for bulk analysis of solid samples", Fresenius' Journal of Analytical Chemistry, 370, 521-526.

Trejos, T., Montero, S., Almirall, J.R., (2003) "Analysis and comparison of glass fragments by laser ablation inductively coupled plasma mass spectrometry (LA-ICP-MS) and ICP-MS)", Analytical and Bioanalytical Chemistry, 376,1255-1264.

U.S. Department of Justice-Federal Bureau of Investigation-Scientific Working Group on Materials Analysis (SWGMAT) (2000) "Forensic Paint Analysis and Comparison Guidelines, http:www.fbi.gov/programs//ab/fsc/backissu/july1999/paintc.htm

U.S. Department of Justice-Federal Bureau of Investigation-Scientific Working Group on Materials Analysis (SWGMAT) (1999 July) Forensic Science Communications: 1(2)

Watling, J.R. (1999) "Novel Application of Laser Ablation Inductively Coupled Mass Spectrometry in Forensic Science and Forensic Archeology", Spectroscopy, 14, 6, 16-32

Watling, J.R., Lynch BF, Herring D (1997) "Use of Laser Ablation Inductively Coupled Plasma Mass Spectrometry for Fingerprinting Scene of Crime Evidence", Journal of Analytical Atomic Spectrometry, 12,195-203.

Zurhaar, A., Mullings, L. (1990) "Characterization of Forensic Glass Samples Using Inductively Coupled mass spectrometry", Journal of Analytical Atomic Spectrometry, 5, 611-617.